The Antibacterial Properties of Oral Mucosa Lamina Propria-Progenitor Cells

A thesis submitted to Cardiff University in accordance with the requirements for the degree of Doctor of Philosophy

January 2016

Emma Board-Davies

Acknowledgements

I would firstly like to thank my supervisors Dr. Lindsay Davies, Prof. Alastair Sloan and Prof. Phil Stephens for their continued support and encouragement throughout the last few years. Particular thanks to Dr. Lindsay Davies who provided guidance and practical help within the lab, in addition to giving me the opportunity to spend time undertaking research at the Karolinska Institutet in Stockholm, Sweden. Support from Prof. Katarina Le Blanc at the Karolinska Institutet has been invaluable, particularly during my visit to Sweden, and I would like to extend my thanks to her group. Further thanks to members of Oral and Biomedical Sciences department, especially the technical staff for providing further support and help along the way.

I have thoroughly enjoyed being a member of the Cardiff Institute of Tissue Engineering and Repair (CITER) and the public engagement events that I have had the opportunity to be a part of. Thanks to Jane Graves for making that happen.

The support of fellow PhD students and early career researchers within the department has been invaluable, both for their experience and friendship – thank you to all who made coming into the lab everyday a happy place to be! I would finally like to thank my parents and Sully for their continued faith in me and for their love and endless support.

Summary

Despite the rich oral microflora, infections within the oral cavity are rare. Rapid wound healing within the oral mucosa occurs, potentially due to the presence of oral mucosa lamina propria-progenitor cells (OMLP-PCs). OMLP-PCs are a novel population of multipotent cells known to possess immunosuppressive properties, through contact-independent mediated mechanisms. Many immunomodulatory soluble factors are also documented to have dual functions as antimicrobials; leading to the hypothesis that OMLP-PCs possess antibacterial properties in addition to their published immunoregulatory actions. The aim of this study was to investigate the antibacterial properties of OMLP-PCs and to define the mechanisms of action. A further aim of this study was to determine whether the antibacterial potential of OMLP-PCs was affected during disease, specifically Graft Versus Host Disease (GVHD). The antibacterial properties of OMLP-PCs were compared between cells isolated from healthy donors and patients with oral chronic GVHD. During this study it was determined that OMLP-PCs possess constitutive antibacterial properties against Gram positive and Gram negative bacteria which are mediated through the release of soluble factors. LL37 and Indoleamine 2,3-Dioxygenase are known to mediated the antibacterial properties of bone marrow-mesenchymal stem cells, however this study determined that these factors did not play a role in the OMLP-PCs antibacterial effects. It was established that osteoprotegerin, haptoglobin and prostaglandin E2 in part mediate the antibacterial effects of OMLP-PCs. For the first time, direct antibacterial properties of osteoprotegerin were demonstrated against Gram positive bacteria. Furthermore, OMLP-PCs isolated from GVHD patients did not display antibacterial properties. It was further established that the secretion of innate cell chemoattractants was dysregulated in OMLP-PCs isolated from GVHD patients compared to healthy controls. This finding demonstrates that during GVHD, the oral mucosa is unable to regulate the oral microflora and sufficiently recruit innate immune cells during infection.

Table of Contents

Abbreviations

ADM: Adrenomedullin

aGVHD: acute graft versus host disease

AMPs: Antimicrobial peptides

APC: Antigen presenting cell

ATP: Adenosine triphosphate

BM-MSC: Bone marrow-mesenchymal stem/stromal cell

CCL: C-C motif chemokine

CCR: c-c chemokine receptor

CFU: Colongy forming unit

cGVHD: Chronic graft versus host disease

CLRs: C-type lectin receptors

CM: Conditioned media

COX: Cyclooxygenase

CXCR: Chemokine c-x-c motif receptor

DC: Dendritic cell

DNA: Deoxyribonucleic acid

DP-MSC: Dental pulp-mesenchymal stem cell

E. coli: *Escherichia coli*

E. faecalis: *Enterococcus faecalis*

ECM: Extracellular matrix

ELISA: enzyme-linked immunosorbent assay

FCS: Fetal calf serum

G-CSF: Granulocyte-colony stimulating factor

GVHD: Graft versus host disease

H. Pylori: Helicobacter pylori

HB: Human defensins

hBD: Human beta defensin

hCAP18: human cathelicidin precursor

HD: human defensin

HLA: Human leukocyte antigen

HNP: Human neutrophil peptides

Hp: Haptoglobin isoform

HSCT: Hematopoietic stem cell transplantation

IDO: Indolamine2,3-dioxygenase

IFNγ: Interferon gamma

Ig: Immunoglobulin

IL-: Interleukin

iPS cell: induced pluripotent stem cells

IRAK: Interleukin-1 receptor associated kinase

IV: Intravenous

JNK/SAP: c-Jun N-terminal kinase/stress-activated protein kinase

K. pneumoniae: *Klebsiella pneumoniae*

LPS: Lipopolysaccharide

LTA: Lipoteichoic acid

MAPK: mitogen-activated protein kinase

MCP-1: Monocyte chemoattractant protein-1

MMPs: Metalloproteinases

mRNA: Messenger ribonucleic acid

MSC: Mesenchymal stem cell

NETs: Neutrophil extracellular traps

NF-$_K$b: Nuclear factor kappa-light-chain-enhancer of activated B cells

NK cell: natural killer cell

NLRs: Nod-like receptors

OMLP-PC: Oral mucosa lamina propria-progenitor cell

OMP: Outer membrane protein

OPG: Osteoprotegerin

P. gingivalis: *Porphyromonas gingivalis*

P. aeruginosa: *Pseudomonas aeruginosa*

P. mirabilis: *Proteus mirabilis*

PAMPs: Pathogen associated molecular patterns

PBMCs: Peripheral blood mononuclear cells

PCR: Polymerase chain reaction

PGD2: Prostaglandin D2

PGE2: Prostaglandin E2

PGN: Peptidoglycan

RANKL: Receptor activator of nuclear factor kappa-B ligand

RLRs: Rig-I like receptors

RNA: Ribonucleic acid

RNS: reactive nitrogen species

ROS: Reactive oxygen species

RT-PCR: Reverse-transcription polymerase chain reaction

S. aureus: Staphylococcus aureus

S. epidermidis: Staphylococcus epidermidis#

S. mitis: Streptococcus mitis

S. mutans: Streptococcus mutans

S. pyogenes: Streptococcus pyogenes

SDF-1: Stromal derived factor-1

T reg cell: T regulatory cell

TGF: transforming growth factor

Th: T helper

TLR: Toll-like receptor

TNF-a: Tumour necrosis factor-alpha

TRAF6: Tumour necrosis factor receptor associated factor 6

TRAIL: Tumour necrosis factor-related apoptosis-inducing ligand

VEGF: Vascular endothelial growth factor

1. General Introduction

1 General Introduction

1.1 Oral Mucosa

The oral mucosa is a vital structure within the oral cavity, involved in thermoregulation, maintaining electrolyte balance and acting as a barrier to micro-organisms (Stephens and Genever, 2007). Macroscopically the tissue is structured into three distinct layers: the oral epithelium, the lamina propria and the submucosal fat layer (Fig. 1.1; Stephens and Genever, 2007).

1.1.1 Epithelium

The epithelium consists of stratified squamous cells, which are mainly keratinocytes in addition to a small number of melanocytes, Langerhans cells and Merkel cells. Within the oral cavity, two different types of epithelium exist; keratinised and non-keratinised epithelium (Dawson et al., 2013). Keratinised epithelium shares structural similarities with skin epithelium, due to the equivalent functions in resisting shear stress and microbial defense. This type of epithelium is found within the gingiva and hard palate, whereas non-keratinised epithelium is found within the soft tissues such as the underside of the tongue and the buccal mucosa (Stephens and Genever, 2007).

1.1.2 Lamina Propria

The lamina propria is the connective tissue layer, which can be further separated into two regions; the papillary and the reticular layers (Stephens and Genever, 2007). The papillary layer is located immediately below the epithelium, with an extracellular matrix (ECM) comprised of glycoproteins, glycosaminoglycans, elastic fibres, proteoglycans and collagen (type I and III). Fibroblasts are thought to primarily produce and re-organise the ECM (Stephens et al., 1996) however, since these studies the identification of a stem cell population within the lamina propria, so termed oral mucosa lamina propria progenitor cells (OMLP-PCs), has been demonstrated (Davies et al., 2010). Further studies are needed to confirm whether the ECM is truly made by the oral fibroblasts, or whether there is an involvement of the OMLP-PCs in tissue homeostasis within the lamina propria.

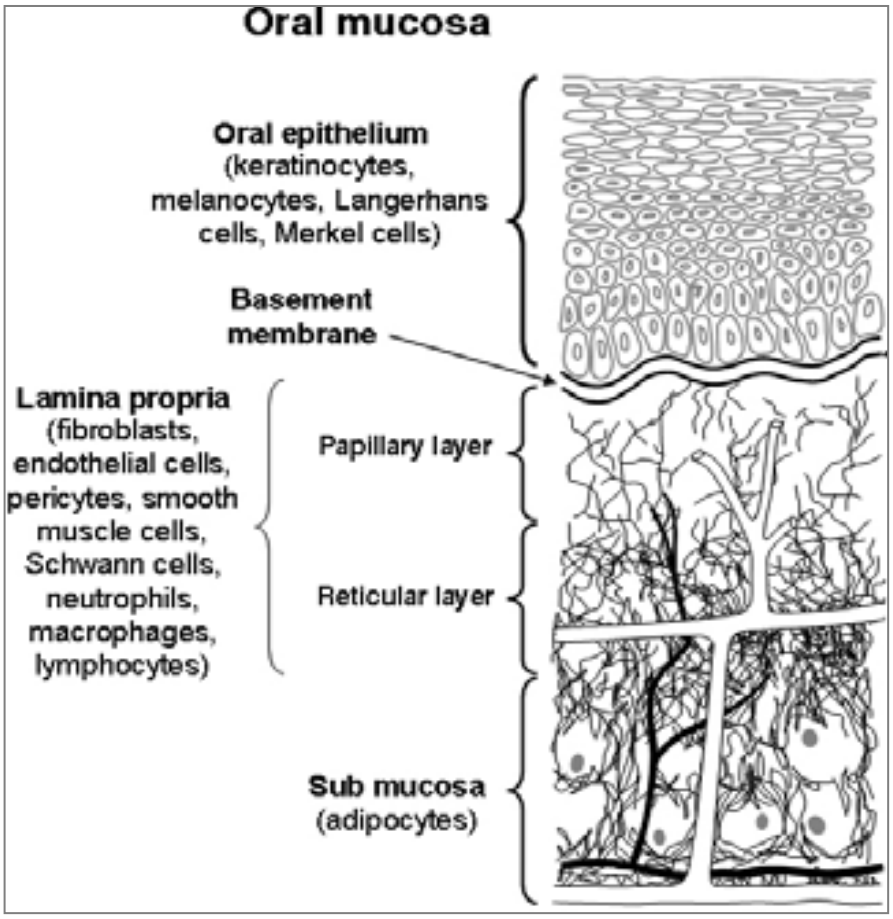

Fig. 1.1: The structure of the oral mucosa (Reproduced from Stephens and Genever, 2007).

A thick reticular layer lays beneath the papillary layer, with an ECM comprising thick bundles of type I collagen, in addition to elastic fibres, glycosaminoglycans, proteoglycans, glycoproteins and fibroblasts (Stephens and Genever, 2007). Immune cells such as dendritic cells (DCs; Hovav, 2014) and cells of the blood vessels such as pericytes are also found dispersed within the lamina propria (Stephens and Genever, 2007).

1.1.3 Submucosa

The submucosa separates the oral mucosa from the underlying muscle and bone. It is comprised of adipocytes and an extensive blood network, providing a nutrient supply and waste removal to the tissue. The submucosal layer also functions as an insulator, preventing excessive heat loss (Stephens and Genever, 2007).

1.2 Oral Microflora

1.2.1 Bacteria

More than 700 different bacterial species have been identified within the human oral cavity (Aas et al., 2005), making the oral cavity the second most bacterially diverse region of the body after the colon (Consortium, 2012). The large number of different bacteria within the mouth is not surprising with its continuous exposure to the external environment, presenting the oral cavity as a major entry point for bacteria. The majority of bacteria are commensals however, some species found in the oral cavity are pathogenic outside the confinement of the oral environment, for example within the respiratory system (Parahitiyawa et al., 2010).

It has been reported that over 60% of bacteria discovered within the oral cavity cannot yet be cultured in standard laboratory conditions, only being identified by molecular techniques (Dewhirst et al., 2010). It has been reported that an average of 56 different bacterial species are dominant in one human mouth. Whilst previous studies have demonstrated that a wide range of bacteria reside within the oral cavity, distinct niches were shown to harbour specific species (Aas et al., 2005). For example, *Streptococcus sanguinis* and *Streptococcus australis* were only found residing on the soft tissues of the mouth and not on hard tissues such as the teeth (Aas et al., 2005). The most commonly found bacteria within the oral cavity were *Gemella, Granulicatella, Streptococcus* and *Viellonella* species, with *Streptococcus*

mitis (*S. mitis*) the most common singular species (Aas et al., 2005). *Streptococcal* species have also been documented by others to be the most abundant species within the oral cavity (Norder Grusell et al., 2013, Dewhirst et al., 2010).

Commensal bacteria play a role in the homeostasis of the oral cavity. These bacteria bind to the surfaces within the oral cavity, limiting the areas in which pathogenic bacteria can bind and subsequently colonise. However, disruptions in the commensal flora can occur through a change in diet, radiation or use of antibiotics (Wade, 2013). For example, in the human gut the use of β lactam antibiotics increases the overall bacterial load. However, a decrease in the bacterial diversity is also noted, with a 20% drop in the number of different bacterial taxa identified after antibiotic use. Furthermore, an increase in *Bacteroides* bacteria is reported, demonstrating the shift of the normal gut flora (Panda et al., 2014).

The microflora of the oral cavity in a healthy individual is distinct from that in a patient with oral disease. Bacterial species, such as *Treponema denticola* and *Porphyromonas gingivalis* (*P. gingivalis*), are associated with periodontal disease. These species are identified within the oral cavity of patients with periodontal disease, but not found in those of healthy subjects (Aas et al., 2005). Higher bacterial counts of *Neisseria* species and *enterobacteria* have also been noted in patients with periodontal disease, compared to healthy individuals (Vieira Colombo et al., 2015). A link between chronic inflammatory periodontitis caused by bacteria and a number of systemic diseases has been documented. Chronic periodontitis is reported to be associated with the incidence of chronic heart failure in men under the age of 60 (Dietrich et al., 2008). It is also thought that the oral cavity provides a reservoir for respiratory pathogens, with direct access to the respiratory organs. Indeed, patients with a history of chronic obstructive pulmonary disease have been associated with a greater number of periodontal tooth attachment loss (Scannapieco and Ho, 2001). The presence of periodontal disease has also been associated with increased systemic complications (such as Graft Versus Host Disease [GVHD], see section 1.9.7.1) following hematopoietic stem cell therapy (HSCT), with prior periodontal treatment hypothesised to improve patient oral outcome (Gürgan et al., 2013). Dental caries is another oral condition associated with bacterial species, such as *Streptococcus mutans* (*S. mutans*). It was found that significantly higher levels of *S mutans* were present in children with caries, compared to healthy controls, in addition to *S. mitis*, *Streptococcus oralis* and *Streptococcus pneumoniae* species *(Becker et al., 2002)*.

1.2.2 Fungi

Candida species, predominantly *Candida albicans* (*C.albicans*), have long been identified within the oral cavity (Arendorf and Walker, 1979). Many different *Candida* species have been isolated from the oral cavity of healthy individuals including *C. albicans*, *Candida parapsilosis*, *Candida tropicalis* and *Candida glabrata,* with *C. albicans* making up over 70% of the *Candida* species within the oral cavity (Ng et al., 2015). In addition to *Candida, Aspergillus and Fusarium* species have been identified in the oral cavity however, these are less abundant than the *Candida* species (Ghannoum et al., 2010). Whilst *Candida* species colonise in the oral cavity as commensals, they can act as opportunistic pathogens causing disease. Overgrowth of the fungus, particularly in immunocompromised individuals, can cause the inflammatory condition candidiasis (Patel et al., 2012).

1.3 Bacterial Cell Wall Structure

The cell wall provides the bacterial cell with shape, whilst preventing the occurrence of cell lysis by regulating internal osmotic pressure (Yount and Yeaman, 2013). It is this structure which divides bacteria into two groups: Gram positive and Gram negative bacteria (Yount and Yeaman, 2013).

1.3.1 Gram Positive Bacteria

The cell wall of Gram positive bacteria (Fig. 1.2, A) consists of polysaccharides covalently linked to peptidoglycan (PGN) (Schäffer and Messner, 2005). Gram positive bacteria have long been further classified into groups by the presence of three specific polysaccharides; teichoic acid (Archibald et al., 1968), teichuronic acid (Ward, 1981) or other acidic or neutral polysaccharides which do not fall under the previous two categories (Araki and Ito, 1989). These polysaccharides are thought to play a role in several different cellular functions of the cell wall such as ion homeostasis, protein binding, folding of extracellular proteins and forming a physical barrier (Schäffer and Messner, 2005).

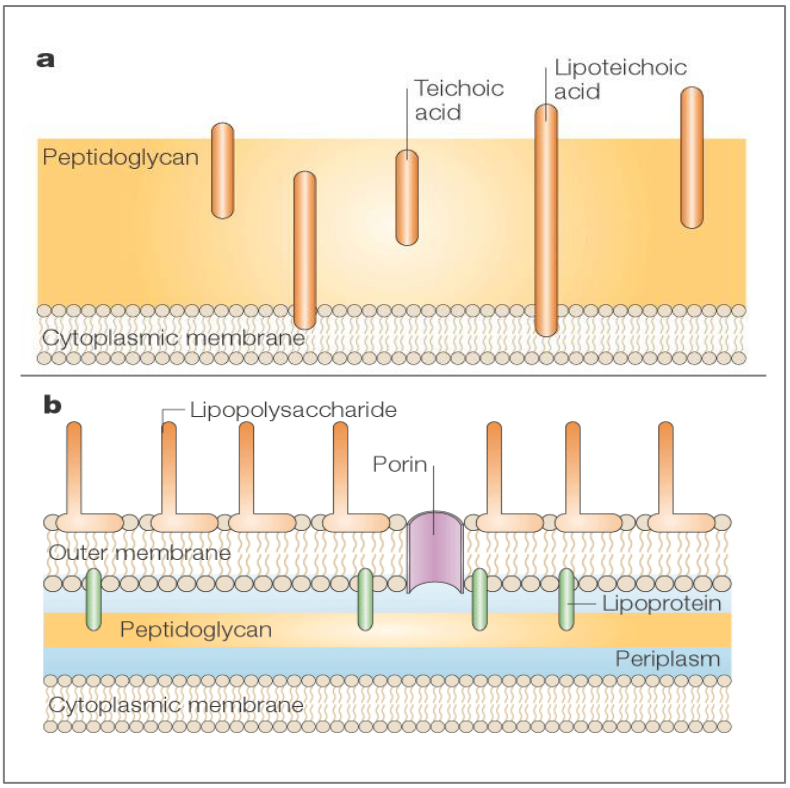

Fig. 1.2: Cell wall structure of **a**: Gram positive and **b**: Gram negative bacteria. (Reproduced from Cabeen and Jacobs-Wagner, 2005).

1.3.2 Gram Negative Bacteria

Gram negative bacterial cell walls (Fig. 1.2, B) also contain a PGN layer, however it is much thinner, usually 1-2 layers thick, and in some cases is a simple monolayer (Labischinski et al., 1991). Surrounding the PGN is a lipopolysaccharide (LPS) outer layer in which either lipoproteins or β-barrel proteins are embedded (Yount and Yeaman, 2013). *Escherichia coli* (*E. coli*) are thought to have over 100 lipoproteins embedded within their LPS layer, however their function is not characterised (Silhavy et al., 2010). Numerous β-barrel proteins have been identified, however few been demonstrated to be essential for bacteria. Deletion of outer membrane protein (OMP)-85 for example in *Neisseria meningitidis* results in a lack of lipids within the outer membrane layer demonstrating the role in OMP-85 in lipid transport (Genevrois et al., 2003).

1.3.3 Cell Wall Synthesis

The bacterial cell wall and its synthesis are targeted by antimicrobials such as β-lactam antibiotics (e.g. penicillin). PGN is the cellular wall component which provides strength and rigidity (Cabeen and Jacobs-Wagner, 2005). This layer is formed by alternating N-acetylglucosamine and N-acetylmuramic acid molecules, linked by peptidyl bridges (Lovering et al., 2012). The cellular synthesis of PGN is highly complex (Fig. 1.3), involving numerous enzymatic reactions (Lovering et al., 2012).

Although PGN is found in both Gram negative and Gram positive cell walls, the major component within Gram negative species is LPS (Wang and Quinn, 2010). LPS molecules are comprised of three components; lipid A, core polysaccharides and O-antigen repeats (Wang and Quinn, 2010). Lipid A is located at the outer membrane and conveys the molecule's hydrophobicity. Both the core polysaccharides and O-antigen repeats are found on the surface of bacterial cells (Wang and Quinn, 2010). Whilst the PGN structure remains consistent between organisms of the same Gram classification, the LPS layers and the proteins embedded can vary greatly (Wang and Quinn, 2010). LPS is a vital structure of Gram negative organisms and its synthesis has been studied to potentially target as part of antibiotic therapy (Fig. 1.4). Disruption in the bacterial cell wall can be fatal for bacteria causing cell lysis, proving an ideal target for natural and synthetic antimicrobials.

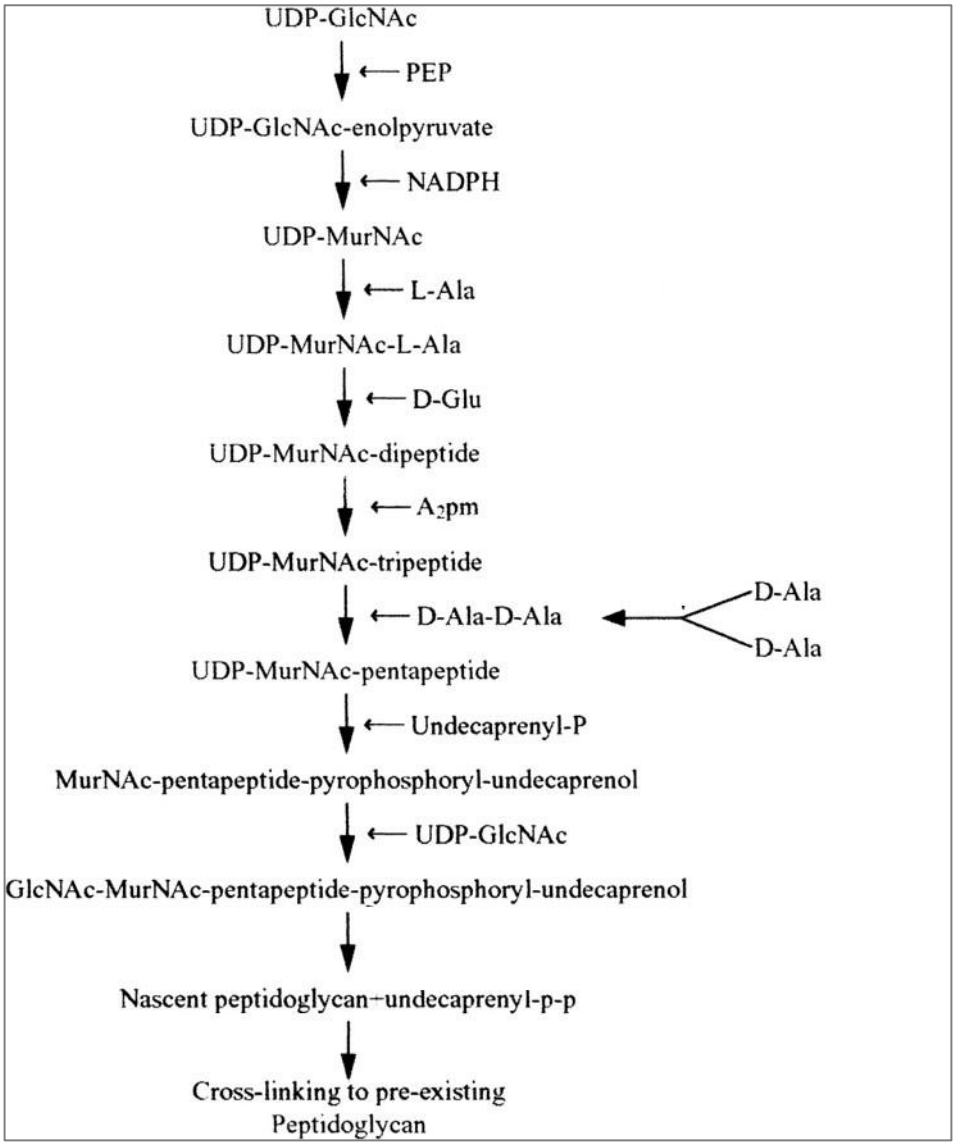

Fig. 1.3: PGN synthesis (Adapted from Katayama et al., 2003).

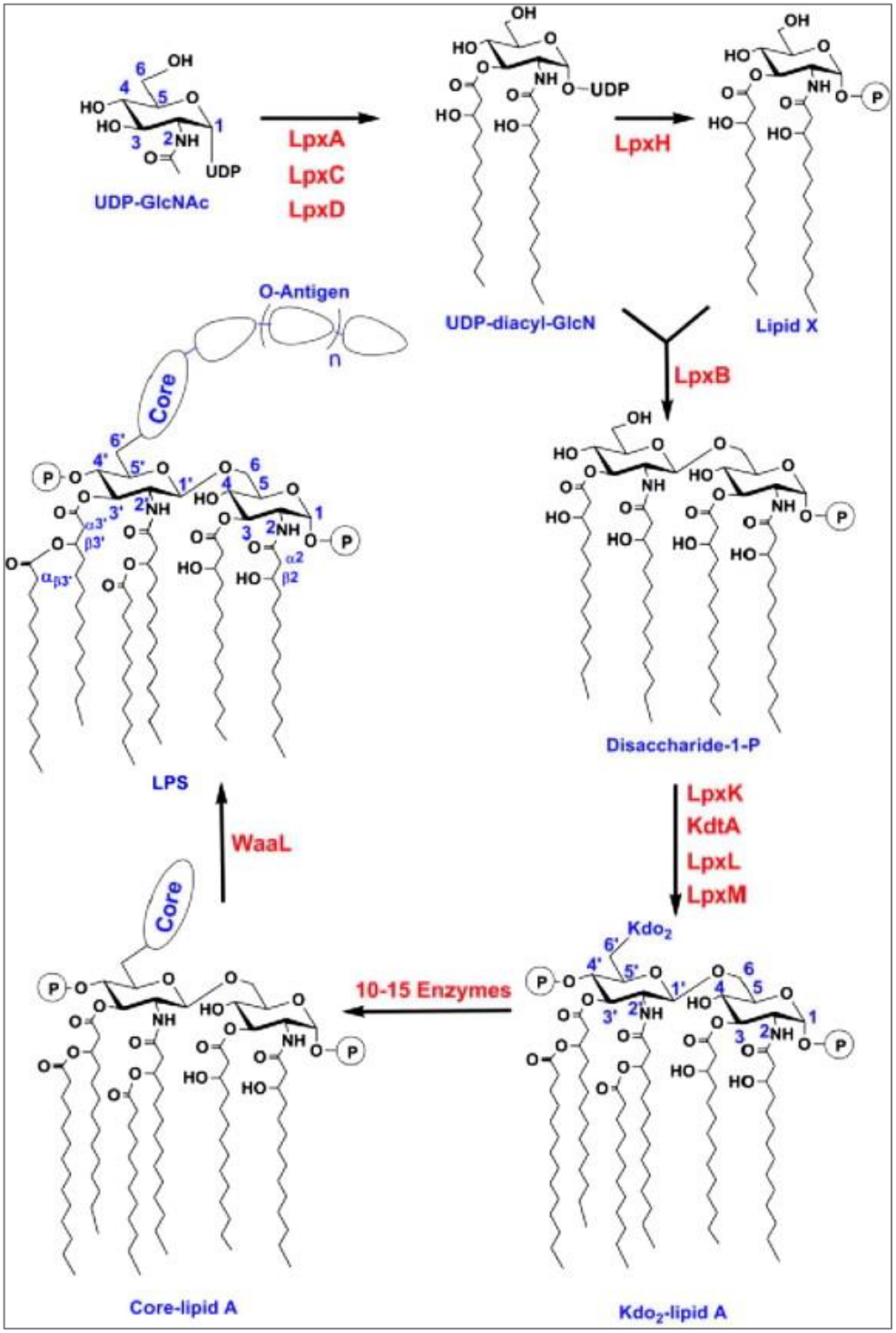

Fig. 1.4: LPS synthesis in *E. coli*. The enzymes for each reaction are shown in red (Reproduced from Wang and Quinn, 2010).

LPS synthesis commences in the bacterial cytoplasm from a uridine diphosphate -N-acetylglucosamine (UDP-GlcNAc) molecule. This molecule is converted into UDP-diacyl-GlcN by the addition of two 3-OH fatty acids chains, catalysed by the enzymes LpxA, LpxC and LpxD (Wang and Quinn, 2010). The hydrolysis of UDP-diacyl-GlcN by LpxH converts this molecule into Lipid X, which is then condensed along with residual UDP-diacyl-GlcN by LpxB to form disaccharide-1-P. The disaccharide molecule is then acted upon by several enzymes, which result in the formation of Kdo_2-lipid A. These enzymes include the kinases LpxK, Kdt, LpxL and LpxM (Wang and Quinn, 2010). The core polysaccharide portion of the LPS is then added to the Kdo_2-lipid A molecule at the inner membrane. The core polysaccharide is comprised of two sections; an inner core, which binds to the Kdo_2-lipid A molecule, and an outer core which connects to the O-antigen repeats. Once the LPS molecule is constructed, it is transported to the outer membrane by a range of enzymes such as LptA-G. The roles of these enzymes include transportation of LPS across the membrane and ensuring correct LPS assembly at the outer surface (Wang and Quinn, 2010).

1.4 Host Response to Bacterial Challenge

Rapid cellular recognition of pathogenic bacteria is vital to initiate immune system defences as quickly as possible. Antigen receptors on the surface of adaptive immune cells, such as B and T lymphocytes, recognise pathogens. These antigen receptors are specific for separate pathogens and depend on the memory of previous infections. However, it can take days to activate adaptive immune cells and carry out sufficient bacterial clearance. It is therefore essential that the host is able to initiate a more rapid defence mechanism. These defences are carried out through innate immune cells, targeting pathogens in a non-specific manner (Fournier and Philpott, 2005).

1.4.1 The Innate Immune System

The innate immune system results in the rapid release of inflammatory cytokines from cells such as neutrophils and macrophages. These cells also serve to phagocytose and kill invading pathogens (Fournier and Philpott, 2005). Residual components from the destruction of the pathogens are presented to cells of the adaptive immune system, which initiates the slower but more specific host defence.

1.4.1.1 Neutrophils

Neutrophils are recruited to sites of infection by interleukin (IL)-8 chemotaxis resulting in the phagocytosis of pathogens. Once phagocytised, pathogens are killed by reactive oxygen species (ROS) and reactive nitrogen species (RNS) produced by the neutrophils (Fialkow et al., 2007). Additionally, neutrophils release granule proteins and chromatin, which form fibres known as neutrophil extracellular traps (NETs). NETs can directly bind Gram positive and Gram negative bacteria, inducing bacterial killing (Brinkmann et al., 2004).

Neutrophils are recruited from the bone marrow during infection, where their life span is noticeably increased (Kim et al., 2011). Their mobilisation by the neutrophil recruitment cascade is a several stage process (Kolaczkowska and Kubes, 2013). During the initial step, neutrophils tether to the surface of endothelial cells within the blood vessels. Endothelial cells are primed for this adhesion by inflammatory mediators such as histamine, resulting in the increased surface expression of the adhesion molecules, P- and E-selectin. The neutrophils roll along the surface of the endothelial cells in the direction of the blood flow. Activation of neutrophils is induced during the rolling process and is facilitated by cytokines such as tumour necrosis factor (TNF)α and IL-1β. Once at the site of infection, neutrophils cease rolling and adhere to the endothelial cells. Chemokines, such as IL-8, provide a signal to the neutrophils to initiate the adhesion to the endothelial surface. Neutrophils migrate out of the vasculature into the site of infection through either a paracellular or transcellular mechanism. Paracellular migration involves neutrophils migrating between two endothelial cells at the cell-to-cell junction. Neutrophils can also migrate directly through an endothelial cell by transcellular migration, however this is less efficient (Burns et al., 2000). During this process endothelial cells send out micro-villi like projections which wrap around the neutrophils. Importantly, neutrophils are not internalised by endothelial cells, but are merely covered by and protected by the endothelium. The final stage is the migration of the neutrophils through the basement membrane, a process facilitated by their production of proteases, such as metalloproteinases (MMPs), which digest the ECM.

1.4.1.2 Monocytes

Monocytes have long been identified by their expression levels of CD14 and CD16 (Passlick et al., 1989). The primary subset of monocytes, termed classical monocytes, display a CD14+CD16- surface expression, making up 90% of the total

monocyte population. The remaining 10% of monocytes is comprised of cells with an expression profile of CD14+CD16+, so termed non-classical monocytes (Ziegler-Heitbrock and Hofer, 2013). The expression of these molecules gives some indication into their function. The ability for CD14 to acts as a co-receptor for toll-like receptor (TLR)4, facilitating LPS signalling is well reported (Wright et al., 1990). Whilst the function of CD16, an Fc receptor, is involved in innate immunity (Clarkson and Ory, 1988).

Classical monocytes can kill bacteria through the production of ROS and the action of phagocytosis (Serbina et al., 2008). Monocytes are recruited from the blood stream during infection and inflammation to affected tissues (Shi and Pamer, 2011). Non-classical monocytes are a major source of pro-inflammatory cytokines such as TNFα. It has been reported that the depletion of CD16+ cells from peripheral blood mononuclear cells (PBMCs) significantly reduces the TNFα secretion induced by LPS by 64% (Belge et al., 2002). In additional to TNFα, the production of IL-1β and a reduced phagocytic phenotype has been documented within the non-classical population of monocytes (Cros et al., 2010).

1.4.1.3 Macrophages

Macrophages are ubiquitous throughout human tissue however, distinct populations are evident within different anatomical locations. For example, microglia, macrophages of the brain, display a different molecular signature to macrophages originating from the spleen (Butovsky et al., 2014). Macrophage populations have a high degree of plasticity, changing their gene expression profiles in response to a range of stimuli. The activation of macrophages results in either M1 (classical activation) or M2 (alternatively activated) macrophage populations, with distinct phenotypes. Interferon (IFN)-γ, LPS or TNFα stimulation to monocyte precursors or tissue-resident macrophages classically activates the cells into an M1 phenotype, which are defined by the secretion of pro-inflammatory cytokines such as TNFα, IL-12 and IL-6. Alternative activation of cells by IL-4 or IL-10 for example, results in an anti-inflammatory M2 phenotype, defined by the secretion of cytokines such as IL-10 (Hume, 2015).

M1 and M2 macrophages have distinct roles with M1 macrophages involved in bacterial defences and M2 in parasite infections (Hume, 2015). Phagocytosis is decreased in M2 macrophages compared to the classically activated M1 population (Varin et al., 2010), with M1 macrophages mediating mycobacteria killing through

nitric oxide (Herbst et al., 2011). Additionally it has been documented that during tuberculosis infection M1 macrophages can induce autpphagy (Matsuzawa et al., 2012) whilst the M2 subset of cells decrease autophagy (Harris et al., 2007). It is thought that the M1 pro-inflammatory macrophages mediate the initial defence during bacterial infection through the induction of inflammation and phagocytosis, while the M2 macrophages predominate at a later stage in order to resolve the increased inflammation and prevent tissue damage (Sica et al., 2015).

1.4.1.4 Dendritic Cells

Dendritic cells (DCs) are phagocytic cells, which provide a link between the innate and adaptive immune system. Described as antigen presenting cells (APCs), DCs process and present antigens to T cells, activating the adaptive immune system (León et al., 2007, Hohl et al., 2009). In addition to the priming of T cells, DCs plays an important role within innate immunity by secreting inflammatory factors such as TNFα and IL-12 after LPS stimulation (Serbina et al., 2003).

DCs can be differentiated from both classical and non-classical monocytes (Sánchez-Torres et al., 2001), generating different phenotypic DCs. DCs originating from the non-classical expressing CD16 monocytes are capable of driving larger T cell responses (such as T cell activation) compared to the classical CD16- monocyte derived DCs (Bajaña et al., 2007).

1.4.2 Toll-like Receptors

TLRs are responsible for identifying pathogenic bacteria by recognising common bacterial motifs know as pathogen associated molecular patterns (PAMPs; Fournier and Philpott, 2005). There have been 10 TLRs identified in humans (Blasius and Beutler, 2010) with all reported to be expressed in the oral cavity (McClure and Massari, 2014). TLR1, 2, 4, 5, 6 and 11 are expressed on the surface of cells which are capable of recognising microbial molecules. The intracellular expression of TLR3, 7, 8 and 9 is found in cellular components such as lysosymes and endosomes, with the receptors adept at detecting microbial nucleic acid (Blasius and Beutler, 2010). The TLR recognition of bacteria is often dependent on the type of cell wall the bacterial organism displays, i.e Gram positive or Gram negative.

1.4.2.1 Gram Negative Bacterial Recognition by TLRs

LPS on the surface of Gram negative bacteria, can induce a response by the human innate immune system via TLR signalling. TLR4 can become activated by LPS via CD14 on the surface of monocytes. LPS is thought to bind to LPS-binding protein, which then binds CD14 (Wright et al., 1990). CD14 bound LPS activates TLR4, activating the nuclear factor kappa-light-chain-enhancer of activated B cells (NF-$_K$b) pathway (Fig. 1.5). Firstly, TLR4 associates with the adapter molecule Myd88 and IL-1 receptor associated kinase (IRAK), before IRAK dissociates and activates TNF receptor associated factor 6 (TRAF6; Heumann and Roger, 2002). The activation of TRAF6 results in activation of the NF-$_K$b pathway; promoting pro-inflammatory cytokine expression (Barton and Medzhitov, 2003) or the c-Jun N-terminal kinase/stress-activated protein kinase (JNK/SAP) pathway (Heumann and Roger, 2002). The apoptotic JNK/SAP pathway has been shown to be activated by Gram negative bacteria such as *Legionella pneumophila* (Welsh et al., 2004).

Yang *et al.* demonstrated that is it the lipid A portion of LPS which activates TLR2, with lipid A alone resulting in activation comparable with LPS. The lipid A activation of TLR2 can induce the NF-$_K$b pathway, resulting in the production of pro-inflammatory cytokines (Yang et al., 1998). Gene expression of TLR2 has been demonstrated in a large variety of lymphoid tissues such as the spleen and lymph nodes and peripheral blood leukocytes, such as macrophages (Yang et al., 1998). Gram negative bacterial infections vary in severity depending on the lipid A structure of the organism (Wang and Quinn, 2010). Some bacteria synthesise lipid A molecules which are not well recognised by the human immune system, such as *Helicobacter pylori* (*H. pylori;* Suda et al., 2001), *P. gingivalis* (Darveau et al., 2004) and *Chlamydia trachomatis* (Heine et al., 2003), which prevents the host from clearing the bacterial infection effectively. The structure of the lipid A molecule i.e. the number of phosphate groups and length of the fatty acids chains, dictates the degree of immune activation (Wang and Quinn, 2010). For example, *E. coli* is a potent activator of the innate immune system as it contains two phosphate groups and six fatty acids chains comprising of 12-14 carbons (Fig. 1.4). The oral pathogen, *P. gingivalis,* is known to activate TLR2. It has been reported that this activation of TLR2 leads to increased receptor activator of NF-κB ligand (RANKL) and therefore increased osteoclast formation. The increased osteoclast formation leads to increased bone resorption, resulting in bone loss (Kassem et al., 2015b).

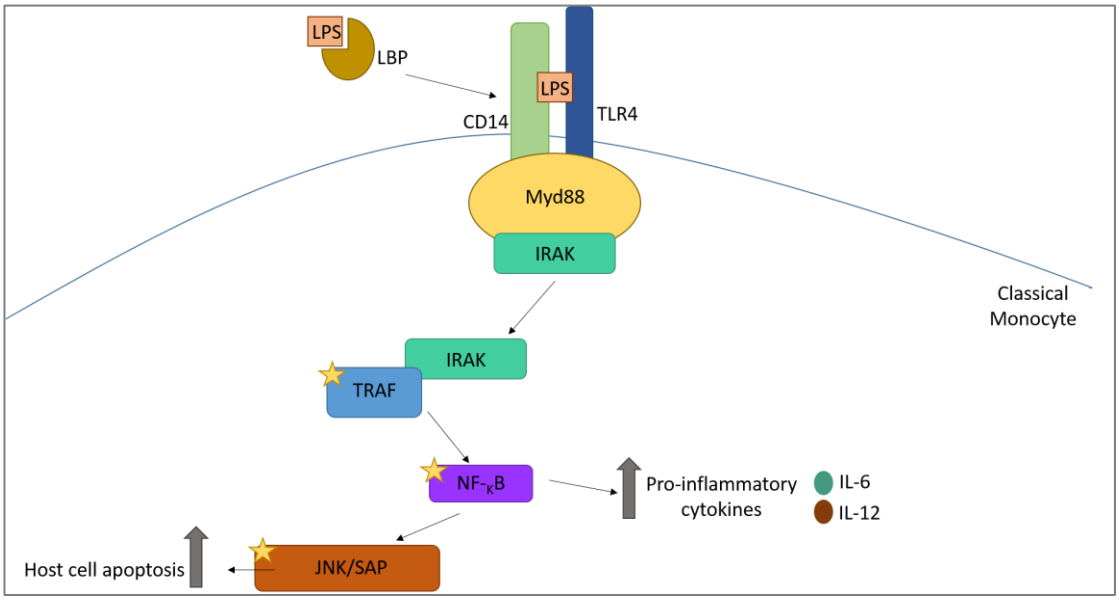

Fig. 1.5: LPS activation of the NF-$_k$B pathway. After binding to LPS binding protein, LPS forms a complex with CD14 causing a further association, with TLR4. This complex then interacts with Myd88 and IRAK, before IRAK dissociates to activate TRAF-6. The activation of TRAF-6 leads to the activation of the NF-$_k$B pathway which increases pro-inflammatory cytokine expression and cause the activation of the JNK/SAP pathway. The JNK/SAP pathway leads to apoptosis of host cells. Yellow stars represent the activation of components.

1.4.2.2 Gram Positive Bacterial Recognition by TLRs

It is widely accepted that TLR2 has a broad range of recognition, recognising bacterial lipoproteins and PGN from the Gram positive staphylococcal species (Yoshimura et al., 1999). Yoshimura *et al.* demonstrated that the pattern of TLR2 recognition was the same from whole *Staphylococcus aureus* (*S. aureus*) and the soluble PGN from the organism. Schröder et al., 2003 provided evidence that lipoteichoic acid (LTA) within the PGN layer of Gram positive species, in addition to PGN itself, activates TLR2 and subsequently the NF-$_k$B pathway. *In vivo* studies have supported the evidence that TLR2 is the vital receptor in Gram positive recognition. Takeuchi et al., 1999 demonstrated that TLR2 deficient mice did not respond to PGN, in addition to TLR2 deficient macrophages, which displayed an impaired response to Gram positive species. Whilst TLR4 is involved in Gram negative recognition, it is not thought to be involved in the recognition of Gram positive species. TLR4 deficient mice did not show any impairment or abnormal responses to PGN (Takeuchi et al., 1999).

1.4.2.3 Viral Recognition by TLRs

TLR3 is the major TLR involved in viral innate immunity. The receptor recognises the double stranded RNA produced by most viruses. The activation of TLR3 by viral RNA leads to the activation of the NF-$_k$B pathway through Myd88 signalling, resulting in the production of type 1 interferons (Alexopoulou et al., 2001). TLR7, 8 and 9 are also involved in viral innate immunity, with TLR7 and 8 able to recognise single stranded RNA, with the recognition of double stranded viral DNA provided for by TLR9. Similarly to the activation of TLR3, the activation for TLR7, 8 and 9 by viral nucleic acids leads to the activation of the NF-$_k$B pathway (Xagorari and Chlichlia, 2008). TLR2 and 4 have also been implicated in the innate recognition of viruses. Viral proteins from organisms such as the Epstein-Barr virus (Gaudreault et al., 2007) and respiratory syncytial virus (Kurt-Jones et al., 2000) have been reported to activate TLR 2 and 4 respectively.

1.4.2.4 Flagella Recognition by TLRs

Flagella are rod-like appendages, comprised of the molecule flagellin, which extend from the outer membrane of some bacteria. Flagellin is a bacterial virulence factor recognised by TLR5. Studies have shown that flagellin from both Gram positive and Gram negative bacteria are capable of activating TLR5, while depletion of the flagellin gene results in no TLR5 activation (Hayashi et al., 2001). Furthermore, the

induction of the flagellin gene in the non-flagellated *E. coli* results in activation of TLR5 (Hayashi et al., 2001). Activation of the receptor leads to NF-$_k$B dependant production of TNFα (Hayashi et al., 2001). In addition to cytokine production, it has been reported that flagellin activation of TLR5 leads to bone loss. The loss of bone demonstrated in murine bones was dependant on the increased RANKL: osteoprotegerin (OPG) ratio, which allows increased osteoclast (bone resorbing cells) formation leading to bone resorption/loss (Kassem et al., 2015a).

1.4.3 Other PAMP Receptors

TLRs are the major receptor family involved in the recognition of pathogens, however several other receptor groups have also been identified to play a role in pathogen recognition and innate immunity. Each of these receptor groups, like the TLRs, result in the activation of the NF-$_k$B pathway.

1.4.3.1 Nod-like Receptors

When activated, Nod-like receptors (NLRs) form inflammasomes, which are caspase activating complexes and facilitate pro-IL-1β maturation (Martinon et al., 2002). NLRs can be activated by a variety of stimuli such as ROS, muramyl dipeptides (mycobacterium cell wall component), flagellin, PGN and viral RNA (Claes et al., 2015), leading to activation of the NF-$_k$B signalling pathway (Silva et al., 2010).

1.4.3.2 RIG-I like Receptors

RIG-I like receptors (RLRs) play a role in anti-viral immunity. Activation of RLRs by viral RNA leads to NF-$_k$B activation and the production of type 1 IFN and the upregulation of antiviral gene expression (Yoneyama et al., 2004). The expression of RLRs is found on most mammalian cells at low levels. Expression levels of RLRs are greatly increased by type 1 IFN during viral infection (Kang et al., 2004, Imaizumi et al., 2005)

1.5 Antimicrobial Peptides

Antimicrobial peptides (AMPs) are cationic proteins which provide a first-line defence against infection (Guaní-Guerra et al., 2010). There are several groups of AMPs (see below). Whilst each class of AMPs differ in structure, they all share a fundamental principle that cationic and hydrophobic amino acids cluster in distinct domains

(Zasloff, 2002). This conveys the amphoteric nature of the molecules. It is thought that cationic AMPs interact with the negatively charged phospholipids on bacterial membranes (Guaní-Guerra et al., 2010), resulting in disruption to the bacterial membrane.

1.5.1 Mechanism of Action

Several methods of how AMPs disturb the bacterial membrane have been proposed (Fig. 1.6). Firstly, the barrel-stave method, where AMPs insert into the bacterial membrane, spanning the entire depth forming a pore. Similar to the barrel-stave method, the toroidal pore method sees the AMPs span the bacterial membrane, forming a pore. The main difference from the barrel-stave method is that the AMPs also associate with the bacterial lipids. The carpet model describes the AMPs coating the bacterial membrane, causing disruption to its structure. AMPs can also interact with the negatively charged bacterial membrane which causes a change in the electrical potential across the membrane in the molecular electroporation model. Finally, the sinking raft model describes when AMPs sink into the bacterial membranes causing the formation of pores, which leads to an increase in membrane permeability (Teixeira et al., 2012).

1.5.2 Cathelicidins

Cathelicidins can modulate the immune system in several ways. They can exert a direct chemoattractive effect on immune cells such as monocytes and $CD4^+$ T lymphocytes and are able to inhibit the transcription of pro-inflammatory cytokines. Cathelicidins are also capable of directly binding bacteria via LPS (Guaní-Guerra et al., 2010).

LL37 is an α-helical protein and the only human cathelicidin (Zanetti, 2005). It is formed from a precursor protein known as hCAP18 (human cathelicidin precursor; (Bowdish et al., 2005) and is cleaved by serine proteases to form the active LL37 (Zanetti, 2005). In sweat, LL37 can be further processed into smaller components which exert increased antimicrobial effects (Izadpanah and Gallo, 2005). LL37 constitutively expressed by cells such as monocytes, natural killer (NK) cells, B and T cells and within tissues such as newborn skin and respiratory epithelia (Zanetti, 2005). LL37 expression is also inducible in keratinocytes, nasal mucosal tissue,

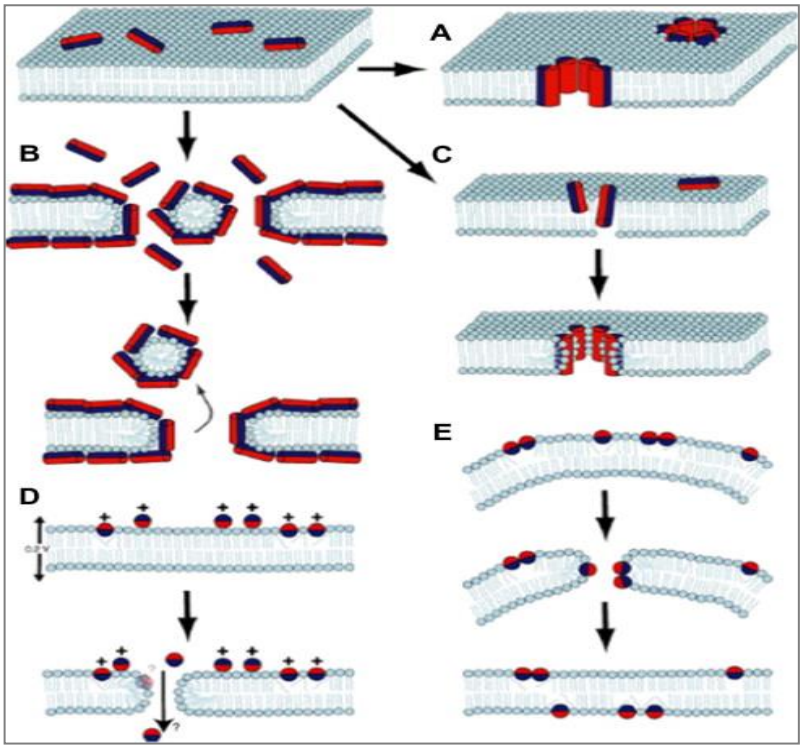

Fig. 1.6: AMPs and their mechanism of action. **A**: Barrel-stave model. **B**: Carpet Model. **C**: Toroidal Pore Model. **D:** Molecular Electroporation Model. **E**: Sinking Raft Model (Reproduced from (Teixeira et al., 2012).

synovial membranes (Zanetti, 2005) and salivary glands by inflammation (Woo et al., 2003) and the peptide is detected in the saliva and gingival crevicular fluid of the oral cavity (Gorr, 2009). The peptide has an array of functions including the direct killing of microorganisms, chemotaxis and wound healing. LL37 is capable of directly binding LPS, inhibiting the LPS induced cellular responses usually seen in infection (Zanetti, 2005), including the release of pro-inflammatory agents such as TNFα and IL-6 (Ngkelo et al., 2012).

LL37 has been demonstrated *in vitro* to provide an antimicrobial effect against Gram negative bacteria (such as *Pseudomonas aeruginosa* [*P. aeruginosa*]*, Salmonella typhimurium* and *E. coli* [Zanetti, 2005]) and Gram positive bacteria (such as *S. aureus, Staphylococcus epidermidis* [*S. epidermidis*] and vancomycin resistance *Enterococci* [Zanetti, 2005]). Although LL37 has demonstrated a wide range of antimicrobial effects, it has not been reported to be an active antifungal against organisms such as *Candida* (Zanetti, 2005). Recently, LL37 has been implicated in the antibacterial effects of bone marrow derived mesenchymal stem cells (BM-MSCs; Krasnodembskaya et al., 2010). It is thought that upon exposure to both Gram positive and Gram negative bacteria, BM-MSCs release LL-37, which provides its direct effects on the microorganisms (Krasnodembskaya et al., 2010). The authors demonstrated that conditioned media (CM) from the BM-MSCs exposed to bacteria decreased the growth of bacteria, which was reversed when the medium was supplemented with an LL37 neutralising antibody.

The dysregulation in oral LL37 is associated with some periodontal diseases. Patients with Morbus Kostman disease, which results in severe periodontitis, are deficient in saliva LL37 (Pütsep et al., 2002). Papillion-Lefèvre syndrome is another condition characterised by severe periodontitis. The syndrome is associated with a deficiency in the serine proteases which cleave hCAP18 into the antimicrobial LL37 peptide. Whilst normal levels of hCAP18 precursor are produced, a limited amount is converted into the active LL37 (de Haar et al., 2006).

It has also been reported that LL37 can aid in the wound healing process. One study demonstrated that in a mouse model of full thickness excisional wounds, encapsulated LL37 decreased the wound closure time by inducing cell migration at the wound site (Chereddy et al., 2014). The expression of IL-6 and vascular endothelial growth factor (VEGF), factors essential to wound healing progression, were found to be increased within the wound tissue in response to the encapsulated

LL37 treatment (Chereddy et al., 2014). Increased expression of VEGF has also been documented in dental pulp cells and periodontal ligament cells after LL37 treatment (Khung et al., 2014, Kittaka et al., 2013). These studies suggest that in addition to its well-known antimicrobial properties, LL37 may also demonstrate wound healing properties.

1.5.3 Defensins

Defensins are peptides of 3.5-4.5 KDa and roughly 30 amino acids in length. They contain an antimicrobial c-terminal and have been found to be involved in the oxygen-independent killing of phagocytosed organisms (De Smet and Contreras, 2005). Defensins are also chemoattractants for immune cells such as monocytes and T lymphocytes (Guaní-Guerra et al., 2010). Defensins contain six cysteine residues, which are highly conserved and form disulphide bonds stabilising the defensin structure (Guaní-Guerra et al., 2010). Human defensins can be divided into two major groups depending on the disulphide bond arrangment: α-defensins and β-defensins.

1.5.3.1 Alpha-defensins

Six α-defensins have been identified in humans, four of which are constitutively expressed in neutrophil granules. These defensins are referred to as human neutrophil peptides (HNP) 1-4 (Guaní-Guerra et al., 2010). HNP1-4 display broad spectrum antibacterial properties against Gram positive and Gram negative bacteria (Ericksen et al., 2005), in addition to antiviral effects against adenoviruses (Smith et al., 2010). These peptides are also chemoattractants and can cause the down regulation of pro-inflammatory cytokine expression (Guaní-Guerra et al., 2010).

Human defensins (HD) 5 and 6 are constitutively expressed in Paneth cells of the small intestine. HD5 displays antibacterial properties against both Gram positive and Gram negative bacteria (Ericksen et al., 2005), whereas it was thought HD6 was not antibacterial. However, by mimicking the intestinal environment, studies have demonstrated that HD6 displays antibacterial activity against commensal bacteria of the gut (Schroeder et al., 2015). Within the oral cavity, α-defensins are found within the saliva (HNP1, 2, 3) and gingival crevicular fluid (HNP1, 2, 3, 4; Gorr, 2009).

1.5.3.2 Beta-defensins

There have been six β-defensins identified in humans, hBD1-6 (Guaní-Guerra et al., 2010), with hBD1-4 more extensive studied. β-defensins are larger than the α-defensins, approximately 40 amino acids in length, and are produced primarily by epithelial cells (Guaní-Guerra et al., 2010).

Table 1.1 demonstrates the anatomical distribution of each β-defensin's expression. These AMPs display a broad spectrum of antimicrobial activity against organisms such as Gram positive bacteria, Gram negative bacteria, yeast and some viruses (Dale and Fredericks, 2005). β-defensins also play a role in the immunomodulatory effects following bacterial invasion by inducing the production of inflammatory cytokines such as TNF-α and IL-1 in keratinocytes (Guaní-Guerra et al., 2010). Human BDs -1, -2 and -3 are detected in the oral fluids such as saliva and gingival crevicular fluid (Gorr, 2009), with the supressed levels of hBD-1 and -2 within the saliva associated with oral candidiasis (Tanida et al., 2003).

1.5.4 Lipocalin-2

The major expression of the Lipocain-2 gene is found within neutrophils, with lower expression reported in the renal tubular cells and hepatocytes (Cowland and Borregaard, 1997). Lipocalin-2 is released at sites of infection by neutrophils and functions to sequester the bacterial siderophores (bacterial iron-binding compounds; (Goetz et al., 2002). This action of lipocalin-2 prevents iron-chelation by microorganisms resulting in iron-deprived bacteria. The growth of *E. coli* is inhibited 20-fold in the presence of lipocalin-2, which can be reversed by the addition of iron (Goetz et al., 2002). *In vivo* studies have demonstrated that lipocalin-2-deficient mice display greater bacterial infection compared with control mice (Flo et al., 2004).

1.5.5 Adrenomedullin

Adrenomedullin (ADM) is a cationic peptide containing one disulphide bond. It is proteolytically generated from a 185 amino acid pro-form into the mature 52 amino acid ADM (Khurshid et al., 2015). The peptide is detected in human saliva (Kapas et al., 2004) and gingival crevicular fluid (Lundy et al., 2006) and possesses diverse antibacterial properties. ADM displays antibacterial activity against Gram positive bacteria such as *S. epidermidis* and Gram negative bacteria such as *Pseudomonas* species (Gröschl et al., 2009). Gröschl et al. further demonstrated no antifungal activity of ADM against *C. albicans* (Gröschl et al., 2009).

Table 1.1: β-defensin distribution (Guaní-Guerra et al., 2010).

β - defensin	Area of AMP production	Expression	Antimicrobial activity	References
hBD1	Epithelial cells of the respiratory and urinary tracts	Constitutive	*Staphylococcus aureus*[1] *Escherichia coli*[1] *Enterococcus faecalis*[2] *Candida albicans*[3] *Candida krusei*[3] *Candida parapsilosis*[3]	(Chen et al., 2005)[1] (Lee and Baek, 2012)[2] (Aerts et al., 2008)[3] (Harder et al., 2000)[4]
hBD2	Skin and urinary, gastrointestinal & respiratory epithelia	Inducible by IL-1α, IL-1β, TNFα, IFNγ, LPS	*Pseudomonas aeruginosa*[4] *Staphylococcus aureus*[1] *Escherichia coli*[1] *Entercoccus faecalis*[2] *Candida albicans*[3] *Candida krusei*[3] *Candida parapsilosis*[3]	
hBD3	Skin and found in saliva	Inducible	*Staphylococcus aureus*[1] *Escherichia coli*[1] *Entercoccus faecalis*[2] *Candida albicans*[3] *Candida krusei*[3] *Candida parapsilosis*[3]	
hBD4	Testicles, stomach and uterus	Inducible	*Enterococcus faecalis*[2]	
hBD5 hBD6	Epididymis			

1.5.6 Statherin

Statherin is a 5.4kDa cationic peptide secreted by parotid and submandibular glands (Isola et al., 2008) and is found in saliva (Wilmarth et al., 2004) and gingival crevicular fluid (Pisano et al., 2005). Statherin displays antibacterial activity against anaerobic bacteria isolated from the oral cavity such as *Peptostreptococcus* strains (Kochańska et al., 2000) and the fungus *C. albicans* (Johansson et al., 2000).

1.5.7 C-C motif ligand 28 (CCL28)

CCL28 is a peptide comprised of 128 amino acids secreted by salivary glands and detected in saliva (Khurshid et al., 2015). It has been reported that human CCL28 demonstrates a diverse antimicrobial activity against the fungus *C. albicans* in addition to Gram positive bacteria (*S. mutans, Streptococcus pyogenes* [*S. pyogenes*] and *S. aureus*) and Gram negative bacteria (*P. aeruginosa* and *Klebsiella pneumoniae* [*K. pneumoniae*]; (Hieshima et al., 2003).

1.5.8 Azurocidin

Azurocidin is a 37KDa cationic peptide expressed in azurophil granules of neutrophils (Khurshid et al., 2015). Azurocidin displays potent antibacterial activity against Gram negative bacteria, potentially due to its affinity to LPS (Linde et al., 2000). Additionally, azurocidin can act as a chemoattractant to monocytes and macrophages leading to enhanced phagocytosis of microorganisms by these immune cells (Soehnlein and Lindbom, 2009).

1.5.9 Neuropeptides

The two neuropeptides, calcitonin gene related peptide and substance P, are both detected in human gingival crevicular fluid (Awawdeh et al., 2002) and saliva (Dawidson et al., 1997), whilst within the oral cavity neuropeptide Y and vasoactive intestinal peptide are exclusively found in saliva (Dawidson et al., 1997). These neuropeptides display diverse antimicrobial activities against the fungus *C. alibicans,* Gram positive bacteria *E. coli, S. mutans* and *Enterococcus faecalis (E. faecalis*), and Gram negative bacteria *P. aeruginosa* and *Lactobacillus acidophilus* (El Karim et al., 2008). *S. aureus* is not susceptible to any of these neuropeptides (El Karim et al., 2008).

1.5.10 Therapeutic Use of AMPs

Cationic AMPs have been identified in leukocytes and other host cells in most species. Their antimicrobial functions, which are often directed at multiple microorganisms, provides a foundation for developing AMP based therapeutics (Devocelle, 2012). AMP therapies can be used alone or in combination with antibiotics (Marr *et al*., 2006), providing a synergistic antimicrobial effect (Devocelle, 2012). Whilst they display antimicrobial actions, they also demonstrate immunomodulatory properties such as modulating cytokine release (Zanetti, 2005). For example, it has been demonstrated that LL37 can act as a chemoattractant for immune cells such as mast cells (Bąbolewska and Brzezińska-Błaszczyk, 2015). Additionally, LL37 has been reported to decrease the production of the pro-inflammatory cytokines TNFα and IL-17, while increasing the anti-inflammatory factors IL-10 and transforming growth factor (TGF)β in mycobacteria infected macrophages (Torres-Juarez et al., 2015). This demonstrates the ability of LL37 to modulate macrophages during infection. Maturation of langerhans cell-like DCs is potently induced by hBD3. Furthermore the expression of c-c chemokine receptor type 7 (CCR7), a mediator of chemotactic responses, is increased on the surface of langerhans cell-like DCs by hBD3 (Ferris et al., 2013).

However, there are some obstacles, which must be overcome to ensure a positive outcome for AMP therapy. AMPs are rapidly degraded or excreted, resulting in a need for high initial doses to maintain therapeutic levels. This raises concerns regarding AMPs reaching toxic levels (Devocelle, 2012). If administrated orally, the peptides will encounter hydrolytic enzymes such as pepsin and trypsin through the digestive system. Similarly, if administered intravenously, proteases in the blood can also cause proteolytic degradation of the peptides (Haney and Hancock, 2013). Modifying AMPs to incorporate non-natural D-isomers of amino acids can alter the stereochemistry of the peptides, decreasing their susceptibility to proteases (Haney and Hancock, 2013).

This has led to the development of synthetic AMPs as therapeutic agents, which are produced to provide effective antimicrobial action against a specific organism, whilst displaying low toxicity in humans at the therapeutic index (Fjell et al., 2012). There are currently over 15 different peptide-based therapies in clinical trials for anti-infective and anti-inflammatory actions (Table 1.2; Devocelle, 2012).

Table 1.2: Antimicrobial peptides in clinical trials, (Adapted from (Fjell et al., 2012).

Name	Description	Application	Trial Phase	Comments
Pexignan	Derived from frog skin	Topical antibiotic	III	No advantage over current therapies
Omiganan	Cationic – derived from indolicidin	Topical antiseptic for the prevention of catheter infections	III	Efficacy shown
Omiganan	Cationic – derived from indolicidin	Acne	II/III	Efficacy shown
Iseganan	Derived from protegrin-1	Oral mucositis in patients undergoing radiation therapy	III	No advantage over current therapies
Hlf1-11	Cationic- derived from lactoferrin	Bacteraemia & fungal infections in immunocompromised patient who have had haematopoietic stem cell transplants	I/II	Efficacy shown
XOMA 629	Derived from a bactericidal permeability-increasing protein	Impetigo	IIA	-
PAC-133	Derived from histatin -3 and -5	Oral candidiasis	IIB	Efficacy shown
CZEN-002	Derived from α-melanocyte-stimulating hormone	Vulvovaginal candidiasis	IIB	Efficacy shown
OP-145	Derived from LL-37	Chronic middle-ear infections	II	Efficacy shown
Ghrelin	Endogenous host-defence peptide	Chronic respiratory infection and cystic fibrosis	II	Inflammation suppression
PMX-3006	Mimetic of defensin	*Staphylococcus species* skin infections	II	-
Delmitide	Derived from HLA 1	Inflammatory bowel disease	II	Efficacy similar to other therapies
Plectasin	Fungal defensin	Microbial diseases	Pre-clinical	Excellent efficacy in animal models
HB1345	Synthetic lipohexapeptide	Acne	Pre-clinical	Promising pre-clinical studies

The majority of synthetic peptide therapies in clinical trials remain in phase II demonstrating efficacy against a range of applications such as acne, impetigo, oral candidiasis and chronic middle-ear infection (Devocelle, 2012). A synthetic peptide derived from LL-37, OP-145, has completed phase II clinical trials, demonstrating proof of efficacy against chronic bacterial mid-ear infection (Clinical trial reference number: ISRCTN84220089; (Fjell et al., 2012). Other synthetic peptides have progressed further into phase III trials. Omiganan, a peptide trialled as a topical antiseptic against catheter infections and acne treatment, has shown efficacy (Clinical trial reference numbers: NCT00231153; https://clinicaltrials.gov/ct2/show/NCT00231153?term=NCT00231153&rank=1 and NCT00608959; https://clinicaltrials.gov/ct2/show/NCT00608959?term=NCT00608959&rank=1 (ClinicalTrials.gov). Omiganan, as a topical gel, had previously been shown *ex vivo* to express potent antimicrobial activity against Gram negative bacteria, Gram positive bacteria and yeast in a dose-dependent manner (Rubinchik et al., 2009). While Omiganan demonstrated positive results in phase II/III trials, Pexigana, a synthetic peptide derived from frog skin, has not demonstrated any advantage over currently used therapies as a topical antibiotic (Clinical trial reference numbers: NCT00563433; https://clinicaltrials.gov/ct2/show/NCT00563433?term=NCT00563433&rank=1 and NCT00563394; https://clinicaltrials.gov/ct2/show/NCT00563394?term=NCT00563394&rank=1 (ClinicalTrials.gov).

1.5.11 Antimicrobial peptide resistance

The antimicrobial activity of AMPs has been maintained over millions of years with very little bacterial resistance documented (Peschel and Sahl, 2006). AMPs target fundamental structures within bacterial cells, which are too costly to compromise in order to develop resistance (Gallo et al., 2002). For bacteria to display resistance to all AMPs, bacteria would need to redesign their membrane ensuring differences were conveyed in the composition (Zasloff, 2002). This is a pursuit too great for bacteria to undertake. However, several resistance mechanisms are displayed by bacteria to overcome the action of AMPs (Fig. 1.7). Partial resistance has been conveyed by bacteria, such as *S. aureus* and group A *Streptococcus* (Gallo and Nizet, 2008) by decreasing their membrane negative charge, preventing the binding of AMPs (Izadpanah and Gallo, 2005). Bacteria have also developed a proteolytic degradation resistance method. This type of resistance involves bacteria producing peptidases and proteases which aim to cleave linear AMPs such as LL37 (Peschel and Sahl, 2006). *S. pyogenes* and *P. gingivalis* are examples of bacteria which produce such

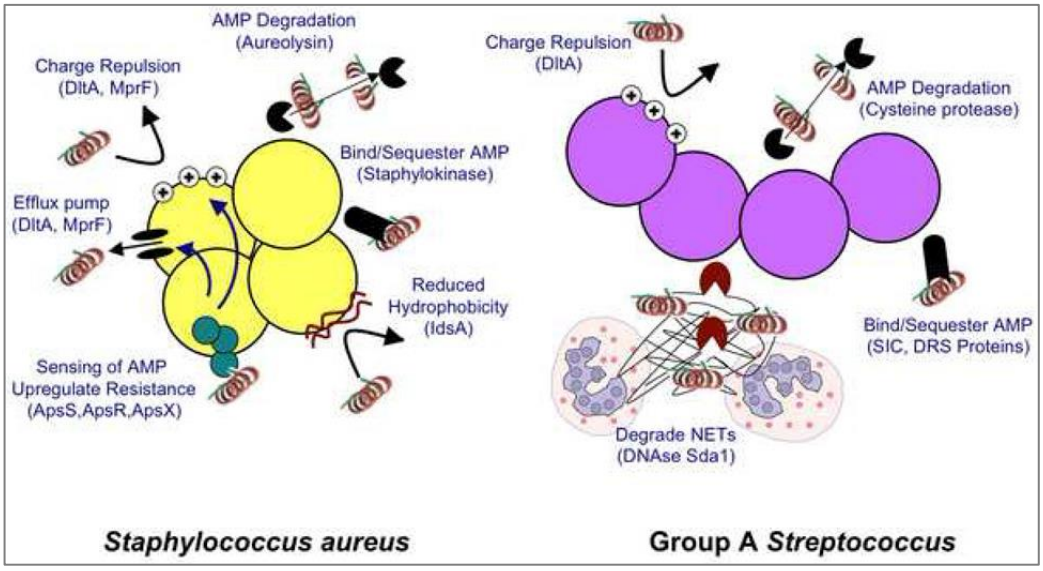

Fig. 1.7: Bacterial mechanisms to convey AMP resistance. Bacteria can decrease their negative charge to prevent AMP binding, release enzymes which cause the degradation of AMPs, sequester AMPs to prevent AMP action and express efflux pumps which actively pump AMPs out of bacterial cells. (Reproduced from (Gallo and Nizet, 2008).

enzymes (Peschel and Sahl, 2006). The addition of disulphide bonds to an AMP structure can increase the peptide's resistance to proteolytic degradation. *S. aureus* has also developed an exoprotein, staphylokinase, which binds and inactivates α-defensins, while *Neisseria gonorrhoeae* and *Neisseria meningitides* express a multidrug exporter, of which LL37 is a substrate (Peschel and Sahl, 2006).

1.6 Antimicrobial Proteins

Antimicrobial proteins provide an additional component to the innate immune system, which act to reduce bacterial infection. They often co-exist with AMPs leading to speculation that they may act synergistically. These proteins demonstrate antimicrobial activity by either degrading a specific cellular component of the microorganism or limiting a vital compound needed for the microorganism's survival (Janeway et al., 2005).

1.6.1 Histatins

Histatins are histidine-rich proteins present within human saliva, playing a vital role in limiting oral infections (De Smet and Contreras, 2005). The major histatins are histatin-1, -3 and -5, with all other histatins existing as degradation products of these. Histatins provide anti-fungal activity against *Candida* (Dale and Fredericks, 2005) in addition to antibacterial effects (De Smet and Contreras, 2005). They are thought to exert their antimicrobial actions via bacterial membrane independent methods. Histatin-5 enters the microbial cells by binding to a 67KDa histatin-binding protein found in bacterial membranes (Edgerton et al., 1998), resulting in cessation of the bacterial cell cycle. Cell respiration is inhibited, depleting adenosine triphosphate (ATP) and the formation of ROS is seen (De Smet and Contreras, 2005). The antifungal activity of histatin-5 is mediated through the protein's ability to penetrate the cells of pathogens, disrupting intracellular processes such as mitochondrial ATP production (Luque-Ortega et al., 2008). Studies have demonstrated that the level of histatins in patient saliva is negatively associated with levels of *Candida* (Sugimoto et al., 2006). Histatin-5 has been reported to decrease *C. albicans* growth within human oral epithelium and reduce host cell apoptosis (Moffa et al., 2015), demonstrating the ability of histatin-5 to reduce *C. albicans* colonisation within the oral cavity.

1.6.2 Indolamine 2,3-dioxygenase

Indolamine 2,3-dioxygenase (IDO) is the rate limiting enzyme involved in tryptophan degradation. It is induced by IFNγ in several cells such as macrophages, fibroblasts

(Hucke et al., 2004), some stem cell populations (Meisel et al., 2004, Davies et al., 2012) and by LPS to display its antibacterial properties (O'Connor et al., 2009). The action of IDO at the site of infection leads to a depletion in the essential amino acid tryptophan; causing an inhibition of the growth of tryptophan-dependant microorganisms (Hucke et al., 2004). Such microorganisms affected include the pathogenic bacteria *B streptococci*, *Enterococci* (Hucke et al., 2004) and *S. aureus* (Schroten et al., 2001). IDO has been reported to provide protection against bacterial infection in human heart valve and vascular allografts (Saito et al., 2008). The allografts displayed a reduced proliferation of methicillin-resistant *S. aureus*, mediated by the induction of IDO.

IDO has also been demonstrated to act in an immunomodulatory capacity. It has long been reported that T cells are not capable of proliferating in a tryptophan deficient environment (Munn et al., 1999); therefore the depletion of tryptophan by IDO suppresses T cell proliferation, limiting the immune response. However, further studies have demonstrated that the metabolites generated by IDO result in selective apoptosis of T helper (Th)1, but not Th2, cells (Fallarino et al., 2003).

The expression of IDO has been noted in several stem cell populations. Wada *et al.,* reported that upon IFNγ stimulation, periodontal ligament stem cells, BM-MSCs and dental pulp stem cells significantly increased the expression of IDO. OMLP-PCs also demonstrate increased IDO expression upon exposure to allo-activated lymphocytes in addition to IFNγ (Davies et al., 2012). It was further noted that these stem cell populations significantly decreased the proliferation of PBMCs in transwell experiments (Wada et al., 2009, Davies et al., 2012). These experiments demonstrated that the immunosuppressive properties of these stem cells are conveyed in part by a contact-independent manner, utilising soluble factors such as IDO (Wada et al., 2009). Several other studies have also reported IDO expression in BM-MSCs upon IFNγ stimulation, which mediates the cell's ability to inhibit T cell proliferation (Meisel et al., 2004, Ryan et al., 2007). This IDO-mediated theory has been confirmed by the restoration in T cell proliferation with the addition of the IDO antagonist 1-methyl-L-tryptophan (English et al., 2013).

IFNγ-induced IDO can be increased by the pro-inflammatory cytokines TNF-α and IL-1 (Nisapakultorn et al., 2009, Shirey et al., 2006). Both TNF-α and IL-1β have been found at elevated levels in chronic periodontitis (Graves and Cochran, 2003), which has led to the notion that these cytokines cause further activation of IDO thereby

preventing an excessive immune response (Nisapakultorn et al., 2009). A similar theory of IDO-induced protection in periodontitis has also been proposed by Konermann et al., 2012. The IDO expression in human periodontal ligament cells was seen to increase when exposed to inflammatory cytokines, specifically IFNγ and IL-1β by real-time PCR. It was proposed that periodontal ligament cells counteract the immune response in periodontitis by upregulating IDO.

1.6.3 Lysozyme

Lysozyme is 1,4-β-N-acetylmuramidase, which targets the PGN in bacterial cell walls. Lysozyme degrades the linkages between the N-acetylglucosamine and N-acetylmuramic acid molecules within the PGN, compromising its structure (Ellison and Giehl, 1991). Due to the mechanism of action, Gram positive bacteria, with exposed PGN, are highly susceptible to lysozyme. Gram negative bacteria however, are reasonably resistant to lysozyme, as their PGN layer is not exposed and the lysozyme is unable to penetrate the outer membrane (Ellison and Giehl, 1991). Lysozyme is one of the dominant proteins found in human breast milk, providing antibacterial protection to an infant (Lönnerdal, 2003) and is additionally found within the fluids of the oral cavity such as saliva and gingival crevicular fluid (Gorr, 2009).

1.6.4 Lactoferrin

Lactoferrin binds with high affinity to iron, a vital compound for bacteria (Ellison and Giehl, 1991). The chelation of iron by lactoferrin deprives bacteria of this essential compound. Bacterial biofilm formation by *P. aeruginosa* and *B. cepacia* has been shown to be stimulated by iron (Berlutti et al., 2005). Therefore, it has been suggested that lactoferrin chelation of iron inhibits the formation of bacterial biofilms (Jenssen and Hancock, 2009). It has also been proposed that enzymatic cleavage of lactoferrin results in antibacterial peptides, active against a range of bacteria including some resistant to the lactoferrin protein itself (Tomita et al., 1991). The activity of these antibacterial peptides was conserved in the presence of increased iron, unlike lactoferrin, suggesting an alternative mechanism to iron chelation. This is further supported by the lack of iron-binding residues in the peptide structures (Bellamy et al., 1992). These peptides, namely lactoferricin, have been shown to provide antibacterial protection against a range of bacteria such as *E. coli, K. pneumoniae, P. aeruginosa* and *S. aureus*. Lactoferricin treatment of the above bacteria significantly decreases the bacterial growth compared to bacterial cultures alone. It is thought the peptides act in a bactericidal manner as they cause the

viability of *E. coli* to rapidly decrease (Tomita et al., 1991). Levels of lactoferrin are detected in the saliva and gingival crevicular fluid of the oral cavity (Gorr, 2009)

Studies have shown that lactoferrin can provide lysozome with access to the PGN layer of Gram negative bacteria. Lactoferrin binds the LPS layer, removing it from the outer membrane (Ellison and Giehl, 1991). This allows lysozyme to degrade the linkages within the PGN layer, compromising the microorganism's structure.

1.6.5 Calprotectin

Calprotectin is a calcium binding protein found in the cytoplasm of neutrophils, which is also capable of binding zinc (Clohessy and Golden, 1995). It is found to be increased in inflammatory conditions and in bacterial invasion it's binding to zinc, a vital growth requirement for many microorganisms, is competitive thereby reducing the availability of this mineral to bacteria (Dale and Fredericks, 2005). Clohessy and Golden, 1995 demonstrated that calprotectin significantly inhibits the growth of the fungus *C. albicans.* This growth inhibition is reversed when zinc is supplemented into the culture medium, demonstrating the role of zinc chelation in calprotectin's mechanism of action. Calprotectin has also been shown to display antimicrobial effects against *S. aureus, S. epidermidis, E. coli* and *Klebsiella* species (Brandtzaeg et al., 1995).

1.6.6 Haptoglobin

Haptoglobin is an acute phase glycoprotein produced by the liver. It is formed from 2 alpha and 2 beta chains, with three possible isoforms; Hp1-2, Hp2-1 and Hp2-2 (Sadrzadeh and Bozorgmehr, 2004). The variation in isoforms is a result of differing alpha chain configurations, thereby determining the level of activity displayed by the protein. It is the alpha-1 chain which conveys the greatest activity, with the Hp1-1 isoform of haptoglobin demonstrating the highest activity level (Eaton et al., 1982).

Haptoglobin is known to be both antibacterial and immunomodulatory. It is the ability of haptoglobin to bind haemoglobin, causing depletion in iron, which gives the protein its antibacterial functions. Specifically, haptoglobin's antibacterial properties against iron-dependent *E. coli* have long been reported (Eaton et al., 1982). The production of TNFα and IL-12 by monocytes in response to LPS is suppressed by haptoglobin *in vitro* (Arredouani et al., 2005) and during inflammatory conditions, such as endometriosis, haptoglobin serum levels are elevated (Polak et al., 2015). This

demonstrates the potential anti-inflammatory effects of haptoglobin. For critically ill patients suffering with sepsis, an association between increased haptoglobin plasma concentrations and a decrease in mortality has also been reported (Janz et al., 2013). It is thought that haptoglobin binds excess free haemoglobin, preventing haemoglobin-induced tissue injury.

1.7 Osteoprotegerin

The main function of the glycoprotein OPG within bone remodelling process is well defined. OPG is a decoy receptor for RANKL. When bound to RANKL, OPG prevents the RANKL mediated osteoclast maturation, limiting the bone resorption phase of the bone remodelling process (Jin et al., 2015). The secretion of OPG from BM-MSCs has been reported, and it's role thought to be involved in the bone remodelling process described above (Oshita et al., 2011). OPG is detected within the oral fluids of the human oral cavity, and is reported to be decreased in patients with periodontitis (Bostanci et al., 2007, Mogi et al., 2004, Liu et al., 2003, Balli et al., 2015). However, each of the studies have analysed the data in relation to the RANKL:OPG ratio and its effect on bone remodelling. No study has investigated the potential involvement of OPG directly on periodontitis and bacterial infection.

TNF-related apoptosis-inducing ligand (TRAIL) is also a ligand for OPG and known to induce apoptosis (Chaudhari et al., 2006) and necrosis (Jouan-Lanhouet et al., 2012). The induction of apoptosis is mediated by the activation of death domain receptors -4 and -5 by TRAIL (Chaudhari et al., 2006) and suppressed by TRAIL binding of the decoy receptor OPG (Sandra et al., 2006). It has been reported that TRAIL decreases the OPG release from MSCs (Corallini et al., 2011), potentially through decreasing the phosphorylation of p38/mitogen-activated protein kinase (MAPK). It has been speculated that p38/MAPK may regulate OPG mRNA as a decrease in OPG by TRAIL can be mimicked by an inhibitor of p38/MAPK (Corallini et al., 2011).

OPG has also been implicated in modulatory aspects of the immune system, although no correlation as to an antibacterial effect has been reported. TRAIL-induced lymphocyte apoptosis is inhibited by OPG (Emery et al., 1998), whilst the regulation of B cell development is OPG dependent (Yun et al., 2001). OPG knock-out mice demonstrate disruptions in B cell populations with increased proliferative

capacity of pro-B cells and an accumulation of transitional B cell populations. OPG has also been reported to play a role in monocyte chemotaxis, inducing their migration in a dose-dependent manner; a process which is inhibited by blocking the receptor syndecan-1 (Mosheimer et al., 2005).

1.8 Prostaglandin E2

Prostaglandin E2 (PGE2) is a lipid produced by immune cells during inflammation (Agard et al., 2013). A number of immunomodulatory effects of PGE2 have been reported. Macrophage phagocytosis is inhibited by PGE2 in a dose-dependent manner (Aronoff et al., 2004), in addition to the inhibition of lymphocyte activation and proliferation (Kalinski, 2012) and NK cell proliferation (Sotiropoulou et al., 2006). A number of stem cell populations such as BM-MSCs (Aggarwal and Pittenger, 2005, Sotiropoulou et al., 2006) and the orally isolated periodontal ligament stem cells (Ding et al., 2010) and gingival stem cells (Su et al., 2011) have been reported to secrete PGE2 as an immunomodulatory mechanism. Both the BM-MSC mediated myeloid cell maturation and lymphocyte cell inhibition is dependent on the secretion of PGE2, with PGE2 blockade preventing these BM-MSC effects *in vitro* (Yañez et al., 2010). The production of PGE2 from BM-MSCs can be stimulated *in vitro* by direct co-culture with T lymphocytes. TNFα stimulation of BM-MSCs can further induce PGE2 production, with additional synergistic effects when in combination with IFNγ (Hegyi et al., 2012).

The production of PGE2 within the oral cavity has been associated with the periodontitis. Elevated levels of PGE2, up to an average of 83ng/ml, are reported in the gingival crevicular fluid of patients with periodontitis (Preshaw and Heasman, 2002). Furthermore, the inhibition of PGE2 production by the COX2 inhibitor Celeoxib reduced the symptoms of periodontitis. It has been reported that Celeoxib reduces gum bleeding after dental probing and improves tooth attachment, compared to a placebo in periodontal patients (Yen et al., 2008).

The synthesis of PGE2 is controlled by cyclooxygenase (COX) enzymes and is regulated by a number of inflammatory stimuli including the bacterial-derived stimuli LPS (Agard et al., 2013). Both the COX1 and COX2 enzymes can synthesise PGE2 from the precursor arachidonic acid (Fig. 1.8). Although the expression of COX1 is constitutive, the expression of COX2 is induced by inflammatory stimuli (Park et al.,

2006). While both Gram positive and Gram negative bacteria are known to induce PGE2 synthesis through COX2, higher levels are induced in macrophages by the Gram negative group of bacteria (Hessle et al., 2003). However, the direct effects of PGE2 on bacterial growth are not well known.

1.9 Stem Cells

Stem cells are defined by their self-renewal capacity and ability to differentiate into specialised cell types (Fagan, 2013)**.** Stem cells are found within embryonic tissues in addition to postnatal and adult tissues. Embryonic stem cells are found within the inner cell mass of a blastocyte during early embryonic development and are defined as pluripotent, with the potential to differentiate into each of the three germ layers (Fig. 1.9). After embryogenesis, most organs contain multipotent tissue-specific stem cell populations which maintain each organ throughout a lifetime (Nisbet 2004). It is the local environment, known as the stem cell nice, which dictates the self-renewal and differentiation properties of the tissue resident stem cells. After injury for example, signals within the stem cell niche initiate stem cell expansion and differentiation to replace damaged tissue (Sakaki-Yumoto et al., 2013). Adult stem cells are categorised into three groups; neural stem cells, mesenchymal stem cells (or mesenchymal stromal cells [MSCs]), and hematopoietic stem cells (Fig. 1.10). The neural stem cells give rise to cells on the central nervous system, whereas mesenchymal stem cells differentiate into cells of connective tissues. Hematopoietic stem cells are the cells which develop into the cells of the immune system such as neutrophils and T lymphocytes.

There is an ethical debate surrounding the use of embryonic stem cell for scientific research, as human embryonic stem cells are harvested during embryonic development, preventing further embryo growth (Westphal, 2002). Due to the debate surrounding embryonic stem cells, much research has shifted towards the use of

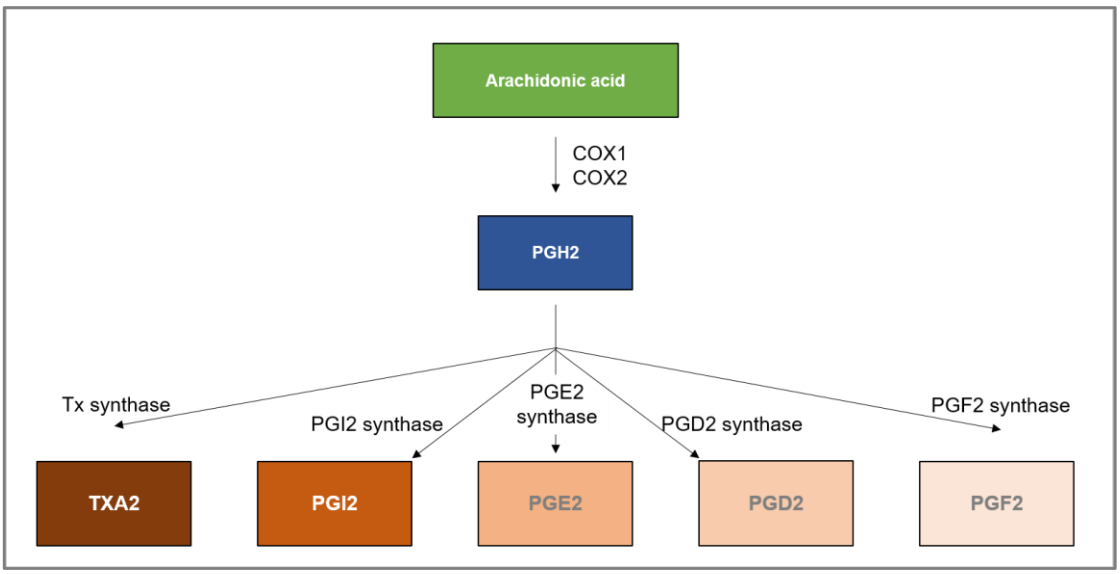

Fig. 1.8: Production of prostaglandins (PG) from Arachidonic acid. Arachidonic acid is metabolised by either COX1 or COX2 to form PGH2. The metabolism of PGH2 by thromboxane (Tx) synthase produces TXA2, while the metabolism by specific PG synthase enzymes results in the production of PGI2, PGE2, PGD2 and PGF2 (Wang and Dubois, 2006).

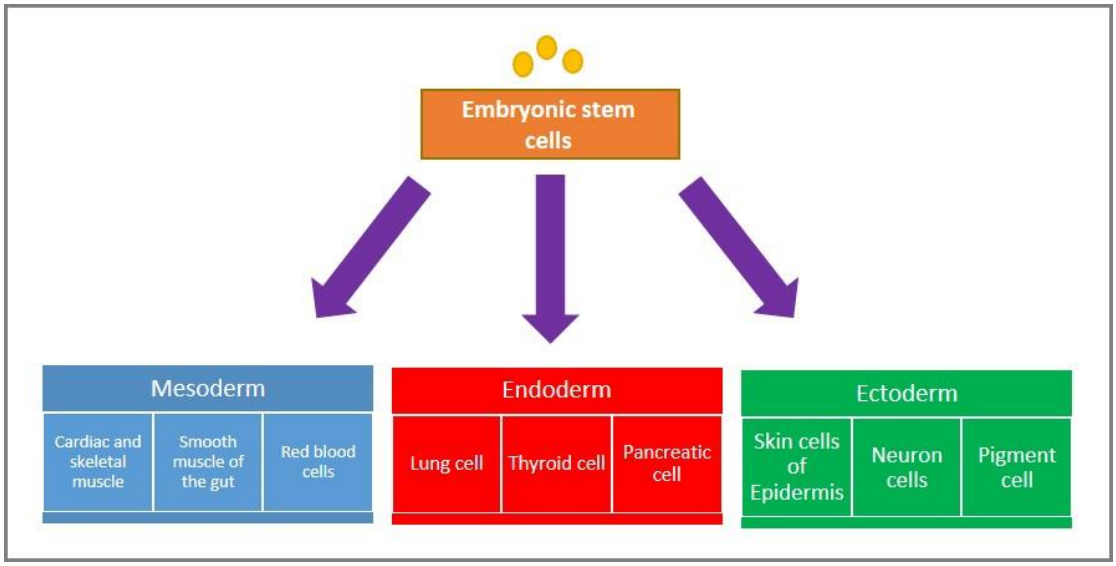

Fig. 1.9**:** Embryonic stem cell development. Embryonic stem cells differentiate to form all three germ layers; the mesoderm, endoderm and ectoderm. Each of these germ layers develops further into the specialised cells and tissues of the human body.

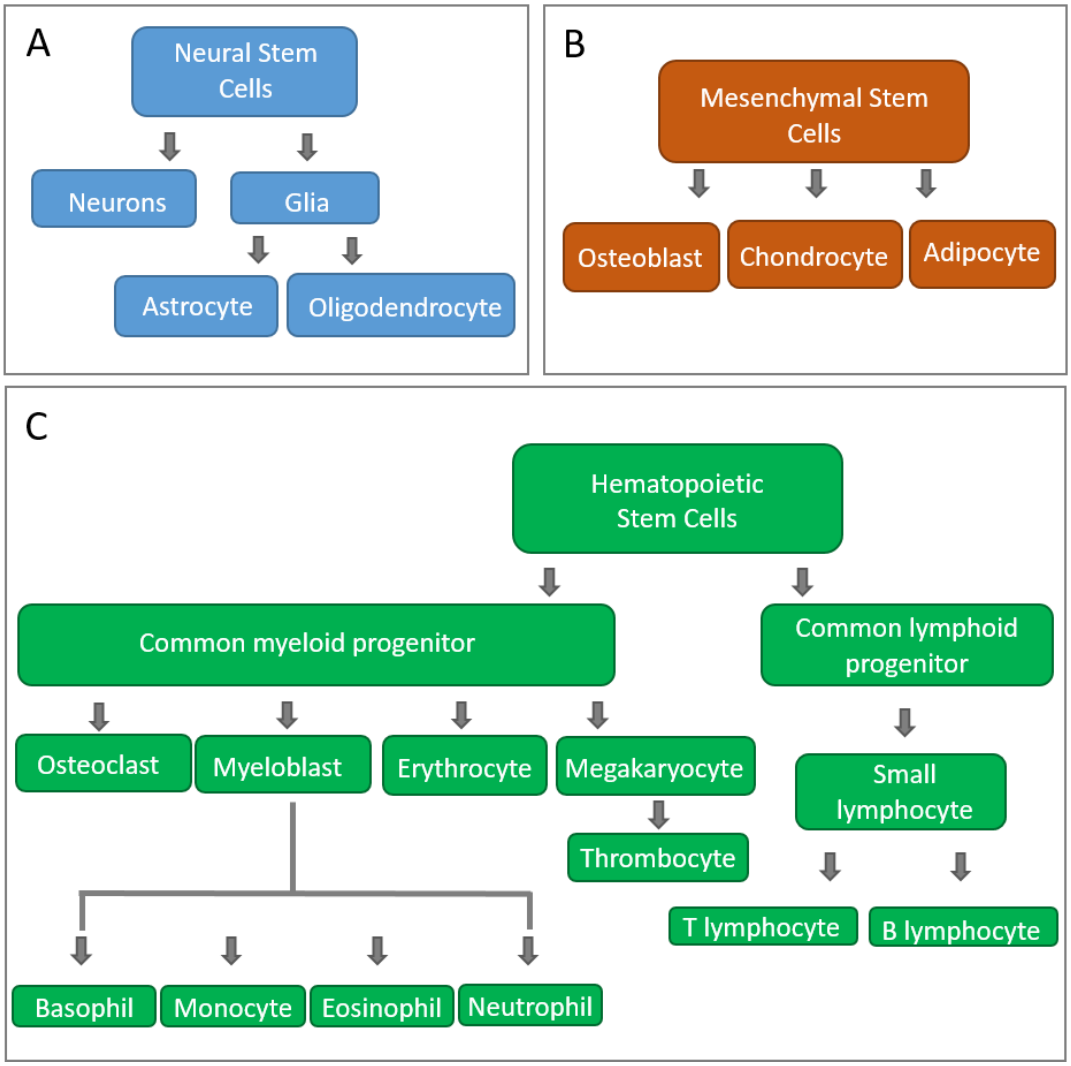

Fig. 1.10: Adult stem cell differentiation pathway. A: The differentiation of neural stem cells into the specialised cells of the central nervous system, neurons, glia, astrocytes and oligodentrocytes. B: Mesenchymal stem cells differentiation potential into the cells that comprise bone (osteoblasts), cartilage (chrondrocytes) and fat (adipocytes), C: Hematopoietic stem cell differentiation into immune cells. Hematopoietic stem cells have the capacity to differentiate into terminal cell types such as monocytes, neutrophils, T lymphocytes and B lymphocytes.

adult stem cells, or induced pluripotent stem (iPS) cells. Adult stem cells can be retrieved from an array of tissues from a consenting donor, while iPS cells can be generated from cells taken from either the patient or a consenting donor. Induced PS cells were first generated in 2006 from murine fibroblasts, by inserting pluripotent genes into the cellular genone (Takahashi and Yamanaka, 2006). The production of iPS cells has made a large impact on the stem cell field, nearly eliminating the need for embryonic stem cells.

1.9.1 Mesenchymal Stromal Cells

MSCs are defined by a distinct set of criteria established in 2006 by the International Society for Cellular Therapy. Firstly, cells must adhere to plastic under standard culture conditions and secondly express the following cell surface markers; CD105, CD73 and CD90. The lack of CD45, CD34, CD14 or CD11b, CD79α or CD19 and human leukocyte antigen (HLA) surface molecules expression is equally important to confirm the MSC classification (Dominici et al., 2006). The differentiation capability is the final set of criteria cells must meet, being able to differentiate into cells of the mesoderm lineage such as osteoblasts, adipocytes and chondroblasts (Dominici et al., 2006).

Standardisation of MSC criteria was needed as MSC definitions prior to this were ambiguous and varied. Scientists had a range of opinions as to the characteristics of MSCs and the methods to isolate and expand the cells in culture (Dominici et al., 2006). The defined criteria has allowed for standardisation of MSC research across different laboratories and countries. MSCs were first isolated from the bone-marrow (Friedenstein et al., 1968) and have remained the primary source of cells for research however, further MSC populations have been discovered in a range of tissues such as adipose (Rebelatto et al., 2008) and articular cartilage (Dowthwaite et al., 2004).

Despite MSC populations from different sources sharing phenotypic characteristics such as a fibroblast-like morphology and expression of surface antigen markers (Jeon et al., 2015), differences in key properties between different MSC populations has been demonstrated. Rates of cell proliferation, in addition to a differential genomic (Chen et al., 2015a) and proteomic expression profile between populations has been reported, contributing to processes involving the regulation of apoptosis and oxidative stress responses, amongst others (Jeon et al., 2015).

1.9.2 Oral Mucosa Lamina Propria-Progenitor Cells

OMLP-PCs were first isolated in 2010 from disease-free buccal mucosal biopsies. The OMLP-PCs were clonally derived, forming a homogeneous cell population displaying a fibroblast-like morphology (Davies et al., 2010). The clones were selected by differential adhesion to fibronectin before the expression of several stem cell markers was assessed. OMLP-PCs were found to have positive expression of the stem cell markers CD44, CD90, CD105 and CD166, but found not to express the hematopoietic markers CD34 and CD45. These findings confirm that the OMLP-PCs are not from a haematopoietic or fibrocyte origin (Davies et al., 2010). The OMLP-PCs were found to stain positively for the neural crest markers Slug, Snail, Twist and Sox10, confirming their origin is of the neural crest. These progenitor cells are capable of differentiating down both mesenchymal and ectodermal lineages forming cells such as osteoblasts, adipocytes and chroncytes cells (Fig. 1.11; Davies et al., 2010). A buccal mucosal biopsy is easy to obtain involving a minimally invasive procedure. The location of the biopsy allows for rapid healing after the process with little/no scar formation (Davies et al., 2010). This makes OMLP-PCs a viable option as a source of patient treatment.

1.9.3 Stem Cells and the Immune System

1.9.3.1 Immunomodulatory Properties of MSCs

MSCs have been shown to possess immunomodulatory properties by manipulating cells of the immune system though the release of soluble factors (Fig. 1.12; Atoui and Chiu, 2012). MSCs modulate several subsets of T cell populations. The proliferation of pro-inflammatory cytokine secreting $CD4^+$ and $CD8^+$ T cells is inhibited by MSCs, whereas the expansion of the IL-10 producing T regulatory (T reg) cells is increased. IDO has been repeatedly reported to play a role in MSC immunosuppression. Once activated by IFNγ, MSCs release IDO resulting in the degradation of tryptophan (Ghannam et al., 2010a). PGE2 is another factor thought to play a role in MSC immunosupression by inhibiting the mitogenesis of T cells. The production of PGE2 by MSCs is also upregulated upon IFNγ activation (Ghannam et al., 2010a). It was shown that in murine MSCs, the production of nitric oxide was noted, which was thought to play a role in the inhibition of T cell proliferation. However, nitric oxide secretion could not be detected from human MSCs (Ghannam et al., 2010a). It has been proposed that murine MSCs increase nitric oxide in response to inflammatory

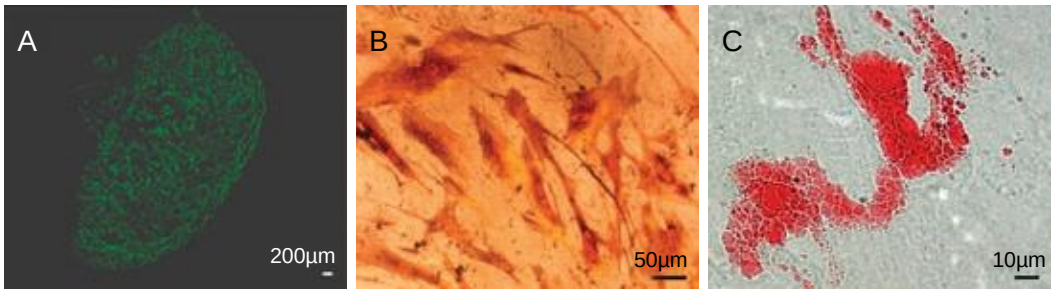

Fig. 1.11: OMLP-PC differentiation capacity. OMLP-PCs can differentiate down the chondrogenic lineage (A: aggrecan immunohistochemistry), form osteoblastic cells (B: Staining for calcium deposition) and adipogenic cells (C: Oil red staining of lipid droplets). (Images reproduced from (Davies et al., 2010).

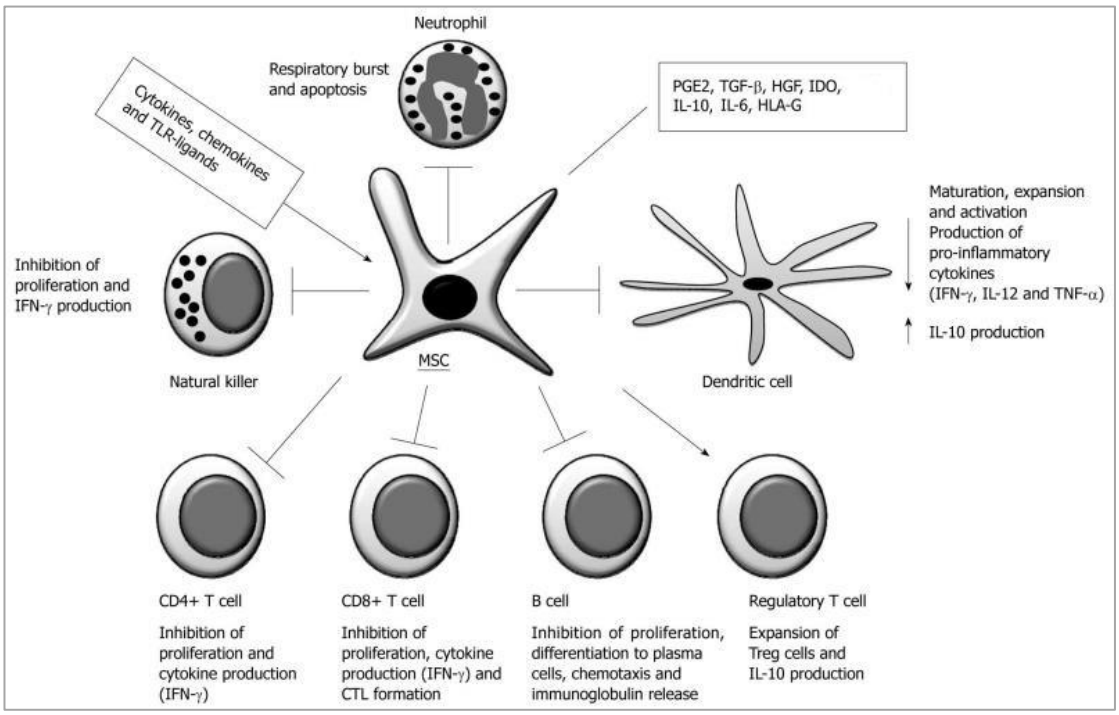

Fig. 1.12: MSC inhibitory effect on immune cells (reproduced from (Djouad et al., 2009, Bassi et al., 2011). MSCs are stimulated by cytokines, chemokines and TLR-ligands to produce immunomodulatory factors such as PGE2, IDO and IL-6. MSCs inhibit the proliferation and cytokine production from $CD4^+$ and $CD8^+$ T cells. The expansion of T reg cells and their production of the anti-inflammatory IL-10 in promoted by MSCs. The proliferation and differentiation of B cells is inhibited by MSCs and the maturation of DCs, in addition to their expansion and production of pro-inflammatory cytokines is also inhibited. Neutrophil respiratory burst and apoptosis is stimulated by MSCs, in addition to the inhibition of NK cell proliferation.

stimuli, while human MSCs respond by inducing IDO activity, demonstrating differential species specific responses (Meisel et al., 2011). Further T cell effects have been demonstrated, with the inhibition of $CD4^+$ T cell differentiation into Th1 effector cells by MSCs reported (Bassi et al., 2011, Ghannam et al., 2010b). The inhibition leads to a shift in the Th populations to an increase in the Th-2 phenotype. This therefore leads to decreased IFNγ production and increased IL-4 production, resulting in a more anti-inflammatory phenotype (Bassi et al., 2011). Further differentiation by $CD4^+$ T cells into the IL-17 producing Th17 cells has also been reported to be inhibited by MSCs, resulting in the lack of pro-inflammatory IL-22, TNFα and IFNγ production by these reduced populations of Th cells (Ghannam et al., 2010b).

The proliferation of B cells is inhibited by MSCs in addition to immunoglobulin (Ig) M, IgG and IgA production (Bassi et al., 2011). The reduction in Ig production by MSC conditioned media (CM) has been demonstrated, with the CC chemokine ligands (CCL) 2 and 7 identified in mediating Ig loss. Neutralisation of CCL2 has been reported to restore production, whereas only a partially restoration is observed by neutralising CCL7 (Rafei et al., 2008).

DC differentiation, maturation and activation is inhibited by MSCs. This results in an altered secretome profile of DCs with increased anti-inflammatory IL-1 and decreased pro-inflammatory IL-12, TNFα and IFNγ production (Bassi et al., 2011). The effects of MSCs on DCs are established during both direct and transwell culture of MSCs with DCs, demonstrating the role of soluble factors (Chen et al., 2015b).

The pro-inflammatory M1 phenotype of macrophages is altered by MSCs, shifting macrophage populations into the anti-inflammatory M2 phenotype (Dayan et al., 2011, Nakajima et al., 2012, Melief et al., 2013). An increase in IL-10 was reported with M1 to M2 polarisation by MSCs (Dayan et al., 2011), mediated by MSC IL-6 production (Melief et al., 2013). There is also evidence to suggest PGE2 mediates IL-10 secretion from macrophage populations. Antagonists to the prostaglandin EP2 and EP4 receptors inhibits the MSC mediated IL-10 production by macrophages (Németh et al., 2009).

Overall MSCs have an immunosuppressive effect of the immune system, shifting to a more anti-inflammatory state by reducing pro-inflammatory cytokine production and increasing anti-inflammatory cytokines such as IL-10.

The oral cavity provides a reservoir of different MSC populations such as gingival mesenchymal stem cells, dental pulp-MSCs (DP-MSCs) and periodontal ligament stem cells. Like other MSC populations, the orally derived MSCs display immunomodulatory properties such as the ability to suppress PBMC proliferation (Zhang et al., 2009, Tomic et al., 2011, Wada et al., 2009). Furthermore, it has been demonstrated that the DP-MSC immunosuppression is mediated by TGFβ (Tomic et al., 2011) while each orally derived MSC population can be induced to express immunosuppressive factors such as IDO, by IFNγ (Zhang et al., 2009, Wada et al., 2009). Moreover, MSC populations, such as human salivary gland MSCs, demonstrate chemotactic effects, such as the ability to cause directed migration of neutrophils (Brandau et al., 2014).

1.9.3.2 Immunosuppressive Properties of OMLP-PCs

It has been found that the OMLP-PCs possess immunomodulatory properties. OMLP-PCs were demonstrated to significantly suppress the proliferation of peripheral blood lymphocytes in a dose- and contact-independent manner (Davies et al., 2012). Significant suppression of lymphocyte proliferation remained when 0.001% OMLP-PCs to responder cells was examined. The removal of OMLP-PCs from the lymphocyte co-culture restored the lymphocyte proliferation, demonstrating that OMLP-PCs do not induce anergy (unpublished data, personal communication with Dr L. Davies). It was shown that the lymphocyte proliferation was not simply suppressed via the induction of cell death by both trypan blue exclusion and annexin V staining. The contact-independent nature of the immunomodulation was established using Transwell systems, where the OMLP-PCs were physically separated from the responder cells, suggesting the importance of soluble factors. One such factor, IDO, has been investigated (Davies et al., 2012) due to its immunosuppressive effects against primary human T cells (Forouzandeh et al., 2008). The activity of the IDO protein was only reported in OMLP-PCs once the cells had been exposed to IFNγ, and was not constitutively expressed.

1.9.4 Antibacterial Properties of MSCs

MSCs from the bone-marrow and umbilical cord blood have been shown to exhibit direct antibacterial properties against a small range of both Gram positive and Gram negative bacteria (Krasnodembskaya et al., 2010, Sung et al., 2016). MSCs significantly reduced the number of bacterial colony forming units (CFU) of *E. coli, P. aeruginosa* and *S. aureus* compared to bacteria cultured in the absence of cells. It

was also investigated whether CM of MSCs would display the same antibacterial effect. It was shown that MSCs CM that had previously been exposed to bacteria significantly reduced the bacterial CFU. This effect was not seen from MSC CM from cells in standard culture in the absence of bacteria (Krasnodembskaya et al., 2010, Sung et al., 2016). This demonstrates that the MSCs do not constitutively display antibacterial properties, but upon bacterial exposure secrete an antibacterial agent(s) into the medium. An antibacterial factor, LL-37, was investigated as a potential mechanism of action. LL37 was observed to increase in BM-MSCs pre-exposed to *E. coli* by RT-PCR and ELISA (Krasnodembskaya et al., 2010). Animal studies have shown that in a model of bacterial-induced sepsis, MSCs increase bacterial clearance and upregulate LL37 secretion (Lee et al., 2011). Umbilical cord-MSCs have also demonstrated similar antibacterial effects *in vitro*, with hBD-2 explored as a potential mechanism. It has been reported that secreted levels of hBD-2 are increased from umbilical cord-MSCs after exposure to *E. coli*, which correlated with increased levels of TLR2 and TLR4 (Sung et al., 2016). A knockdown of TLR4 eliminated the induction of hBD-2 and the antibacterial effects of the umbilical cord-MSCs. The antibacterial effects of MSCs were restored by the addition of hBD-2 into the culture medium. This demonstrates the involvement of TLR4-mediated production of hBD-2 in the antibacterial effects of umbilical cord-MSCs.

1.9.4.1 MSC Therapy for Bacterial Infections

BM-MSCs express TLR1, 2, 3, 4, 5, 6 and 9 (Cho et al. 2006), demonstrating their ability to recognise bacterial stimuli and therefore respond to the infection. Animal studies using *E. coli* induced murine pneumonia have shown that overall MSCs reduce lung injury and improve survival (Gupta et al., 2012). Bacterial clearance was seen to increase with MSC treatment in addition to upregulating lipocalin-2 production (Gupta et al., 2012). *Ex vivo* studies have also demonstrated the benefit of MSC therapy for bacterial infections. Lee et al., 2013 infused MSCs into human lungs after inducing *E. coli* associated pneumonia. A significant reduction in CFU/ml of *E. coli* within the alveolar fluid was seen after MSC therapy, which was not replicated by fibroblast infusion. Increasing the MSC dose further decreased the bacterial load, indicating a dose-dependent response. To assess whether the MSCs released antibacterial factors as a mechanism of action, the alveolar fluid exposed to MSCs and *E. coli* was tested for antibacterial properties. The fluid exposed to the bacteria significantly reduced the CFU/ml of *E. coli*, demonstrating MSCs had released factors into the surrounding environment. In addition to the secretion of

antibacterial agents, Lee *et al*., demonstrated increased levels of phagocytosis, indicating a further mechanism of bacterial clearance (Lee et al., 2013). Both human BM-MSCs and microvesicles derived these cells demonstrate increased survival of *E coli* induced-acute lung injury mice in a dose-dependent manner (Monsel et al., 2015). The increased survival rate was associated with an increased monocyte phagocytosis, decreased bacterial load and a decrease of the pro-inflammatory cytokine TNFa. Similar effects of MSC treatment have been demonstrated for *K. pneumoniae*-induced acute lung injury (Hackstein et al., 2015). Increased murine survival was observed in combination with reduced aveolar pro-inflammatory cytokines such as TNFα**,** in addition to decreased IFNy and IL-17 secreting T cell subsets. Furthermore, both CM and extracellular vesicles derived from both human and murine BM-MSCs ameliorate the effects of the fungal *Aspergillus* hyphal extract, which otherwise induced a murine model representative of severe refractory asthma. Both lung inflammation and the $CD4^+$ T cell Th2 and Th17 phenotype were reduced after the CM or extracellular vesicle treatment (Cruz et al., 2015). Similar effects of MSC extracellular vesicles on bacterial-induced conditions are yet to be examined.

MSCs are now being evaluated in the treatment of sepsis in animal models. Sepsis is a condition in which the response to an infection is dysregulated within the host (Lombardo et al., 2015). This dysregulation leads to a disproportionally high pro-inflammatory response due to the increase in activation of PAMP receptors such as TLRs. Therapies to successfully treat sepsis are not available, whilst the condition continues to become amongst the most comment causes of death amongst hospitalised patients (Mayr et al., 2014). The potential for MSCs in the treatment of *P. aeruginosa* induced sepsis has been explored. Murine models of bacterial induced sepsis were infused with MSCs. The intravenous (IV) administration of MSCs significantly increased the survival of the mice while demonstrating a reduction in the numbers of bacteria within the blood (Krasnodembskaya et al., 2012). The reduction in bacterial numbers was attributed to increased phagocytosis of peripheral monocytes. The specific antiseptic mechanism of MSCs is not clearly defined, but MSCs are thought to contribute in several ways. The pro-inflammatory state of patients is facilitated by the apoptosis of many resolving immune cells (Kusadasi and Groeneveld, 2013). MSCs have been shown to reduce the apoptosis of neutrophils through IL-6 mediated mechanisms (Raffaghello et al., 2008), which could aid in the control of the pro-inflammatory state for septic patients. Studies have also shown that MSCs can effectively reverse the inflammatory position from a pro-inflammatory to an anti-inflammatory state. Németh and colleagues demonstrated that MSC infusion into

a murine model of sepsis significantly reduced the serum levels of the pro-inflammatory cytokines TNFα and IL-6, both of which are known to be key in the development of sepsis (Németh et al., 2009). Furthermore, it was shown that the serum levels of the anti-inflammatory IL-10 were increased, even at 3 hours post MSC infusion. The study expanded to look at the influence of immune cells on the MSC antiseptic action. T, B and NK cells were not found to play a role however, when monocytes and macrophages were depleted, the MSC infusion failed to have an effect. It was also found that the monocytes and macrophages were the source of the anti-inflammatory IL-10 levels. The authors found that bacterial LPS exposure activated the NF-$_k$B pathway, which induced the production of COX2 dependant PGE_2 from MSCs. The prostaglandin then modifies the macrophage secretome by reducing TNFα and IL-6 levels and increasing IL-10 (Németh et al., 2009).

1.9.5 MSCs as a cell-based therapy

There are currently almost 500 clinical trials which are registered to assess MSC-based therapy (ClinicalTrials.gov). MSCs are thought to home to sites of injury, making them suitable candidates for cell-based therapies (Wei et al., 2013). The directed migration is thought to involve several cytokines and chemokines. For example, the chemokine receptor C-X-C chemokine receptor type 4 (CXCR4) found to be expressed on the surface of MSCs responds to the secretion gradient of stromal cell-derived factor-1 (SDF-1) from the sites of tissue damage. Over-expression of the receptor in MSCs has been demonstrated to improve the cell engraftment at the site of injury (Cheng et al., 2008). It has also been reported that direct co-culture of *H. pylori* with BM-MSCs results in an increased BM-MSC surface expression of CXCR4, enhancing the migration of the cells towards a SDF-1a gradient (Fakhari et al., 2014). Another chemokine noted to be involved in MSC migration is macrophage inflammatory protein 1 alpha (MIP-1α) (Eseonu and De Bari, 2015). Cell migration assays have determined that MIP-1α, again secreted from sites of damage, significantly increases the migration of MSCs *in vitro* (Boomsma and Geenen, 2012).

IV administration of MSCs has been demonstrated to be safe and allows for a large number of MSCs to be delivered. However, tracking studies have established that the overwhelming majority of infused MSCs migrate to the lungs (Assis et al., 2010, Fischer et al., 2009), with minimal numbers migrating to organs such as the heart and kidneys (Assis et al., 2010). When infused into a rat model of myocardial

infarction, the small number of MSCs which migrated to the heart remained 7 days post infusion (Assis et al., 2010, Kraitchman et al., 2005). However, when infused into wild-type mice, infused MSCs were located in the lungs 1hr post infusion, with no viable MSCs detected in any other organ. Furthermore, infused MSCs were not detected in the lungs 24hrs post infusion, demonstrating their short longevity (Eggenhofer et al., 2012).

The engraftment of IV infused MSCs has been investigated in the autopsy material of 18 patients, all of which received MSC IV treatment (von Bahr et al. 2012). Autopsy material from just 8 patients was positive for donor MSC DNA, which was detected mostly within the lung, lymph nodes and intestine. The detection of MSC donor DNA was negatively correlated with the time from infusion, suggesting MSCs are cleared from the patient over time after the IV infusion MSC treatment demonstrating a limited engraftment long term. It was also reported that there was no correlation between MSC engraftment and treatment response, demonstrating that the MSC mechanism of action does not require MSC engraftment.

Research involving MSCs has begun to focus on patient treatment. The overwhelming presence of infused MSCs in the lungs and the short longevity of the cells could limit their application (Eggenhofer et al., 2012), however MSC therapy has proven effective despite this for the treatment of conditions such as GVHD (see section 1.9.7.1). These stem cells are considered immunoprivileged due to their low expression of HLA I and HLA II and a lack of T cell stimulatory molecules (Lee et al., 2011). The immunosuppressive nature of the cells could cause some concern if treating diseases unrelated to the immune system. However, suppression of the immune system by MSCs may not correlate to an increase in infections due to their additional antibacterial properties (Lee et al., 2011). Ease of delivery and the immunoprivilege properties make MSCs ideal drug candidates.

1.9.6 Post Hematopoietic stem cell transplantation Infections

HSCT is a treatment for conditions such as leukaemia and solid tumours (Passweg et al., 2014). However, HSCT transplantation can lead to the development of complications such as GVHD (see section 1.9.7.1) and increased infections (Kedia et al., 2013). The increase in infections is a result of the conditioning regimes (such as chemotherapy and radiation) prior to the HSCT, which target the immune cells of the bone marrow. Additionally, the patient is subjected to immunosuppressive treatment,

to prevent immune rejection of the transplant. This has further effects on the patient's immune system, dampening its ability to fight infections.

Neutropenia (decreased neutrophils) can result from HSCT, predisposing patients to increased infections. The majority of these infections are caused by bacteria (Young et al., 2015) and have the potential to be life threatening in this group of patients. Diverse oral bacterial infections have been documented post-HSCT, caused by microorganisms such as Gram positive cocci, and the Gram negative organisms *K. pneumoniae* and *Enterobacter cloacae* (Vavilov et al., 2015). Fungal infections have also been reported in patients undergoing HSCT. The most common fungal infections within the oral cavity of these patients are caused by *C. albicans*, with patients receiving allogeneic HSCT more susceptible to fungal infections, compared to those who received an autologous HSCT (Markowski et al., 2015). Viral infections, particularly the reactivation of human herpes virus-6 (Shachor-Meyouhas et al., 2015, Inazawa et al., 2015) and Epstein–Barr virus (Inazawa et al., 2015) have also been reported in patients after HSCT.

1.9.7 MSCs in the Treatment of GVHD

1.9.7.1 Graft Versus Host Disease

GVHD can develop in patients who have undergone a biological graft. The disease is defined by the Billingham criteria (Ferrara et al., 2009):

1. The graft must contain cells which are capable of generating an immune response (i.e. immune-competent cells)
2. The recipient must contain antigens which are not present in the graft donor
3. The recipient must not be able to generate an effective immune response against the immune-competent cells from the donor

GVHD arises from the transplantation of stem cells (haematopoietic) or bone marrow for the treatment of conditions such as leukaemia. T cells (the immune-competent cells) within the transplanted tissue will give rise to a reaction against the host's tissue, often when a mismatch in the HLAs from the donor and recipient are detected (Ferrara et al., 2009, Loiseau et al., 2007).

There are two types of GVHD, acute GVHD (aGVHD) and chronic GVHD (cGVHD). The acute condition normally manifests within 100 days of the transplantation, with

chronic GVHD presenting after 100 days and can last a lifetime (Jagasia et al., 2015). The pathogenesis of GVHD, both acute and chronic is broken down into a model developed by Ferrara (Fig. 1.13; Ferrara and Reddy, 2006). Here it is thought that GVHD manifestation occurs in three stages. In the first stage, conditioning of the recipient by chemotherapy and/or radiotherapy prior to transplantation which leads to tissue damage and the release of bacterial products from the gut flora such as LPS. This in turn will cause the second stage of pro-inflammatory cytokine release and the migration of host antigen presenting cells to secondary lymphoid organs such as the lymph nodes. Finally, within the lymph nodes activated antigen presenting cells will present antigen to the donor T cells, leading to their proliferation and differentiation into effector cells. This will stimulate T cell production of IFNy and IL-2. These effector T cells will travel to the target tissues of the host, normally the skin, gut and liver and initiate cellular apoptosis as well as releasing pro-inflammatory cytokines to maintain the process (Ferrara and Reddy, 2006).

Acute GVHD is reported to develop in 50-70% of patients undergoing allogenic transplants, whereas 30-50% develop the cGVHD (Margaix-Muñoz et al., 2015). The diagnosis of aGVHD is based on potential symptoms in up to three organs; the skin, the gastrointestinal (GI) tract and the liver. The skin is the most targeted organ during aGVHD, presenting with maculopapular rash, with the liver the most infrequently affected organ. The GI tract can also be affect during aGVHD, resulting in nausea, vomiting and diarrhoea (Harris et al., 2015).

A larger number of organs may be affected during cGVHD (see Table 1.3) including the oral cavity (Socié and Ritz, 2014). The oral cavity is the second most commonly affected area in chronic GVHD patients, with in some cases being the only tissue affected (Margaix-Muñoz et al., 2015). One study found that 70% and 53% of patients who had undergone haematopoietic stem cell transplantation and bone marrow transplantation respectively, developed cGVHD with oral symptoms (Pavletic et al., 2005). These symptoms include mucositis, gingivitis (bacterial infection) and pain. The pain leads to difficulty in the ability of patients to eat which in turn can lead to weight loss. Overall the oral component of the condition can severely decrease the quality of life for patients. It has been reported that GVHD is associated with a reduction in AMPs within the intestine of mice. The secretion of α-defensins by intestinal Paneth cells regulates the microbial communities within the gut. It has also been reported that in a murine model of aGVHD, the Paneth cells are specifically

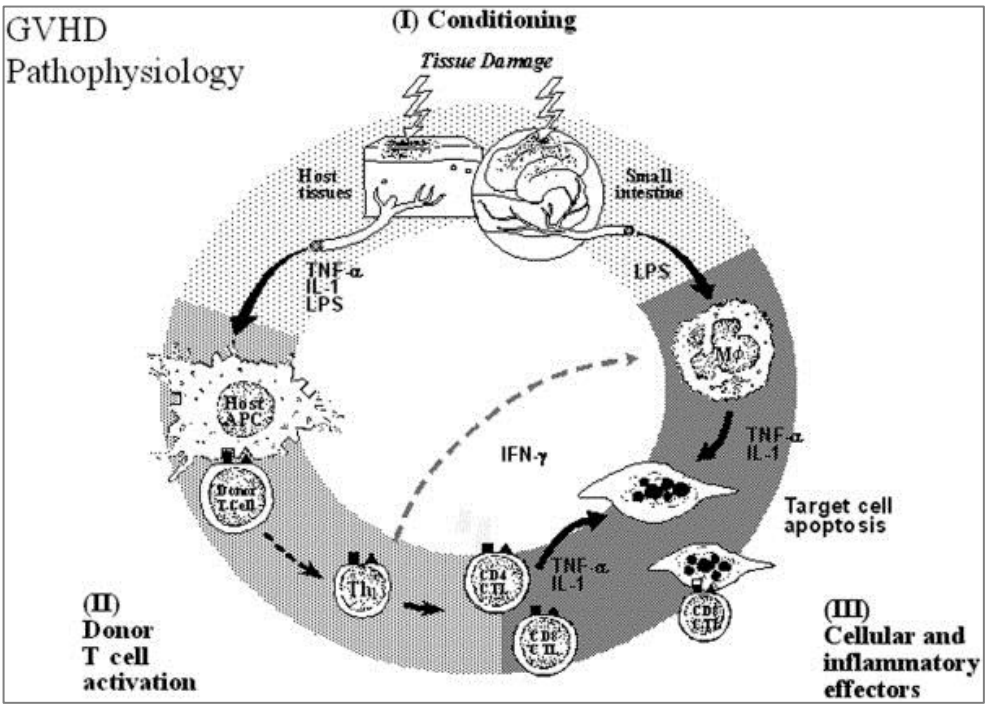

Fig. 1.13: Reproduced from (Ferrara and Reddy, 2006). The pathogenesis of GVHD. Tissue damage is caused by conditioning regimes such as chemotherapy, causing the release of products such as LPS. The release of the bacterial components cause the section of cytokines and the migration of APCs. APCs then present antigen to the donor T cells, resulting in T cell activation and proliferation leading to the development of T effector cells. This process stimulates the production of IFN-y and IL-2. The effector cells are then transported to target tissues where cellular apoptosis occurs.

Table 1.3: Tissue specific symptoms of cGVHD, a non-exhaustive list.

Tissue site	**Symptoms**
Skin	Maculopapular rash, Lichen planus-like rash, Erythema
Nails	Nail loss
Gastrointestinal tract	Diarrhoea, Vomiting, Loss of Weight
Liver	Increased Bilirubin
Oral cavity	Erythema, Gingivitis, Pain, Mucositis, Lichen planus-like rash

targeted, with dramatically less observed in the GVHD mice compared to controls. Furthermore, the loss in Paneth cells was associated with an increase in aGVHD severity in addition to a reduced secretion of α-defensins (Eriguchi et al., 2012). This may pre-dispose the gut changes in microflora. An increase in *E. coli* growth was demonstrated in the aGVHD mice, which was correlated to GVHD severity (Eriguchi et al., 2012). The effect of cGVHD on the secretion of AMPs and potential effects on microbial communities within the oral cavity is yet to be examined.

Currently, conventional treatment of both aGVHD and cGVHD consists of steroids and an immunosuppressive drug such as cyclosporine a, but it has been reported that only two thirds of patients develop a complete response to this treatment (Dhir et al., 2014). It has long been known that patients with steroid refectory GVHD have a decreased survival rate compared to those who respond to steroids (Martin et al., 1990). Further treatment for GVHD patients who do not respond to steroids is given with drugs such as anti-TNFα antibodies (e.g. infliximab) and IL-2 receptor antibodies (e.g. daclizumab) (Dhir et al., 2014). However, the recommendations for treating GVHD from the American Society of Blood and Marrow Transplantation state that there is not enough evidence to support other treatments of GVHD other than steroids (Martin et al., 2012).

1.9.7.1.1 Oral Chronic GVHD

The oral cavity is the second most commonly affected organ during cGVHD, with 45-83% of patients with reported oral involvement (Mays et al., 2013). Oral cGVHD is diagnosed by the presence of lichen-planus like changes characterised by 'hyperkeratotic (thickening) white lines and lacy-appearing lesions' within the oral mucosa (Jagasia et al., 2015). Further symptoms of oral cGVHD include mucositis, gingivitis, erythema and pain, but are not used to diagnose the disease. Treatment for cGVHD often targets multiple organs affected by GVHD, with systemic treatment with corticosteroids the first-line therapy (Margaix-Muñoz et al., 2015). It has been reported that systemic treatment of cGHVD can result in oral improvements in 32% of patients (Inamoto et al., 2012). In patients where the cGHVD progresses despite corticosteroid treatment the disease is termed steroid-refractory. In steroid-refractory patients second-line treatments such as Rituximab may be used. Rituximab treatment is well tolerated (Cutler et al., 2006), with one study reporting clinical improvements in the oral musocas in 6 out of 11 patients (Clavert et al., 2013). Extracorporeal photopheresis is also a second-line treatment for steroid-refractory

patients. Clinical improvements in oral cGVHD have been reported after extracorporeal photopheresis (Dall'Amico and Messina, 2002), with improvements potentially attributed to the apoptosis of neutrophils and a down regulation of the activation markers, CD16, CD54 and CD64, expressed on the surface of neutrophils (Franklin et al., 2015). Patients treated with extracorporeal photopheresis also display higher numbers of T regulatory cells and reduced numbers of $CD4^+$ T cells and B cells (Zhu et al., 2015).

Topical treatments can directly target the oral mucosa during cGVHD treatment. Topical treatments, such as the immunosuppressive drug tacrolimus, have demonstrated promise. One case study demonstrated that in 8 weeks the topical application of tacrolimus effectively relieved the mucosal symptoms in a 41 year old GVHD patient (Eckardt et al., 2004). It has also been reported that topical tacrolimus treatment in combination with an oral hygiene protocol may be an effective treatment for oral cGVHD (Conrotto et al., 2014).

1.9.7.2 MSC Therapy for GVHD

MSC therapy in the treatment of both aGVHD and cGVHD has been explored. MSCs, from donors ranging from HLA-matched to HLA-mismatched, were transplanted in 55 patients with steroid refractory aGVHD in Sweden (Le Blanc et al., 2008). Up to 70% of patients responded to the MSC treatment with no side effects seen throughout the study. The survival rate of steroid resistance GVHD patients was increased from 10% to 52% by the MSC therapy. The majority of responding patients required a single dose of MSCs from any donor however, some patients needed a second and potentially third dose to maintain the therapeutic benefits. There was no difference seen between the HLA-matched and HLA-mismatched MSCs, demonstrating MSCs in a practical therapy without the need for HLA-matching (Le Blanc et al., 2008). Furthermore, complete aberration of aGVHD has been documented in 6 out of 8 patients in another study (Ringdén et al., 2006).

The MSC treatment for cGVHD has also been investigated. One study demonstrate that up to 74% of patients treated with MSCs display clinical improvements with no side effects, with a 2-year survival rate of 77.7%. This study also confirmed that the clinical benefits of MSCs are noted irrespective of donor (Weng et al., 2010). MSC therapy is well tolerated in patients with no side effects documented (Lucchini et al., 2010, Zhou et al., 2010). A further study has demonstrated an arrest in cGVHD development in paediatric patients and a partial clinical response to MSC therapy in 2

out of 3 cGVHD patients, resulting in a decrease in the immunosuppressive treatment required. MSC therapy resulted in a decrease in the plasma levels of the pro-inflammatory cytokines TNFα and IFNγ (Lucchini et al., 2010). Improvements in the clinical scores of 4 patients have been documented in another study, with improvements skin sclerosis and joint mobility observed after MSC therapy (Zhou et al., 2010).

Kordelas et al., have undertaken a novel approach to MSC therapy. With the knowledge that the MSC effects are mediated by the release of soluble factors, and not the cells directly, the authors isolated exosomes from MSC cultures to apply as a GVHD therapy. Due to their size, exosomes can be easily sterilised using filtration and do not necessitate the lengthy expansion times MSCs require as they are not self-replicating. Furthermore, exosomes can be isolated from immortilised MSC cell line cultures, which otherwise could not be used for a cell-based therapies. It was reported that the isolated MSC exosomes contained large quantities of the anti-inflammatory molecules IL-10, TGFβ and HLA-G. Pro-inflammatory cytokine presence in the exosomes was limited to IFNγ and IL-8, with the absence of further molecules such as TNFα, IL-2 and IL-6. With the immunosuppressive properties of the exosomes was confirmed by the reduction in PBMC numbers, the application of exosomes to treat one GVHD patient was conducted. Exosome therapy did not cause any side effects and was well tolerated in the patient and resulted in a decrease in the numbers of pro-inflammatory cytokine secreting PBMCs. The clinical symptoms of GVHD improved within the patient after the treatment such as reduced diarrhoea volume. This study demonstrated the beneficial effects of MSCs even without the presence of MSCs directly (Kordelas et al., 2014).

1.9.7.2.1 MSC Therapy for Oral GVHD

A recent case study has demonstrated the efficacy of local MSC treatment in steroid-refractory cGVHD (Garming-Legert et al., 2015). MSCs were locally injected into 3 ulcerated areas of the buccal mucosa at day 0 and day 8 in a 59 year old male. Clinical improvements were reported at day 2, with a reduction in the ulceration wound and redness of the area and by day 16 the majority of the ulceration at the affected sites had dissolved. The healing capacity of the MSCs is thought to be mediated through soluble factors such as SDF-1, monocyte chemoattractant protein (MCP)-1 and IL-8, which were identified in the MSC secretome (Garming-Legert et

al., 2015). This is currently the only study to examine the effects of local MSC therapy to treat tissue-specific components of GVHD.

The first line treatment of corticosteroids in the treatment of GVHD can prove ineffective against the oral symptoms. One study demonstrated that in group of 283 patients with cGVHD, oral improvements were only observed in 32% of patients (Inamoto et al., 2012). This demonstrates the need for an oral specific treatment. Systemic MSC therapy has proven effective in treating cGVHD with oral involvement. One study demonstrated oral responses to MSC therapy in 15 out of 16 patients (Weng et al., 2010). With the known short longevity, localisation to the lungs (Eggenhofer et al., 2012) and lack of engraftment (von Bahr et al., 2012) of IV infused MSCs into the body, local MSC treatments may provide a more specific effect at the affected tissues. The benefits of MSC treatment could be provided with local injections without the need for systemic infusion, reducing the number of cells needed.

1.9.8 Choosing an Appropriate Stem Cell Source

Autologous stem cell therapies, in which the donor and recipient are the same individual, has distinct advantages over allogeneic therapy, in which donor cells are harvested from a different individual to the recipient. Autologous therapy does not involve the need to identify HLA-matched samples, as the donor cells are native to the recipient (Champlin, 2003). This type of therapy does not require immunosuppressive treatment post-transplantation and therefore there is no risk of developing transplant rejection (Champlin, 2003). The reagents and culture medium used during culture must be considered. Foetal calf serum (FCS) is a commonly used as a medium supplement during cell expansion *in vitro*. As a xenogenic material, the immunoprivileged nature of autologous stem cells could potentially be compromised, with the production anti-bodies directed at FCS demonstrated after MSC infusion (Sundin et al., 2007). Human-derived alternatives, such as human serum, may limit the effects on the immuneprivileged status of autologous stem cell therapies. However, if a patient displays a condition directly relating to the cell source or is genetic, autologous cells are not suitable. Transplantation of such cells would not result in clinical improvement as they would continue to develop the disease.

Allogeneic cell sources overcome this problem, with cells taken from healthy donors. However, the cells are often HLA-matched to limit the immune response by the recipient and there is a risk of GVHD (Champlin, 2003). Allogeneic cell sources with

low immunogenicity would overcome the problems faced by autologous and allogeneic therapies. BM-MSCs display intermediate levels of HLA-I and low levels of HLA-II (Le Blanc et al., 2003). This limited expression of HLA molecules reduces their recognition by the donor immune system, and lowers the potential immune response to the donor cells by the recipient. MSCs are also able to evade the immune system by suppressing the activation and proliferation of a range of cellular components to the immune system (see section 1.9.3.1). This limits the immune response to the cells, potentiating their use as an allogeneic therapy.

BM-MSCs are the gold standard adult stem cells for cell based therapies however, harvesting such cells is an invasive procedure causing the donor discomfort and pain for several days (Chen et al., 2013). A stem cell population has been identified within the oral mucosa (OMLP-PCs) with potential therapeutic value. OMLP-PCs are harvested by a minimally invasive procedure involving a biopsy from the oral mucosa (Davies et al., 2010). The procedure can be undertaken during routine dental procedures as the mucosa is easily accessible. It is also associated with rapid healing and a lack of scar formation, allowing rapid patient recovery with little discomfort and pain.

A number of studies have demonstrated that the numbers of BM-MSCs decrease with age. It has been hypothesised that the decrease in bone mass with age is related to the numbers of progenitor cells. In one study, cells from the bone marrow were harvested from 41 deceased patients ranging in ages (3yrs – 70yrs). The patients' deaths had been as a result of traumatic injury and they had been otherwise healthy individuals. It was found that the number of BM-MSC colony forming units (CFU-F) decreased with age (D'Ippolito et al., 1999). These results have been echoed in numerous studies where the CFU-F of BM-MSC are seen to decrease with age (Nishida et al., 1999, Majors et al., 1997). (Stenderup et al., 2003) reported that BM-MSCs from older patients (68-81yrs) reached a senescent state faster than those from younger donors (18-29yrs). The decrease in proliferative capacity was not associated with a decrease in stem cell numbers with age. However, this study utilised the Stro-1 antibody to identify the BM-MSCs. This antibody may also identify non-stromal cells in the bone-marrow producing false-positive results. These studies have demonstrated that harvesting of BM-MSCs is limited by patient age. Finding an alternative stem cell source, which doesn't decrease with age would be beneficial in harvesting optimal numbers of cells.

1.10 Rationale

The oral cavity contains a rich microbiome, yet recurrent infections are rare (Parahitiyawa et al., 2010). A diverse and multifactorial microbial defence is essential to maintain a healthy oral homeostasis including the effects of innate immune cells and the secretion of antimicrobial factors. Antimicrobial factors are secreted in many areas of the oral cavity such as salivary glands and epithelial cells and are detected within the oral fluids such as saliva (Gorr, 2009). At least 45 different antimicrobial factors have been identified in the oral cavity, such as the defensins, histatins and LL37 (Gorr, 2009). It has been reported that BM-MSCs secret the antimicrobial peptide LL37, which has led to the investigation of the role of OMLP-PCs in oral defence. MSCs have been reported to act as both an immunosuppressant (Ghannam et al., 2010a) and antibacterial (Krasnodembskaya et al., 2010) agent. OMLP-PCs share the immunosuppressive properties of MSCs (Davies et al., 2012), but the antibacterial qualities have yet to be investigated in OMLP-PCs.

1.11 Hypothesis

As OMLP-PCs are one of the key cells involved in the orchestration of oral homeostasis and repair, I hypothesize that such oral progenitors also exhibit antibacterial properties in addition to their immunosuppressive capabilities.

1.12 Aims

The overall objective of this study is to demonstrate the antibacterial properties of OMLP-PCs and their principal mechanisms of action. To achieve this objective the following aims will be addressed:

1. Establish whether OMLP-PCs reduce the growth of both Gram positive and Gram negative bacteria *in vitro*.

2. Determine if OMLP-PCs require licensing by exposure to pro-inflammatory stimuli and/or bacterial products in order to exhibit antibacterial properties or whether their antibacterial properties are constitutive.

3. Elucidate the mechanism of OMLP-PC antimicrobial action through investigation of the role of antibacterial factors produced by OMLP-PCs.

2. Investigating the Antibacterial Properties of OMLP-PCs

2 Investigating the Antibacterial Properties of OMLP-PCs

2.1 Background

Oral soft tissues are continually exposed to the external environment and are thus a critical entry point for potentially harmful bacteria (Parahitiyawa et al., 2010). Surprisingly chronic infections are rare, potentially due to antimicrobial factors secreted by resident cells within tissues such as the salivary glands (Gorr, 2009). Indeed, a decrease in specific antimicrobial factors has been linked with the onset of oral diseases such as periodontitis and deficiencies in the human cathelicidin protein LL37 (Pütsep et al., 2002).

Wound healing within the buccal mucosa is preferential, potentially due to the presence of OMLP-PCs. In addition to their multipotency, OMLP-PCs have been demonstrated to possess potent immunosuppressive properties, significantly suppressing the proliferation of peripheral blood lymphocytes in a dose and contact-independent manner (Davies et al., 2012). The contact-independent nature of this immunomodulation suggests the importance of soluble factors in mediating these effects. MSCs, from numerous sources including the bone marrow (BM-MSCs), have also been demonstrated to have inherent immunosuppressive properties, induced by exposure to IFNγ, a pro-inflammatory cytokine released by subsets of immune cells such as T helper cells (Ghannam et al., 2010). In contrast to OMLP-PCs, the immunosuppressive effects of BM-MSCs on T cell proliferation are thought to act via both contact-dependant and contact-independent methods, potentially suggesting different modes of action between the stem cell sources (Mezey, 2011).

IDO is one of the major soluble factors repeatedly reported to play a role in stem cell mediated immunosuppression, including OMLP-PCs, BM-MSCs and gingival MSCs (GMSCs). The production of the IDO protein is not constitutively produced by these stem cell sources and is only secreted in response to IFNγ, (Davies et al., 2012, Ghannam et al., 2010, Zhang et al., 2009).

Once activated by IFNγ, MSCs release IDO resulting in the degradation and depletion of tryptophan, thereby inducting T cell apoptosis (Ghannam et al., 2010) and the inhibition of T cell proliferation (Yang et al., 2009). Immunosuppressive factors, such as IDO, are also known to have prominent antibacterial actions; IDO inhibits tryptophan-dependent bacteria such as group B *streptococci* (Hucke et al.,

2004) and *E.coli* (Barclay, 1985, Eaton et al., 1982) by the depletion of tryptophan. This knowledge has led to the hypothesis that stem cells can act with dual properties; displaying both immunomodulatory and antibacterial characteristics. However, limited studies have been reported with respect to the potential antibacterial properties of stem/progenitor cells. BM-MSCs have been demonstrated to exhibit antibacterial properties against a small range of both Gram positive and Gram negative bacteria (Krasnodembskaya et al., 2010). Within this study it was reported that BM-MSCs significantly reduced the number of bacterial colony forming units (CFU) of *E. coli, Pseudomonas aeruginosa* and *Staphylococcus aureus* compared to bacteria cultured in the absence of BM-MSCs. The authors demonstrated that CM produced from BM-MSCs that had previously been exposed to bacteria, significantly reduced the bacterial CFU. This effect was not seen when CM was produced from BM-MSCs in standard culture in the absence of bacteria, suggesting that BM-MSCs do not constitutively display antibacterial properties, but upon bacterial exposure can be induced to secrete antibacterial factors; in this case LL37 (Krasnodembskaya et al., 2010). LL37 has also been implicated in BM-MSC mediated antibacterial action *in vivo*, with animal studies using a model of bacterial-induced sepsis demonstrating the ability of BM-MSCs to increase bacterial clearance via upregulation of LL37 secretion (Lee et al., 2011).

This Chapter therefore sought to investigate whether, similar to BM-MSCs, OMLP-PCs display antibacterial properties in addition to their immunosuppressive qualities. Investigations were carried out to determine whether OMLP-PCs are constitutively antibacterial or whether bacterial and/or inflammatory priming is needed to exert suppressive effects against both Gram positive and Gram negative bacteria.

2.1.1 Aims

1. Establish whether OMLP-PCs possess antibacterial properties, acting against both Gram negative and Gram positive bacteria.
2. Investigate OMLP-PC antibacterial mode of action and whether this is via contact dependant or independent mechanisms.
3. Determine whether OMLP-PCs require bacterial or inflammatory priming to exert antibacterial actions against Gram positive and Gram negative bacteria.
4. Investigate the response of OMLP-PCs to bacterial stimuli.

2.2 Materials and Methods

All microbiology reagents were purchased from Oxoid (UK) and tissue culture reagents from Life Technologies Ltd (UK) unless otherwise stated.

2.2.1 Maintenance of Oral Mucosa Lamina Propria Progenitor Cells (OMLP-PCs) and Enriched Oral Fibroblasts (EFs)

OMLP-PCs were previously isolated and characterised by L. Davies (Cardiff University, UK; Davies et al., 2010). The study was approved by the local ethics committee and conducted in accordance with the Declaration of Helsinki. All donors provided written consent. Buccal mucosa biopsies from healthy patients undergoing orthognathic surgery were submerged in 70% (v/v) ethanol prior to enzymatic digestion for 16hrs at 4°C with 2mg/ml dispase II (Sigma, UK) in Dulbecco's Modified Eagle's Medium (DMEM) supplemented with 10% (v/v) foetal calf serum (FCS), 2mM L-glutamine and antibiotics/antimycotics (100 U/ml penicillin G, 100 µg/ml streptomycin sulphate and 0.25 µg/ml amphotericin B), herein referred to as complete medium. The epithelium layer was removed and further digestion into a single cell suspension was carried out in 1mg/ml collaganse A (Roche, UK) in complete medium for 16hrs at 37°C in a 5% CO_2 humidified atmosphere. The single cell suspension was then washed in serum-free medium before plating (20mins at 37°C) onto tissue culture plastic coated with 10µM bovine plasma fibronectin (Sigma, UK) diluted in phosphate buffered saline supplemented with 1mM $CaCl_2$ and 1mM $MgCl_2$ (PBS+). The cells that did not adhere to fibronectin after this 20mins were plated onto fibronectin as before for a further 40mins x2 to ensure all PCs were depleted, and the remaining cells which did not adhere to fibronectin were defined as EFs. The cells which adhered to the fibronectin from the first incubation of 20mins (OMLP-PCs) were cultured in complete medium until colonies formed from a single cell reached $\geq$ 32 cells. Each colony was surrounded by a cloning ring and cells were removed from the plastic using 0.05% Trypsin-EDTA for 10mins at 37°C. The colony derived OMLP-PCs and the EFs were then expanded in complete medium.

Cells in complete medium were frozen in 10% dimethyl sulphoxide (DMSO) for long term storage in liquid nitrogen. Upon removal from liquid nitrogen storage, cells were rapidly thawed in a 37°C waterbath before counting and seeding into a T75 flask as below.

The cell density of confluent flasks was recorded and the population doubling level (PDL) calculated for each OMLP-PC clone, using the formula below;

$$PDL = \frac{log_{10}(confluent\ cell\ density) - log_{10}(initial\ seeding\ density)}{log_{10}(2)}$$

Cells were seeded at a density of $2x10^3$ cells per cm^2 in a T75 flask and trypsinised when they reached approximately 90% confluency. Cells were washed with 10ml PBS before adding 1ml 0.05% Trypsin-EDTA (Life Technologies Ltd., UK) & incubating at 37°C for 5mins. The cell suspension was combined with 7ml of complete medium and centrifuged at 500g for 5mins at room temperature. The medium was removed and the cell pellet re-suspended in 1ml of complete medium. Ten microlitres of the cell suspension was diluted 1:2 with trypan blue (to enable a viable cell count) and counted using a haemocytometer.

2.2.2 Maintenance of Microbiological Stocks

Enterococcus faecalis (*E. faecelis*; NCTC 775), *Pseudomonas aeruginosa* (*P. aeruginosa*; ATCC 15692) and *Streptococcus pyogenes* (*S. pyogenes*; NCTC 8198) were maintained on tryptone soya agar (TSA). *Proteus mirabilis* (*P. mirabilis*; NCTC 11938) was maintained on cysteine lactose electrolyte deficient (CLED) agar to prevent swarming of the bacteria. Bacteria were sub-cultured onto fresh agar plates weekly and stored at 4°C. Stocks of each bacterium were stored in Microbank™ cryovials (Pro-lab diagnostics, UK) at -80°C.

2.2.3 Gram Staining

Gram staining was performed regularly to ensure pure cultures. A loop of bacteria was heat fixed onto a glass slide before staining with crystal violet (1% w/v; Prolab diagnostics, UK) for 1min. Iodine solution (1% w/v iodine, 2% w/v potassium iodide; Prolab diagnostics: UK) was added to the bacteria for 30 seconds, followed by a rapid de-colouration step using acetone (Prolab diagnostics: UK). A final stain of fuschin (0.1% w/v fuschin, 1% v/v ethanol, 0.5% w/v phenol; Prolab diagnostics: UK) was added to the bacteria for 1 min before visualisation under a x100 lens oil emersion light microscope (Provis, Olympus, UK).

2.2.4 Determining Colony Forming Unit Concentration from Overnight Bacteriological Cultures

Single colonies of bacteria (*E. faecalis*, *P. aeruginosa*, *S. pyogenes* and *P. mirabilis*) were grown in brain heart infusion (BHI) broth cultures overnight at 37°C (*S. pyogenes* also required 5% CO_2; *n*=4 colonies per bacteria). At 16 and 23hrs, the cultures were serially diluted and a 50µl volume spiral plated (Whitely Automatic Spiral Plater, Don Whitely Scientific Limited, UK) onto TSA or CLED agar (*P. mirabilis*) and incubated at 37°C overnight. The numbers of colonies on the agar plate were subsequently counted as per the manufacturer's instructions and the total number of colonies/ml was calculated from the counting table (WASP 2 User Manual Section 15.1, Don Whitely Scientific Limited, UK). The dilution necessary to obtain 150CFU units/ml was calculated from the colonies/ml value.

2.2.5 Bacterial Growth Curves

The growth profiles of *E. faecalis*, *P. aeruginosa*, *S. pyogenes* and *P. mirabilis* was examined in BHI broth, Roswell Park Memorial Institute (RPMI) medium supplemented with 10% (v/v) or 20% (v/v) FCS and RPMI supplemented with 10% or 20% (v/v) FCS in combination with 5%, 10% and 20% (v/v) BHI.

A single bacterial colony was grown overnight in 10ml (*E. faecalis, P. mirabilis, P. aeruginosa*) or 20ml (*S. pyogenes*) BHI medium as described in section 2.2.4. The bacterial culture was diluted in PBS to either a 0.5 McFarland standard (dilution of bacteria which has an absorbance of 0.08-0.1 at 600nm), before further diluting 1 in 100, or to 150 CFU/ml into the range of media described above. The final dilutions were added to a 48 well plate in triplicate in a total volume of 0.5 ml per well. Respective sterile media was used as background controls for each condition. The microplate reader (SPECTROstar Omega, BMG-LABTECH or FLUOstar Optima, BMG-LABTECH, Germany) was warmed to 37°C before the plates were inserted. Before each reading, the plates were shaken for 20s before the absorbance was read at 625nm. Readings were taken every 30mins until the bacterial cultures had reached stationary phase (7-14hrs).

2.2.6 Determining Cytotoxicity to BHI Using the LDH Cytotoxicity Assay

Cellular lactate dehydrogenase (LDH) release from OMLP-PCs and EFs was used as a measure of cell death in response to incubation with BHI. LDH is a stable enzyme which is released from cells upon plasma membrane damage (Drent *et al.,* 1996).

The LDH-Cytotoxicity Assay Kit (Abcam, UK) relies on LDH oxidising lactate, which produces nicotinamide adenine dinucleotide (NADH). The NADH then reacts with the WST substrate reagent to produce a colorimetric change.

OMLP-PCs and EFs (*n*=3 independent donors; all with technical triplicates) were seeded at a density of $4x10^4$ cells per well in a 96 well plate and left to settle overnight in complete medium. Subsequently, the CM was removed and the cells were incubated with 200µl of RPMI supplemented with 2mM L-glutamine, 10 or 20% (v/v) FCS and 5, 10 or 20% (v/v) BHI for 8.5hrs at 37ºC/5% CO_2. The provided cell lysis solution was added to a further three wells of cells as 'high' controls. Medium was also incubated for 8.5hrs without the presence of any cells as a 'low' control. Subsequent to incubation, the medium was removed from the cells and stored in fresh 96 well plates at 4ºC overnight. The plates were then centrifuged at 126xg for 5mins, before 10µl of medium from each well was transferred to a new 96 well plate in triplicate. One hundred microliters of the reaction buffer was added to each sample and incubated in the dark for 30mins. Ten microlitres of LDH was also added to 100µl of the reaction buffer and incubated for 30mins as a positive control. The absorbance of each well was read at 450nm and 650nm (reference wavelength). The following equation was used to determine the percentage of cytotoxic cells.

$$Cytotoxicity\ (\%) = \frac{(Test\ sample\ abs - Low\ control\ abs)}{(Hight\ control\ abs - Low\ control\ abs)}\ x\ 100$$

2.2.7 Co-culture of OMLP-PCs or EFs and Live Bacteria

OMLP-PCs (*n*=4 independent donors) at 24-30 PDs were treated +/-100 units/ml recombinant human interferon γ (rhIFNγ ; Sigma Aldrich, UK) for 7 days prior to co-culture with bacteria.

EFs (*n*=3 independent donors) and OMLP-PC +/- IFNγ (*n*=4 independent donors) were seeded into a 24 well plate at a density of $1x10^5$ cells per well in RPMI supplemented with 10% (v/v) FCS and 2mM L-glutamine (no antibiotics were added to the medium). The cells were cultured at 37°C/5% CO_2 overnight to allow adherence to the plate. Subsequent to adhesion, the medium was removed and exchanged for RPMI supplemented with 2mM L-glutamine, 10% (v/v) FCS and 20% (v/v) BHI +/- 150CFU bacteria.

The cells were co-cultured with the bacteria at 37°C/5% CO_2 until the bacteria reached midlog phase (dependant on growth curves from 150 CFU/ml). The CM was removed from the cells, serially diluted and spiral plated (onto TSA or CLED [*P. mirabilis*]) as outlined in section 2.2.4, and incubated overnight at 37°C before counting the bacterial colonies. The remaining CM was centrifuged at 14,000xg for 2mins through a Nanosep MF centrifugal device (Pall, UK) to remove bacteria and stored at -80°C.

2.2.8 Susceptibility Testing of CM from OMLP-PCs or EFs

CM samples from OMLP-PCs and EFs generated in section 2.2.7 (90µl) were cultured with 100 CFU of each bacteria (in a 10µl volume of PBS) in a 96 well plate for 16hrs at 37°C/5% CO_2. The CM was then serially diluted and spiral plated onto TSA or CLED (*P. mirabilis*) as outlined in section 1.2.5 and incubated overnight at 37°C, before the colonies were counted.

To examine whether the constitutive antibacterial properties of the CM could be diluted out, CM samples from OMLP-PCs were diluted 1:2 – 1:100 with RPMI + 10% (v/v) FCS + 20% (v/v) BHI supplemented with 2mM L-glutamine to a final volume of 90µl. One hundred CFU of bacteria was added to the CM, incubated and analysed as above.

2.2.9 Bacterial Viability Assessment with Live/Dead® BacLight™ Bacterial Viability Kit.

Replicates of the above undiluted CM samples were incubated with 100 CFU bacteria as per section 2.2.8 and stained using the Live/Dead® BacLight™ Bacterial Viability Kit (Life Technologies, UK). Briefly, cultures were centrifuged for 5mins and pellets washed in 0.85% w/v NaCl before re-suspending in 1ml of 0.85% w/v NaCl. Three microliters of the bacterial stain (1:1, part A: part B) was added to each culture for 15mins in the dark. Cultures were centrifuged and resuspended in 50µl 0.85% w/v NaCl before 5µl was mounted onto a poly-L-lysine coated glass slide under a glass coverslip using the mountant provided. Fluorescent bacteria were then visualised under a x100 lens oil emersion fluorescent microscope (Provis, Olympus, UK). Both live (green) and dead (red) bacteria were counted in a minimum of 3 fields of view per condition and percentage viability was calculated.

2.2.10 Assessment of OMLP-PCs responses to bacterial stimuli

2.2.10.1 Generation of Bacterial Supernatant and Soluble Protein Extract

A single bacterial colony was grown overnight in 10ml (*E. faecelis, P. mirabilis, P. aeruginosa*) or 20ml (*S. pyogenes*) BHI medium as described in section 2.2.4. Bacteria were diluted to 0.5 McFarland standard in BHI and a further 1:100 into 200ml of BHI. Cultures were grown until midlog phase was reached (as assessed by BHI growth curve).

2.2.10.2 Separation of Bacterial Supernatant

Cultures were centrifuged at 17,000xg for 10mins to pellet the bacteria and the supernatant decanted. The supernatant was filter sterilised using a 0.22µm syringe filter (PVDF membrane, Elkay Laboratory Porducts Ltd, UK) before freezing in aliquots at -20°C for future use.

2.2.10.3 Isolation of Soluble Bacterial Protein Fraction

The bacterial protein was extracted from the pellet using the Qproteome® Bacterial Protein Prep Kit (Qiagen Ltd, UK). Briefly, the bacterial cell walls were disrupted by cell lysis using the provided detergent, allowing the release of the soluble bacterial protein from the cell. The bacterial cells and soluble protein were then centrifuged at 14,000xg and therefore separated. The soluble protein fraction was then pelleted by centrifugation at 16,000xg and washed in ice cold acetone:water (4:1) before being re-suspended in 5ml sterile water.

2.2.10.4 Quantification of Soluble Bacterial Protein

The soluble bacterial protein was quantified using the Pierce® BCA Assay Kit (Thermo Scientific, UK). This assay is dependent on two reactions. The first is the reduction of Cu^{+} to Cu^{2+} by the peptide bonds within the protein sample. Secondly, two bicinchoninic acid (BCA) molecules chelate with a Cu^{+} ion, forming a purple coloured product which absorbs light at a wavelength of 562nm.

A standard curve was produced using known concentrations of bovine serum albumin (BSA; 0 - 2mg/ml). Both the standards and samples were incubated with the BCA solution (50:1, Reagent A:B) for 30mins at 37ºC before the absorbance was

read at 562nm (SPECTROstar Omega, BMG-LABTECH or FLUOstar Optima, BMG-LABTECH, Germany).

2.2.10.5 Visualisation of OMLP-PC Co-culture with Live Bacteria and Bacterial Products

OMLP-PCs clones at 30-34 PDs (*n*=4 independent donors) or EFs at 30-34 PDs (*n*=3 independent donors) were seeded at a density of $4x10^4$ cells/well into a 12 well plate and left to settle overnight in complete medium. The next day, medium was removed and the cells were washed with PBS before being incubated with 2ml RPMI supplemented with 2mM L-glutamine and 10% (v/v) FCS, +/- 50µg/ml of bacterial protein or +/- 20% (v/v) bacterial supernatant or +/- 20% (v/v) BHI +/- 300 CFU live bacteria. Cells were incubated at 37°C/5% CO_2 for 16hrs with images captured every 20mins in 4 fields of view/well using the Multi Label Fluorescence (MLF) Cell IQ System (CM Technologies, Finland; Gen. 2.1). At the conclusion of these time lapse experiments CM were harvested and stored at -80°C until use. The cells were lysed in the cell lysis buffer (RA1) and stored at -80°C for later RNA extraction using the Illustra RNAspin Mini RNA isolation kit (GE Healthcare, Buckinghamshire, UK).

Time-lapse images were combined and converted into videos using the Cell IQ lineage analyser software (CM Technologies, Finland; 4_v.ANA1.0_analyserdemo). Cell tracking was performed using an alternative version of the software: Cell IQ lineage analyser (4 ANA 01 TEST 2). Cells were tracked for 3hrs, as post 3hrs, live bacteria proliferated to the extent whereby visualising the cells was completely obstructed. Forty cells per well were manually tracked and the average speed over the 3 different clones tested (*n*=3 independent donors) was calculated by the Cell IQ lineage analyser software. The cell area of OMLP-PCs incubated with bacterial protein was also recorded using the Cell IQ lineage analyser software (CM Technologies, Finland; 4_v.ANA1.0_analyserdemo) after 16hrs in culture. A minimum of 40 cells were recorded per bacterial protein isolate or control medium.

2.2.10.6 Boyden Chamber Migration Assay

OMLP-PCs clones at 30-34 PDs (*n*=4 independent donors) or EFs at 30-34 PDs (*n*=3 independent donors) were serum starved in RPMI medium for 24hrs before seeding 10,000 cells / cm^2 onto a 10µg rat tail type 1 collagen (First Link, UK) coated insert (ThinCert™ cell culture insert for 24 well plate, Greiner Bio-One, UK). The lower well contained 1ml of either RPMI (control), RPMI + 10% (v/v) FCS (positive control),

RPMI + 50µg *E. faecalis* protein or RPMI + 50µg *P. aeruginosa* protein. Insert cultures were incubated at 37°C/5% CO_2 for 20hrs before cells were fluorescently stained using 8µM Calcein-AM solution (Sigma Aldrich, UK) for 45mins at 37°C/5% CO_2. Inserts were washed in PBS and submerged into a 20% (v/v) trypsin-PBS solution for 10mins at 37°C/5% CO_2. Two hundred microliters of each sample was transferred to a black Nunc™ MicroWell™ 96-Well plate (Thermo Scientific, UK) in triplicate before the fluorescence was read at an excitation wavelength of 480nm and an emission wavelength of 520nm. The fluorescence of each well was compared to the fluorescence of the control wells.

2.2.11 Statistical Analysis

All statistical analysis was performed using SPSS statistics (IBM®, UK; Version 20). Variance analysis was performed using Levene's test, where significant variability was assumed where $P \leq 0.05$. Statistical analysis for comparing means was performed using a One-way ANOVA test with a post hoc Tukey test (where equal variance) or a Games-Howell test (where variances were unequal). Statistical significance was assumed where $P \leq 0.05$.

2.3 Results

2.3.1 OMLP-PCs and EFs in culture

OMLP-PCs (n=4 independent donors) and EFs (n=3 independent donors) were expanded in complete media. Both cell types demonstrated a typical bipolar, fibroblast-like morphology at a PD 24-30 (Fig. 2.1 A-G). All OMLP-PC clones were previously phenotyped for their positive cell surface expression of CD44, CD90, CD105 and CD166 and negative expression of the haematopoietic markers CD45 and CD34 (Davies et al., 2010). No variation in the growth profiles or gene expression was noted in cells derived from different patients, or during culture.

2.3.2 Gram Staining of Bacteria

Bacteria were Gram stained monthly to ensure purity of cultures. The PGN component within the cell wall of Gram positive bacteria, *E. faecalis* (Fig. 2.2 A) and *S. pyogenes* (Fig. 2.2 B), stained purple using crystal violet stain, whilst the LPS component of the cell wall of Gram negative bacteria, *P. aeruginosa* (Fig. 2.2 C) and *P. mirabilis* (Fig. 2.2 D), stained pink with fuchsin.

2.3.3 Bacteria Growth Curves: Growth Profiles of E. faecalis, S. pyogenes, P. aeruginosa and P. mirabilis

The growth profiles for each bacterium were examined between 16 and 48hrs dependent on when the bacterial strain reached stationary phase. Further experiments would utilise the bacteria up to midlog phase, hence the complete growth profiles of each bacterium were examined to ensure transition from log into stationary phase. The growth of all bacteria was investigated in BHI and RPMI (supplemented with 2mM L-glutamine and 10 or 20% FCS) ±5, 10 or 20% BHI to establish an optimal growth medium supportive of both bacteria and OMLP-PCs/EFs. Each bacterium was added to the medium at both a 1:100 of a 0.5 McFarland standard and at 150 CFU/ml. To calculate 150 CFU of each bacteria, the total CFU/ml were determined. Bacterial cultures derived from a single CFU were taken at 16 and 23hrs and spiral plated onto appropriate agar. Colonies were counted and the total CFU/ml calculated (Table 2.1).

All bacteria displayed a standard sigmoidal growth pattern within each of the media tested. Each bacterium reached a higher optical density (OD) value within the RPMI

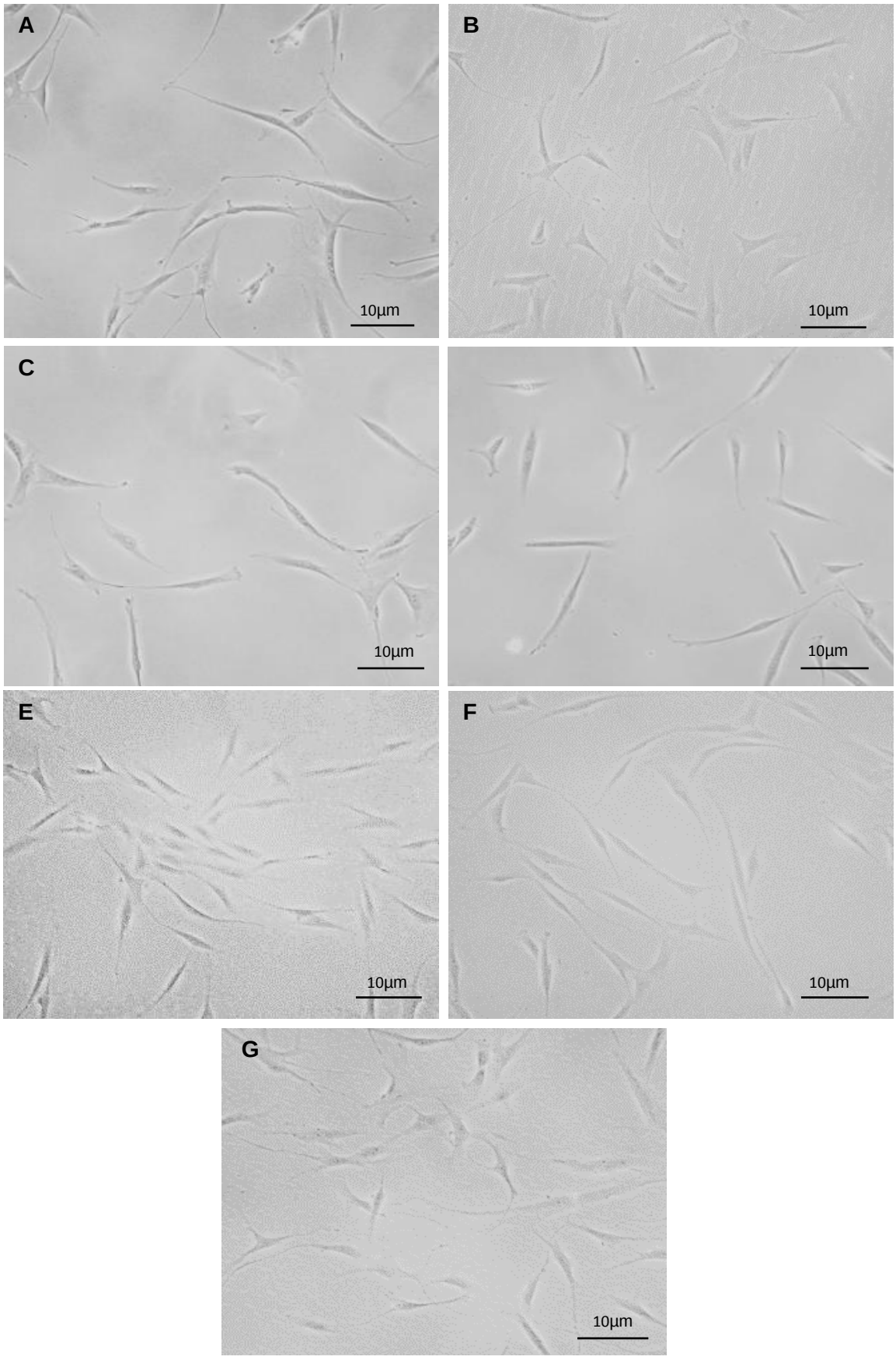

Fig. 2.1: Photomicrographs of each OMLP-PC clone and EF in culture. OMLP-PCs: (A) 17XV, (B) 11Li, (C) 2α (D) 1XXI and EFs: (E) XVI, (F) XXVIII, (G) XXI, PD 24-30. Bar = 10µm.

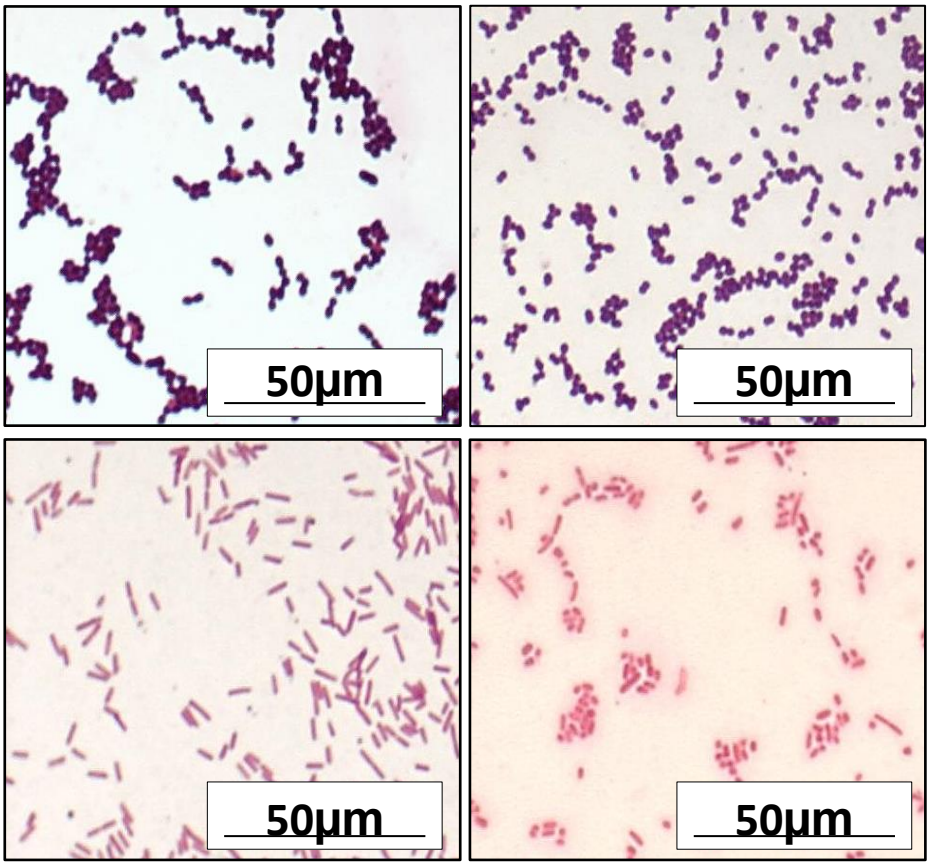

Fig. 2.2: Photomicrographs of bacteria showing Gram positive bacteria (A) *E. faecalis*, (B) *S. pyogenes*, and Gram negative bacteria (C) *P. aeruginosa*, (D) *P. mirabilis*. Bar = 50µm.

Table 2.1: Bacterial Counts at 16hrs and 23hrs

Bacteria	**16hrs bacterial count / ml**	**23hrs bacterial count / ml**
E. faecalis	**3.36×10^8** (range: $2.8 \times 10^8 – 4.05 \times 10^8$)	**3.62×10^8** (range: $2.95 \times 10^8 – 4.4 \times 10^8$)
S. pyogenes	**1.99×10^8** (range: $1.4 \times 10^8 – 2.5 \times 10^8$)	**3.225×10^7** (range: $2.7 \times 10^7 – 3.45 \times 10^7$)
P. aeruginosa	**2.71×10^9** (range: $2 \times 10^9 – 3.3 \times 10^9$)	**1.4×10^9** (range: $1.2 \times 10^9 – 1.7 \times 10^9$)
P. mirabilis	**1.402×10^9** (range: $1.06 \times 10^9 – 1.6 \times 10^9$)	**2.05×10^9** (range: $1.9 \times 10^9 – 2.2 \times 10^9$)

media when supplemented with BHI suggesting a more supportive growth environment (Supplementary Data).

The growth profiles for each bacterium in BHI alone and RPMI supplemented with 2mM L-glutamine, 10% FCS and 20% BHI are shown in Fig. 2.3 - Fig. 2.10, with the time taken to reach each growth phase in each medium detailed in Table 2.2 (growth curves for all other media are provided in Supplementary Data). These growth curves demonstrate that *E. faecalis*, *S. pyogenes*, *P. aeruginosa and P. mirabilis* all display reproducible growth patterns in both BHI and supplemented RPMI + 20% BHI. All bacteria demonstrate a lag phase with absorbance values close to 0, which develops into a short log phase (as seen by the rapid increase in absorbance values) before reaching stationary phase. The absorbance values in this last phase remain relatively constant over the time period examined.

2.3.4 Determining the Cytotoxicity of BHI to OMLP-PCs/EFs

All bacteria demonstrated improved growth in RPMI (supplemented with 2mM L-glutamine and 10% or 20% FCS) medium when further supplemented with BHI. The toxicity of BHI to OMLP-PCs and EFs was therefore examined to ensure that the BHI did not affect the viability of the mammalian cells. Cytotoxicity was measured using LDH as a marker – an active enzyme released upon cellular membrane damage.

OMLP-PCs/EFs were incubated for 8.5hrs with the RPMI medium + 10% or 20% FCS, ±5, 10 or 20% BHI before percentage cytotoxicity was calculated. No significant cytotoxicity to the different media was observed within either cell type ($P \geq 0.05$; Fig. 2.11).

Based on these findings, and those outlined in section 2.3.3, further experiments have utilised RPMI (supplemented with 2mM L-glutamine and 10% FCS) + 20% BHI as an optimal growth media for both bacterial and mammalian cells with each bacteria grown to the midlog point marked on the appropriate graphs (Fig. 2.3 - Fig. 2.10),

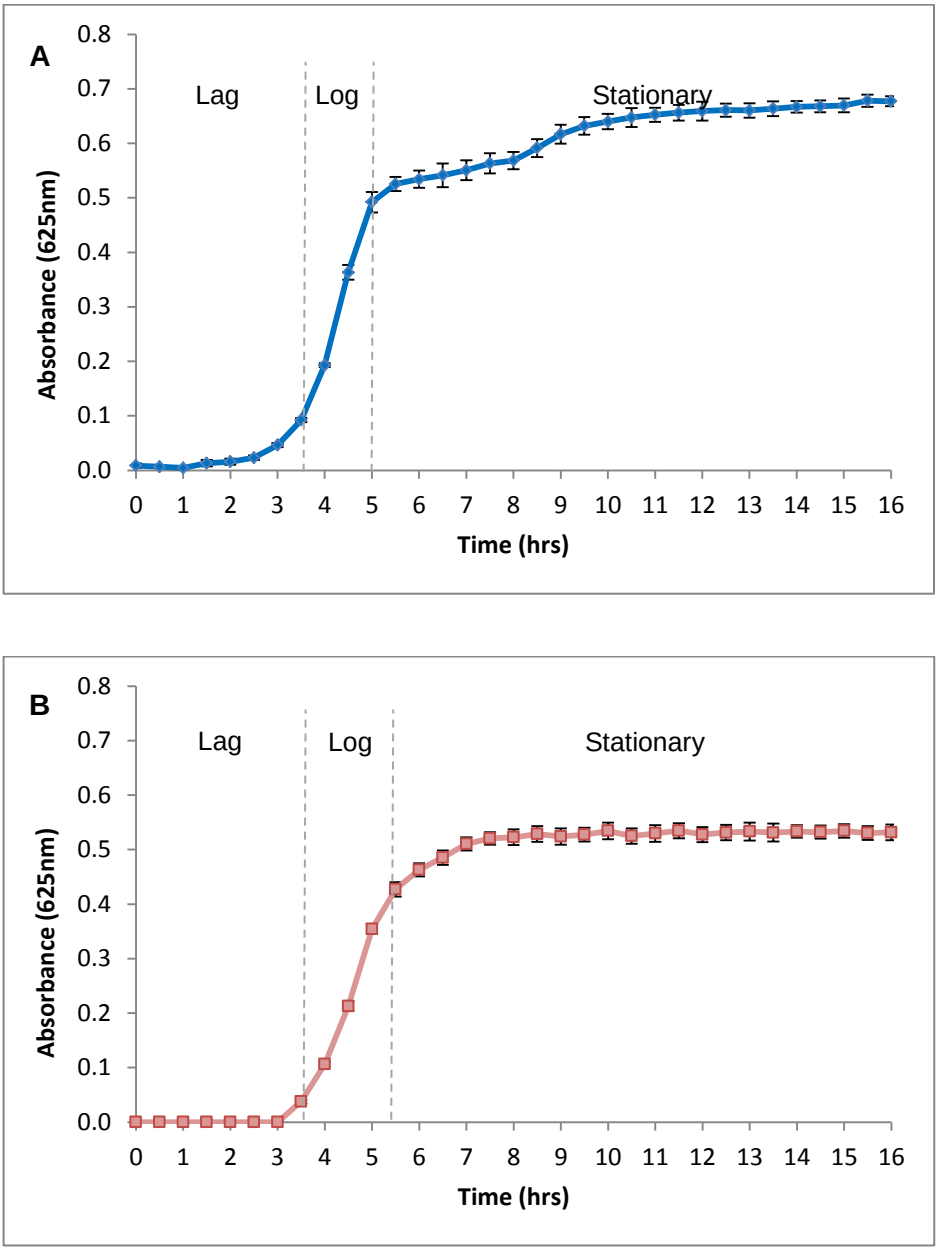

Fig. 2.3: Growth profile of *E. faecalis* from an initial inoculation of 1:100 of a 0.5 McFarland Standard over 16hrs. (A) BHI and (B) RPMI supplemented with 2mM L-glutamine, 10% FCS and 20% BHI. Data expressed as absorbance at 625nm +/- SD of the mean.

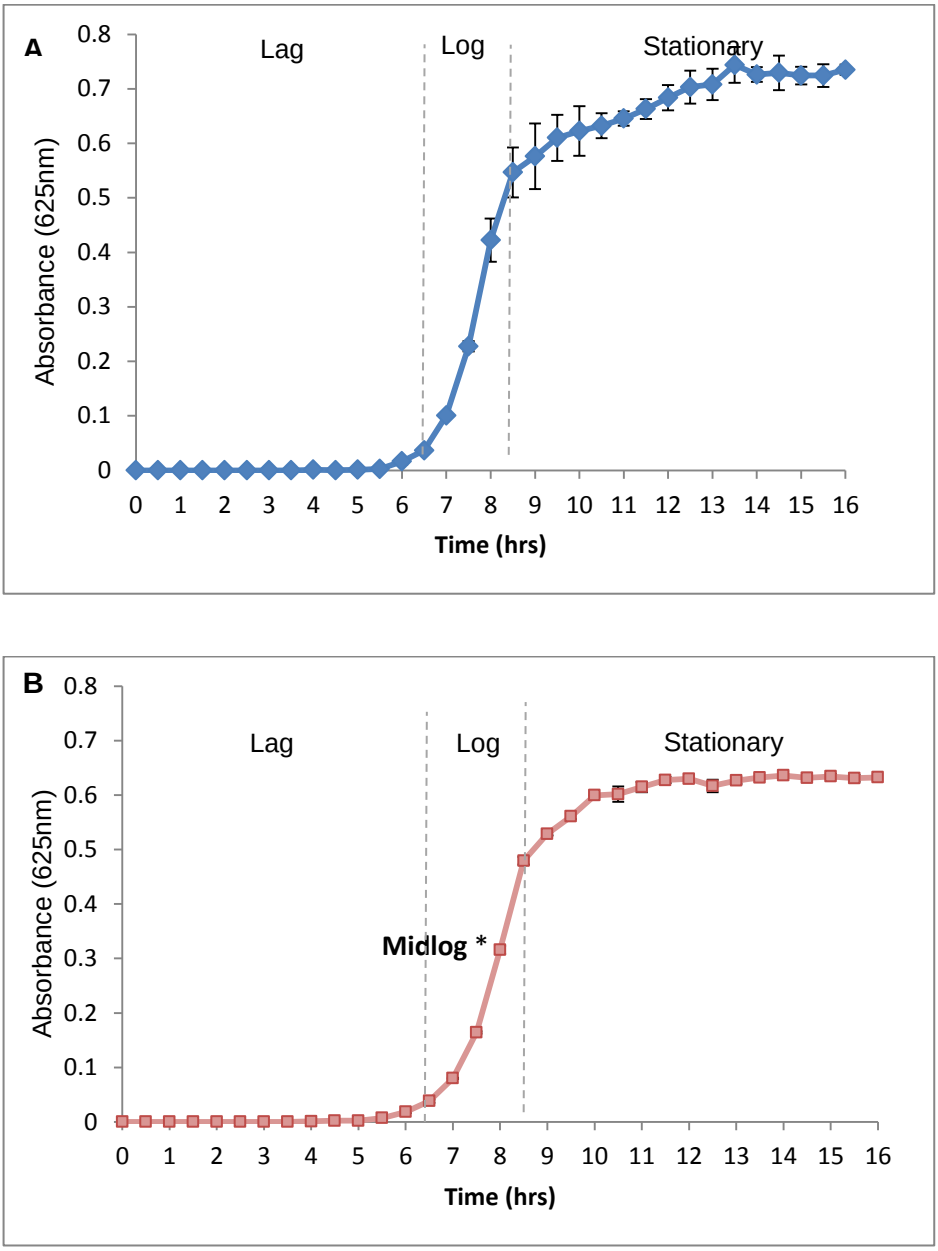

Fig. 2.4: Growth profile of *E. faecalis* from an initial inoculation of 150CFU over 16hrs. (A) BHI and (B) RPMI supplemented with 2mM L-glutamine, 10% FCS and 20% BHI. *Midlog point used in future experiments. Data expressed as absorbance at 625nm +/- SD of the mean.

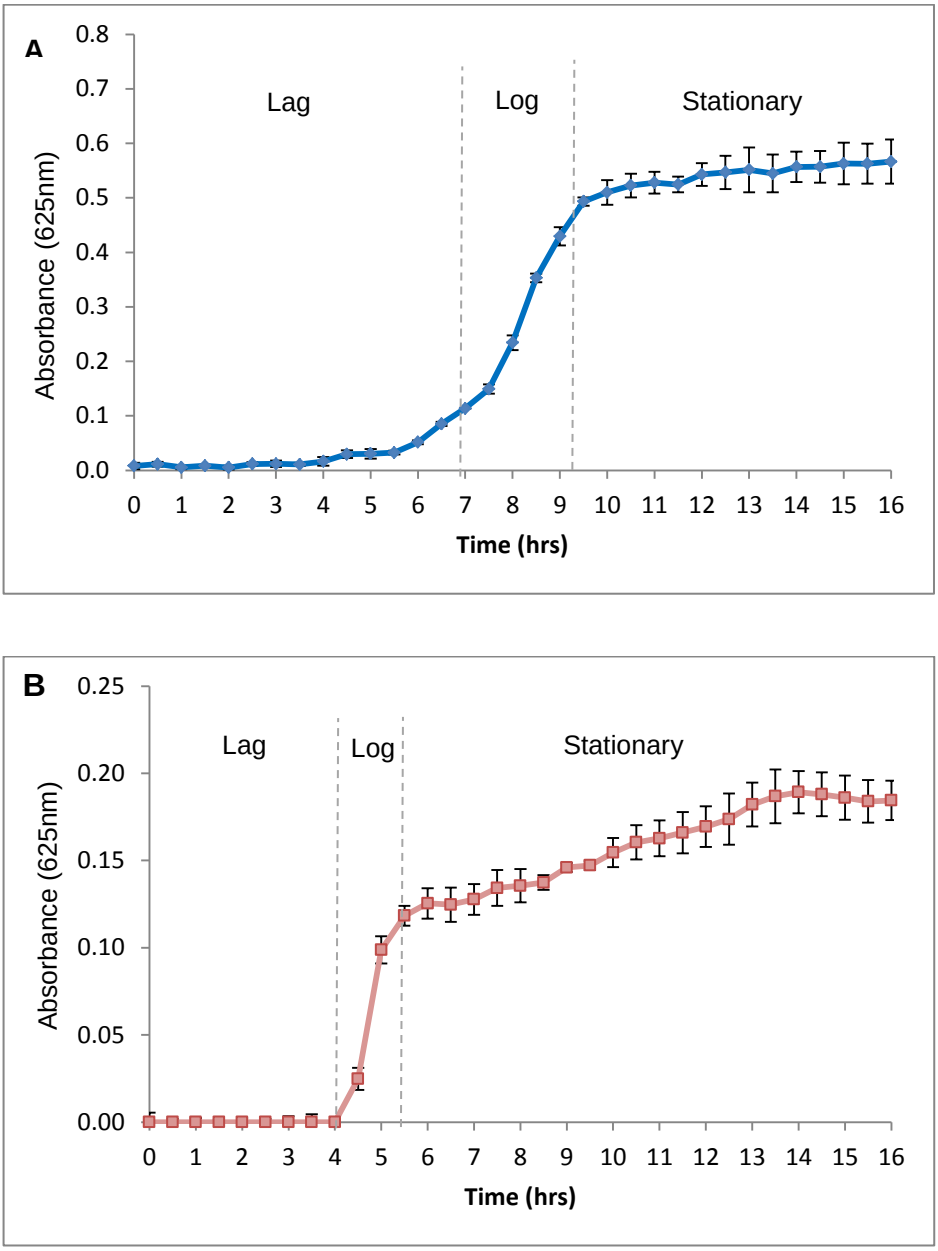

Fig. 2.5: Growth profile of *S. pyogenes* in (A) BHI and (B) RPMI supplemented with 2mM L-glutamine, 10% FCS and 20% BHI over 16hrs from an initial inoculation of 1:100 of a 0.5 McFarland. Data expressed as absorbance at 625nm +/- SD of the mean.

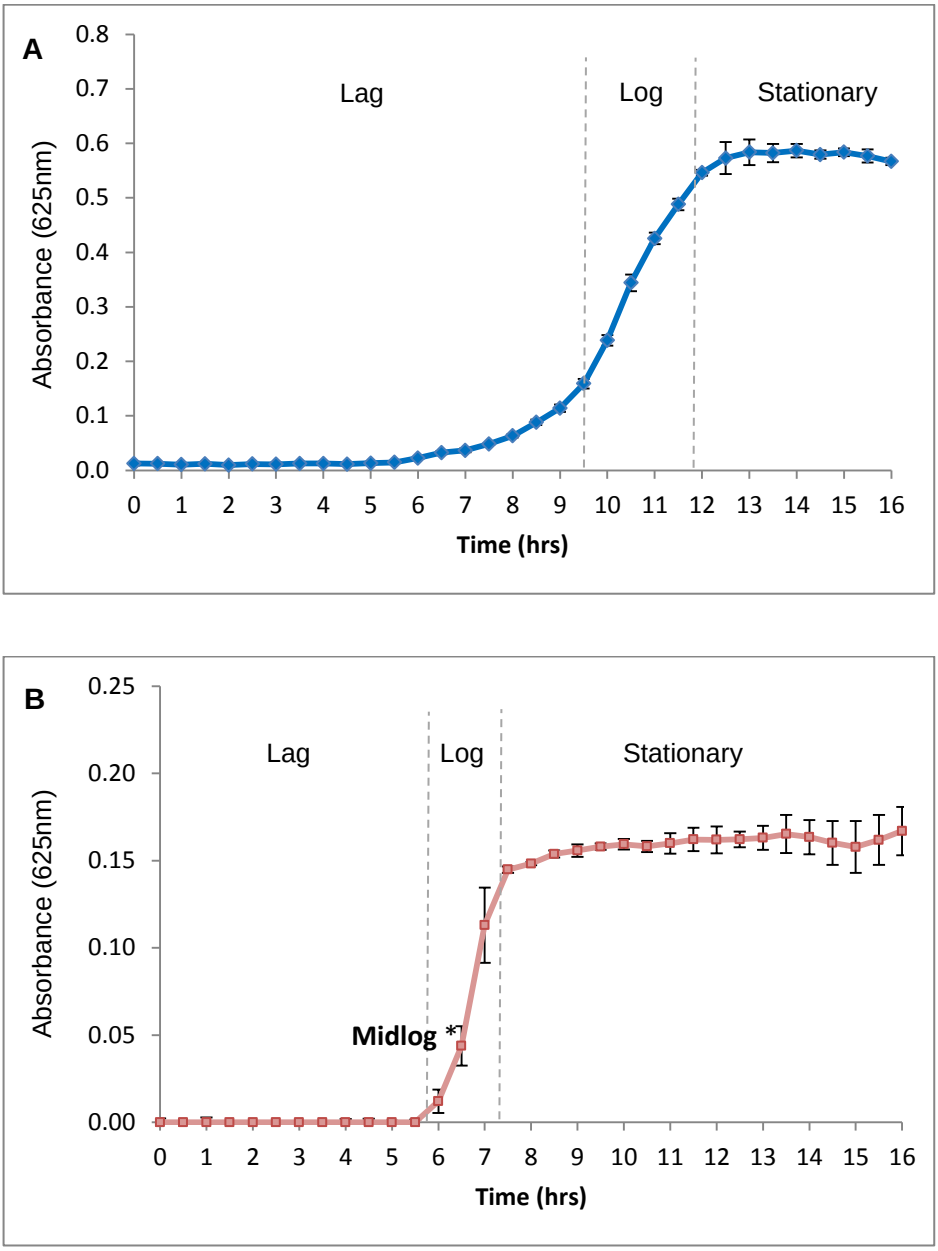

Fig. 2.6: Growth profile of *S. pyogenes* in (A) BHI and (B) RPMI supplemented with 2mM L-glutamine, 10% FCS and 20% BHI over 16hrs from an initial inoculation of 150 CFU. *Midlog point used in future experiments. Data expressed as absorbance at 625nm +/- SD of the mean.

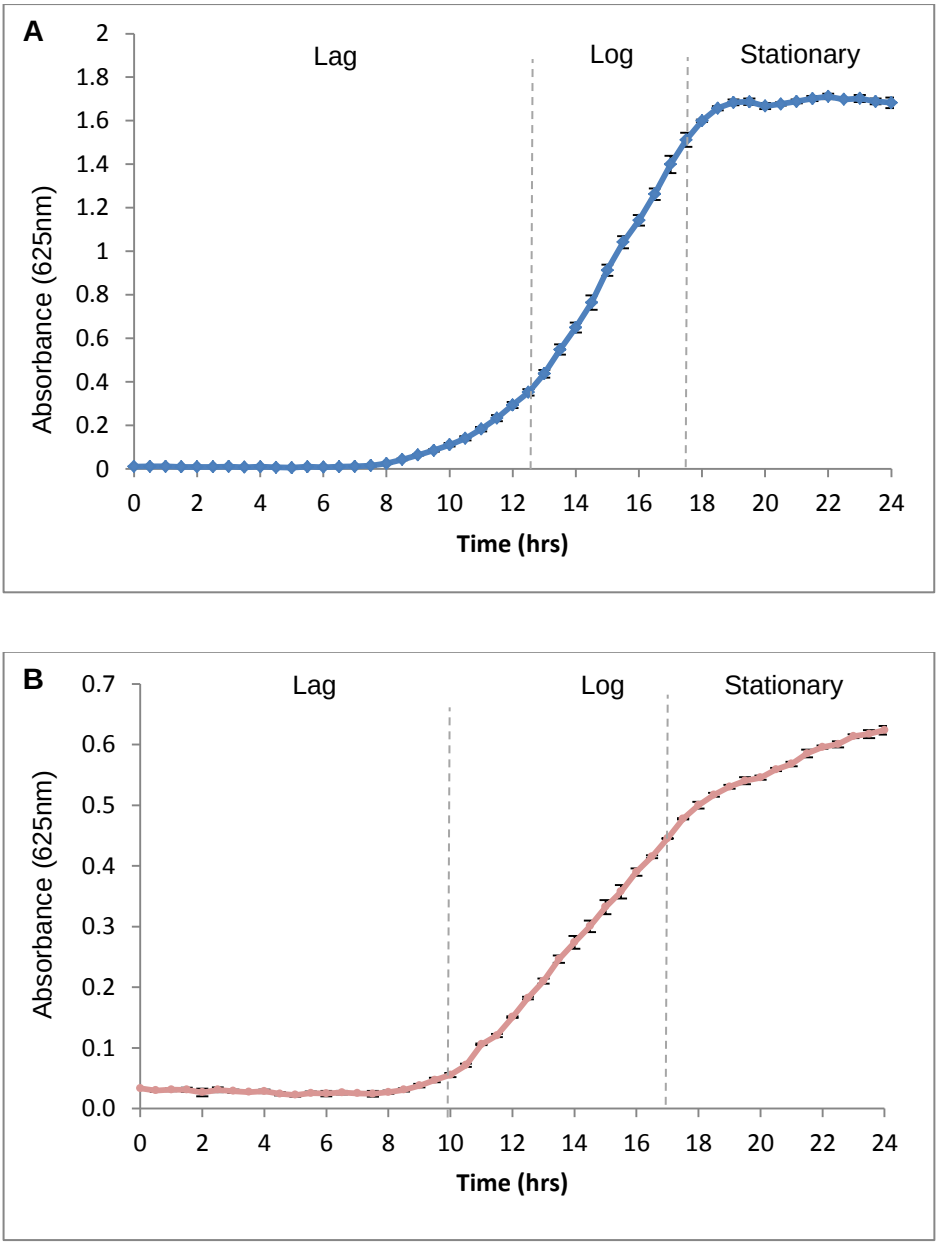

Fig. 2.7: Growth profile of *P. aeruginosa* in (A) BHI and (B) RPMI supplemented with 2mM L-glutamine, 10% FCS and 20% BHI over 24hrs from an initial inoculation of 1:100 of a 0.5 McFarland. Data expressed as absorbance at 625nm +/- SD of the mean.

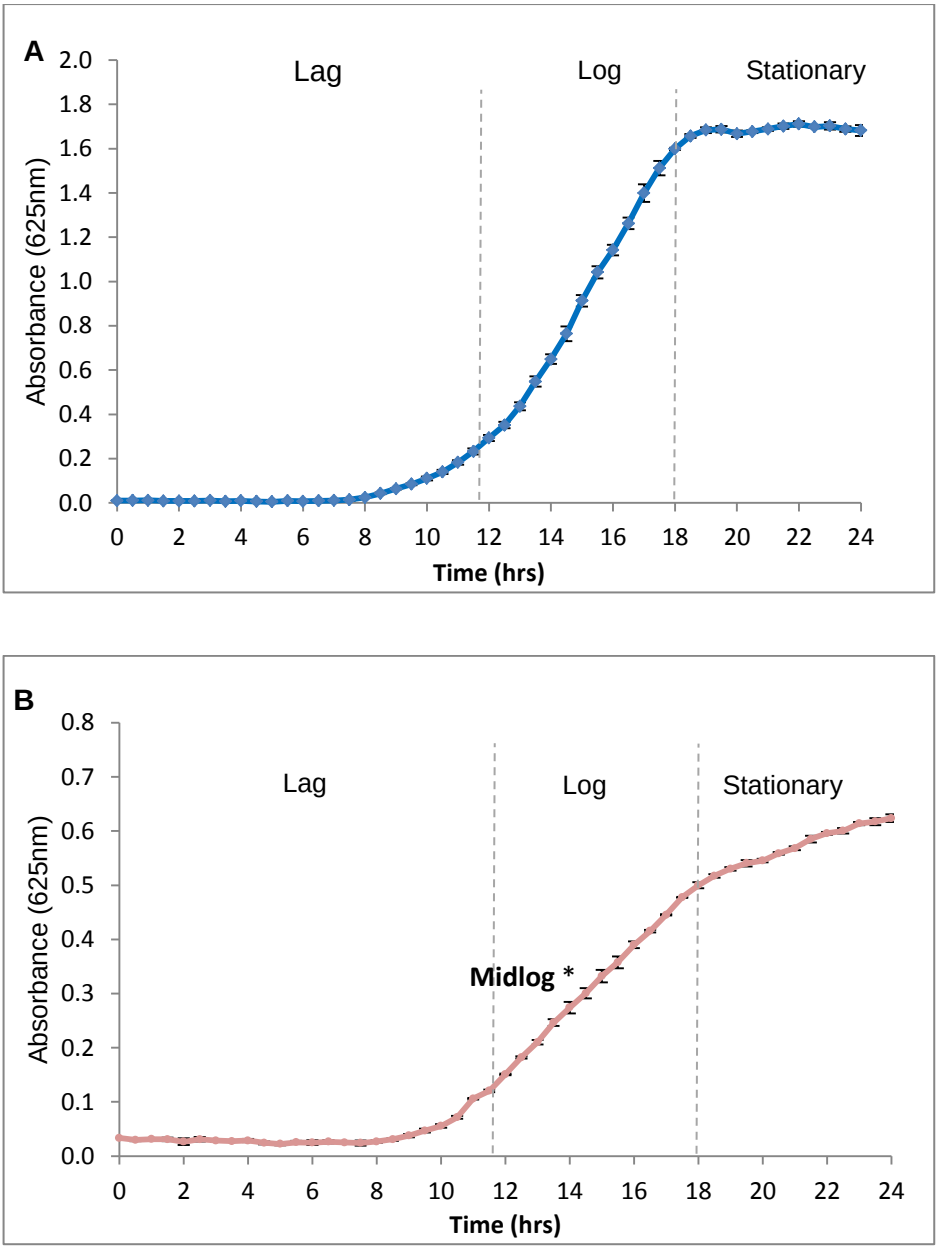

Fig. 2.8: Growth profile of *P. aeruginosa* in (A) BHI and (B) RPMI supplemented with 2mM L-glutamine, 10% FCS and 20% BHI over 24hrs from an initial inoculation of 150 CFU. *Midlog point used in future experiments. Data expressed as absorbance at 625nm +/- SD of the mean.

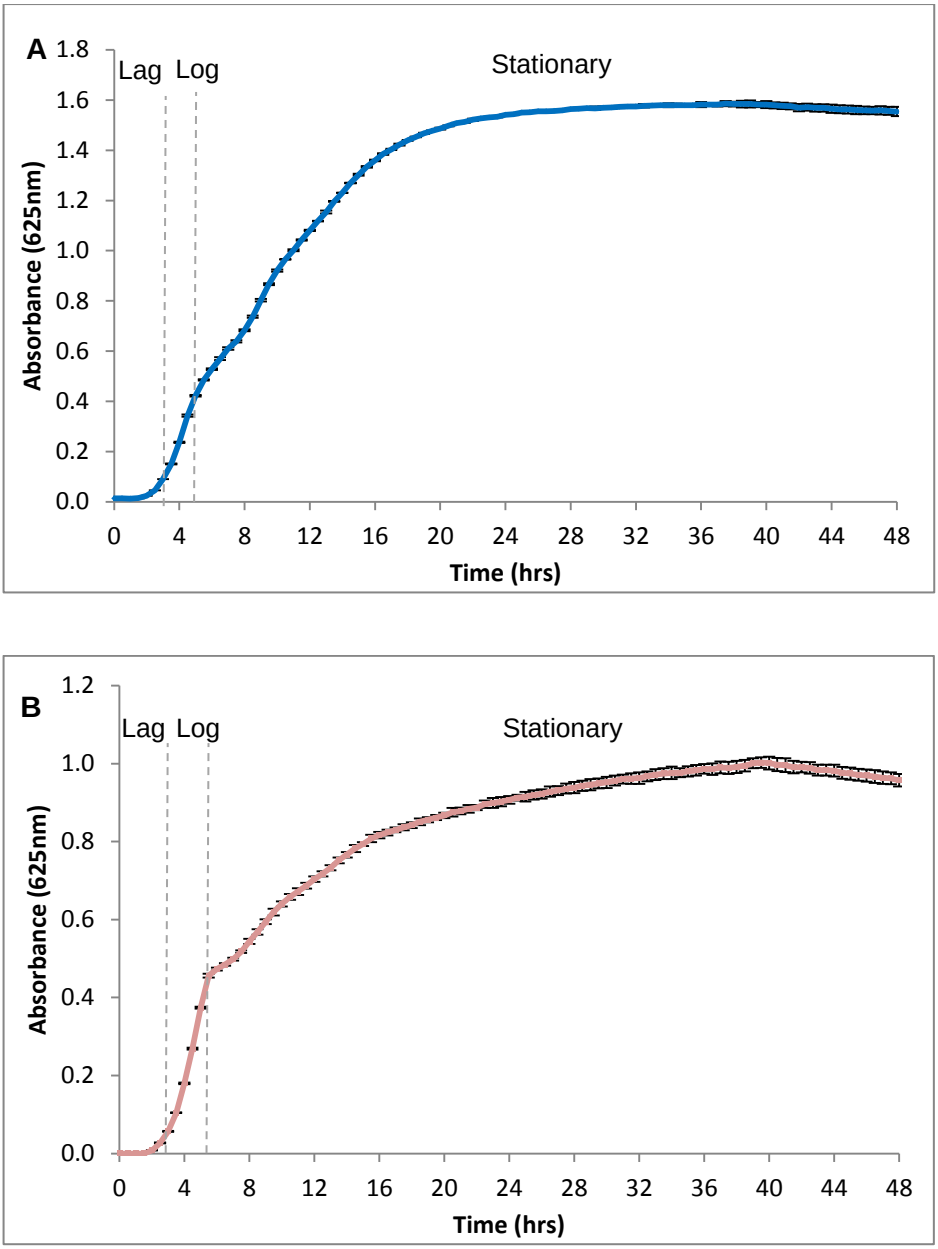

Fig. 2.9: Growth profile of *P. mirabilis* in (A) BHI and (B) RPMI supplemented with 2mM L-glutamine, 10% FCS and 20% BHI over 48hrs from an initial inoculation of 1:100 of a 0.5 McFarland. Data expressed as absorbance at 625nm +/- SD of the mean.

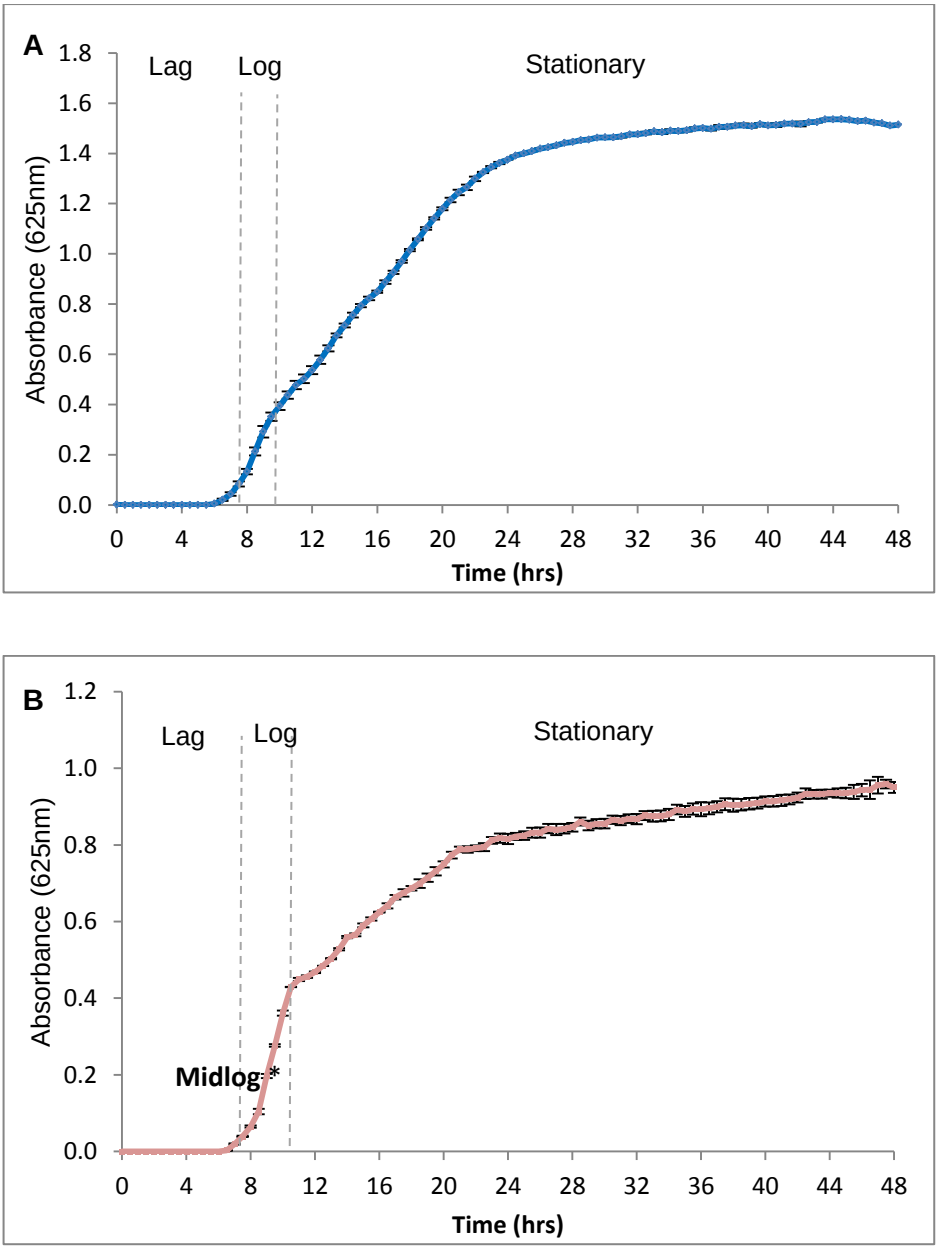

Fig. 2.10: Growth profile of *P. mirabilis* in (A) BHI and (B) RPMI supplemented with 2mM L-glutamine, 10% FCS and 20% BHI over 48hrs from an initial inoculation of 150 CFU. *Midlog point used in future experiments. Data expressed as absorbance at 625nm +/- SD of the mean.

Table 2.2: Summary of the time in which each bacterium enters the different growth phases from both an initial inoculation of 1:100 of 0.5 McFarland standard and 150CFU in both media examined.

Media and bacterial dilution	**BHI: 1:100 of 0.5 McFarland standard**		**RPMI: 1:100 of 0.5 McFarland standard**		**BHI: 150CFU**		**RPMI: 150CFU**	
Growth phase: **Bacteria**	Log (hrs)	Stationary (hrs)	Log (hrs)	Stationary (hrs)	Log (hrs)	Stationary (hrs)	Log (hrs)	Stationary (hrs)
E. faecalis	2	5	3.5	5.5	6.5	8.5	6.5	8.5
S. pyogenes	7	9.5	4	5.5	9.5	12	6	7.5
P. aeruginosa	13	17.5	10	17	12	18	12	18
P. mirabilis	3	5	3	5	7	10	8	11

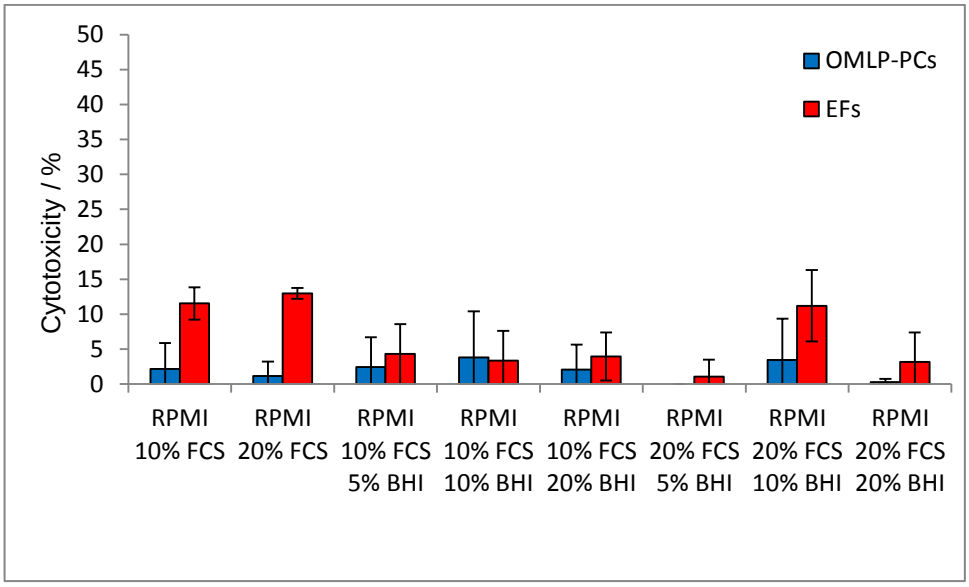

Fig. 2.11: The effect of RPMI supplemented with 10% or 20% FCS +/- BHI 5%, 10% or 20% on the viability of OMLP-PCs (*n*=4 independent donors) and EFs (*n*=3 independent donors) as measured by the release of LDH from the cells. Percentage viability calculated from a positive control of lysed cells with 100% cytotoxicity. Data expressed as percentage cytotoxicity +/- SD of the mean.

2.3.5 OMLP-PCs Suppress the Growth of Gram positive and Gram Negative Bacteria in Co-culture.

OMLP-PCs or EFs were co-cultured in direct contact with bacteria to determine whether oral mucosa cells possess antibacterial properties and whether this effect is specific to the PCs. Live bacteria (*E. faecalis, S. pyogenes*, *P. aeruginosa, and P. mirabilis*) were co-cultured with EFs or OMLP-PCs (pre-treated ± IFNγ for 7 days) for 8, 7, 14 and 9hrs respectively to replicate the time required for each bacterium to normally reach midlog phase. Subsequently the CM (containing the bacteria) was aspirated and spiral plated onto agar to assess bacterial growth.

Data within Fig. 2.12 is expressed as percentage bacterial growth compared to bacteria only controls (set at 100%). Bacterial growth in the presence of EFs did not significantly differ from control conditions ($P \geq 0.05$; Fig. 2.12 A-D). In contrast OMLP-PCs significantly decreased the percentage bacterium growth compared controls ($P \leq 0.01$; Fig. 2.12 A-D). This effect was seen irrespective of pre-treatment with IFNγ or Gram classification ($P \leq 0.01$; Fig. 2.12 A-D).

2.3.6 OMLP-PCs Constitutively Suppress the Growth of Bacteria through the Release of Soluble Factors

CM generated from section 2.2.7 was incubated with 100 CFU of each bacterium overnight (independent of the presence of any mammalian cells). Cultures were serially diluted and spiral plated onto agar before bacterial colonies were counted.

CM from OMLP-PCs significantly decreased the growth of each bacterium ($P \leq 0.001$), irrespective of whether this CM was derived from cells which had previously been stimulated by IFNy and/or bacterial exposure or not (Fig. 2.13 A, B and Fig. 2.14 A, B). Neither the CM from EFs (+/- bacterial exposure) or bacterial supernatants had any effect on bacterial growth (Fig. 2.13 A, B and Fig. 2.14 A, B). CM derived from OMLP-PCs which had previously been exposed to *S. pyogenes* had a further significant effect on decreasing bacterial growth ($P \leq 0.001$; Fig. 2.13 B).

2.3.7 OMLP-PC Secretome Reduces Bacterial Growth via a Bacteriostatic Mechanism

CM generated from section 2.2.7 was incubated with 100CFU of each bacterium overnight. Cultures were stained using the Live/Dead® BacLight™ Bacterial Viability Kit. Bacteria were counted and percentage viability calculated. Fig. 2.15 – 2.18

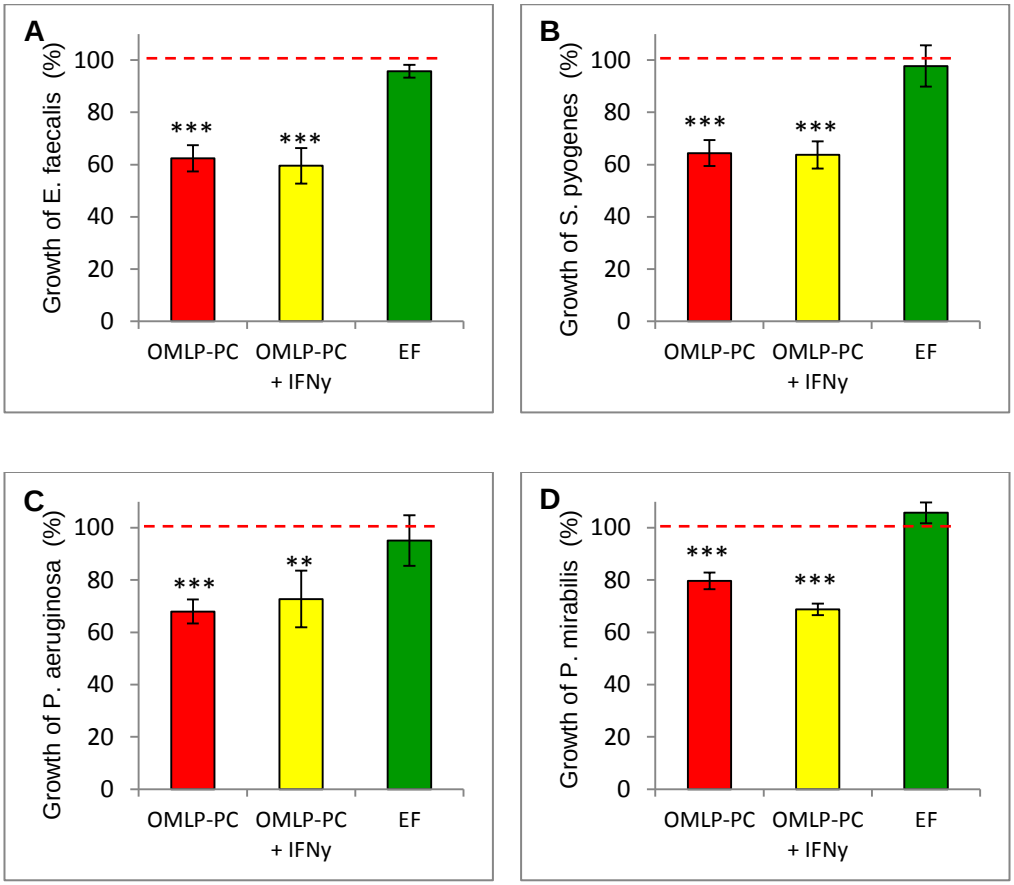

Fig. 2.12: The effect of OMLP-PCs on the growth of bacteria in co-culture. The growth of (A) *E. faecalis*, (B) *S. pyogenes*, (C) *P. aeruginosa* and (D) *P. mirabilis* after incubation with OMLP-PCs (n=4) or EFs (n=3). Data expressed as percentage bacterial growth +/- SD of the mean with bacteria only controls set to 100%. ** $P \leq 0.01$ *** $P \leq 0.001$

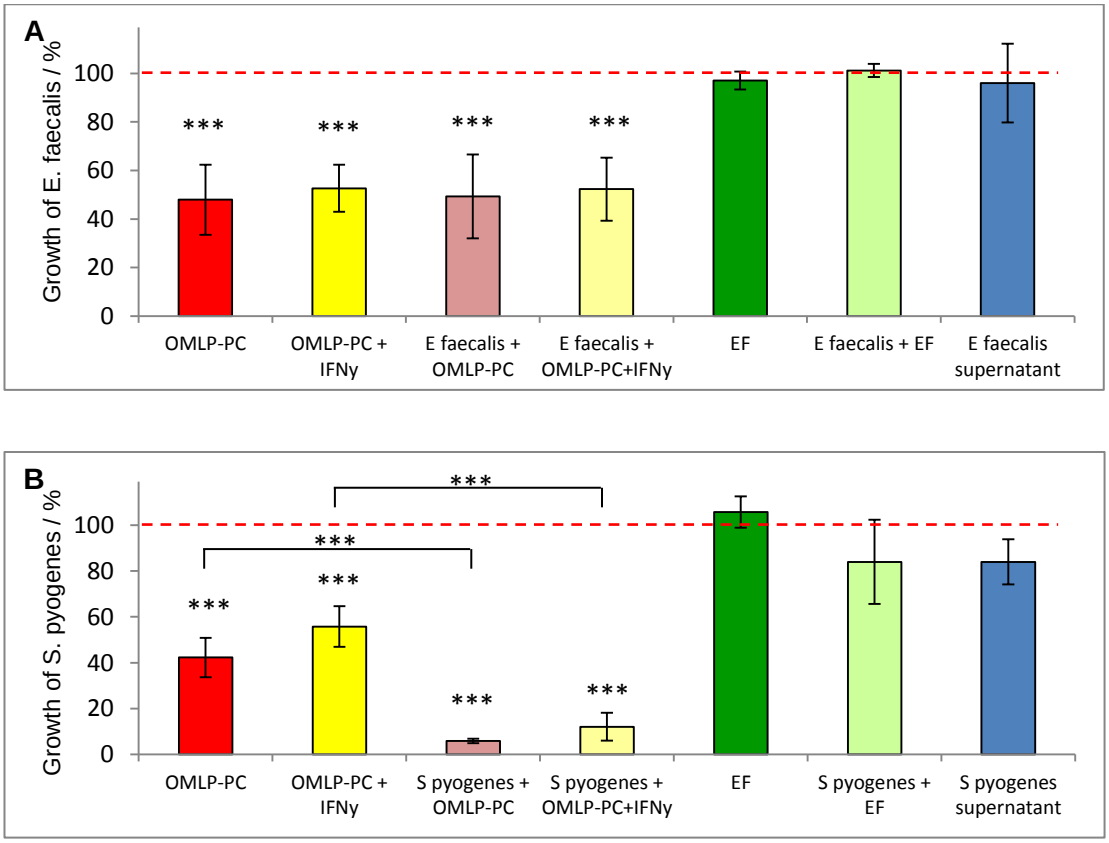

Fig. 2.13: The effect of CM from OMLP-PCs on the growth of Gram positive bacteria. The growth of (A) *E. faecalis* and (B) *S. pyogenes* after incubation with CM from OMLP-PCs (n=4), EFs (n=3) or bacterial supernatant (n=3). Data expressed as percentage bacterial growth +/- SD of the mean with bacteria only controls set to 100%. Statistics are compared to the bacteria only control unless otherwise stated. ***P≤0.001

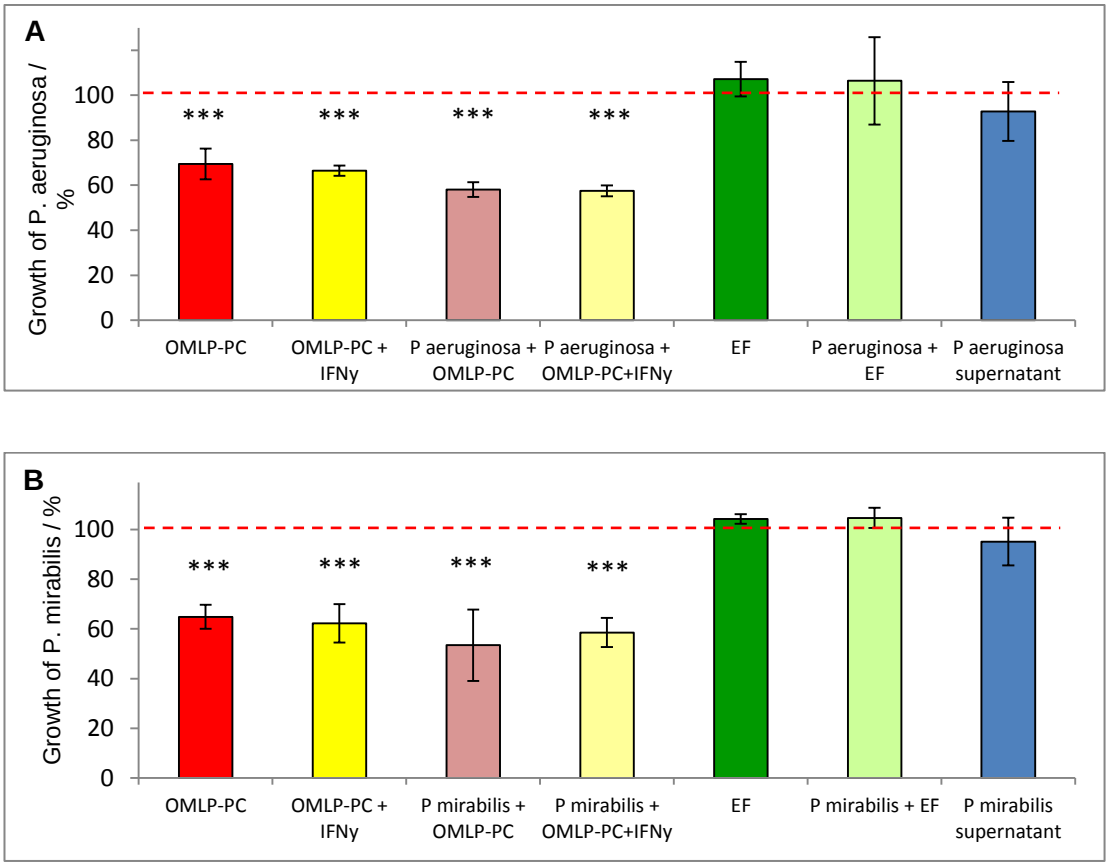

Fig. 2.14: The effect of CM from OMLP-PCs on the growth of Gram negative bacteria. The growth of (A) P. aeruginosa and (B) P. mirabilis after incubation with CM from OMLP-PCs (n=4), EFs (n=3) or bacterial supernatant (n=3). Data expressed as percentage bacterial growth +/- SD of the mean with bacteria only controls set to 100%. Statistics are compared to the bacteria only control. ***P≤0.001

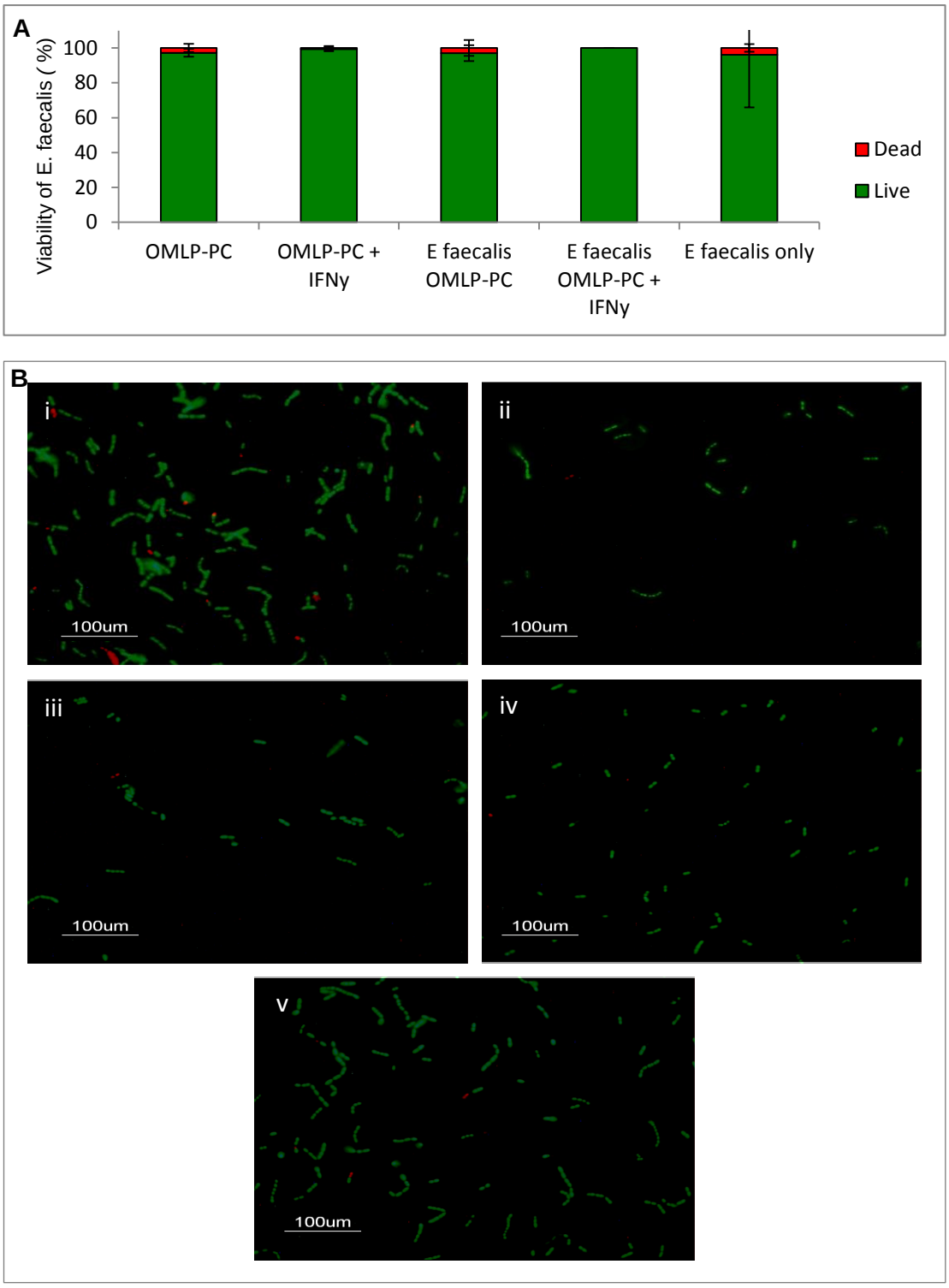

Fig. 2.15: Percentage viability of *E. faecalis* after incubation with CM from OMLP-PCs. (A) Percentage of live (green) and dead (red) bacterial cells after incubation with CM derived from OMLP-PCs (n=4). Data expressed as percentage of bacterial cells +/- SD of the mean. Representative images (B) for *E. faecalis* incubated with CM from (i) OMLP-PCs, (ii) OMLP-PCs + IFNγ, (iii) *E. faecalis* primed OMLP-PCs, (iv) *E. faecalis* primed OMLP-PCs + IFNγ, (v) no medium (*E. faecalis* only control).

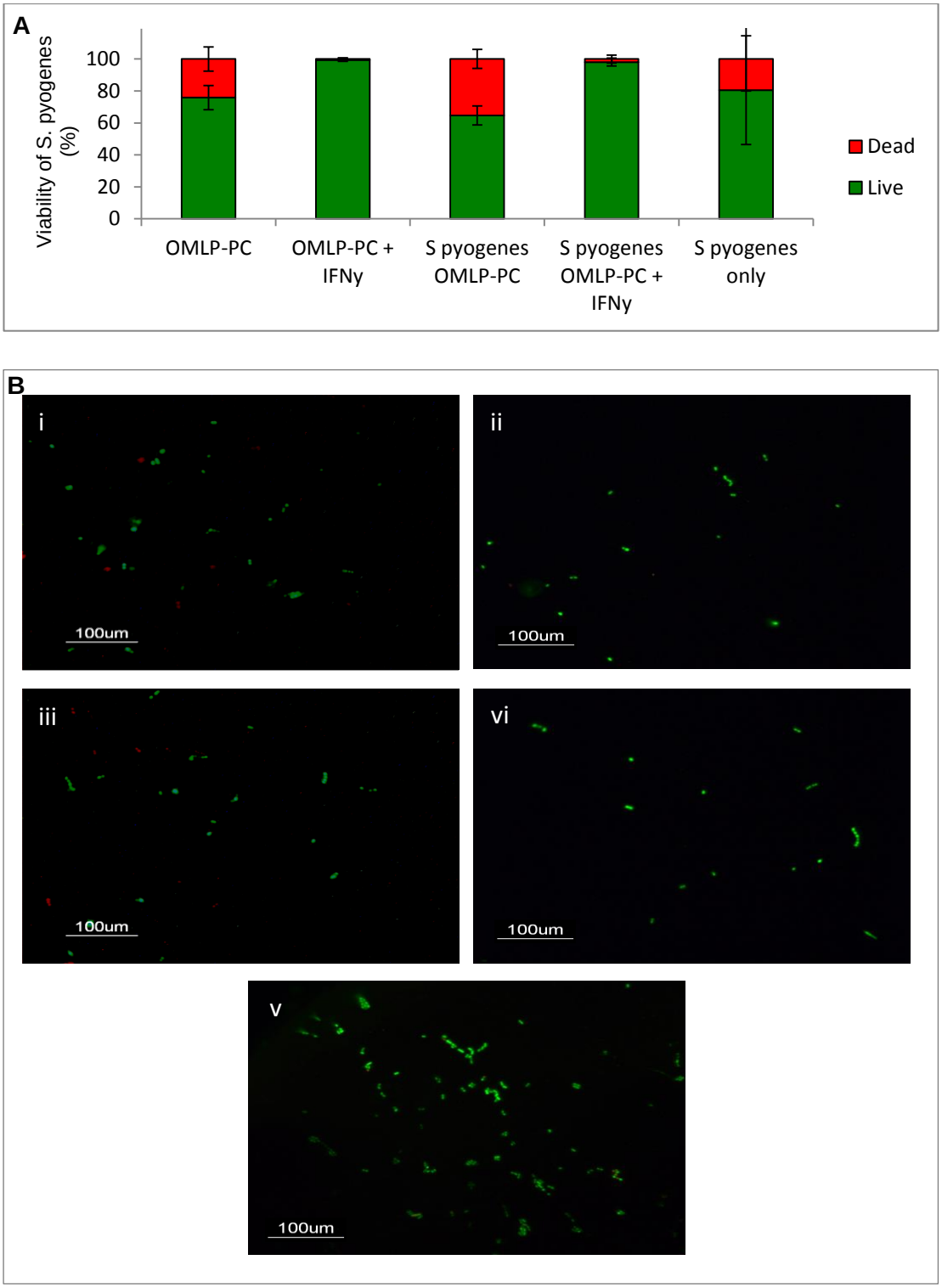

Fig. 2.16: Percentage viability of *S. pyogenes* after incubation with CM from OMLP-PCs. (A) Percentage of live (green) and dead (red) bacterial cells after incubation with CM derived from OMLP-PCs (n=4). Data expressed as percentage of bacterial cells +/- SD of the mean. Representative images (B) for *S. pyogenes* incubated with CM from (i) OMLP-PCs, (ii) OMLP-PCs + IFNγ, (iii) *S. pyogenes* primed OMLP-PCs, (iv) *S. pyogenes* primed OMLP-PCs + IFNγ, (v) no medium (*S. pyogenes* only control).

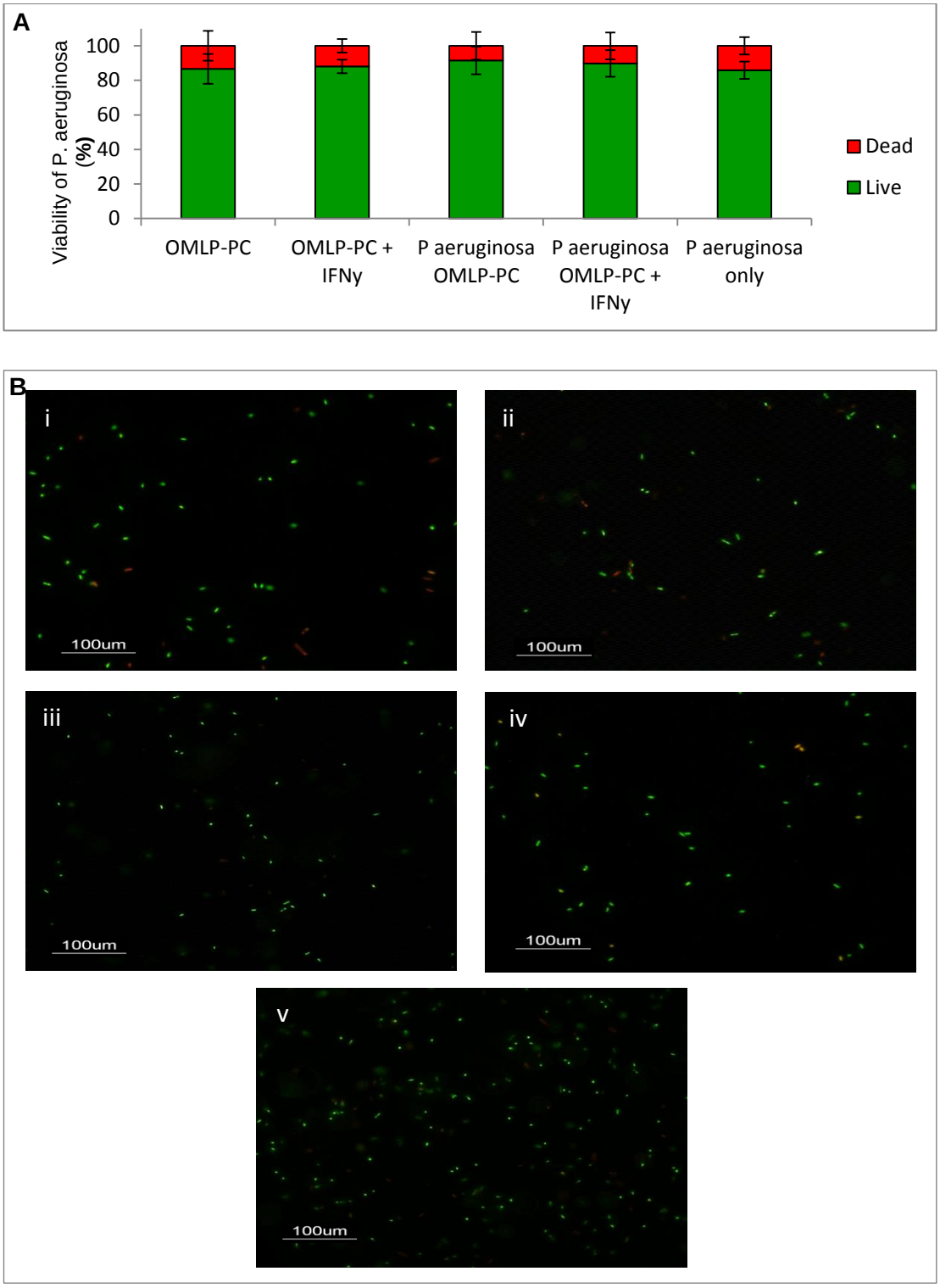

Fig. 2.17: Percentage viability of *P. aeruginosa* after incubation with CM from OMLP-PCs. (A) Percentage of live (green) and dead (red) bacterial cells after incubation with CM derived from OMLP-PCs (n=4). Data expressed as percentage of bacterial cells +/- SD of the mean. Representative images (B) for *P. aeruginosa* incubated with CM from (i) OMLP-PCs, (ii) OMLP-PCs + IFNγ, (iii) *P. aeruginosa* primed OMLP-PCs, (iv) *P. aeruginosa* primed OMLP-PCs + IFNγ, (v) no medium (*P. aeruginosa* only control).

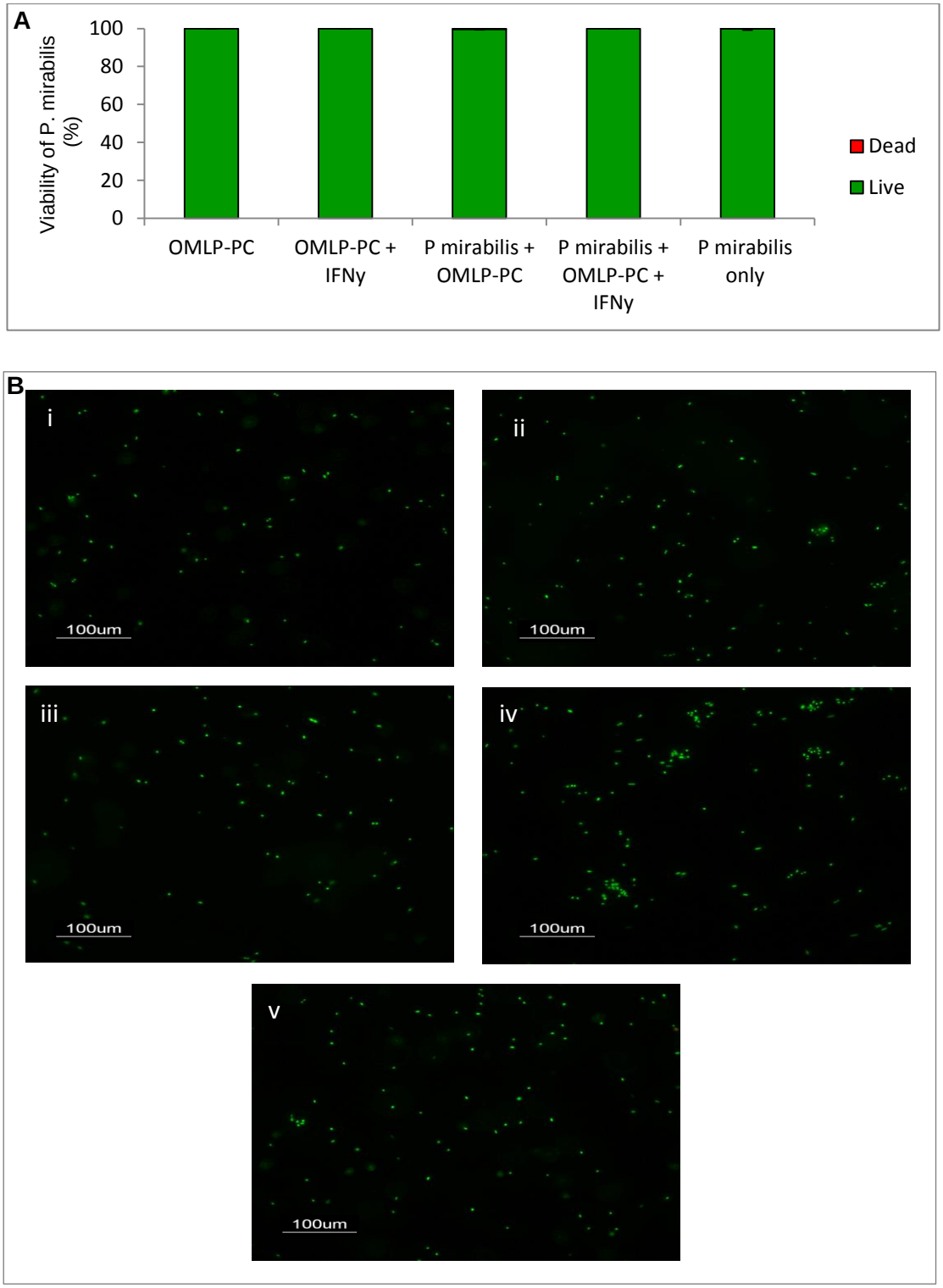

Fig. 2.18: Percentage viability of *P. mirabilis* after incubation with CM from OMLP-PCs. (A) Percentage of live (green) and dead (red) bacterial cells after incubation with CM derived from OMLP-PCs (n=4). Data expressed as percentage of bacterial cells +/- SD of the mean. Representative images (B) for *P. mirabilis* incubated with CM from (i) OMLP-PCs, (ii) OMLP-PCs + IFNγ, (iii) *P. mirabilis* primed OMLP-PCs, (iv) *P. mirabilis* primed OMLP-PCs + IFNγ, (v) no medium (*P. mirabilis* only control).

demonstrate that the bacterial viability (live:dead ratio) was not adversely affected by exposure to CM derived from OMLP-PCs when compared to that of bacteria only cultures ($P \geq 0.05$; Fig. 2.15 – Fig. 2.18) suggesting that suppression of bacterial growth by OMLP-PC CM occurs through a bacteriostatic rather than bacteriocidal effect.

2.3.8 OMLP-PCs Antibacterial Factors are Dose Dependent

CM samples derived from section 2.2.7 were diluted up to 1 in 100 into RPMI (supplemented with 2mM L-glutamine and 10% FCS and 20% BHI). Diluted samples were incubated with 100CFU of each bacterium for 16hrs before spiral plating onto agar and colonies counted.

Undiluted CM from OMLP-PCs (+/- IFNy, +/- bacterial exposure) significantly decreased the growth of each bacterium as in section 2.3.6 ($P \leq 0.01$; Fig. 2.19 – Fig. 2.22), with medium derived from OMLP-PCs exposed to *S. pyogenes* further decreasing the growth of *S. pyogenes* (Fig. 2.20). Bacterial growth continued to be significantly decreased when the CM samples were diluted 1 in 2 and 1 in 5 ($P \leq 0.01$), however further dilutions of 1 in 10 and 1 in 100 of the samples did not cause a significant effect on bacterial growth ($P \geq 0.05$; Fig. 2.19 – Fig. 2.22), confirming the dose-dependent effect of the OMLP-PCs.

2.3.9 OMLP-PCs Respond to Bacterial Stimuli

2.3.9.1.1 OMLP-PCs Reduce Their Migratory Speed When Exposed to Live Bacteria or Bacterial Supernatant

OMLP-PCs were incubated for 16hrs with bacterial protein, bacterial supernatant or live bacteria, with images of OMLP-PCs (n=4) or EFs (n=3) taken every 20mins to investigate the behaviour of the cells when cultured with live bacteria or their products. The migratory speed of the cells was determined (Fig. 2.23 – Fig. 2.26).

Cells were tracked over a 3hr period as after this time, the view of those incubated with bacteria were obstructed by dividing bacteria. No notable changes in cell

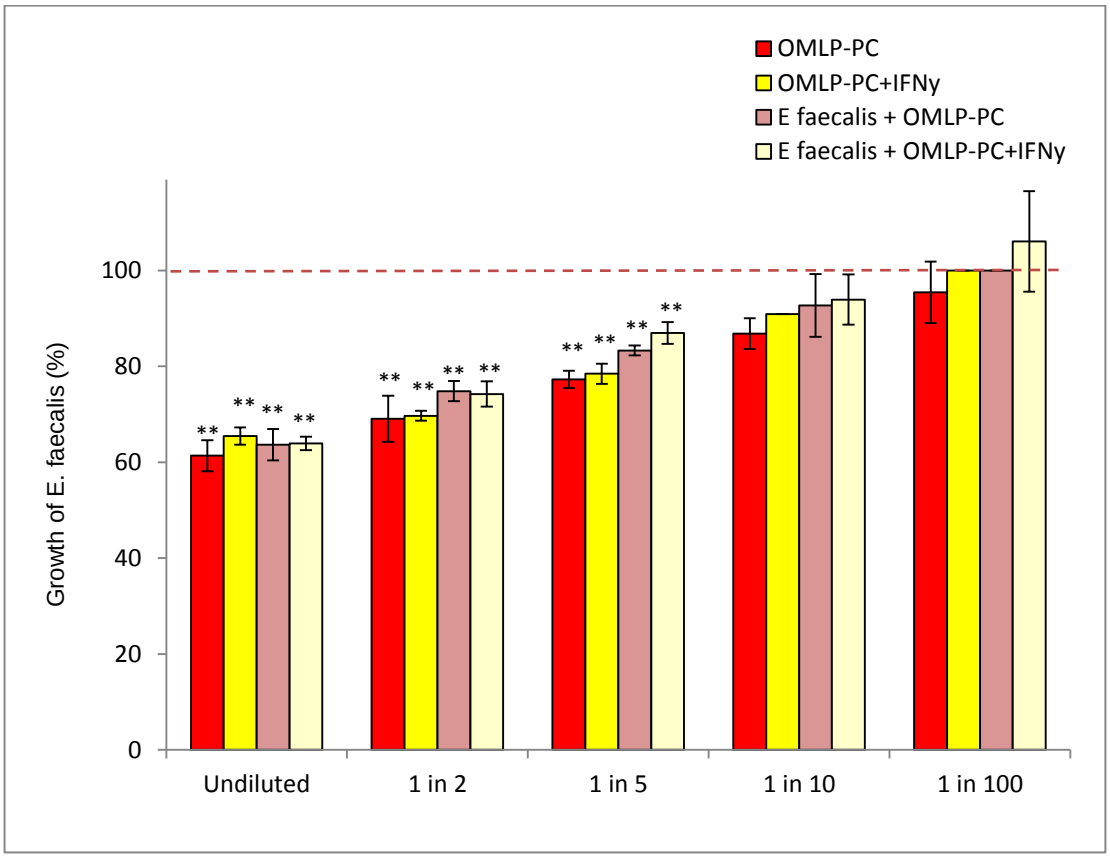

Fig. 2.19: The effect of a dilution series of CM from OMLP-PCs on the growth of *E. faecalis*. Percentage of *E. faecalis* after incubation with CM (n=3) from undiluted to 1 in 100. Data expressed as percentage bacterial growth +/- SD of the mean with *E. faecalis* only controls set to 100%, represented by the red dotted line. All statistics compared to *E. faecalis* only control. **P≤0.01.

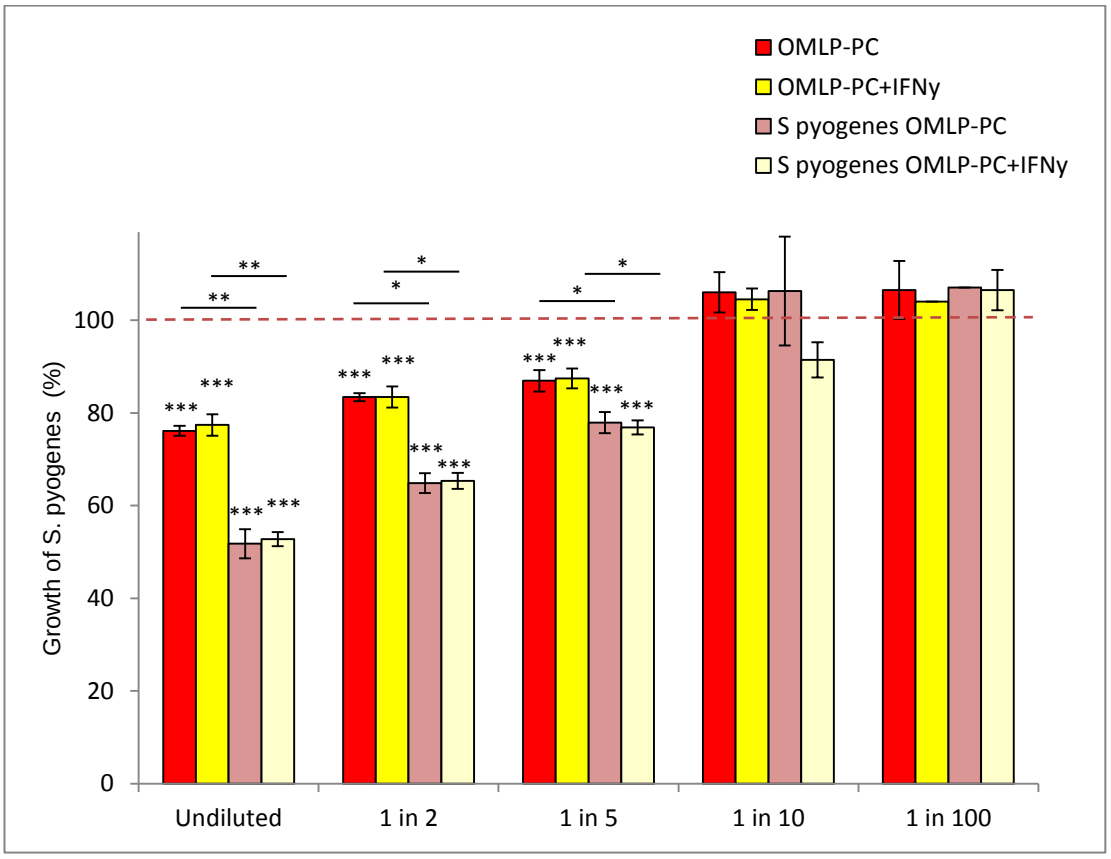

Fig. 2.20: The effect of a dilution series of CM from OMLP-PCs on the growth of *S. pyogenes*. Percentage of *S. pyogenes* after incubation with CM (n=3) from undiluted to 1 in 100. Data expressed as percentage bacterial growth +/- SD of the mean with *S. pyogenes* only controls set to 100%, represented by the red dotted line. All Statistics compared to *S. pyogenes* only control unless otherwise stated. *P≤0.05, **P≤0.01, ***P≤0.001.

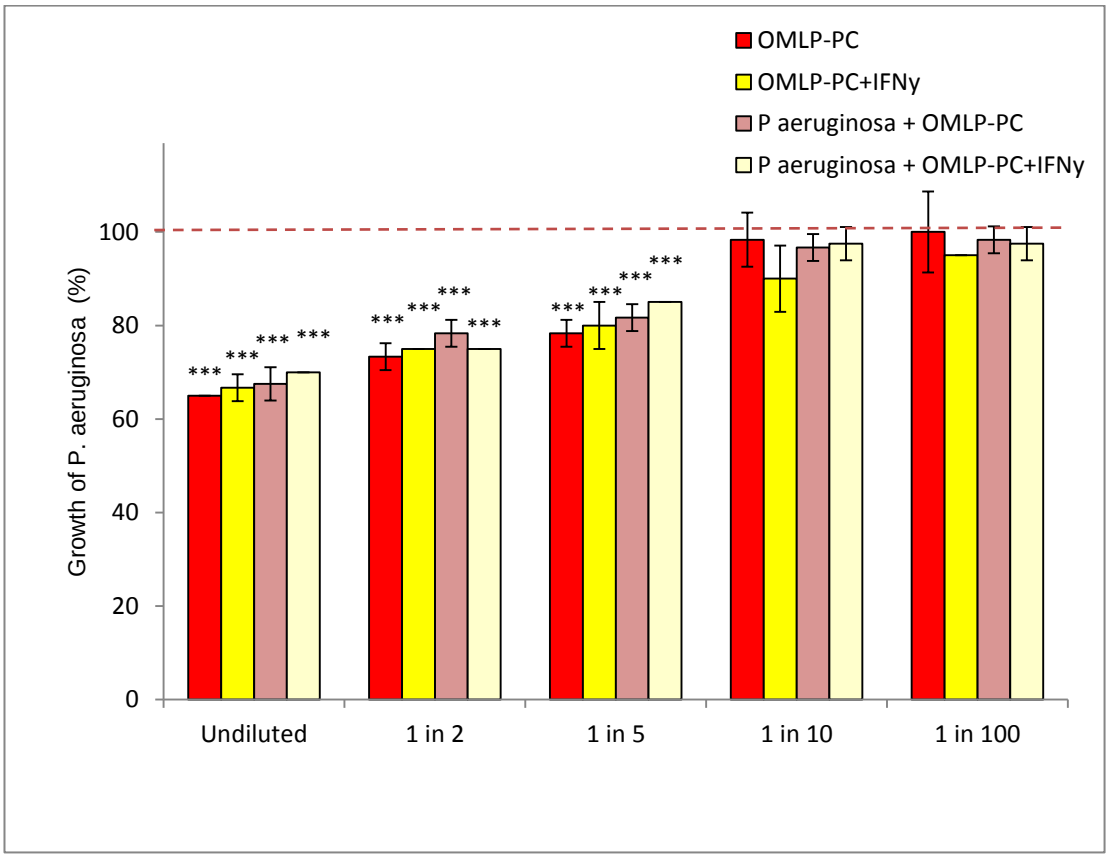

Fig. 2.21: The effect of a dilution series of CM from OMLP-PCs on the growth of *P. aeruginosa*. Percentage of *P. aeruginosa* after incubation with CM (n=3) from undiluted to 1 in 100. Data expressed as percentage bacterial growth +/- SD of the mean with *P. aeruginosa* only controls set to 100%. Statistics compared to *P. aeruginosa* only control. ***P≤0.001.

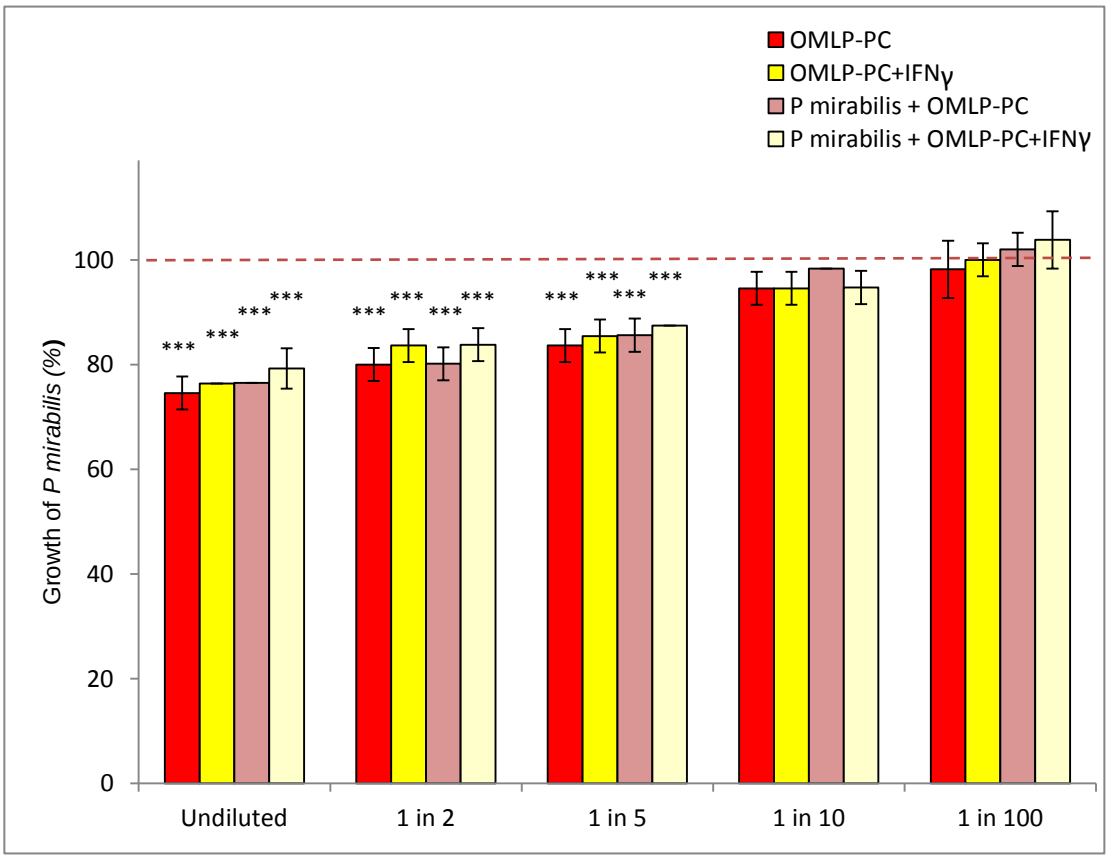

Fig. 2.22: The effect of a dilution series of CM from OMLP-PCs on the growth of *P. mirabilis*. Percentage of *P. mirabilis* after incubation with CM (n=3) from undiluted to 1 in 100. Data expressed as percentage bacterial growth +/- SD of the mean with *P. mirabilis* only controls set to 100%. Statistics compared to *P. mirabilis* only control. ***P≤0.001.

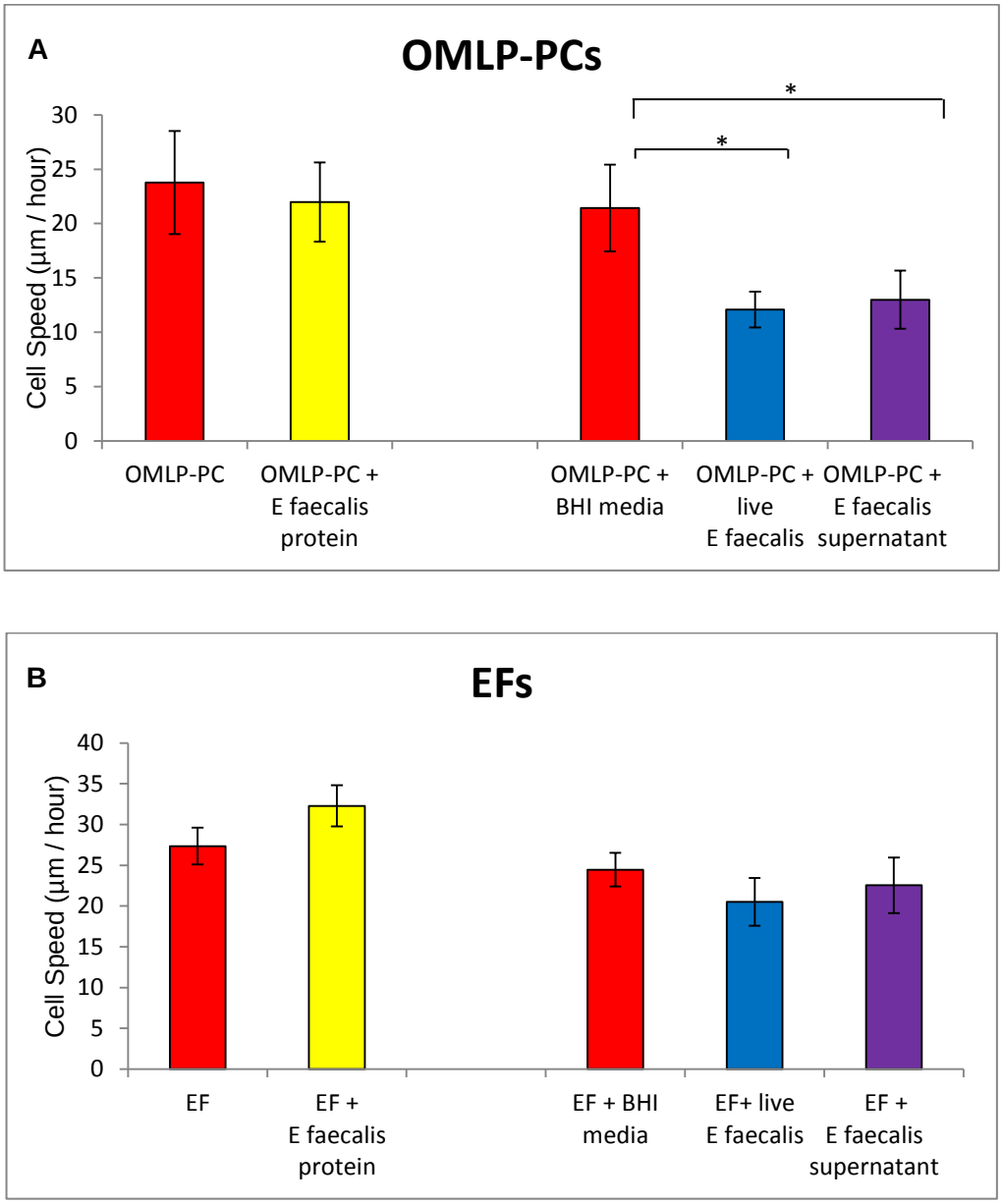

Fig. 2.23: Migratory speed of cells after incubation with *E. faecalis* stimuli. Cell speed of OMLP-PCs (n=4) (A) and EFs (n=3) (B) after incubation with *E. faecalis* protein, live *E. faecalis* or *E. faecalis* supernatant. BHI media was used as a control for both live *E. faecalis* and *E. faecalis* supernatant samples. Data expressed as cell speed +/- SD of the mean. *P≤ 0.05

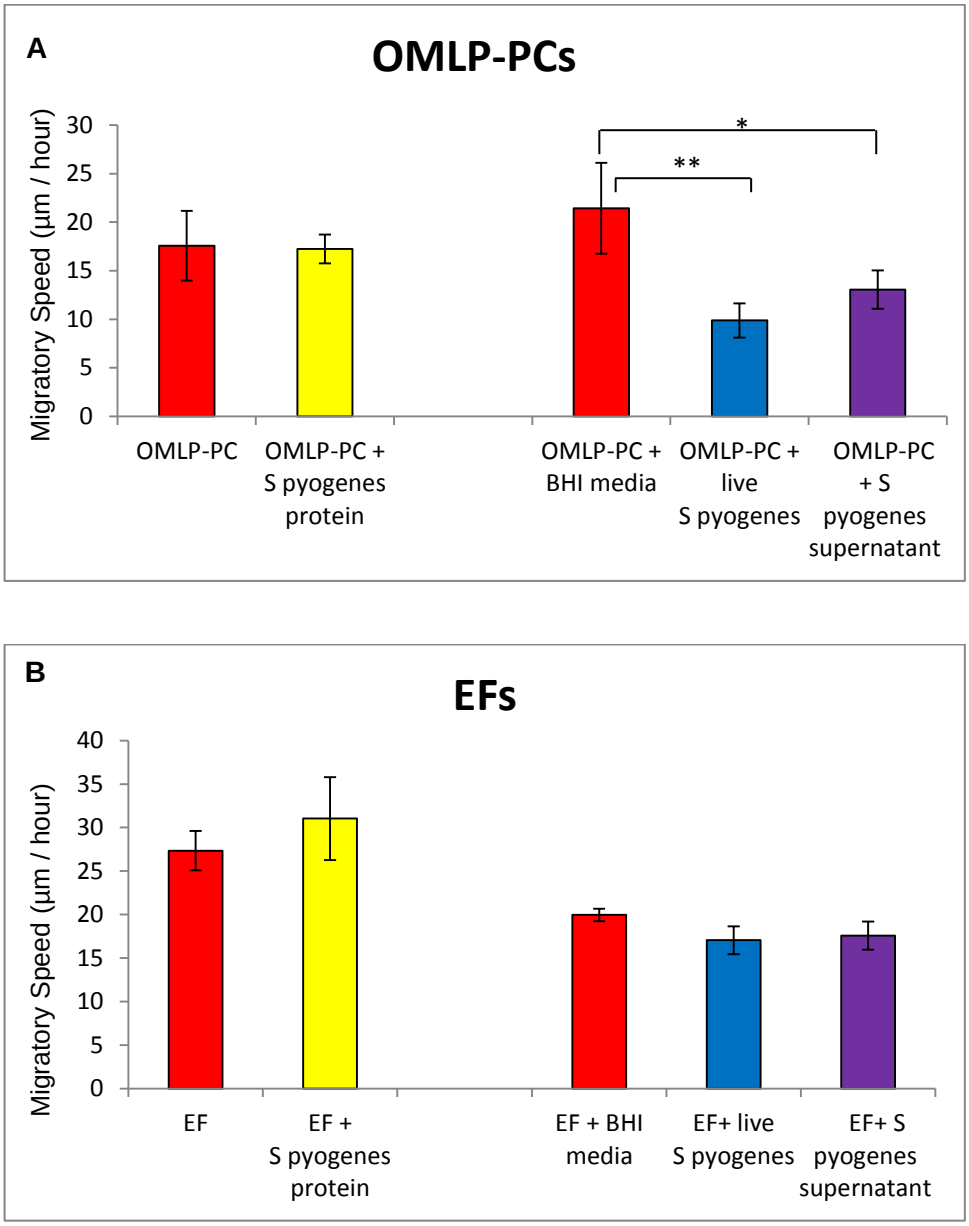

Fig. 2.24: Migratory speed of cells after incubation with *S. pyogenes* stimuli. Cell speed of OMLP-PCs (n=4) (A) and EFs (n=3) (B) after incubation with *S. pyogenes* protein, live *S. pyogenes* or *S. pyogenes* supernatant. BHI media was used as a control for both live *S. pyogenes* and *S. pyogenes* supernatant samples. Data expressed as cell speed +/- SD of the mean. *P≤0.05, ** P≤0.01

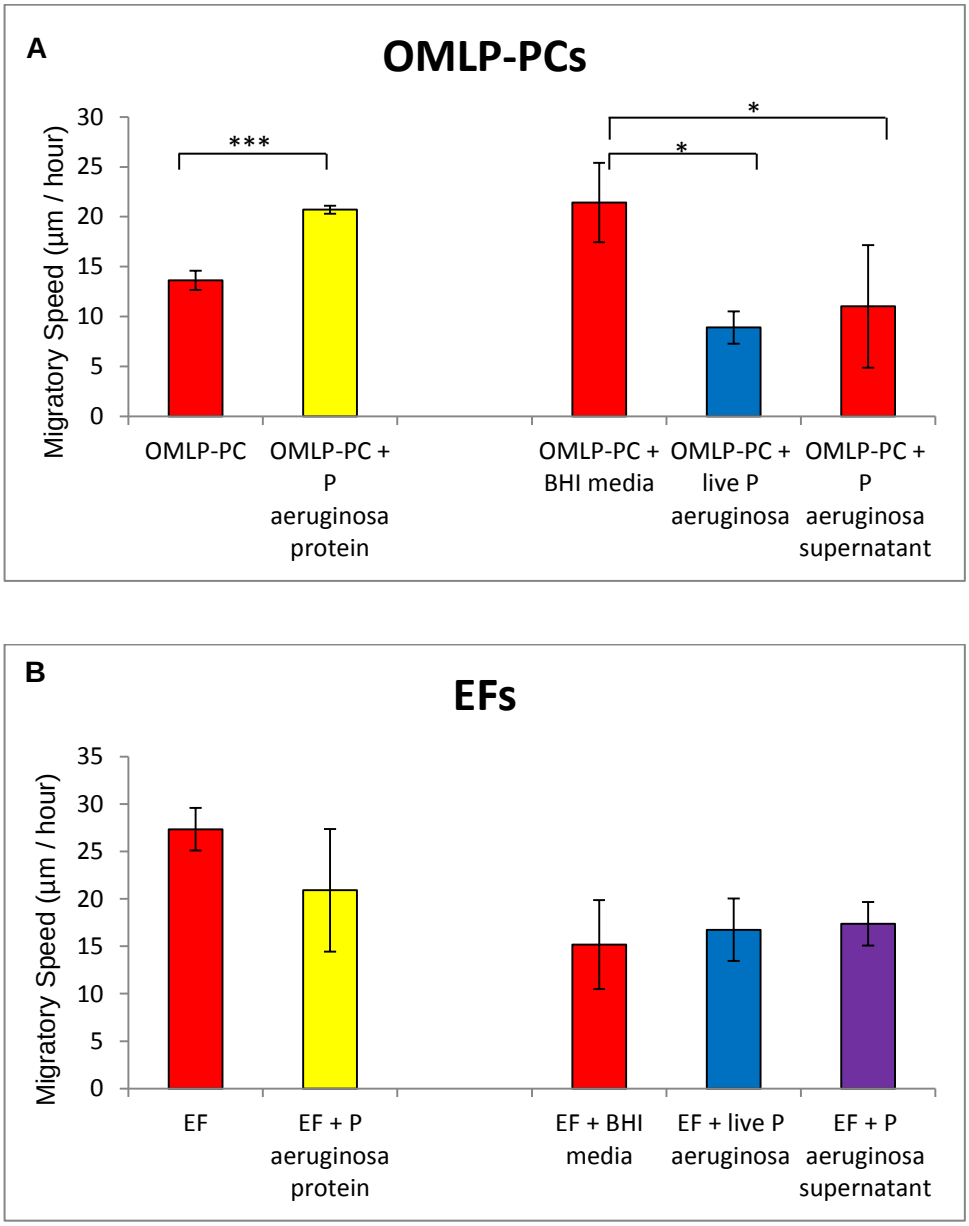

Fig. 2.25: Migratory speed of cells after incubation with *P. aeruginosa* stimuli. Cell speed of OMLP-PCs (n=4) (A) and EFs (n=3) (B) after incubation with *P. aeruginosa* protein, live *P. aeruginosa* or *P. aeruginosa* supernatant. BHI media was used as a control for both live *P. aeruginosa* and *P. aeruginosa* supernatant samples. Data expressed as cell speed +/- SD of the mean. *P≤0.05, *** P≤0.001

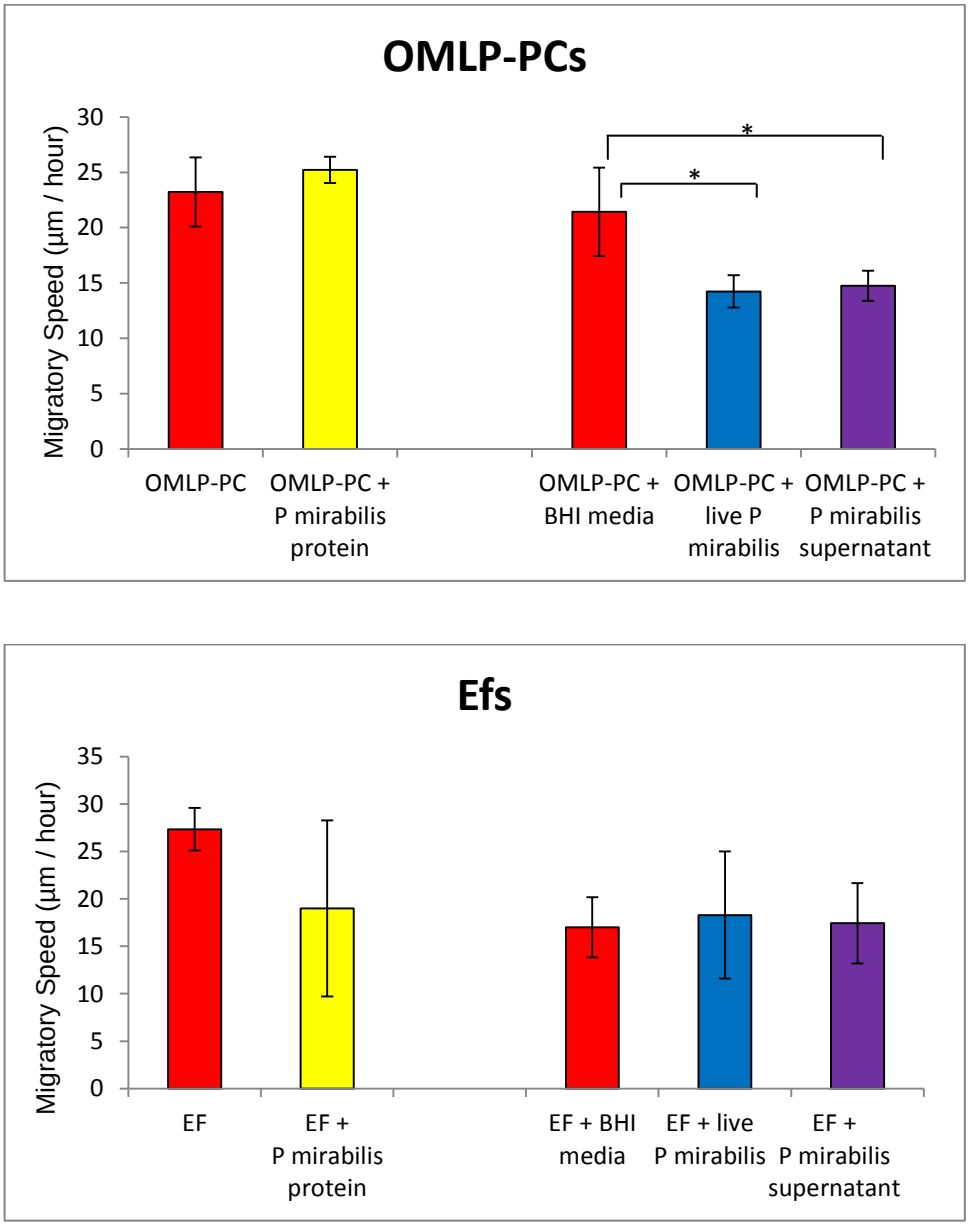

Fig. 2.26: Migratory speed of cells after incubation with *P. mirabilis* stimuli. Cell speed of OMLP-PCs (n=4) (A) and EFs (n=3) (B) after incubation with *P. mirabilis* protein, live *P. mirabilis* or *P. mirabilis* supernatant. BHI media was used as a control for both live P. mirabilis and *P. mirabilis* supernatant samples. Data expressed as cell speed +/- SD of the mean. *P< 0.05.

morphology were observed over the culture period when cells were incubated in control media, RPMI supplemented with 2mM L-glutamine and 10% (v/v) FCS.

OMLP-PCs moved significantly slower when exposed to live bacteria up to this 3hr time period ($P \leq 0.05$; Fig. 2.23 – Fig 2.26), whereas the EFs did not display any changes to their speed ($P \geq 0.05$).

OMLP-PCs moved significantly slower when exposed to bacterial supernatant, irrespective of the bacteria Gram classification of the bacteria ($P \leq 0.05$; Fig. 2.23 – Fig 2.26), while EFs remained at a constant speed compared to the control ($P \geq 0.05$).

Irrespective of the bacteria utilised, oral cells incubated with bacterial protein appeared to migrate towards and directly interact with this protein (Supplementary Data Stick: Movie 1-4). Over time, the majority of the bacterial protein appeared to become associated with the OMLP-PCs rather than remain free within the medium (Fig. 2.27 – Fig. 30). This effect was observed irrespective of whether bacteria were Gram positive (*E. faecalis* and *S. pyogenes*) or Gram negative (*P. mirabilis* and *P. aeruginosa*). The speed of OMLP-PC movement did not significantly alter when exposed to bacterial protein ($P \geq 0.05$), with the exception of protein extracted from *P. aeruginosa* ($P \leq 0.001$) (Fig. 2.23 – Fig 2.26). This suggests that OMLP-PCs respond to factors secreted by OMLP-PCs rather than the intracellular soluble proteins of the bacteria examined here.

2.3.9.1.2 Bacterial Protein Does Not Affect the Cell Area of OMLP-PCs

While the migratory speed of OMLP-PCs did not change in response to bacterial protein, the morphology appeared to change. The cell area of OMLP-PCs was therefore recorded after 16 hours in culture. It was demonstrated that OMLP-PCs did not change their cell area in response to bacterial protein isolated from Gram positive or Gram negative bacteria (Fig. 2.31).

2.3.9.2 OMLP-PCs Do Not Migrate Towards Bacterial Protein

It was hypothesised that OMLP-PCs may migrate towards bacterial protein after analysis presented in section 2.3.9.1 Boyden chamber analysis was therefore carried out to assess the migration of the cells towards Gram positive (*E. faecalis*) and Gram negative (*P. aeruginosa*) bacterial protein.

Neither OMLP-PCs nor EFs displayed any migration towards the bacterial protein utilising this system (Fig. 2.32). A positive control of 10% FCS was used, which significantly increased the migration of the EFs but not the OMLP-PCs. The OMLP-PCs baseline migration was comparable to levels induced by FCS in the EFs (Fig. 2.32). This suggested that OMLP-PCs were inherently more migratory at baseline compared to the EFs.

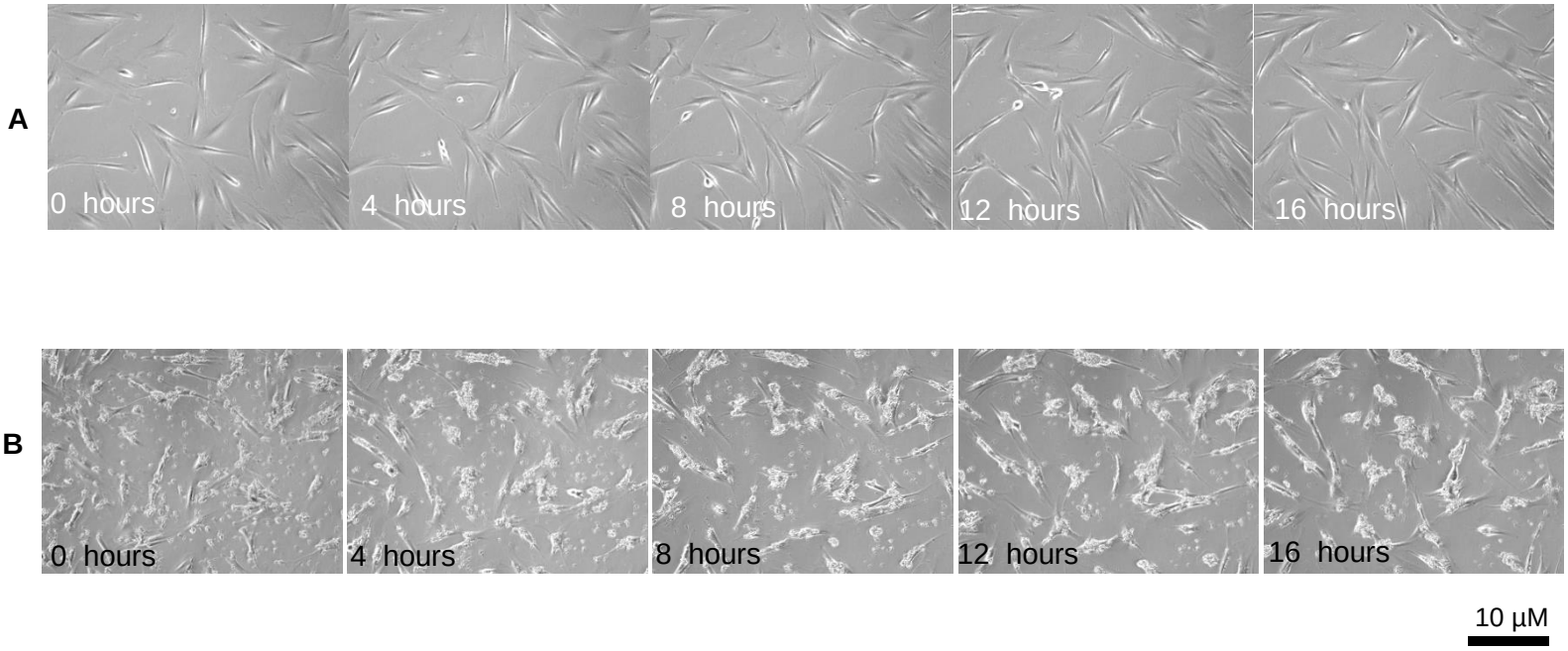

Fig. 2.27: Micrograph images of OMLP-PCs in (A) control media or (B) with protein extracted from E. faecalis (B) over a time course of 16 hours. OMLP-PCs appeared to remain healthy with no considerable changes in morphology when incubated with bacterial protein. OMLP-PCs physically interacted with protein extracted from *E. faecalis*, and by 16 hours the majority of protein was interacting with the OMLP-PCs and was not free within the medium. Bar = 10µM.

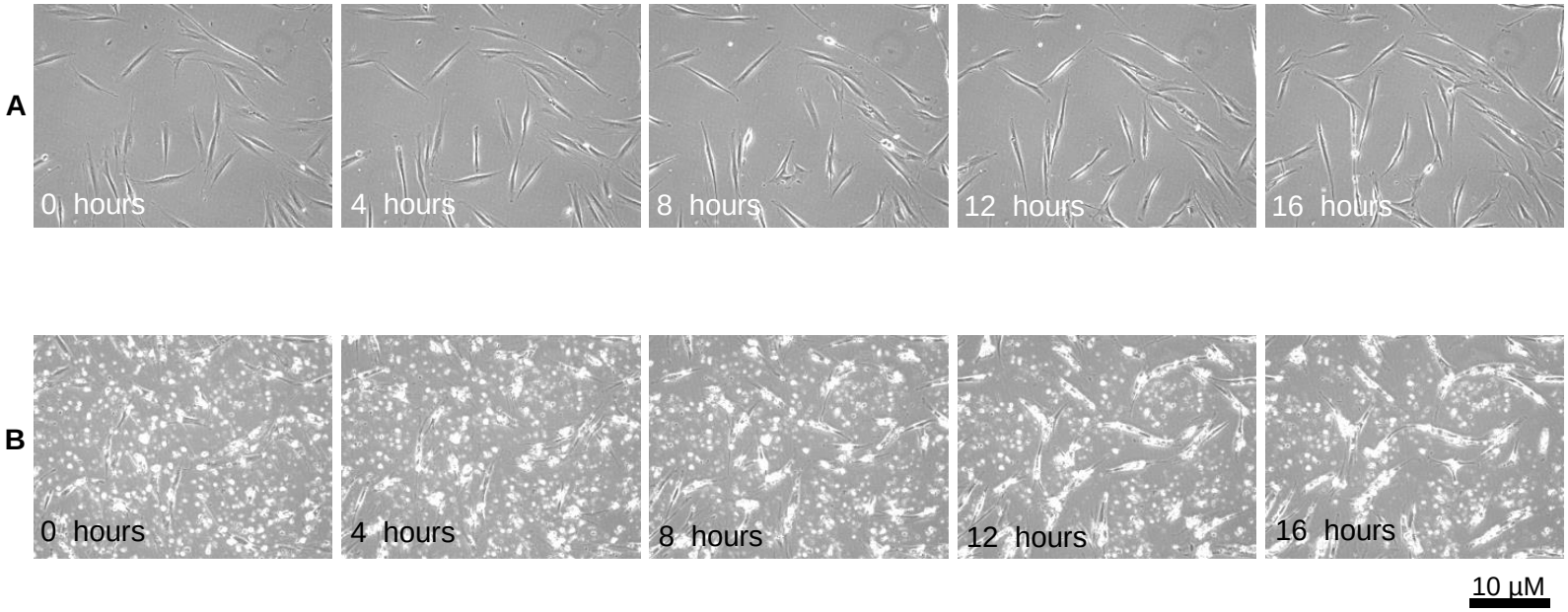

Fig. 2.28: Micrograph images of OMLP-PCs in (A) control media or (B) with protein extracted from *S. pyogenes* (B) over a time course of 16 hours. OMLP-PCs appeared to remain healthy with no considerable changes in morphology when incubated with bacterial protein. OMLP-PCs physically interacted with protein extracted from *S. pyogenes*, and by 16 hours the majority of protein was interacting with the OMLP-PCs and was not free within the medium. Bar = 10µM.

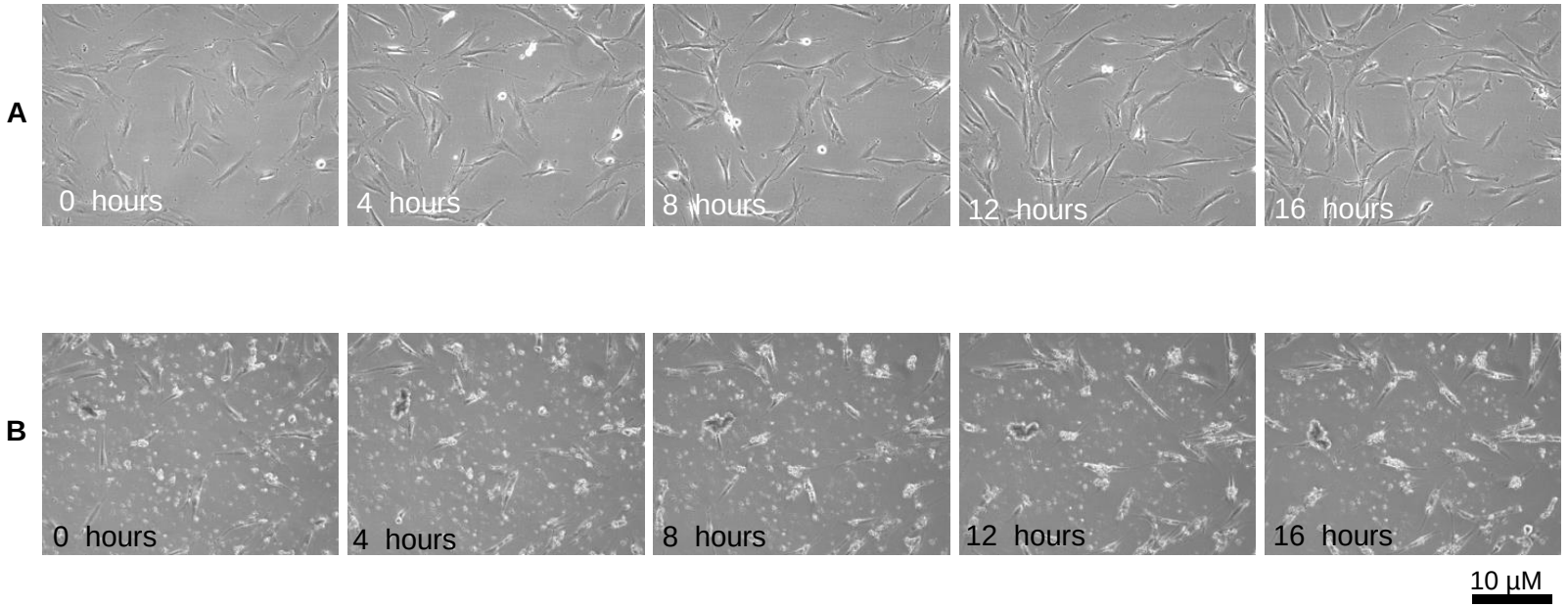

Fig. 2.29: Micrograph images of OMLP-PCs in (A) control media or (B) with protein extracted from *P. aeruginosa* (B) over a time course of 16 hours. OMLP-PCs appeared to remain healthy with no considerable changes in morphology when incubated with bacterial protein. OMLP-PCs physically interacted with protein extracted from *P. aeruginosa*, and by 16 hours the majority of protein was interacting with the OMLP-PCs and was not free within the medium. Bar = 10µM.

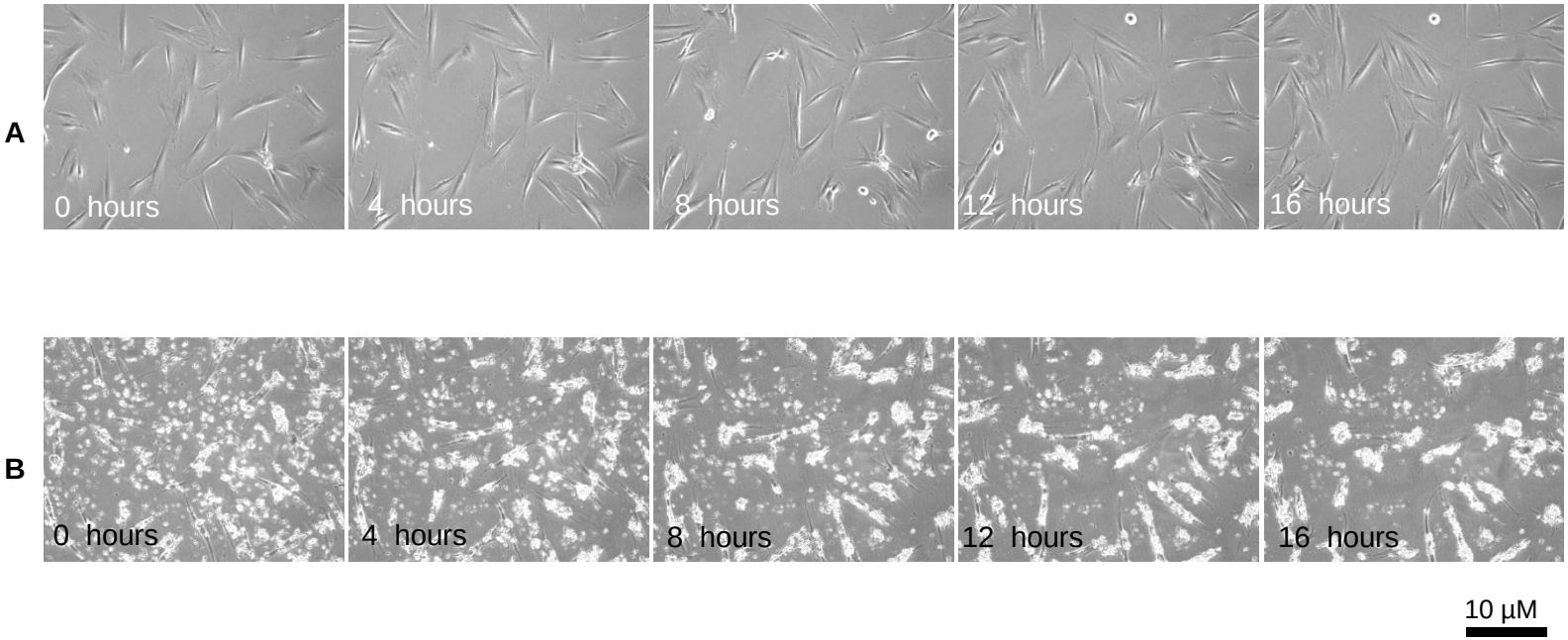

Fig. 2.30: Micrograph images of OMLP-PCs in (A) control media or (B) with protein extracted from *P. mirabilis* (B) over a time course of 16 hours. OMLP-PCs appeared to remain healthy with no considerable changes in morphology when incubated with bacterial protein. OMLP-PCs physically interacted with protein extracted from *P. mirabilis*, and by 16 hours the majority of protein was interacting with the OMLP-PCs and was not free within the medium. Bar = 10µM.

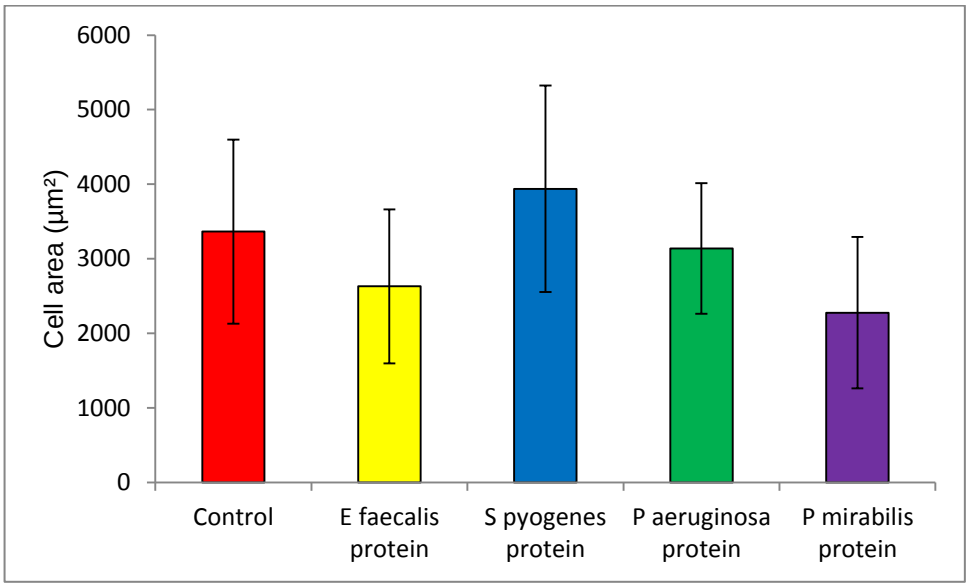

Fig. 2.31: The effect of bacterial protein on OMLP-PC area. Area of OMLP-PCs (n=3) after incubation with bacterial protein isolated from *E. faecalis, S. pyogenes, Paeruginosa* or *P. mirabilis*, +/- SD of the mean.

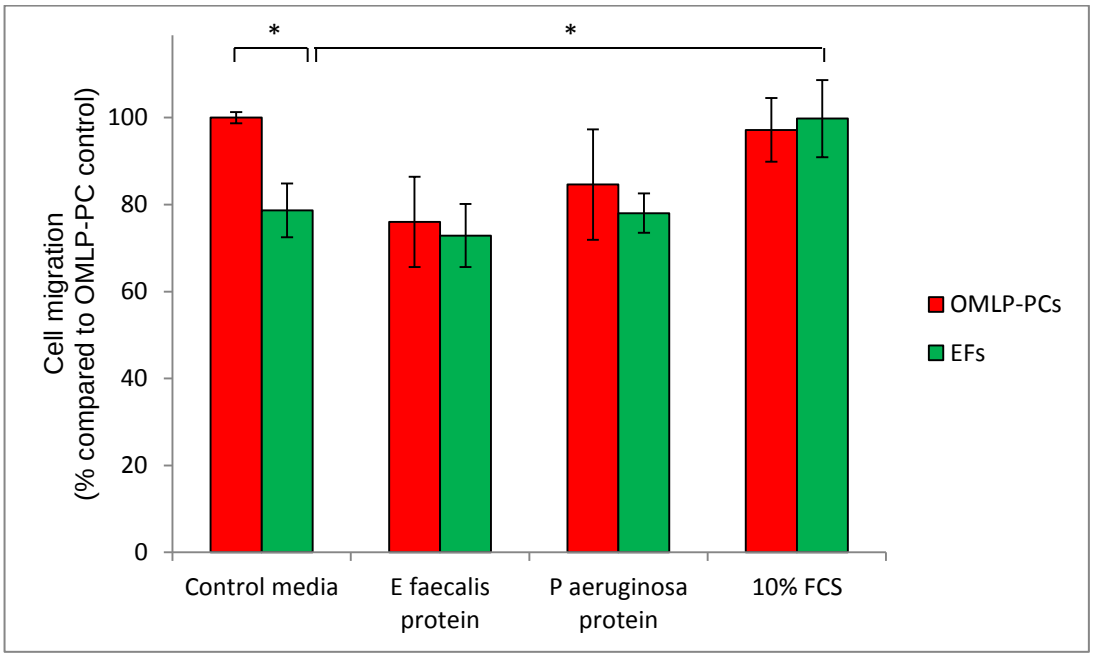

Fig. 2.32: The effect of bacterial protein on directional cell migration. OMLP-PCs (n=3) and EFs (n=3) migration after incubation with *E. faecalis* protein or *P. aeruginosa* protein. FCS was used as a positive control. Data expressed as a percentage of cells compared to migratory OMLP-PCs in control media +/- SD of the mean.

*P< 0.05

2.4 Discussion

BM-MSCs display both immunosuppressive (Ghannam et al., 2010) and antibacterial (Krasnodembskaya et al., 2010) properties. Potentially, these properties may be common to many stem and PC populations. The recent discovery that OMLP-PCs display immunosuppressive qualities (Davies et al., 2012) has led to the investigations in this Thesis into the potential antibacterial properties of OMLP-PCs.

Cells from the oral cavity provide promising potential as antimicrobial cells as the mouth is constantly rich in a dynamic population of micro-organisms (Parahitiyawa et al., 2010). It is clear that there must be an antimicrobial strategy in the oral cavity to prevent recurrent infections. Several cell populations have already been identified to play a role (e.g. oral epithelial cells and the salivary gland) by secreting antibacterial factors (Gorr, 2009). However, due to the diversity in the microbial population of the mouth the secretion of multiple antimicrobial peptides or proteins is likely. The secretion of LL37 by BM-MSCs (Krasnodembskaya et al., 2010) suggests that OMLP-PCs may also secrete an antimicrobial agent(s) to aid in oral defences.

This study aimed to investigate the antibacterial properties of OMLP-PCs in host defence. Investigations have focussed on determining whether OMLP-PCs decrease the CFU of bacteria, while further studies will concentrate on potential antibacterial factors released by these cells.

The growth of bacteria in tissue culture medium was demonstrated to be limited compared to growth in the standard microbiology medium BHI. To increase the growth of bacteria, BHI was supplemented to the RPMI tissue culture medium, which in some cases restored the growth of bacteria to a level comparable to that seen in BHI medium. It was important to assess the effect of the BHI supplementation on OMLP-PC and EF viability as later experiments involved co-culturing the cells with bacteria. The addition of 5, 10 or 20% BHI to the RPMI medium did not cause any significant cytotoxicity to either the OMLP-PCs or EFs. This demonstrated that RPMI supplemented with BHI medium could be utilised in the later co-culture studies.

The first aim of the study, to establish whether OMLP-PCs decrease the growth of Gram positive and Gram negative bacteria was addressed. The study demonstrated that OMLP-PCs act in an antibacterial manner by reducing the growth of both Gram positive and Gram negative bacteria, a phenomenon not replicated by the EFs. The EF cells were used as a control cell type; illustrating that the OMLP-PCs actively

decrease the growth of bacteria and do not simply decrease the bacterial numbers due to depletion of nutrients within the culture media. The lack of antibacterial properties of the EFs also demonstrates that this is not a property of all cells within the buccal mucosal, and despite the rich microbial environment from which they originate, it is a property specific to the OMLP-PCs.

The decrease in bacterial growth by OMLP-PCs was seen irrespective of pre-treatment with IFNγ. The IFNγ stimulation is required to activate the immunosuppressive activity of MSCs through the induction of IDO (Ghannam et al., 2010), while IDO is also induced by IFNγ in OMLP-PCs (Davies et al., 2012). This observation demonstrates that the induction of IDO from OMLP-PCs does not contribute to the antibacterial properties. Furthermore this study begins to address the third aim of this chapter: to determine whether OMLP-PCs require inflammatory or bacterial priming to exert antibacterial actions against Gram positive and Gram negative bacteria. It was demonstrated that the inflammatory stimulus IFNγ was not required for OMLP-PCs to display the antibacterial properties, nor was exposure of bacteria to OMLP-PCs. This illustrates that OMLP-PCs are constitutively antibacterial, a mechanism differing from that of the BM-MSCs, which only display antibacterial properties upon exposure to bacteria (Krasnodembskaya et al., 2010). It is possible that the constitutive mechanism of OMLP-PCs may be a consequence of *in vivo* priming to the cells, due to the rich microbiome from which the cells originate.

The contact independent antibacterial mechanism of OMLP-PCs was confirmed when it was demonstrated that the CM samples retained the constitutive antibacterial properties of the cells. These studies confirm that OMLP-PCs secrete antimicrobial factors, confirming a similar mechanism to the BM-MSCs (Krasnodembskaya et al., 2010). While pre-stimulation of the cells to IFNγ or previous bacterial exposure was not required for the CM of OMLP-PCs to demonstrate antibacterial properties, OMLP-PCs exposed to *S. pyogenes* demonstrated enhanced antibacterial properties within the CM. *Streptoccocal* species are hugely prevalent within the oral cavity (Aas et al., 2005), with exposure of the cells to such bacteria possible *in situ.* This may explain the heightened response of the OMLP-PCs to *S. pyogenes,* as cells may recognise this genus. Further investigations could fully evaluate the effects of bacteria commonly found in the oral cavity on the antibacterial properties of OMLP-PCs.

Importantly, these studies demonstrate that the antibacterial properties of OMLP-PCs can be lost through dilution. CM samples were diluted up to 1 in 100. It was found that CM samples retained their antibacterial properties when diluted up to 1 in 5, but beyond this the antibacterial effect was not observed. This illustrates the dose-dependent antibacterial mechanism of OMLP-PCs, a phenomenon which has yet to be investigated within the CM of BM-MSCs.

It has also been demonstrated during this study that the antibacterial properties of OMLP-PCs are of a bacteriostatic mechanism and not bactericidal. By staining bacterial cultures with LIVE/DEAD® fluorescent dyes it was determined that the number of dead bacterial cells did not increase when bacterial cultures were incubated with the CM derived from OMLP-PCs. From this it can be concluded that the overall effect of the soluble factors released by OMLP-PCs is a bacteriostatic effect.

To address the forth aim live bacteria, bacterial supernatant and bacterial protein were incubated with OMLP-PCs for 16hrs and migratory cell speed was determined using time-lapse microscopy. The time-lapse photomicrographs of the OMLP-PCs incubated with live bacteria, bacterial supernatant and bacterial protein demonstrated no morphological changes to the cells over time suggesting they remained healthy throughout the incubation period. Some interesting findings were made with respect to the cells incubated with the bacterial protein.

The Cell-IQ system utilised as part of these investigations is able to capture Z-stacks of cells, however there was an extensive build-up of bacterial protein on the cells. Therefore, analysis using a suitable Z stack range could not be performed to evaluate the protein from its outer surface down to the cell membrane. It was therefore not possible to determine whether the protein was bound to the cell surface, or had become internalised by the cells. Further investigations are warranted to delineate the fate of this protein, such as the use of scanning electron microscopy to visualise if the protein is internalised or bound to the surface of OMLP-PCs. Whilst the morphology of OMLP-PCs exposed to bacterial protein did not notably change over time, there were some differences compared to the morphology of OMLP-PCs cultured in the absence of stimuli. However, this was not manifested by any change in cell area, yet the cells incubated with bacterial protein appeared thinner and longer with some cells sending out processes to interact with the protein in the surrounding environment. This suggests that the OMLP-PCs can rapidly respond to the presence

of bacterial proteins, adapting their shape to permit direct interaction with this exogenous agent. The mechanism by which the OMLP-PCs 'sense' the protein has yet to be explored. One candidate pathway is via Phosphoinositide-3-Kinase (PI3K) signalling which has been implicated in microbial killing by neutrophils (Kulkarni et al., 2011). Neutrophils engulf the microbes exposing the micro-organisms to antimicrobial proteins such as lysozyme and lactoferrin and reactive oxygen species (ROS; Moraes and Downey, 2003). However, it was noted that the production of the ROS was inhibited following PI3K inhibition (Kulkarni et al., 2011). Furthermore, animal studies have demonstrated that mice deficient in PI3K display impaired ROS production in response to bacterial LPS (Hirsch et al., 2000). Recently, it has been reported that the PI3K isoform, p110γ, is the major form of the enzyme involved in ROS production (Nigorikawa et al., 2012). Superoxide production cannot be induced by PI3K in p110γ knock-out mice (Nigorikawa et al., 2012). These studies illustrate the importance of PI3K in the host defence against bacterial infection. PI3K could potentially be involved in recognising the bacterial protein which may cause downstream effects in aiding bacterial clearance. Repeating the experiments using a PI3K inhibitor could confirm its involvement in the behaviour of OMLP-PCs in response to the bacterial protein, while immunocytochemistry could also been used to localise the transport and production of PI3K.

The speed of the OMLP-PC migration significantly decreased when exposed to live bacteria or bacterial supernatant from both Gram positive and Gram negative bacteria, but not in response to isolated intracellular bacterial protein. This suggests that OMLP-PCs respond to factors secreted by OMLP-PCs, rather than the intracellular bacterial proteins examined here. The decrease in migratory speed after bacterial stimuli could be a result of cells transferring resources into antibacterial mechanisms rather than migration. Further investigations will determine if the OMLP-PCs release antimicrobial factors in response to bacterial stimuli.

Neither the migration of OMLP-PCs nor EFs increased when exposed to bacterial protein. A positive control of 10% FCS was used to stimulate the migration of each cell type. The migration of the EFs significantly increased upon FCS exposure; however the OMLP-PCs migration was not altered. The baseline migration of the OMLP-PCs was comparable to the FCS stimulated migration of EFs, suggesting OMLP-PCs are inherently more migratory at baseline compared to EFs. This could potentially be a result of *in vivo* priming of the OMLP-PCs, having already been stimulated to migrate by the presence of bacteria or bacterial products *in situ*.

Throughout this Thesis chapter it has been demonstrated that EFs cannot respond to bacterial stimuli or display antibacterial properties despite the rich microbial environment from which both EFs and OMLP-PCs originate, hence the *in situ* priming having no effect on EFs. Higher concentrations of FCS could be used to assess the maximal migratory potential of the OMLP-PCs and examine whether the migratory potential of OMLP-PCs is greater than the EFs at all FCS concentrations.

2.4.1 Conclusion

The aim of this study was to investigate the antibacterial properties of OMLP-PCs. Work within this chapter demonstrated that OMLP-PCs are antibacterial, reducing the growth of both Gram positive and Gram negative bacteria. Furthermore, it was established that neither inflammatory nor bacterial stimuli was required to induce this property, illustrating the constitutive antibacterial nature of the cells.

The antibacterial properties of the OMLP-PCs were retained within the CM of the cells, indicating that antibacterial factors are released by the PCs into the culture medium. This effect was dose-dependent, with dilutions of the CM beyond 1 in 5 not displaying any antibacterial properties. The antibacterial mechanism was further investigated, with confirmation of the bacteriostatic effect by OMLP-PCs demonstrated using live/dead staining of the bacterial cultures. The antibacterial response of the CM was enhanced when the cells were previously exposed to *S. pyogenes.* This could be a result of OMLP-PC recognition of the *Streptococcal* genus, as these bacteria are a dominant genus within the oral cavity

This chapter has determined that OMLP-PCs are antibacterial through the release of antimicrobial factors, a property scarcely investigated in stem cell/PC populations. Further investigations have focussed on the soluble factors released by OMLP-PCs and their potential antibacterial effects against Gram positive and Gram negative bacteria.

3. Elucidating the Soluble Mechanisms Mediating the Antibacterial Effects of OMLP-PCs

3 Elucidating the Soluble Mechanisms Mediating the Antibacterial Effects of OMLP-PCs

3.1 Background

The immunosuppressive properties of OMLP-PCs are mediated through the cellular release of soluble factors (Davies et al., 2012). Many of the identified immunomodulatory factors are known to additionally demonstrate antibacterial effects, leading to the hypothesis that OMLP-PCs possess both immunosuppressive and antibacterial properties through the secretion of such factors. This hypothesis has been demonstrated to some extent for BM-MSCs, with the secretion of IDO (Krampera et al., 2006) and LL37 (Krasnodembskaya et al., 2010) documented.

IDO is an enzyme capable of degrading tryptophan, an essential factor for tryptophan-dependant bacteria such as Group B *Streptococci*, *Enterococci* (Hucke et al., 2004) and *Staphylococcus aureus* (Schroten et al., 2001). IDO activity is undetected in resting OMLP-PCs, but with high levels of IFNγ can be induced (Davies et al., 2012). IDO induction in response to bacterial exposure is yet to be investigated.

LL37 is an AMP constitutively expressed in immune cells such as monocytes and natural killer cells (Zanetti, 2005), and inducible in areas such as the salivary glands by inflammation (Woo et al., 2003). LL37 directly binds LPS on the surface of bacteria, supressing LPS-induced host responses, such as pro-inflammatory cytokines release, during infection (Zanetti, 2005). It has been reported that LL37 demonstrates antibacterial properties against a range of bacteria such as the Gram positive *S. aureus* and vancomycin resistance *enterococci* and Gram negative *E. coli* and *P. aeruginosa* (Zanetti, 2005). It has also been reported that the secretion of LL37 is induced by bacteria in BM-MSCs, which partially mediated the antibacterial properties of BM-MSCs described in this study (Krasnodembskaya et al., 2010).

The role of OPG is well known within bone remodelling, acting as a decoy receptor for RANKL. The binding of OPG to RANKL prevents osteoclast maturation and therefore slows the bone resorptive phase of the process (Jin et al., 2015). This glycoprotein has been identified within the secretome of BM-MSCs, but is not thought

to play a role in the BM-MSC-mediated immunosuppression (Le Blanc et al., 2004). OPG has also been identified as a decoy receptor for TRAIL. TRAIL induces apoptosis (Chaudhari et al., 2006) through the activation of death domain receptor, with apoptosis suppressed when TRAIL is bound to OPG (Sandra et al., 2006). The decrease of OPG within the oral cavity has been well documented during periodontitis, a condition associated with the bacterium *Porphyromonas gingivalis* (Bostanci et al., 2007, Mogi et al., 2004, Liu et al., 2003). However, each study has investigated the levels of OPG in relation to the bone remodelling process, rather than examining any potential antibacterial effect.

Another glycoprotein, haptoglobin, is known to possess both antibacterial and immunomodulatory properties (Sadrzadeh and Bozorgmehr, 2004). Three forms of haptoglobin have been identified within humans, Hp1-1, Hp1-2 or Hp2-2, dependant on the chains present. Comprising of two α and two β chains, the isoform of the α chain dictates the form and the level of activity. The presence of the α1 chain leads to a higher activity level, with the Hp1-1 form displaying the greatest level of activity. The antibacterial mechanism of haptoglobin is through effective binding of haemoglobin and therefore depletion of iron (Eaton et al., 1982), which is an essential environmental factor for many bacteria and fungi (Barclay, 1985). Production of haptoglobin by the liver and its presence within plasma during inflammation is well known (Huntoon et al., 2008) however, the secretion by a stem/progenitor cell population has yet to be reported.

A factor known to be secreted from stem cell populations is PGE2, a lipid produced by COX enzymes (Park et al., 2006), which demonstrates immunomodulatory properties, with immune cells the primary source during inflammation (Agard et al., 2013). Whilst PGE2 is known to inhibit innate cell functions such as the phagocytosis of macrophages, direct effects of PGE2 on bacterial growth are less reported. In addition to its effect on innate immune cells, PGE2 is able to suppress the activation and proliferation of T cells (Kalinski, 2012). The synthesis of PGE2 is regulated by a number of inflammatory stimuli including the bacterial-derived stimuli LPS (Agard et al., 2013). Whilst both Gram positive and Gram negative bacteria are known to induce PGE2 expression in macrophages, higher levels are induced by the Gram negative group of bacteria (Hessle et al., 2003). The secretion of PGE2 is well documented from stem cell populations, with BM-MSCs (Aggarwal and Pittenger, 2005, Sotiropoulou et al., 2006), periodontal ligament stem cells (Ding et al., 2010)

and gingival stem cells (Su et al., 2011) reported to secrete PGE2, which plays a role in the immunomodulation of these cell types.

The aim of this chapter is to begin to elucidate the antibacterial mechanism of action of OMLP-PCs. Previously, it was demonstrated within chapter 2 that OMLP-PCs mediate their antibacterial effects through contact independent mechanisms i.e. the release of soluble factors. Furthermore, it was demonstrated that these factors are constitutively secreted. This chapter aims to identity the proteins within the OMLP-PC secretome which play a role in the antibacterial effects. The antibacterial activity of identified factors was also assessed with reference to and secreted concentration required to elicit an effect. Additionally, blocking of the identified factors within the secretome has been used to further validate the role of each factor in the OMLP-PC mediated antibacterial effects.

3.1.1 Aims

1. To investigate the potential antibacterial factors expressed and secreted by OMLP-PCs
2. To examine the antibacterial activity of identified factors
3. Establish whether blocking specific antibacterial factors inhibits the antibacterial properties of OMLP-PCs

3.2 Materials and Methods

3.2.1 Investigation of mRNA Expression of Antimicrobial Factors in OMLP-PCs

3.2.1.1 RNA Isolation

RNA was isolated from OMLP-PCs after co-culture experiments described in section 2.2.7 using the Illustra RNAspin Mini RNA isolation kit. The RNA isolation method used is shown in Fig. 3.1. Briefly, cells were directly added to the cell lysis buffer provided and stored at -80ºC until required. The lysed cells were passed through an RNAspin Mini Filter at 11,000xg for 1 min, to reduce viscosity. The RNA binding conditions were altered by adding 70% ethanol, before the RNA was bound to a silica membrane. Salts were removed from the membrane using the Membrane Desalting Buffer provided, allowing DNase to effectively remove contaminating DNA. Finally, the membrane was washed 3 times before the RNA was eluted in 100µl of RNase-free water. The RNA was then quantified using a NanoVue (28-9232-16; GE Healthcare, UK) and the quality assessed by evaluation of the A260/A280 and A260/A230 ratios.

3.2.1.2 cDNA Synthesis

cDNA was synthesised from 0.5µg of total RNA. RNA was added to 1µl random hexamer primers (Promega Ltd, Southampton, UK) and incubated at 70°C for 5mins. The RNA and primer mix was supplemented with 1µl RNasin, 1µl Moloney murine leukemia virus reverse transcriptase, 5µl reverse transcriptase buffer and 5µl deoxynucleotide triphosphates (dNTPS; Promega, Southampton, UK). The reaction volume was made up to 50µl with DNase-free water (Sigma Aldrich, UK) and incubated at 25°C for 10mins, 42°C for 1hr followed by 95°C for 5mins (Unocyclyer, VWR, UK).

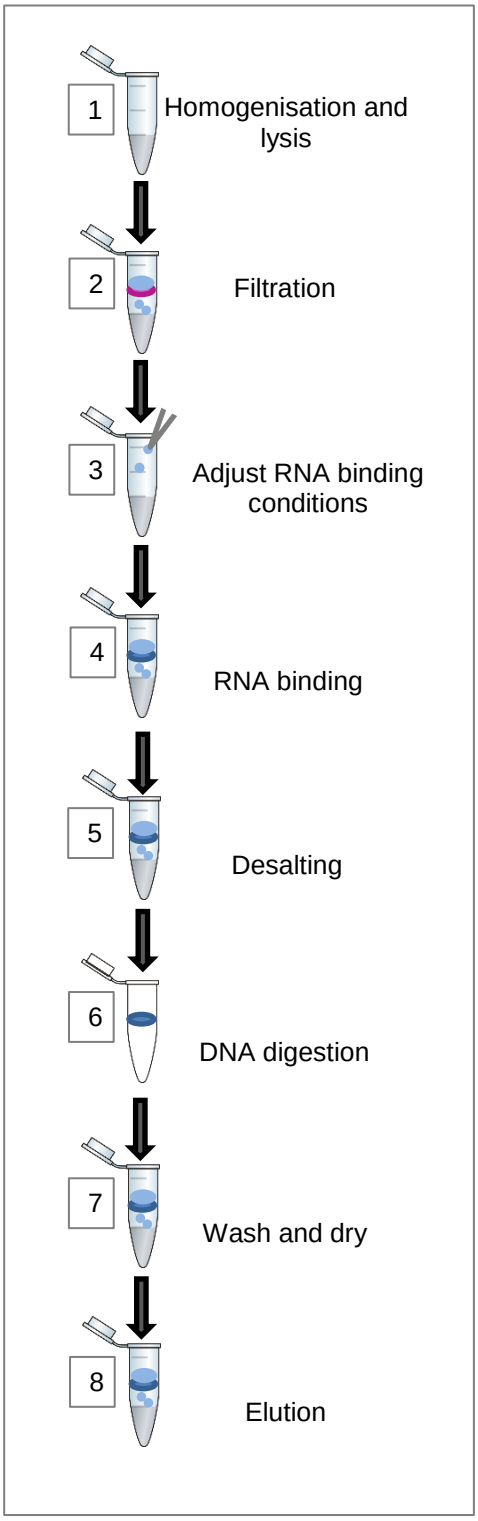

Fig. 3.1: RNA Isolation: 1: Cell lysis. 2: Cells filtered to reduce viscosity. 3: The binding conditions altered using 70% ethanol to allow RNA binding. 4: RNA bound to membrane. 5: Membrane desalted. 6: Contaminating DNA digested using DNase. 7: Membrane is washed and dried. 8: RNA eluted using RNase-free water.

3.2.1.3 Quantitative Polymerase Chain Reaction (qPCR)

Three µl of diluted cDNA (1 in 5) was added to 10 µmol of both forward and reverse primers and 4.75µl of Fast SYBR® Green Master Mix (Life Technologies Ltd, Paisley, UK). The volume of each well was made up to 10µl with DNase-free water. Water was used as a negative control. Primers were designed using basic local alignment search tool (BLAST) from NCBI (http://blast.ncbi.nlm.nih.gov/) and purchased from MWG Biotech (Germany). Primer sequences are outlined in table 3.1

The PCR was carried out using a standard PCR reaction protocol, with an initial denaturation at 95°C, followed by 40 cycles of 95°C for denaturation for 3s and annealing/extension 60°C for 30s (ABI 6000 Prism, Life Technologies Ltd, UK).

Data was analysed using the Δ ΔCT method, by which each sample was compared to its own β-actin level, before being compared to the control sample group.

3.2.2 Investigation of the Secretion of Antimicrobial Factors in OMLP-PCs

Conditioned media (CM) samples were generated from section 2.2.7.

3.2.2.1 Quantification of IDO Activity in Conditioned Media from OMLP-PCs

The concentration of the IDO metabolite, L-kynurenine was determined as a measure of IDO activity. The method used was adapted from Mahanonda *et al.,* 2007. Briefly, 300µl CM from the experiments outlined in section 2.2.7 was mixed with 150µl of 30% (v/v) trichloroacetic acid and centrifuged for 5 minutes at 8000xg. Seventy-five µl of each supernatant was added to 75µl of Ehrlich's reagent (20mg/ml p-dimethylbenzaldehyde [Sigma Aldrich, UK] dissolved in pure glacial acetic acid [Sigma Aldrich, UK]) in a 96 well plate in triplicate. The absorbance of each well was read at 490nm (Microplate autoreader EL311, Bio-Tek Instruments, USA). Concentrations of L-kynurenine in each sample were determined using a standard curve produced using known concentrations of L-kynurenine (0-100µM; Sigma Aldrich, UK) prepared in unconditioned medium pre-centrifuged at x8000g with 30% (v/v) trichloroacetic acid.

Table 3.1: Primer sequences for qPCR reactions.

Primer target	**Primer sequence**
β-actin (housekeeping gene)	F: AGG GCA GTG ATC TCC TTC TGC ATC CT R: CCA CAC TGT GCC CAT CTA CGA GGG GT
IDO	F: GCG ATG TTG GAA ATA GCT TC R: CAG GAC GTC AAA GCA CTA AA
LL37	F: CTG CTG GGT GAT TTC TTC C R: TCT GTC CTG GGT ACA AGA TTC C
OPG	F:GAA GGG CGC TAC CTT GA GAT R:GCA AAC TGT ATT TCG CTC TGG
COX2	F:CTT CAC GCA TCA GTT TTT CAA G R: TCA CCG TAA ATA TGA TTT AAG TCC AC
RANKL	F: TGA TTC ATG TAG GAG AAT TAA ACA GG R: GAT GTG CTG TGA TCC AAC GA
TRAIL	F:GC TCT GGG CCG CAA AAT R:GCT CTG GGC CGC AAA AT

3.2.2.2 Quantification of OPG Secretion in Conditioned Media from OMLP-PCs

Secreted levels of OPG were determined using an enzyme-linked immunosorbent assay (ELISA: R&D systems, UK), and was performed as per the manufacturer's protocol. A 96 well microplate was coated with 100µl of the capture antibody (2µg/ml) in PBS, covered and incubated overnight at room temperature. Each well was washed for a total of three times using the wash buffer provided (0.05% Tween® 20 in PBS, pH 7.2-7.4). Wells were subsequently blocked with the supplied Reagent Diluent (1% bovine serum albumin [BSA], pH 7.2-7.4, 0.2µm filtered) for 1hr at room temperature. The microplate was washed as before, followed by the addition of 100µl of sample (diluted 1 in 5) or standard (0-4ng/ml) for 2hrs. The wells were washed before the addition of 100µl detection antibody (200ng/ml diluted in reagent diluent and 2% heat inactivated normal goat serum) for a further 2hrs. After washing, 100µl of the supplied Streptavidin-horseradish peroxidase (HRP) (diluted 1 in 40) was added to each well for 20mins in the dark. A final wash step was applied before 100µl of the substrate solution (1:1 Part A [H_2O_2]: Part B [Tetramethylbenzidine]) was added for 20mins in the dark. Fifty µl of stop solution (2N H_2SO_4) was added to each well before the absorbance at 450nm, with a reference wavelength of 540nm was determined (SPECTROstar Omega, BMG-LABTECH or FLUOstar Optima, BMG-LABTECH, Germany). Concentrations of OPG were determined using a standard curve of OPG provided. The data was linearised by plotting the log of OPG concentrations against the log of the absorbance values. Concentrations were read using the equation of the line and data re-transformed and compared to an OPG standard of known concentrations.

3.2.2.3 Quantification of Secreted PGE2 in Conditioned Media from OMLP-PC

The secretion of PGE2 from OMLP-PCs and EFs was determined using a Prostaglandin E_2 Parameter Assay Kit (R&D Systems, UK), as per the manufacturer's protocol. CM samples (150µl) generated in section 2.2.7 and PGE2 standard provided (0-2500pg/ml) were incubated with 50µl of the provided primary antibody for 1hr with agitation. Non-specific binding wells were included containing only the provided calibrator diluent (a buffered protein base with preservatives), in which the standards were diluted. Fifty µl of the PGE2 conjugate was added directly to each sample (excluding the non-specific binding wells) and incubated for a further

2hrs on an orbital shaker at 500 revolutions per minute (RPM). Each well was washed thoroughly with the wash buffer provided (0.05% Tween® 20 in PBS, pH 7.2-7.4) before 200µl of the substrate solution (1:1 Part A [H_2O_2]: Part B [Tetramethylbenzidine]) was added, and incubated for 30mins in the dark. After the 30mins incubation, 100µl stop solution (2N H_2SO_4) was added and the absorbance of each well recorded at 450nm and 540nm (SPECTROstar Omega, BMG-LABTECH or FLUOstar Optima, BMG-LABTECH, Germany). Concentrations of PGE2 were determined using a standard curve of PGE2 provided. The data was linearised by plotting the mean absorbance of each standard on a linear y-axis and the log of the concentration on the x-axis. Concentrations were read using the equation of the line and data re-transformed and compared to a PGE2 standard of known concentrations.

3.2.2.4 Western Blot Analysis of OPG and Haptoglobin Secretion from OMLP-PCs

3.2.2.4.1 Protein Quantification by Bicinchoninic Acid Protein Assay

The protein content of CM samples generate from section 2.2.7 were determined by bicinchoninic acid (BCA) protein assay (Pierce; ThermoFisher Scientific, UK). Briefly, 25µl of CM was added to 200µl of working reagent, prepared according to the manufacturer's protocol (50:1 Part A [sodium carbonate, sodium bicarbonate, bicinchoninic acid and sodium tartrate in 0.1M sodium hydroxide]: Part B [4% cupric sulphate]). Samples were incubated at 37°C for 30mins before the absorbance was read at 562nm (SPECTROstar Omega, BMG-LABTECH or FLUOstar Optima, BMG-LABTECH, Germany). The concentration of protein in each sample was determined using a standard linear curve of albumin standards provided, diluted in unconditioned media.

3.2.2.4.2 Protein Separation by Polyacrylamide gel electrophoresis

CM (25µg total protein) was combined with x3 Laemmli sample buffer (0.125M Tris, 0.004% Bromophenol Blue, 20% Glycerol, 4% Sodium dodecyl sulfate [SDS], pH 6.8). Where sample reduction was required, 10% 2β-mercaptoethanol was added to the above and samples incubated at 96°C for 5mins. (Note: to separate native proteins neither SDS nor 2β-mercaptoethanol was added). The 25 µg samples were then separated through a 4–15% Mini-PROTEAN® TGX™ Gel (Biorad, UK) at 200V for 45mins (Mini-PROTEAN® Tetra Vertical Electrophoresis Cell, Biorad UK) in

running buffer (25mM Tris [Sigma Aldrich, UK]), 192mM Glycine [Fisher Scientific, UK], 0.1% Sodium dodecyl sulfate [SDS; Sigma Aldrich, UK]). Pre-stained Kaleidoscope molecular weight standards (10-250kDa; BioRad, UK) were loaded (8µl) to compare samples. Gels were subsequently carried forward for Western blot analysis (see section 3.2.2.4.4).

3.2.2.4.3 2 Dimensional-Polyacrylamide Gel Electrophoresis

CM samples (180µg) from section 2.2.7 were processed through a 2D Clean-Up Kit (GE Healthcare, UK). Briefly, proteins were precipitated using the precipitant and co-precipitant provided and centrifuged at 12,000xg for 5mins. The proteins were then washed in the ice-cold wash buffer provided and pellets air-dried. Pellets were re-suspended in 116µl of 7M Urea, 2M Thiourea, 2% 3-[(3-cholamidopropyl)dimethylammonio]-1-propanesulfonate [CHAPS] followed by 1% Bromophenol Blue, 2µl immobilized pH gradient [IPG] buffer (GE Healthcare, UK) and 6.25µl 50nM Dithiothreitol (DTT).

Samples (180µg) were pipetted into the strip holder and the Immobiline DryStrip pH 3-10, 7 cm (GE Healthcare, UK) placed on top. The sample and Immobiline® DryStrip were coated in Immobiline® DryStrip cover fluid (GE Healthcare, UK) and placed onto the Isoelectric Focussing Unit (GE healthcare, UK) and the following protocol applied: rehydration at 20°C for 12hrs, step & hold 500V 1hr, gradient 1000V 2hrs, step & hold 1000V 1hr, gradient 8000V 2hrs and step & hold 8000V 8hrs.

The Immobiline DryStrip was equilibrated in 4.5ml 1x NuPAGE LDS Sample Buffer (Life Technologies, UK) supplemented with 0.5ml 1x NuPAGE Sample Reducing Agent (Life Technologies, UK) for 15mins with agitation. The Immobiline DryStrip was then added to 5ml of an alkylating solution of 1x NuPAGE LDS Sample Buffer supplemented with 23.2mg/ml Iodoacetamide for 15mins with agitation.

The Immobiline DryStrip was then inserted into the well of a NuPAGE® Novex® 4-12% Bis-Tris ZOOM® Protein Gel (1.0 mm, IPG well: Life Technologies, UK). A rhOPG standard (R&D Systems, UK; 30ng) and pre-stained Kaleidoscope molecular weight standards (BioRad, UK) were mixed and added to the control well as a guide. Proteins were separated through the gel at 200V for 50mins. Gels were carried forward for western blot analysis (see section 3.2.2.4.4).

3.2.2.4.4 Western Blot Detection of OPG and Haptoglobin

Western blot analysis was carried out on gels from sections 3.2.2.4.2 and 3.2.2.4.3. Samples loaded were transferred onto a Polyvinylidene fluoride (PVDF: GE Healthcare, UK membrane) for OPG detection, or a nitrocellulose membrane (Hybond™ECL™; GE Healthcare, UK) for haptoglobin detection, at 15V for 30mins (Trans-Blot® SD Semi-Dry Transfer Cell, Biorad UK). The membranes were subsequently blocked for 1hr in blocking buffer (Tris buffered saline [TBS], 0.2% (v/v) Tween®20, 5% (w/v) skimmed milk powder) with agitation. The membranes were probed with the primary antibody (OPG: Monoclonal Human Osteoprotegerin/ TNFRSF11B Antibody, 0.1µg/ml; R&D Systems and Haptoglobin: Polyclonal Rabbit Anti-Human Haptoglobin, 1.2µg/ml; Dako, UK) diluted in blocking buffer for 1hr at room temperature (OPG) or overnight at 4°C (haptoglobin). The membranes were washed in the blocking buffer before incubation with secondary antibody (OPG: HRP Conjugated Polyclonal Rabbit Anti-Goat Antibody, 25µg/ml; Dako, UK, Haptoglobin: HRP Conjugated Polyclonal Swine Anti-Rabbit, 0.1µg/ml: Dako, UK) in blocking buffer for 1hr at room temperature. The membranes were washed in TBS before development using ECL™ Prime and exposure to Hyperfilm (GE Healthcare).

3.2.3 Examining the Level of Antimicrobial Activity of OPG, Haptoglobin and PGE2

RhOPG (0-100ng/ml; R&D Systems, UK), haptoglobin from pooled human plasma (0-1µg/ml; Sigma Aldrich, UK) or 0-100ng/ml PGE2 (Cambridge Bioscience, UK) were incubated with 150CFU/ml of Gram positive (*E. faecalis* or *S. pyogenes*) or Gram negative (*P. aeruginosa* or *P. mirabilis*) bacteria for 7-14hrs (established midlog for each bacteria). Bacterial cultures were serially diluted and spiral plated (Don Whitley Scientific Limited, UK) onto TSA or CLED (*P. mirabilis*) agar and incubated at 37°C overnight. The number of colonies grown on the agar plates was counted and bacterial CFU/ml was calculated from the manufacturer's counting table (WASP 2 User Manual Section 15.1, Don Whitely Scientific Limited, UK).

It was also investigated whether OPG in combination with haptoglobin or PGE2 had an additive or synergistic effect against bacterial growth. OPG (10ng/ml) and haptoglobin (1ng/ml) or PGE2 (10ng/ml) were incubated with the above Gram positive and Gram negative bacteria for 7-14hrs. Cultures were serially diluted before spiral plating onto appropriate agar, and the colonies counted.

Furthermore, the antibacterial potential of OPG against oral specific bacterial strains was examined. *S. salivarius* and *S. oralis* were isolated from the oral mucosa of patients with oral squamous cell carcinoma at the Dental Hospital of University Hospital Wales after local research ethical approval and in accordance with the Declaration of Helsinki. OPG (0-100ng/ml) was cultured with 100CFU of either *S. salivarius* or *S. oralis* for 16hrs at 37ºC/5%CO_2. Bacterial cultures were serially diluted and spiral plates onto TSA. The number of colonies grown on the agar was counted, and CFU/ml determined as above.

3.2.3.1 Viability of Bacterial Cultures after Incubation with OPG, Haptoglobin or PGE2

Bacteria from section 3.2.3 were stained using the LIVE/DEAD® BacLight™ Bacterial Viability Kit (Life Technologies) as per the manufacturer's instructions after incubation with rhOPG, haptoglobin or PGE2. Briefly, bacterial cultures were pelleted by centrifugation at 14,000xg for 1min and re-suspended in 0.85% (w/v) NaCl or 70% isopropanol (negative control) and incubated for 1hour at room temperature. Bacterial cultures were again centrifuged at 14,000xg for 1min and re-suspended in 1ml 0.85% (w/v) NaCl before incubating with 3µl of dye (1:1, SYTO® 9 nucleic acid stain, propidium iodide) for 15mins in the dark. Cultures were centrifuged at 14,000xg for 1min and re-suspended in 50µl 0.85% (w/v) NaCl before 5µl of each sample was transferred onto a Poly-L-lysine glass slide (Fisher Scientific, UK) and mounted under a coverslip using the provided mountant.

The bacteria were visualized by fluorescence microscopy (Olympus, UK) at x100 magnification under oil emersion. Live (green) and dead (red) bacterial cells were subsequently counted using Image Pro-Plus software v6.0 (Media Cybernectics, USA). Individual bacteria in a minimum of 4 fields of view were counted per condition.

3.2.3.2 Blocking OPG and Haptoglobin in Conditioned Media of OMLP-PCs

CM samples (90µl) from section 2.2.7 were incubated with 100CFU of Gram positive (*E. faecalis* and *S. pyogenes*) +/- 0.6µg/ml of human OPG neutralizing antibody (concentration sufficient enough to block ten times of the amount of OMLP-PC secreted OPG, calculated from EC50 value; R&D Systems) or with Gram negative (*P. aeruginosa* and *P. mirabilis*) bacteria +/- 24µg/ml of polyclonal rabbit anti-human

haptoglobin antibody (Sharpe-Timms et al., 2002); Dako, UK) in a 96 well plate for 16hrs at 37°C/5% CO_2. After 16hrs, bacterial cultures were serially diluted and spiral plated onto appropriate agar and incubated at 37°C overnight and the number of colonies grown on the agar plates were counted (as section 3.2.3).

3.2.3.3 OPG Binding to Gram Positive Bacterial Cell Wall Components

Surface plasmon resonance (SPR) was conducted using Biacore™ T200 (GE Healthcare, UK). The surface of the gold plated chip (GE Healthcare, UK) was activated using 75mg/ml 1-ethyl-3-(3dimethylaminopropyl) carbodiimide (EDC: GE Healthcare, UK) and 11.5mg/ml N-hydroxysuccinimide (NHS: GE Healthcare, UK) before 50µg/ml human OPG Antibody (R&D Systems, UK) in 20mM Sodium acetate at pH 4.5 was injected over the chip. The chip was then deactivated using 1M ethanolamine hydrochloride at pH 8.5. To immobilise rhOPG, 50µg/ml in PBS was injected over the antibody-bound chip. A second injection of the rhOPG was performed to ensure maximal binding was achieved. PGN (Sigma Aldrich, UK) and lipoteiochic acid (LTA; Sigma Aldrich, UK) were injected (0µg/ml – 50µg/ml in PBS) over different cells of the chip containing the immobilised rhOPG as well as chips containing no rhOPG or antibody (as a negative control) at a flow rate of 30µl/min. PGN or LTA were allowed to bind to the rhOPG for 40s with a further 3mins for the dissociation period. Data was analysed using the Biacore™ T200 Software v2.0 (GE Healthcare, UK**).**

3.2.4 Statistical Analysis

All statistical analysis was performed using SPSS statistics (IBM®, Version 20). Variance analysis was performed using Levene's test, with significant variability assumed where $P<0.05$. Statistical analysis for comparing means was performed using a one-way analysis of variance (ANOVA) test with a post hoc Tukey test (where equal variance) or a Games-Howell test (where variances were unequal). Statistical significance was assumed where $P<0.05$.

3.3 Results

3.3.1 OMLP-PCs Do Not Express LL37

RNA was extracted from OMLP-PCs (n=4; +/- IFNγ) and EFs (n=3), which had been cultured with live bacteria and cDNA was synthesised. The molecular levels of LL37 were subsequently determined using qPCR. It was found that LL37 was not expressed in OMLP-PCs irrespective of IFNγ priming and/or bacterial exposure or within EFs (+/- bacterial exposure; Note that the cycle time [CT] values were $\geq$ 37; Fig. 3.2 A-D). Unstimulated BM-MSC cDNA was also analysed as a positive control to ensure primers were functioning (Fig. 3.2 A-D).

3.3.2 IDO is Induced by IFNγ, but not Modulated by the Presence of Bacteria in OMLP-PCs

CM samples and extracted RNA was obtained from OMLP-PCs (n=4; +/- IFNγ) and EFs (n=3), which had been cultured with live bacteria. The molecular levels of IDO were determined using qPCR and IDO activity was assessed in the CM by measuring the metabolite L-kynurenine. Both the molecular expression (Fig. 3.3 A-D) and the activity (Fig. 3.4 A-D) of IDO were induced by IFNγ ($P \leq 0.05$). IDO levels were undetectable in OMLP-PC samples at resting state or after exposure to bacteria in the absence of IFNy. Co-culturing IFNγ primed OMLP-PCs with live bacteria had no further effect on the IDO levels compared to IFNγ priming alone. IDO was not expressed in EF samples, irrespective of bacterial exposure (Fig. 3.3 A-D), however IFNγ stimulation of EFs did induce IDO expression and activity ($P \leq 0.05$; Fig. 3.5 A-B). Furthermore, the induced expression of IDO by IFNγ in EFs was significantly less compared to the induction of IDO by IFNγ in OMLP-PCs.

3.3.3 PGE2 as an Antibacterial Mediator

3.3.3.1 OMLP-PCs Express COX2 and Secrete PGE2

CM samples and extracted RNA was obtained from OMLP-PCs (n=4) (+/- IFNγ) and EFs (n=3) generated in section 2.2.7, which had been cultured with live bacteria. cDNA was synthesised from the extracted RNA and the molecular levels of COX2 were subsequently determined using qPCR. The secreted levels of PGE2 within the CM were determined using ELISA. COX2 was constitutively expressed in OMLP-PCs

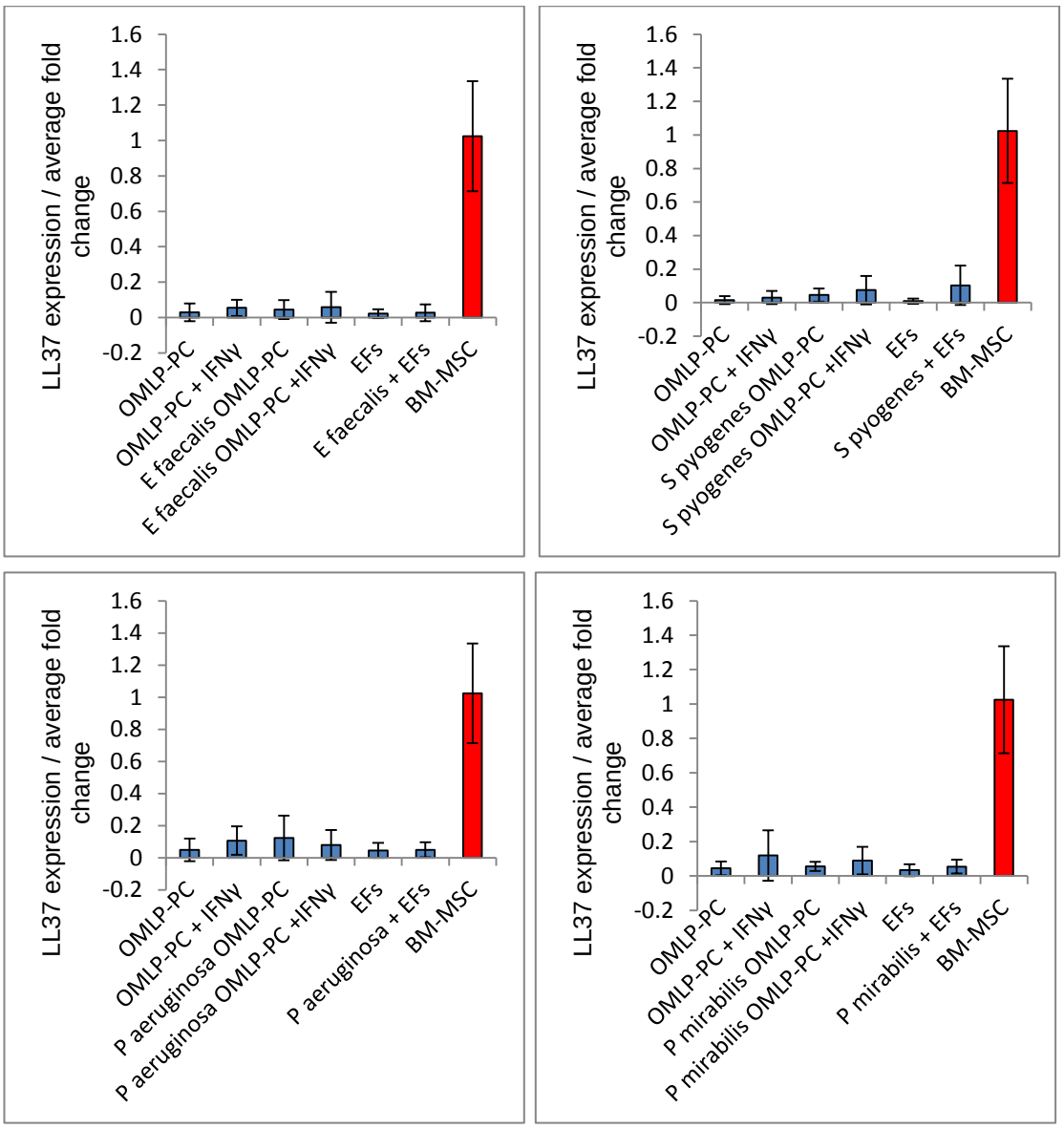

Fig. 3.2: LL37 expression in OMLP-PCs (n=4) and EFs (n=3). Expression of LL37 in OMLP-PCs +/-IFNγ priming and/or exposure to (A) *E. faecalis*, (B) *S. pyogenes*, (C) *P. aeruginosa* or (D) *P. mirabilis*. LL37 expression in BM-MSCs (n=3) as a positive control. Data is expressed as average fold change to BM-MSC, +/- SD of the mean.

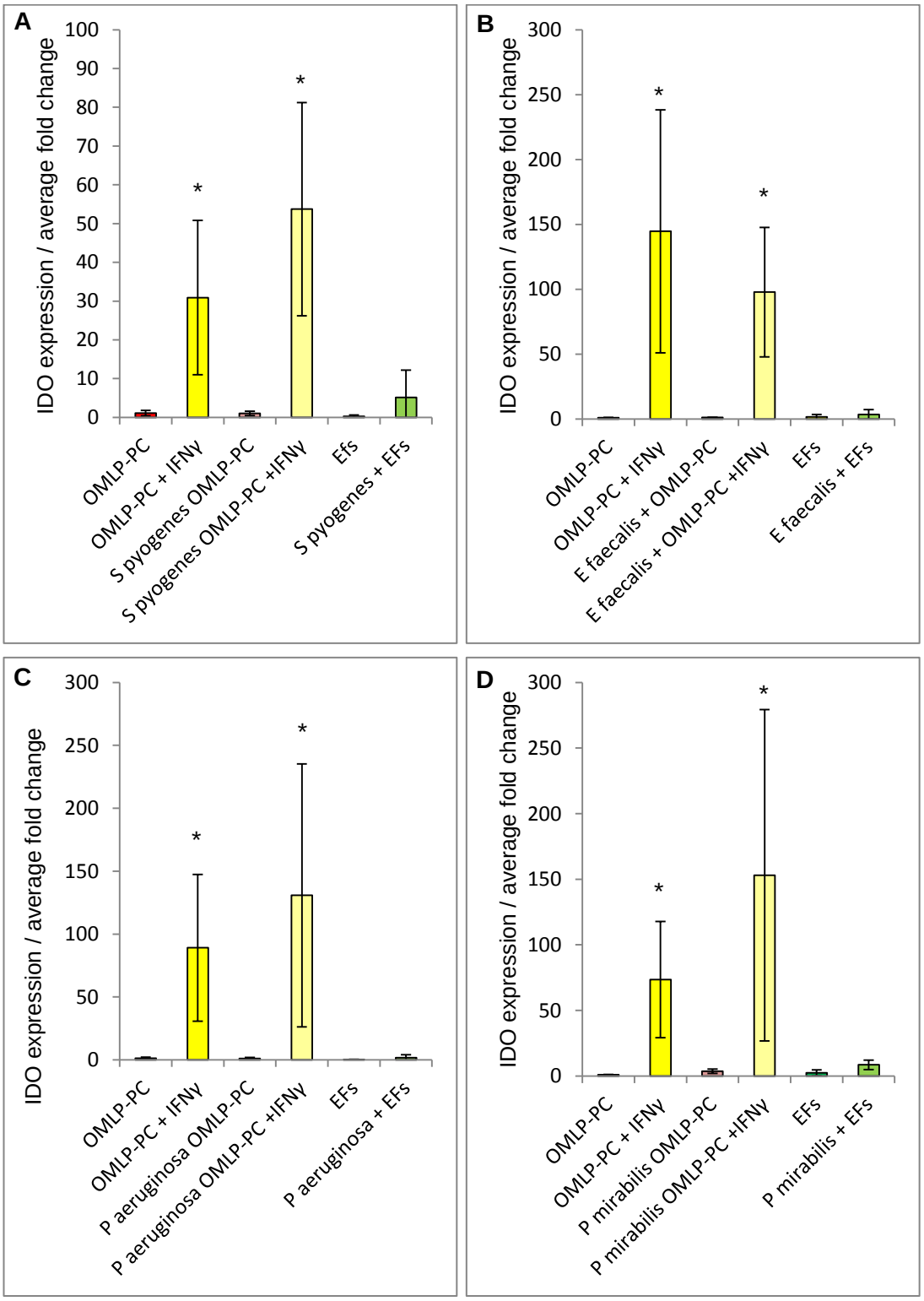

Fig. 3.3: IDO expression in OMLP-PCs (n=4) and EFs (n=3). IDO expression in OMLP-PCs +/-IFNγ priming and/or exposure to (A) *E. faecalis*, (B) *S. pyogenes*, (C) *P. aeruginosa* or (D) *P. mirabilis*. Data is expressed as average fold change to OMLP-PCs, +/- SD of the mean. Statistics compared to OMLP-PC. *P≤0.05.

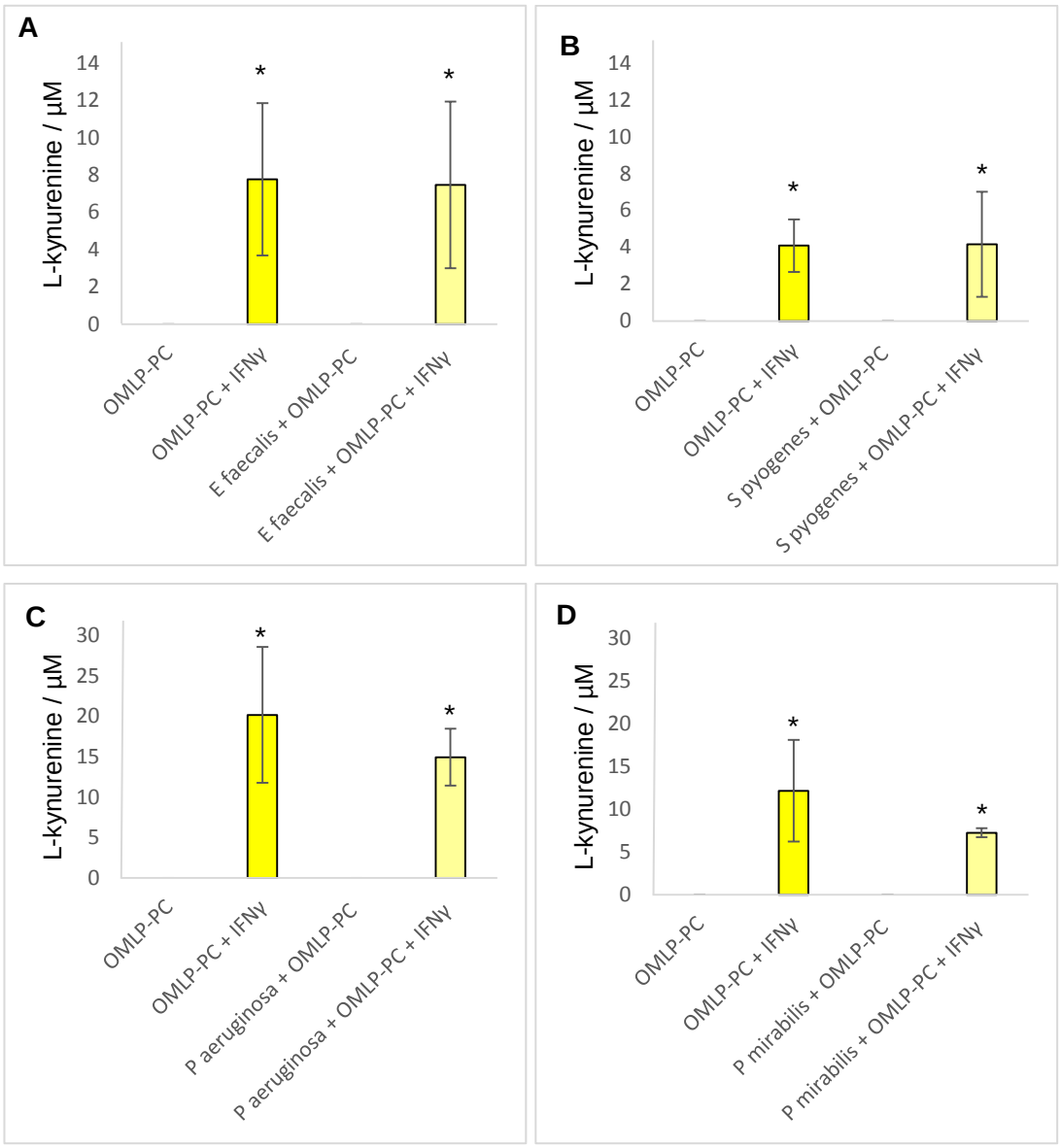

Fig. 3.4: IDO activity in OMLP-PCs (n=3). IDO activity was assessed by measuring the metabolite L-kynurenine in OMLP-PCs +/- IFNγ priming and/or exposure to (A) *E. faecalis*, (B) *S. pyogenes*, (C) *P. aeruginosa* or (D) *P. mirabilis*, +/- SD of the mean. Statistics compared to OMLP-PC (A-D) *P≤0.05.

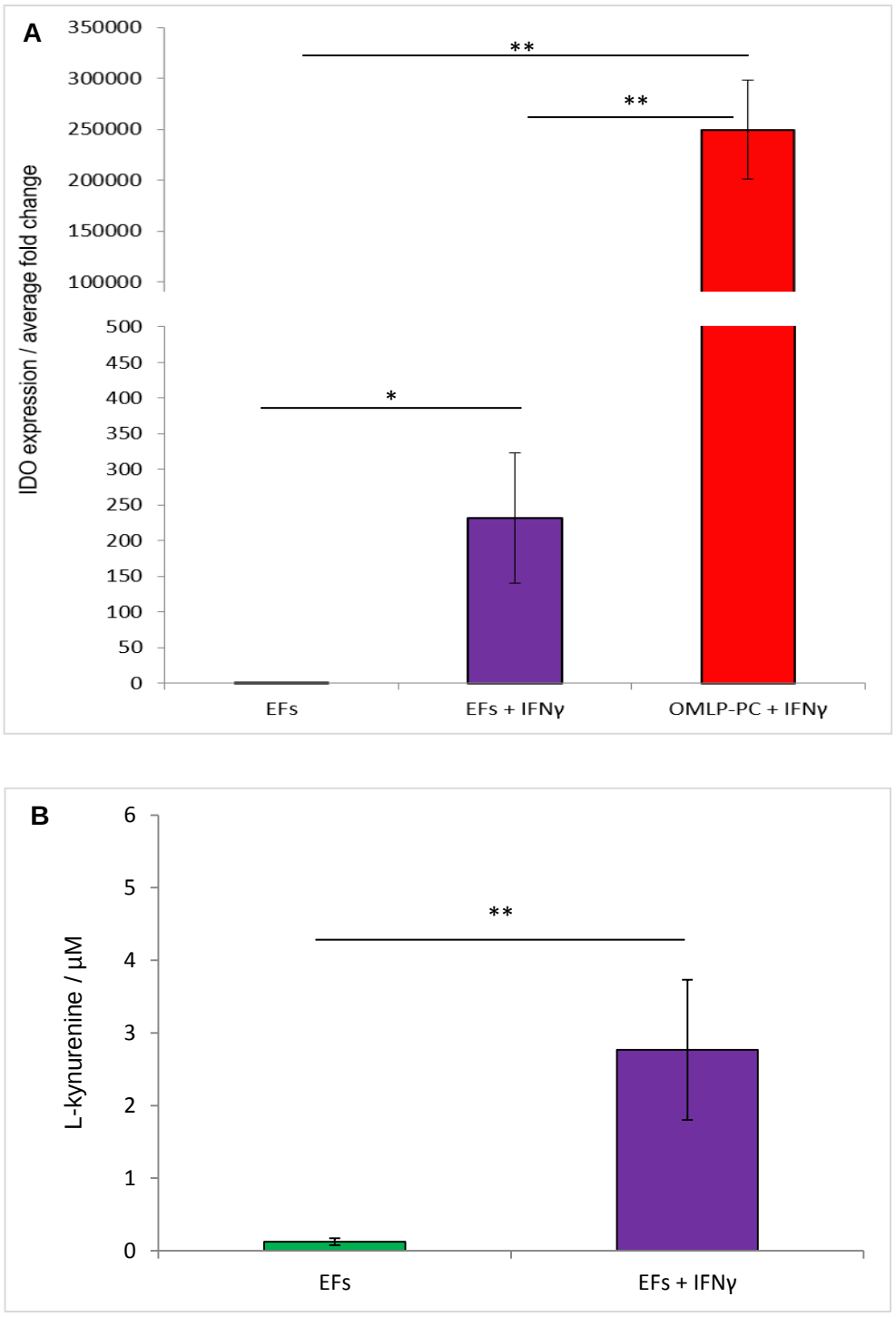

Fig. 3.5: IDO expression and activity in EFs +/- IFNγ. (A) The expression of IDO in EFs +/- IFNγ. OMLP-PCs + IFNγ as a positive control. Data expressed as average fold change compared to EFs. (B) The activity of IDO measured by the IDO metabolite L-kynurenine in EF +/- IFNγ. All data +/- SD of the mean. **P≤0.05, **P≤0.01.

irrespective of IFNγ and/or Gram positive bacterial exposure (Fig. 3.6 A, B). However, exposure to Gram negative bacteria in combination with IFNγ priming, significantly increased the expression of COX2 within OMLP-PCs ($P \leq 0.05$; Fig. 3.6 C, D). COX2 expression was detected in EFs, at similar levels to the constitutive OMLP-PC expression (Fig. 3.6 A-D). Similarly to the expression profile of COX2, secreted levels of PGE2 were constitutively detected at an average of 1.57pg/ml, and significantly increased to an average of 7.7pg/ml ($P \leq 0.05$) by a combination of IFNγ priming and Gram negative bacterial exposure to OMLP-PCs (Fig. 3.7 C, D). The constitutive secretion of PGE2 from EFs at an average of 0.15ng/ml was significantly less ($P \leq 0.05$; Fig. 3.7 A-D) compared to that from the OMLP-PCs at 1.5ng/ml.

3.3.3.2 PGE2 is Antibacterial Through a Bacteriostatic Mechanism

PGE2 (0-100ng/ml, n=3) was incubated 150CFU/ml live bacteria, to assess the effect of PGE2 on bacterial growth. PGE2 significantly reduced the growth of both Gram positive bacteria, *E. faecalis* and *S. pyogenes* ($P \leq 0.05$; Fig. 3.8 A, B) at 1ng/ml and the growth of the Gram negative *P. mirabilis* at 10ng/ml ($P \leq 0.05$; Fig. 3.8 D). There was no effect on the growth of the Gram negative bacterium *P. aeruginosa* after incubation with PGE2 ($P \geq 0.05$; Fig. 3.8 C).

Cultures of *E. faecalis, S. pyogenes* or *P. mirabilis* incubated with 10ng/ml PGE2 (antibacterial levels for all susceptible bacterium) from above were stained using the Live/Dead® BacLight™ Bacterial Viability Kit. Bacteria were counted and percentage viability calculated. PGE2 did not affect the bacterial viability (live:dead ratio) compared to bacteria only cultures ($P \geq 0.05$; Fig. 3.9 A-C), confirming that PGE2 suppresses bacterial growth through a bacteriostatic mechanism rather than a bactericidal mechanism.

3.3.4 Haptoglobin as an antibacterial mediator

3.3.4.1 Haptoglobin is Secreted by OMLP-PCs

The levels of Haptoglobin within CM samples from section 2.2.7 were initially examined using ELISA. However, the levels fell below the first lower detection limit of the standard curve (3.13ng/ml) and were therefore not reliable (data not shown). Haptoglobin was therefore detected using Western blot analysis. The secretion of haptoglobin from OMLP-PCs and EFs was detected, and the presence of all β, α1 and α2 chains were noted (Fig. 3.10).

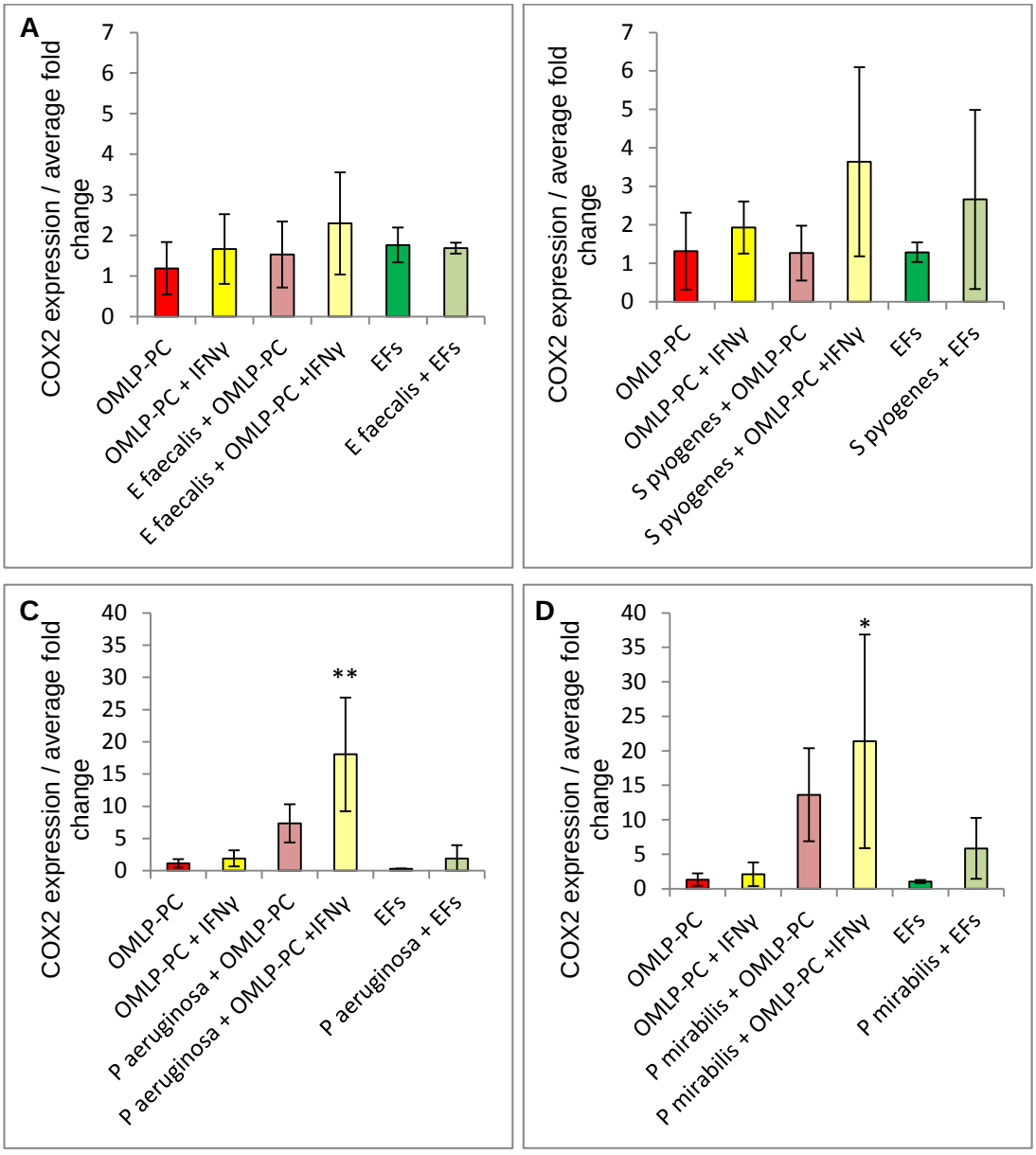

Fig. 3.6: COX2 expression in OMLP-PCs (n=4) and EFs (n=3). The expression of COX2 in OMLP-PCs (+/- IFNγ) and EFs +/- exposure to (A) *E. faecalis*, (B) *S. pyogenes*, (C) *P. aeruginosa* and (D) *P. mirabilis.* Data expressed as the average fold change compared to OMLP-PCs, +/- SD of the mean. Statistics compared to OMLP-PC. *P≤0.05, **P≤0.01

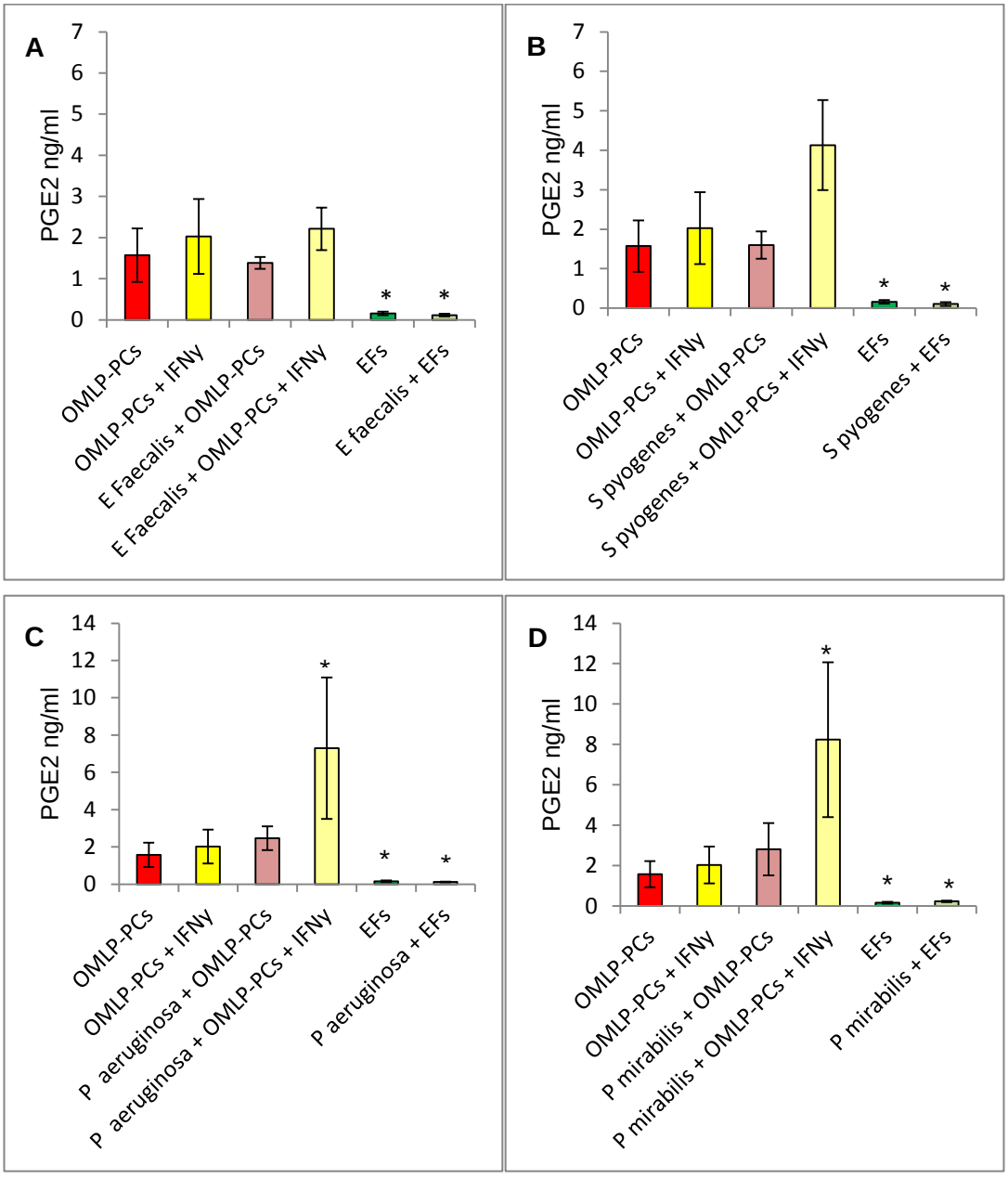

Fig. 3.7: PGE2 secretion from OMLP-PCs (n=4) and EFs (n=3). The secretion of PGE2 from OMLP-PCs (+/- IFNγ) and EFs +/- (A) *E. faecalis*, (B) *S. pyogenes*, (C) *P. aeruginosa* and (D) *P. mirabilis*, +/- SD of the mean. Statistics compared to OMLP-PCs. *P≤0.05

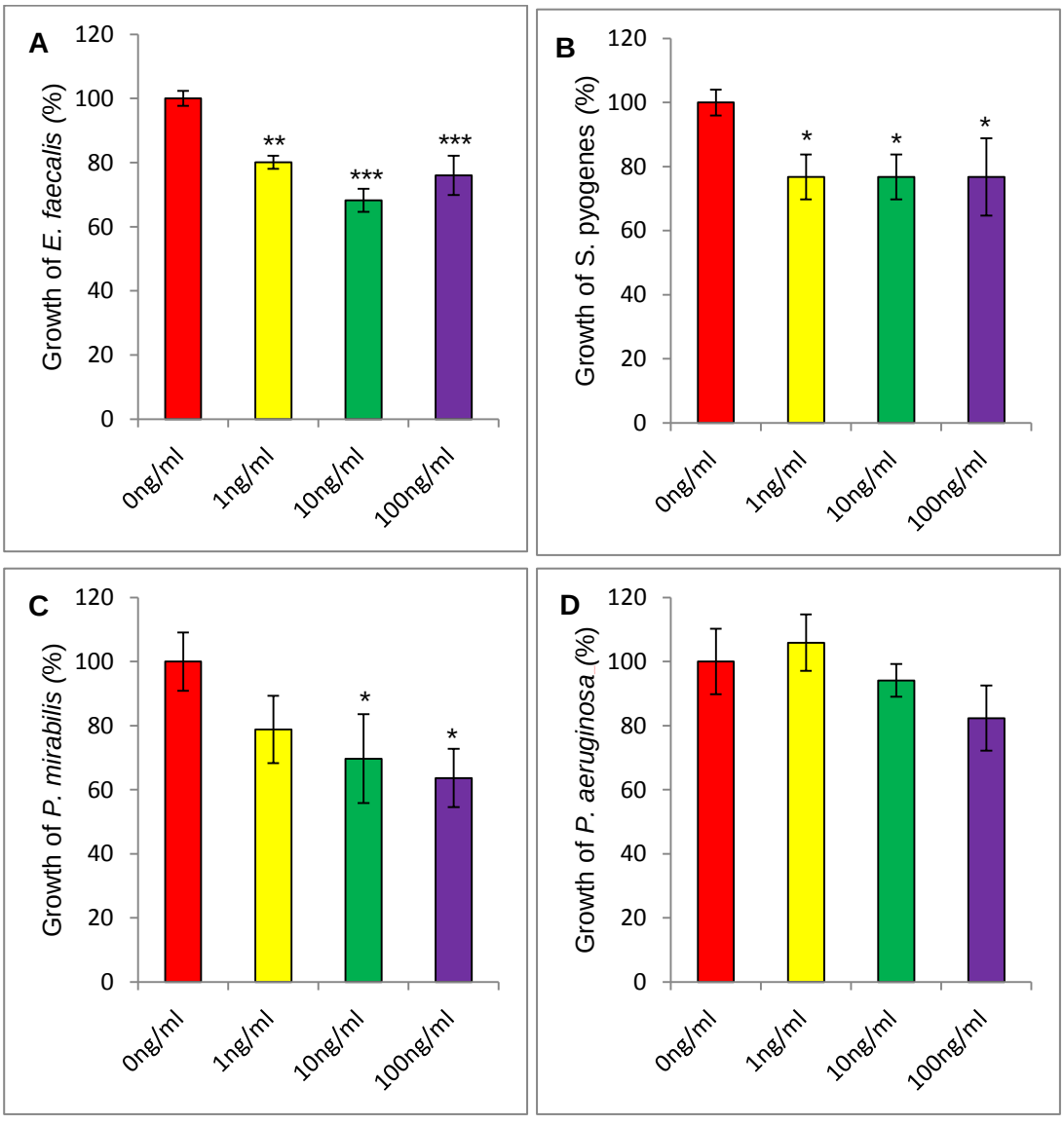

Fig. 3.8: The effect of PGE2 on bacterial growth (n=3). The growth of (A) *E. faecalis*, (B) *S. pyogenes*, (C) *P. aeruginosa* and (D) *P. mirabilis* after culturing with PGE2. Data expressed as percentage bacterial growth, +/- SD of the mean. Statistics compared to 0ng/ml. *P≤0.05, **P≤0.01, ***P≤0.001

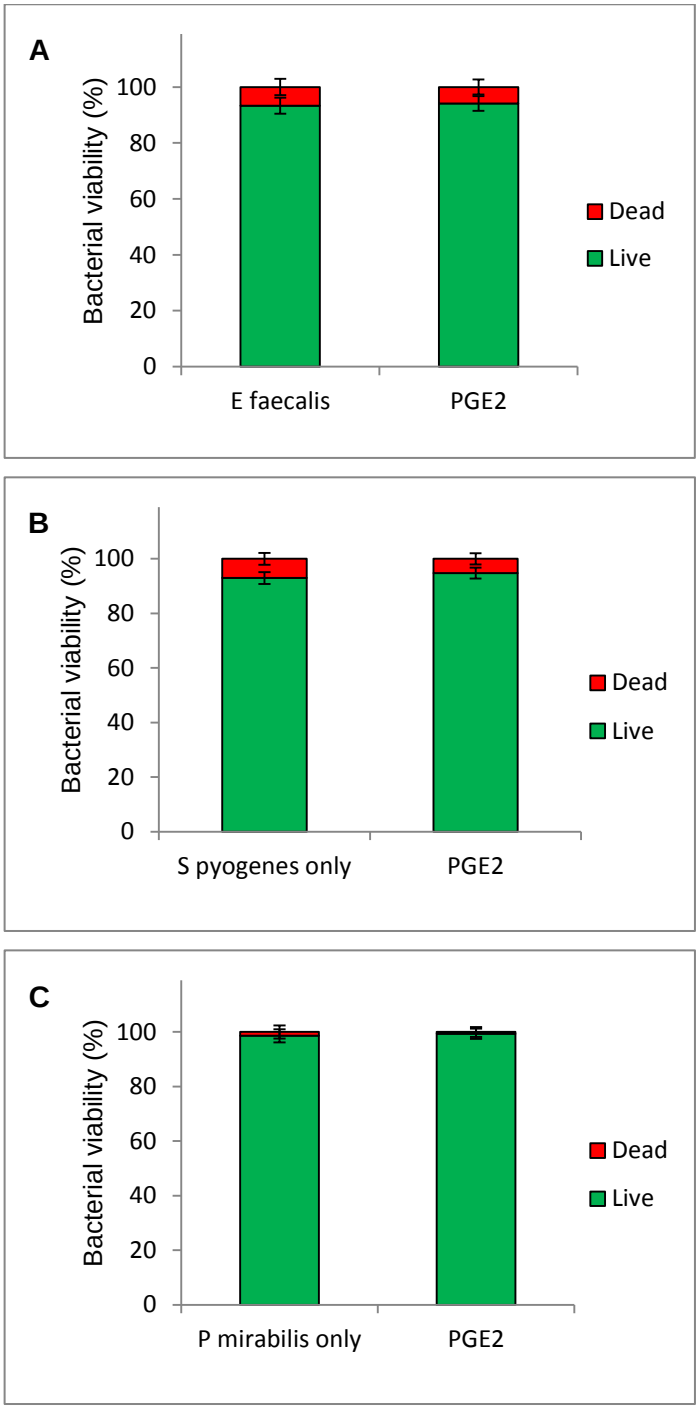

Fig. 3.9: The effect of PGE2 on bacterial viability (n=3). The viability (live [green]: dead [red] ratio) of (A) *E. faecalis*, (B) *S. pyogenes*, (C) *P. mirabilis* after culture with PGE2. Data expressed as percentage live or dead cells, +/- SD of the mean.

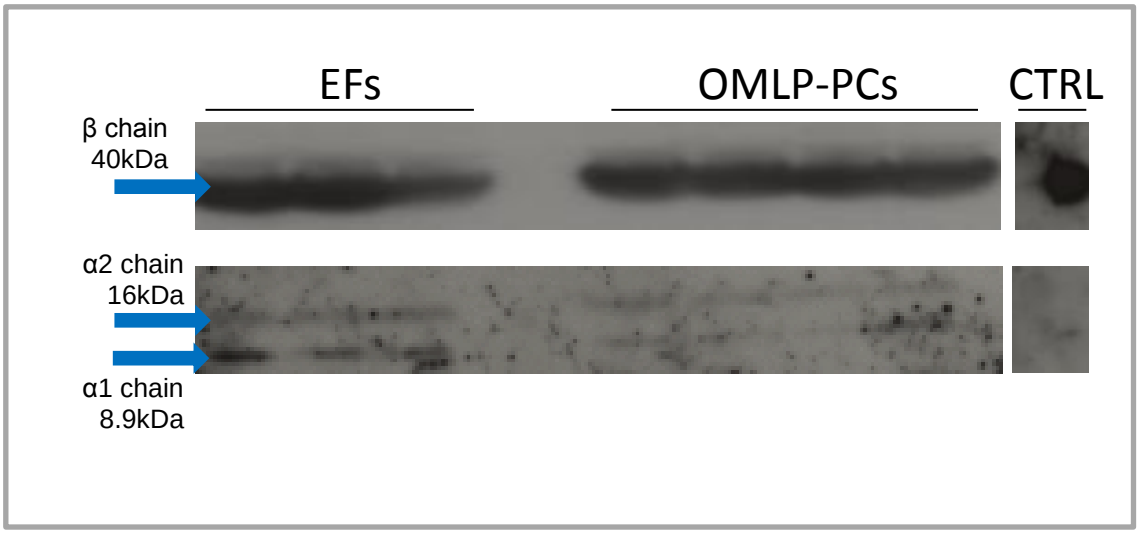

Fig. 3.10: Haptoglobin secretion by EFs (n=3) and OMLP-PCs (n=4). Western blot image demonstrating the presence of the β, α1 and α2 chains from both EFs and OMLP-PCs. Note that the both images are of the same membrane at different exposures. A positive control of Haptoglobin is represented in the CTRL lane.

3.3.4.2 Haptoglobin is Antibacterial Against Gram Negative Bacteria Through a Bacteriostatic Mechanism

Haptoglobin (0-1µg/ml, n=3: Dako, UK) was incubated with 150CFU/ml live bacteria to assess its effects on bacterial growth. Haptoglobin had no effect on the growth of the Gram positive bacteria *E. faecalis* and *S. pyogenes* ($P \geq 0.05$; Fig. 3.11 A, B). However, the growth of the Gram negative bacteria *P. aeruginosa* and *P. mirabilis* was significantly inhibited at 50pg/ml ($P \leq 0.001$; Fig. 3.11 C, D).

Gram negative bacterial cultures incubated with antibacterial levels of haptoglobin were stained using the Live/Dead® BacLight™ Bacterial Viability Kit. Haptoglobin had no significant effect on the bacterial viability (live:dead ratio) of the bacteria compared to bacteria only cultures ($P \geq 0.05$; Fig. 3.12 A, B), demonstrating it's bacteriostatic mechanism of action.

3.3.4.3 Blocking Haptoglobin Restores the Growth of Bacteria

CM samples from section 2.2.7 were incubated with 100CFU Gram negative bacteria (*P. aeruginosa* and *P. mirabilis*) +/- a haptoglobin blocking antibody. By blocking the secreted haptoglobin, the growth of both *P. aeruginosa* and *P. mirabilis* was fully restored, irrespective of whether the OMLP-PCs had previously been exposed to the bacteria or not ($P<0.01$; Fig. 3.13 A, B).

3.3.5 OPG as an Antibacterial Mediator

3.3.5.1 OPG is Constitutively Expressed by OMLP-PCs

Transcriptional and secreted levels of OPG were assessed within samples generated in section 2.2.7. OPG gene expression was analysed using qPCR whilst secreted protein levels were assessed using ELISA. OPG was constitutively expressed (Fig. 3.14 A-D) and secreted (Fig. 3.15 A-D) by OMLP-PCs, irrespective of IFNγ priming and/or bacterial exposure ($P \geq 0.05$). The expression and secretion of OPG was also noted in the EFs at similar levels to the OMLP-PCs (Fig. 3.14 A-D and Fig. 3.15 A-D), with mRNA expression further increased by Gram negative bacterial exposure to EFs ($P \leq 0.05$; Fig. 3.14 C, D).

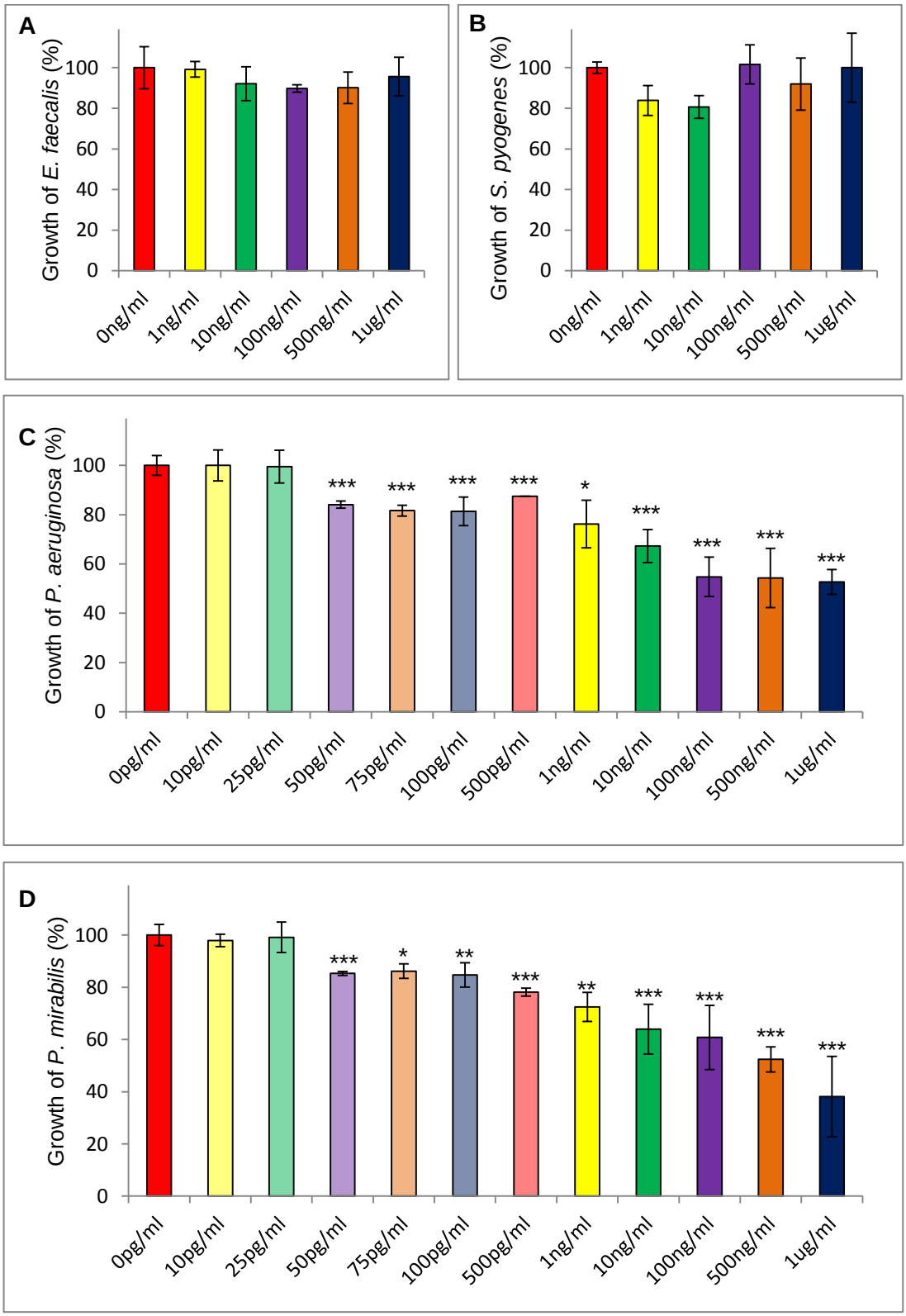

Fig. 3.11: The effect of haptoglobin (n=3) on bacterial growth. The growth of (A) *E. faecalis*, (B) *S. pyogenes*, (C) *P. aeruginosa* and (D) *P. mirabilis* after culture with haptoglobin. Data expressed as percentage bacterial growth, +/-SD. Statistics compared to 0pg/ml. *P≤0.05, **P≤0.01, **P≤0.001. Statistics compared to 0pg/ml.

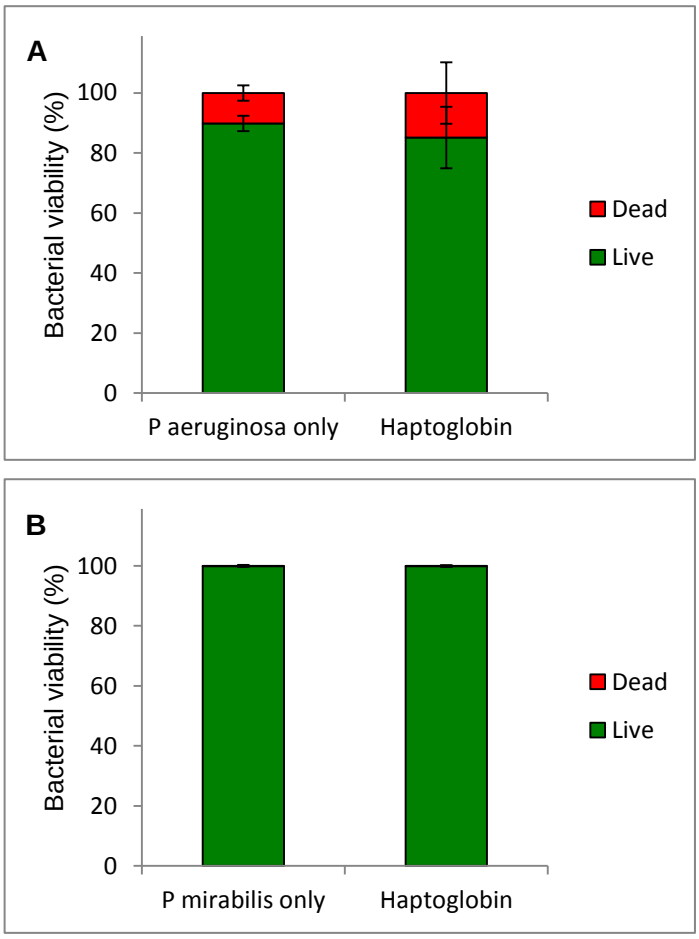

Fig. 3.12: The effect of haptoglobin on bacterial viability. The viability (live [green]: dead [red] ratio) of (A) *P. aeruginosa* and (B) *P. mirabilis* after culture with haptoglobin. Data expressed as percentage of live or dead cells, +/- SD of the mean.

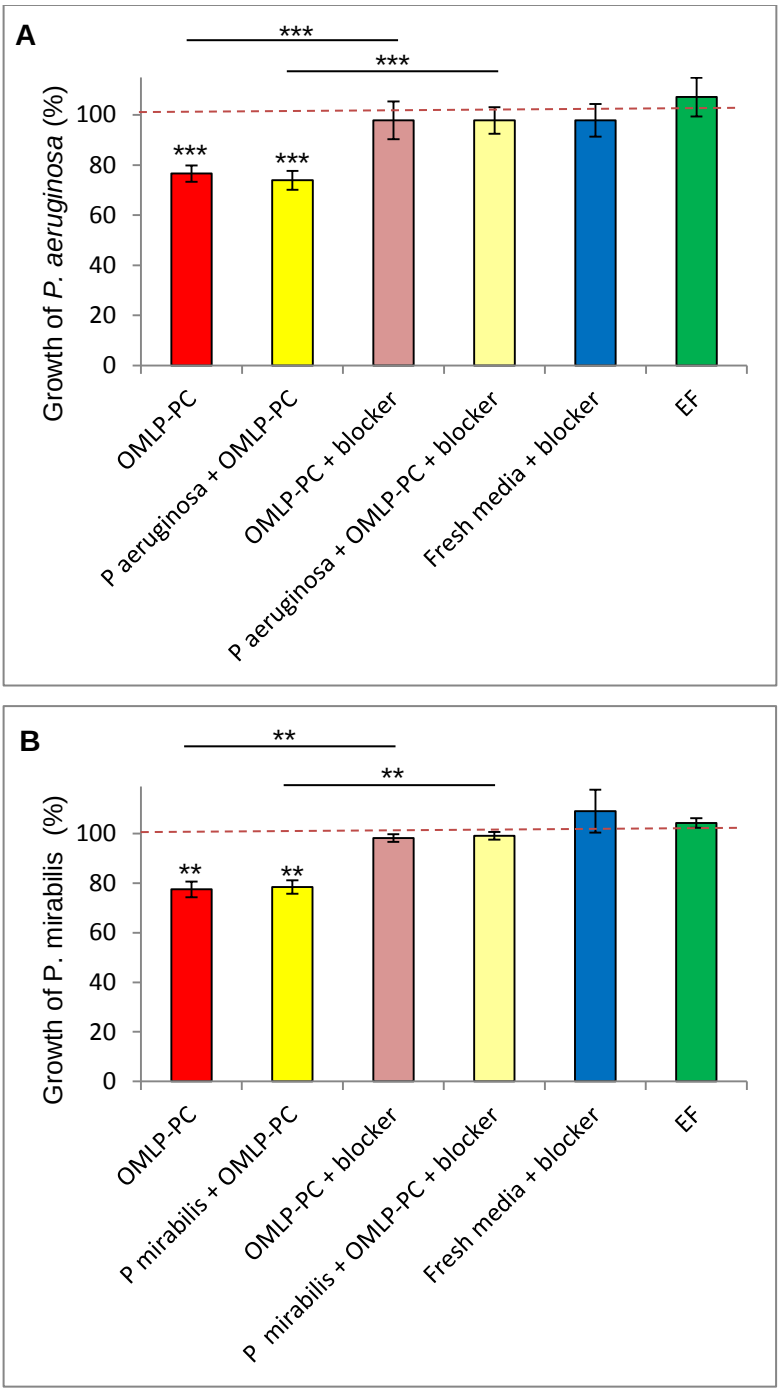

Fig. 3.13: The effect of blocking haptoglobin in the CM of OMLP-PCs (n=4). The growth of (A) *P. aeruginosa* and (B) *P. mirabilis* after incubation with OMLP-PC derived CM +/- a haptoglobin blocking antibody and EF derived CM (n=3). Data expressed as percentage bacterial growth, +/- SD of the mean. Statistics compared to bacteria only controls (represented by the red dotted line), unless otherwise stated. **P≤0.01, ***P≤0.001.

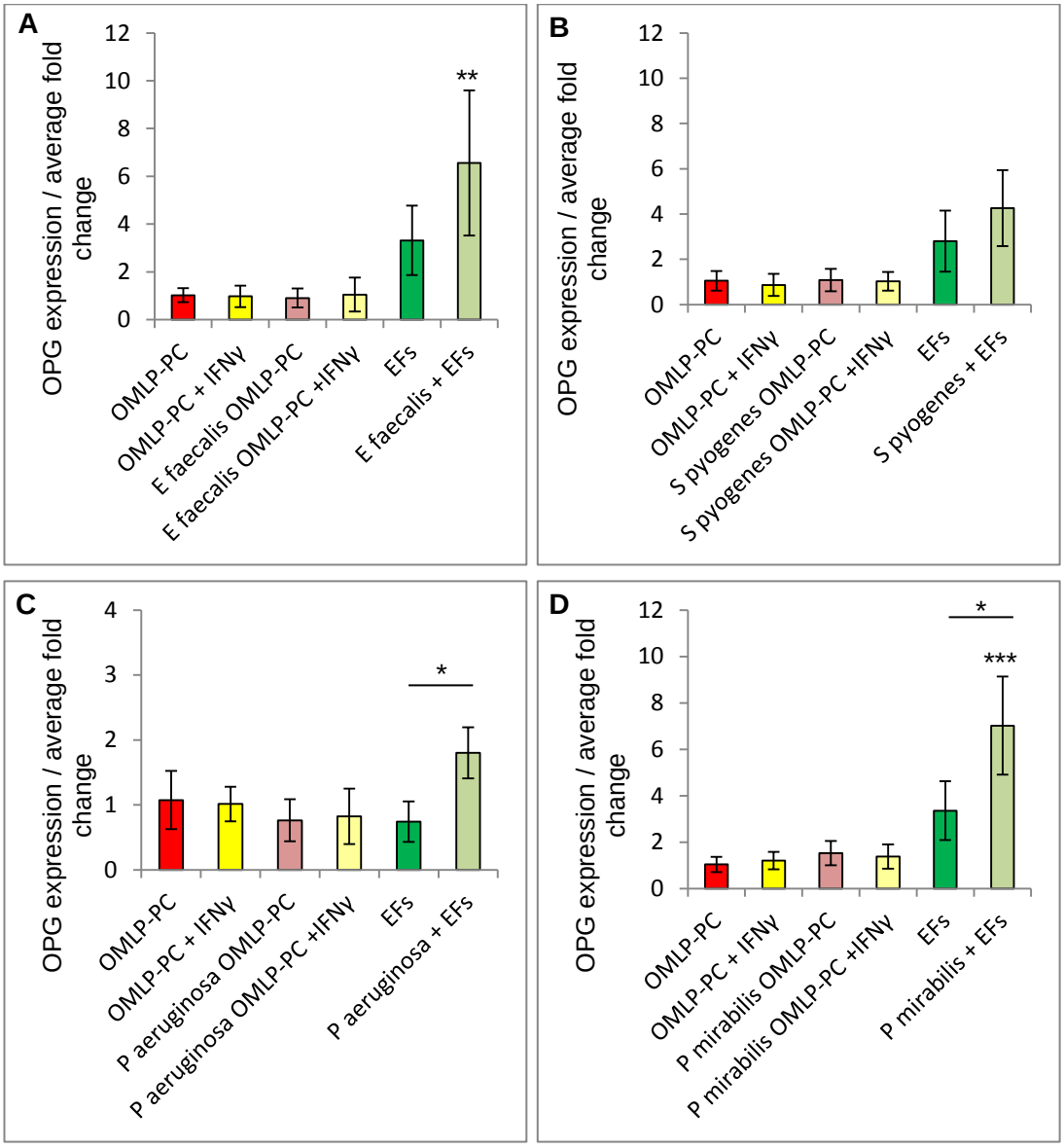

Fig. 3.14: OPG expression in OMLP-PCs (n=4) and EFs (n=3). The expression of OPG in OMLP-PCs (+/- IFNγ) and EFs +/- exposure to (A) *E. faecalis*, (B) *S. pyogenes*, (C) *P. aeruginosa* and (D) *P. mirabilis*. Data expressed as the average fold change compared to OMLP-PCs, +/- SD of the mean. Statistics compared to OMLP-PC, unless otherwise stated. *P≤0.05, **P≤0.01, ***P≤0.001.

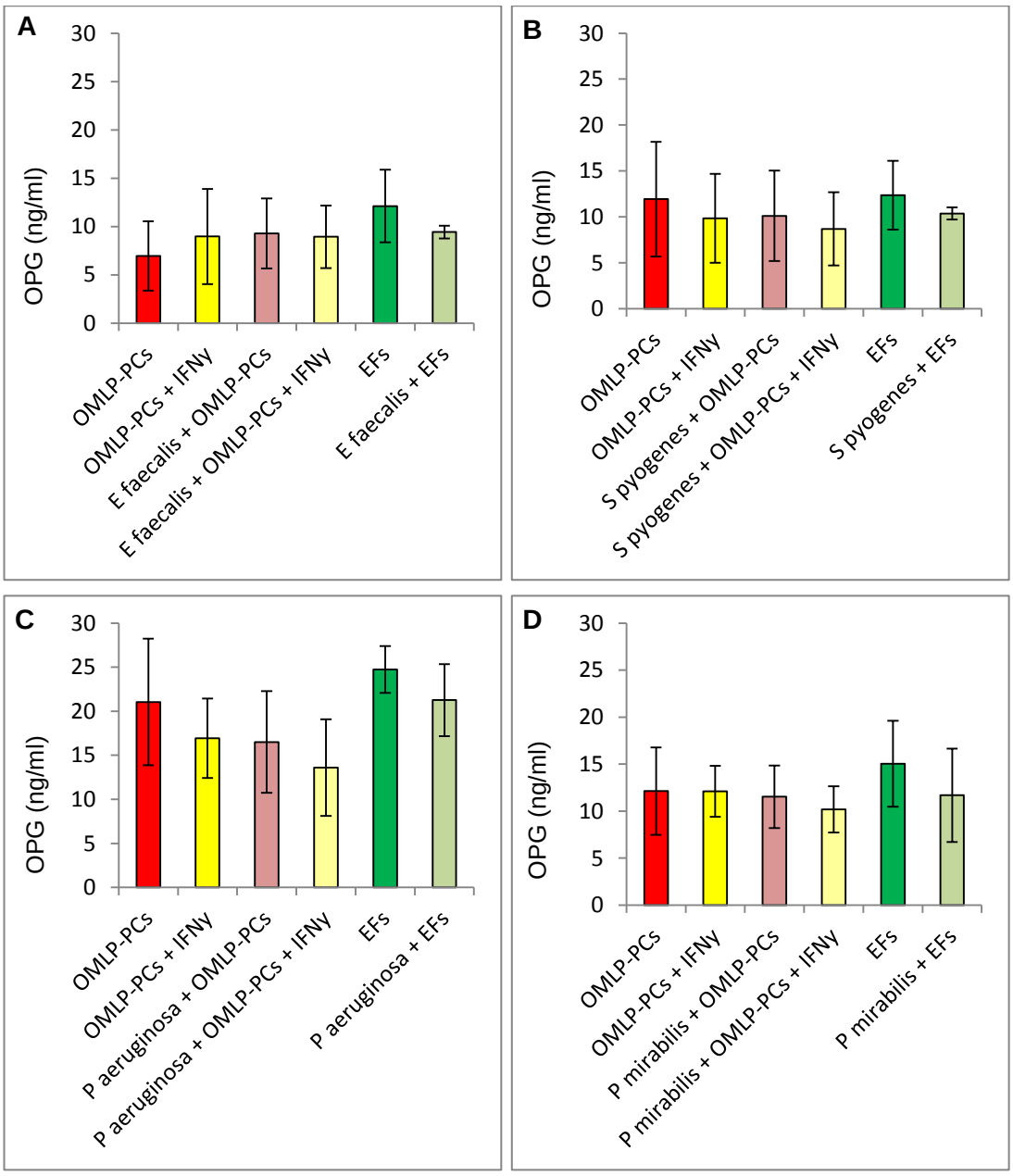

Fig. 3.15: OPG secretion from OMLP-PCs (n=4) and EFs (n=3). The secretion of OPG from OMLP-PCs (+/- IFNγ) and EFs +/- exposure to (A) *E. faecalis*, (B) *S. pyogenes*, (C) *P. aeruginosa* and (D) *P. mirabilis,* +/- SD of the mean.

3.3.5.2 OPG is Antibacterial against Gram Positive Bacteria Through a Bacteriostatic Mechanism

OPG (0-100ng/ml, n=3) was cultured with 150CFU/ml live bacteria to assess its effect on bacterial growth. The growth of the Gram positive bacteria *E. faecalis* and *S. pyogenes* was significantly inhibited by OPG at 5ng/ml ($P \leq 0.001$; Fig. 3.16 A, B). OPG had no significant effect on the growth of the Gram negative bacteria *P. aeruginosa* and *P. mirabilis* ($P \geq 0.05$; Fig. 3.16 C, D).

Gram positive bacterial cultures incubated with antibacterial levels of OPG from above were stained using the Live/Dead® BacLight™ Bacterial Viability Kit. Bacteria were counted and percentage viability calculated. The bacterial viability (live:dead ratio) was not affected by OPG compared to bacteria only cultures ($P \geq 0.05$; Fig. 3.17 A, B), demonstrating a bacteriostatic mechanism by OPG.

3.3.5.3 Blocking OPG Partially Restores the Growth of Bacteria

OMLP-PC CM samples from section 2.2.7 were incubated with 100CFU Gram positive bacteria (*E. faecalis* or *S. pyogenes*) +/- an OPG neutralising antibody. By blocking OPG within the CM, the growth of both *E. faecalis* ($P \leq 0.05$; Fig. 3.18 A) and *S. pyogenes* ($P \leq 0.001$; Fig. 3.18 B) was partially restored, irrespective of whether the OMLP-PCs had previously been exposed to the bacteria.

3.3.5.4 OPG Does Not Act in an Additive or Synergistic Effect with Haptoglobin or PGE2

It was investigated whether OPG acted in an additive or synergistic effect with haptoglobin or PGE2. Antibacterial levels of OPG were cultured with Gram positive and Gram negative bacteria +/- antibacterial levels of either haptoglobin or PGE2. As shown in Fig. 3.16, OPG significantly reduces the growth of Gram positive bacteria. The combined culture of OPG and haptoglobin or PGE2 had no further effect on the bacterial growth of either Gram positive or Gram negative bacteria compared to OPG, haptoglobin or PGE2 in culture alone ($P \geq 0.05$; Fig. 3.19 A-D and Fig. 3.20 A-D).

3.3.5.5 OPG is Antibacterial against Oral Specific Strains

To my knowledge this is the first study to demonstrate that OPG has antibacterial properties. To further extrapolate the potential effect to the oral cavity, OPG was

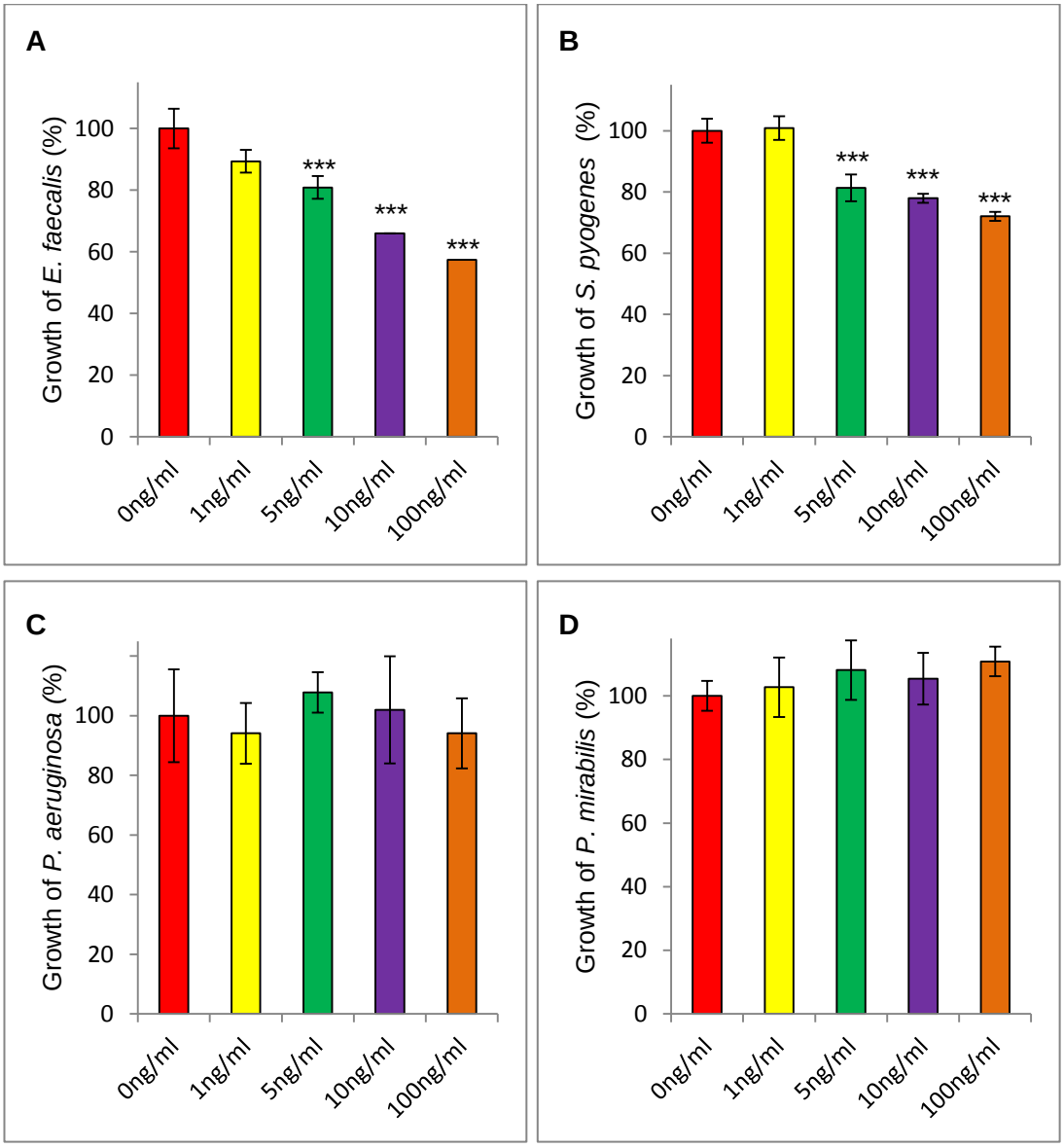

Fig. 3.16: The effect of OPG on bacterial growth (n=3). The growth of (A) *E. faecalis*, (B) *S. pyogenes*, (C) *P. aeruginosa* and (D) *P. mirabilis* after culture with OPG. Data expressed as percentage bacterial growth, +/-SD. Statistics compared to 0ng/ml. ***P≤0.001.

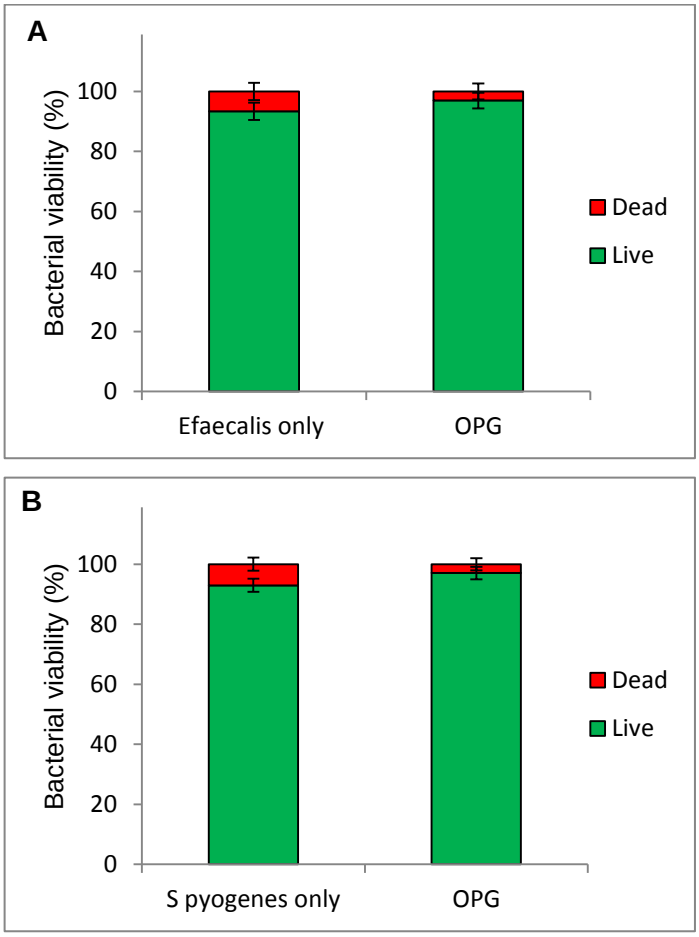

Fig. 3.17: The effect of OPG on bacterial viability. The viability (live [green]: dead [red] ratio) of (A) *E. faecalis* and (B) *S. pyogenes* after culture with OPG. Data expressed as percentage of live or dead cells, +/- SD of the mean.

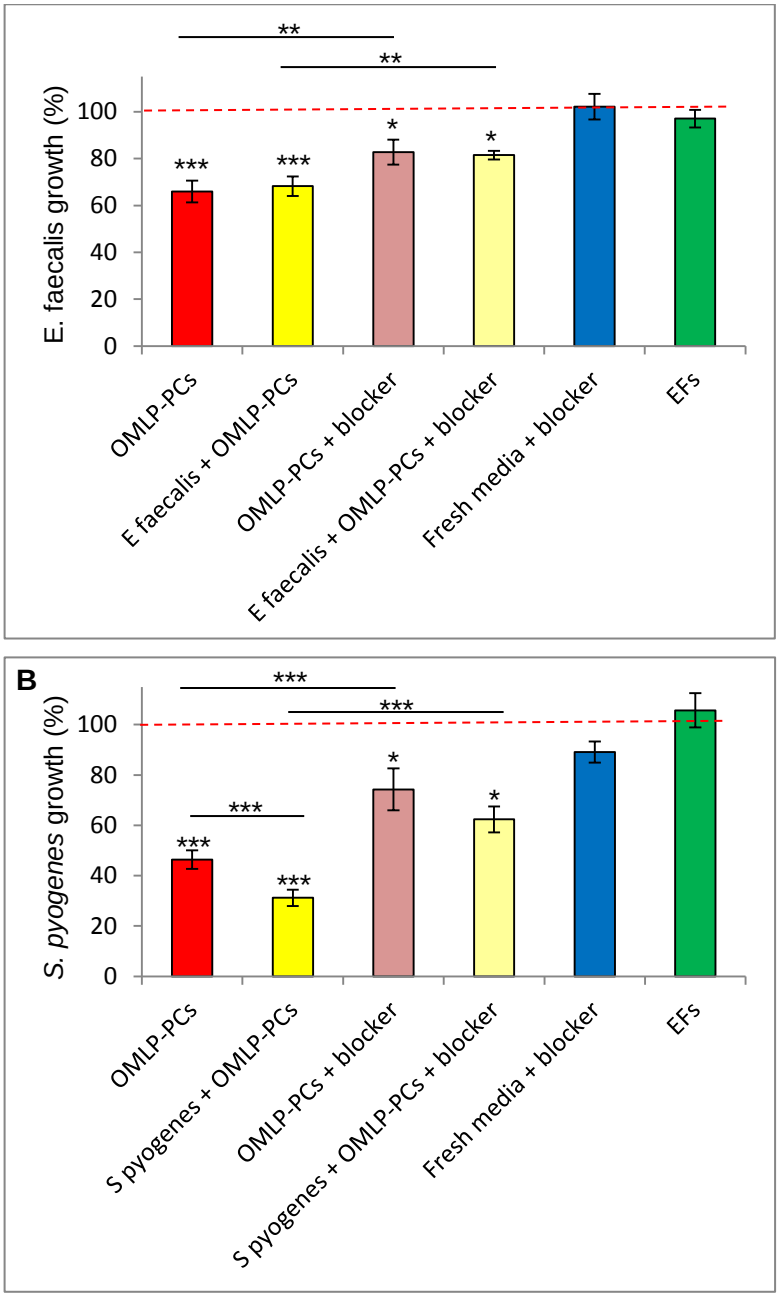

Fig. 3.18: The effect of blocking OPG in the CM of OMLP-PCs (n=4). The growth of (A) *E. faecalis* and (B) *S. pyogenes* after incubation with OMLP-PC derived CM +/- an OPG neutralising antibody and EF derived CM (n=3). Data expressed as percentage bacterial growth, +/- SD of the mean. Statistics compared to bacteria only controls (represented by the red dotted line), unless otherwise stated. **P≤0.01, ***P≤0.001.

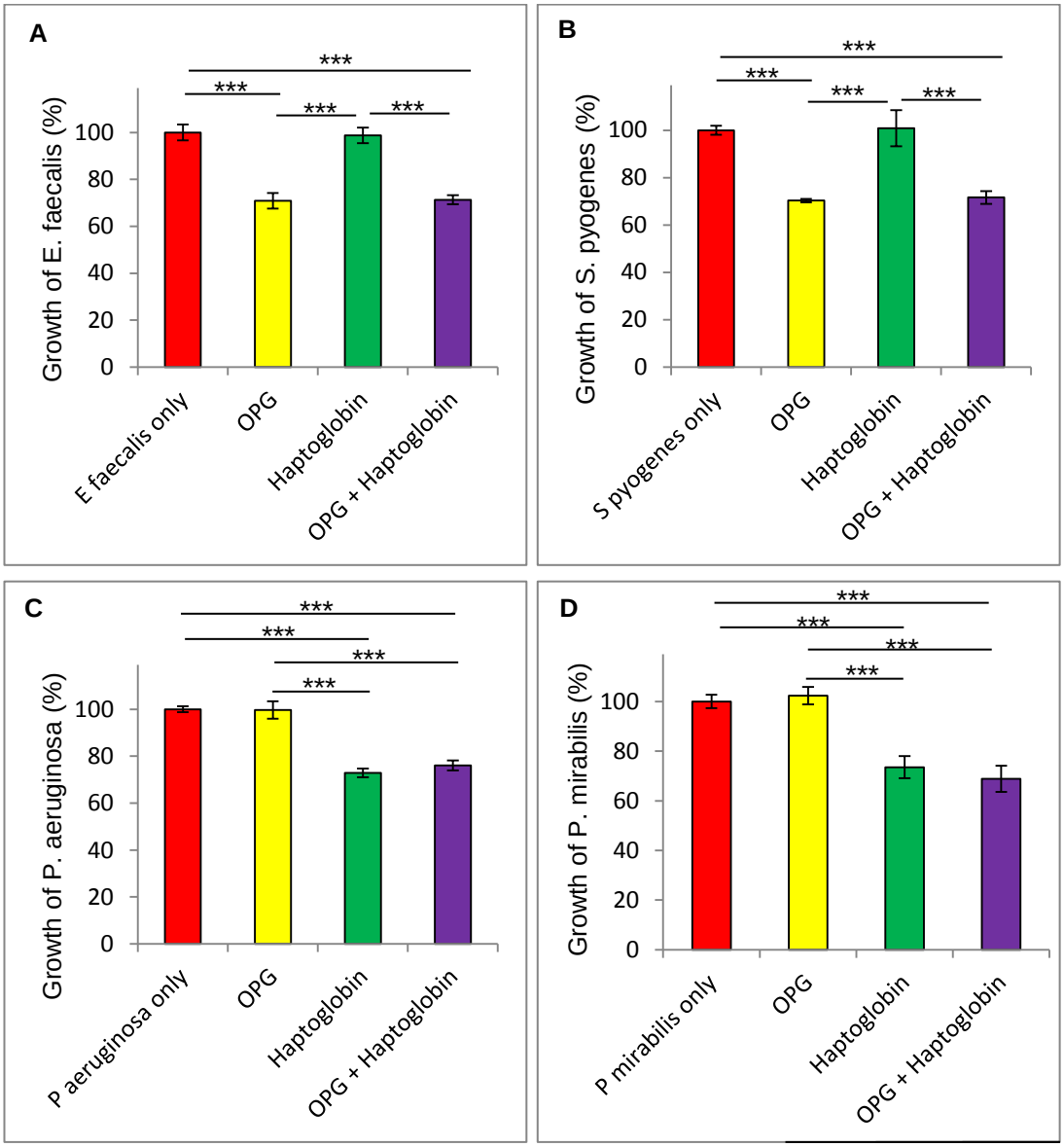

Fig. 3.19: The effect of OPG and haptoglobin combined culture (n=3) on bacterial growth. OPG and haptoglobin cultured with (A) *E. faecalis*, (B) *S. pyogenes*, (C) *P. aeruginosa* and (D) *P. mirabilis*. Data expressed as percentage bacterial growth. +/- SD of the mean. ***P≤0.001.

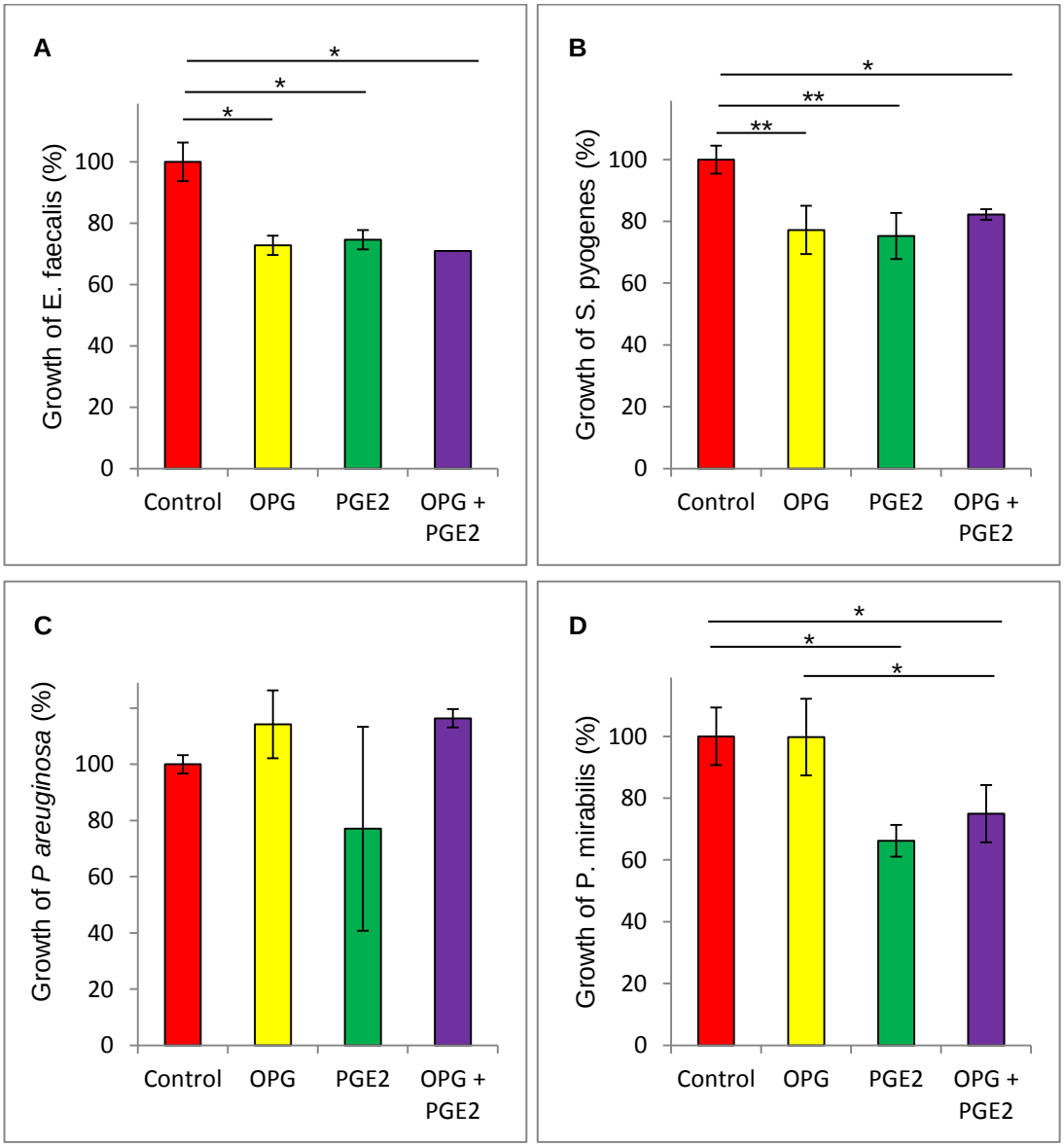

Fig. 3.20: The effect of OPG and PGE2 combined culture (n=3) on bacterial growth. OPG and PGE2 cultured with (A) *E. faecalis*, (B) *S. pyogenes*, (C) *P. aeruginosa* and (D) *P. mirabilis*. Data expressed as percentage bacterial growth. +/- SD of the mean. *P≤0.05, **P≤0.01.

cultured with the *Streptococcus* species, *S. salivarius* and *S. oralis,* isolated from the oral mucosa of patients with oral squamous cell carcinoma. OMLP-PC CM demonstrated enhanced antibacterial effects against *S. pyogenes* (section 2.3.6), potentially due to *in vivo* priming. It was for this reason that orally isolated *Streptococcus* species were chosen to assess the antibacterial effects of OPG on oral specific bacteria. OPG significantly reduced the growth of both *S. salivarius* and *S. oralis* at 5ng/ml, comparable to the non-orally derived Gram positive bacteria ($P \leq 0.001$ and $P \leq 0.05$ respectively; Fig. 3.21A, B).

3.3.5.6 Differences in the Secreted OGP from OMLP-PCs and EFs

To assess why secreted OPG had an antibacterial phenotype when secreted by OMLP-PCs but not from EFs, levels of potential protein inhibitors from EFs were examined in addition to potential structural differences within the OPG proteins.

3.3.5.6.1 OPG is Not Inhibited by Cellular Expression of TRAIL or RANKL by EFs

The expression of TRAIL and RANKL were examined within cDNA samples generated from section 2.2.7 using qPCR. Secreted levels of TRAIL were also assessed in CM samples by ELISA. The mRNA expression of RANKL was not detected in either OMLP-PCs or EFs (data not shown). The expression and secretion of TRAIL was comparable between OMLP-PCs and EFs ($P \geq 0.05$; Fig. 3.22 A, B).

3.3.5.6.2 OPG Secreted by OMLP-PCs and EFs Displays the Same Molecular Weight

The secreted OPG within CM samples from section 2.2.7 was identified using Western blot analysis. Samples were examined under non-reducing, reducing and native conditions to assess any potential differences in the secreted OPG structure from OMLP-PCs and EFs, which would affect the migration during electrophoresis, in addition to performing 2D gel electrophoresis. OPG from OMLP-PCs and EFs demonstrated the same molecular weight when exposed to each of the above conditions, with dimers (non-reducing and native; Fig. 2.23 A, C) and monomers (reducing; Fig. 2.23 B) identified at the same molecular weight for OMLP-PCs and EFs. However, the charge of the OPG appears to shift to a more negative charge in the EFs compared with OPG secreted from OMLP-PCs as shown by the Western blot analysis of the 2D electrophoresis gels (Fig. 2.24 G).

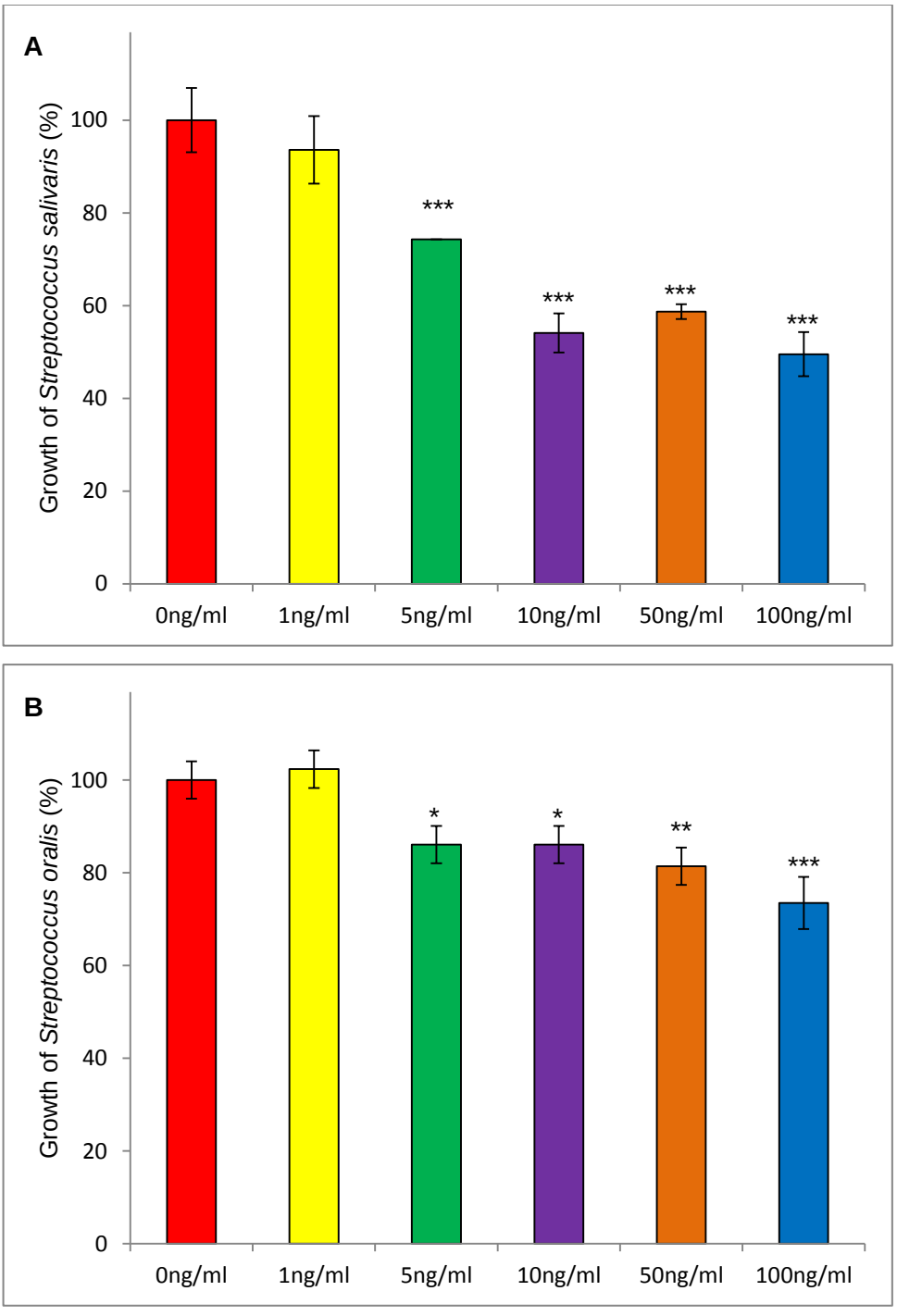

Fig. 3.21: The effect of OPG on oral specific bacterial strains. OPG (n=3) cultured with *Streptococcus salivaris* (A) and *Streptococcus oralis* (B). Data expressed as percentage bacterial growth, +/-SD. Statistics compared to 0ng/ml. *P≤0.05, **P≤0.01, ***P≤0.001.

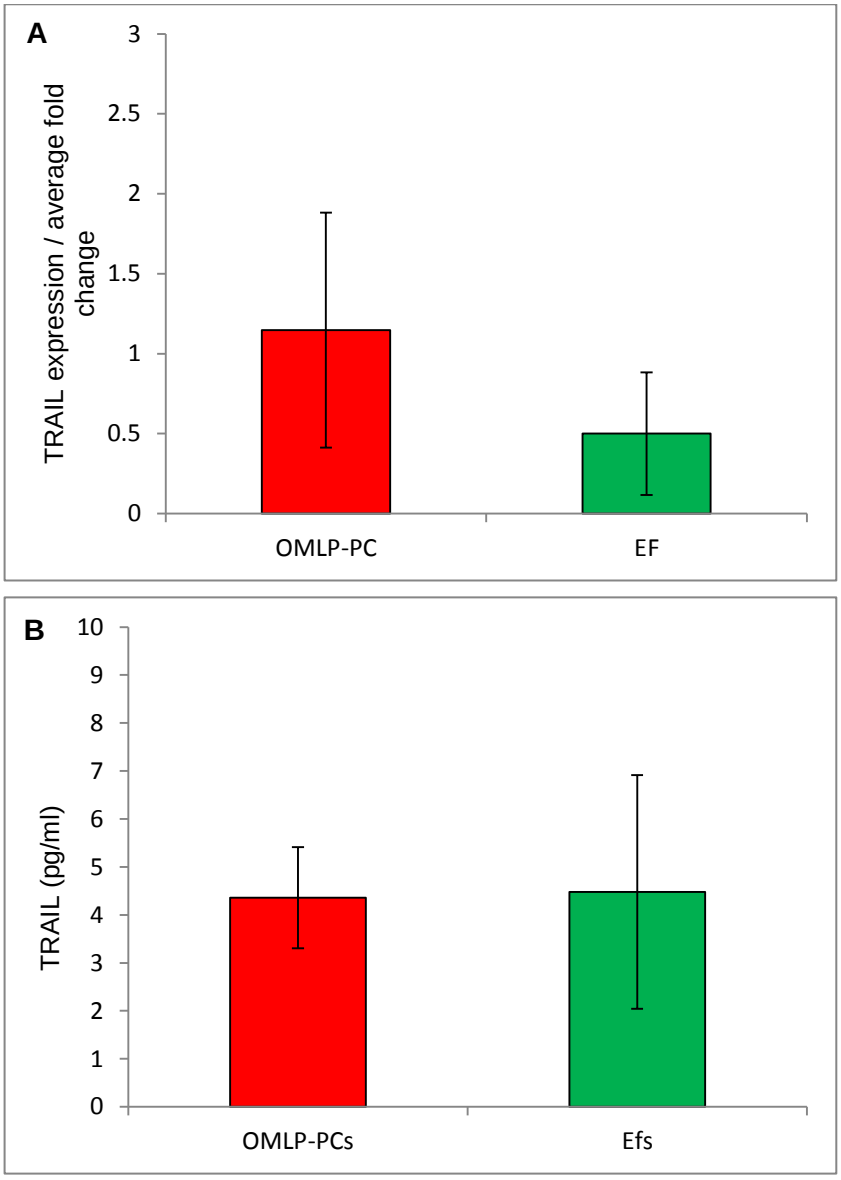

Fig. 3.22: TRAIL expression in OMLP-PCs (n=4) and EFs (m=3). The mRNA expression (A) and secretion (B) of TRAIL in OMLP-PCs and EFs. mRNA expression data represented as the average fold change compared to OMLP-PCs. +/- SD of the mean. Note: ELISA sensitivity 0-1500pg/ml.

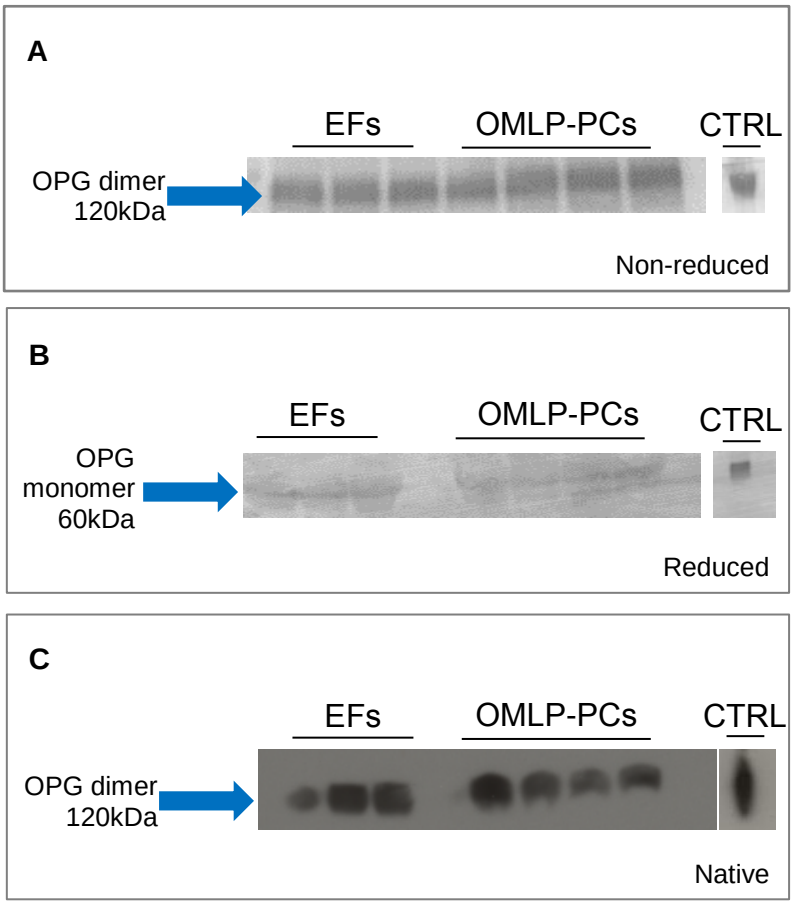

Fig. 3.23: Western blot detection of OPG in EFs (n=3) and OMLP-PCs (n=4). OPG detection in CM of OMLP-PCs and EFs subjected to (A) non-reducing, (B) reducing and (C) native conditions. A positive control of rhOPG is demonstrated in the CTRL lane.

.

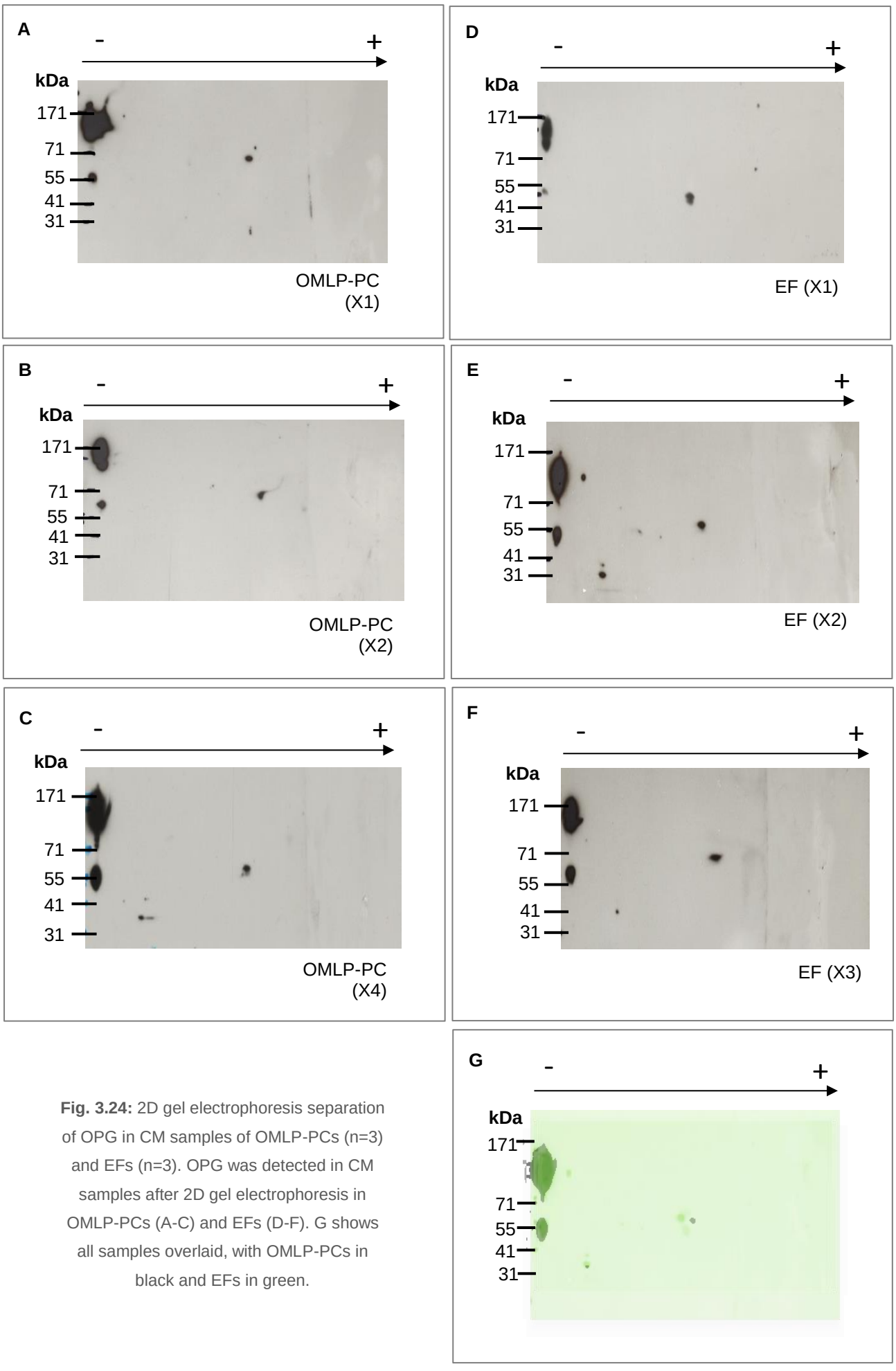

Fig. 3.24: 2D gel electrophoresis separation of OPG in CM samples of OMLP-PCs (n=3) and EFs (n=3). OPG was detected in CM samples after 2D gel electrophoresis in OMLP-PCs (A-C) and EFs (D-F). G shows all samples overlaid, with OMLP-PCs in black and EFs in green.

3.3.5.7 OPG Binds Lipoteichoic Acid on the Surface of Gram Positive Bacteria

To further examine the antibacterial mechanism of OPG, SPR was performed to investigate potential binding sites of OPG on the surface of Gram positive bacteria. Successful antibody binding to the gold plated chip and subsequent immobilisation of OPG was demonstrated (Fig. 3.25 A, B). Following OPG immobilisation, PGN or LTA was injected over the surface with binding to OPG measured. It was found that PGN did not bind to OPG (Fig. 3.26 A), whereas LTA bound to OPG in a concentration dependant manner (Fig. 3.26 B). Note that the molecular weight value for LTA was unavailable hence analysis of the binding kinetics could not be performed.

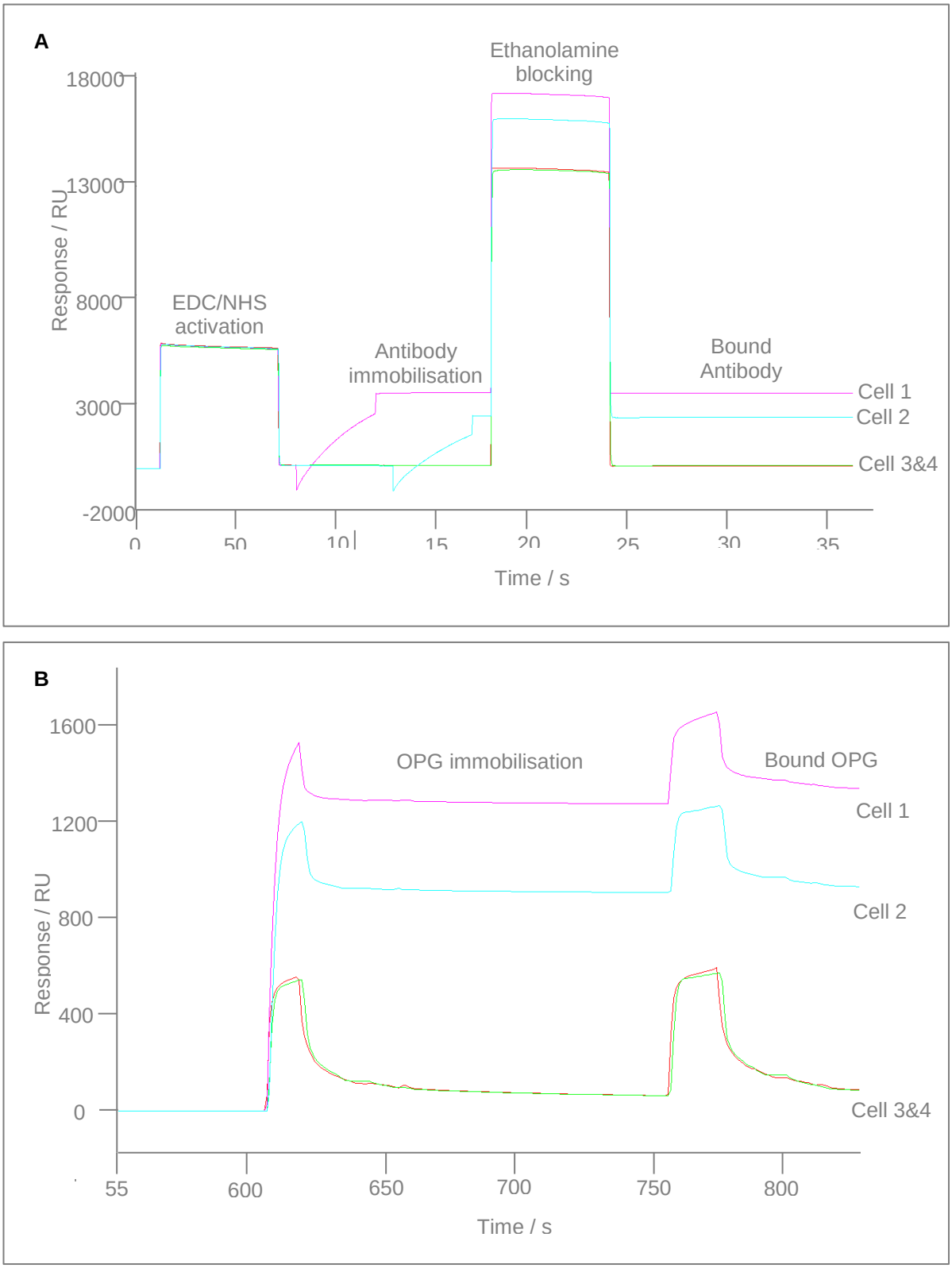

Fig. 3.25: OPG immobilisation for SPR. Successful antibody immobilisation (A) and OPG binding to the antibody (B) for SPR.

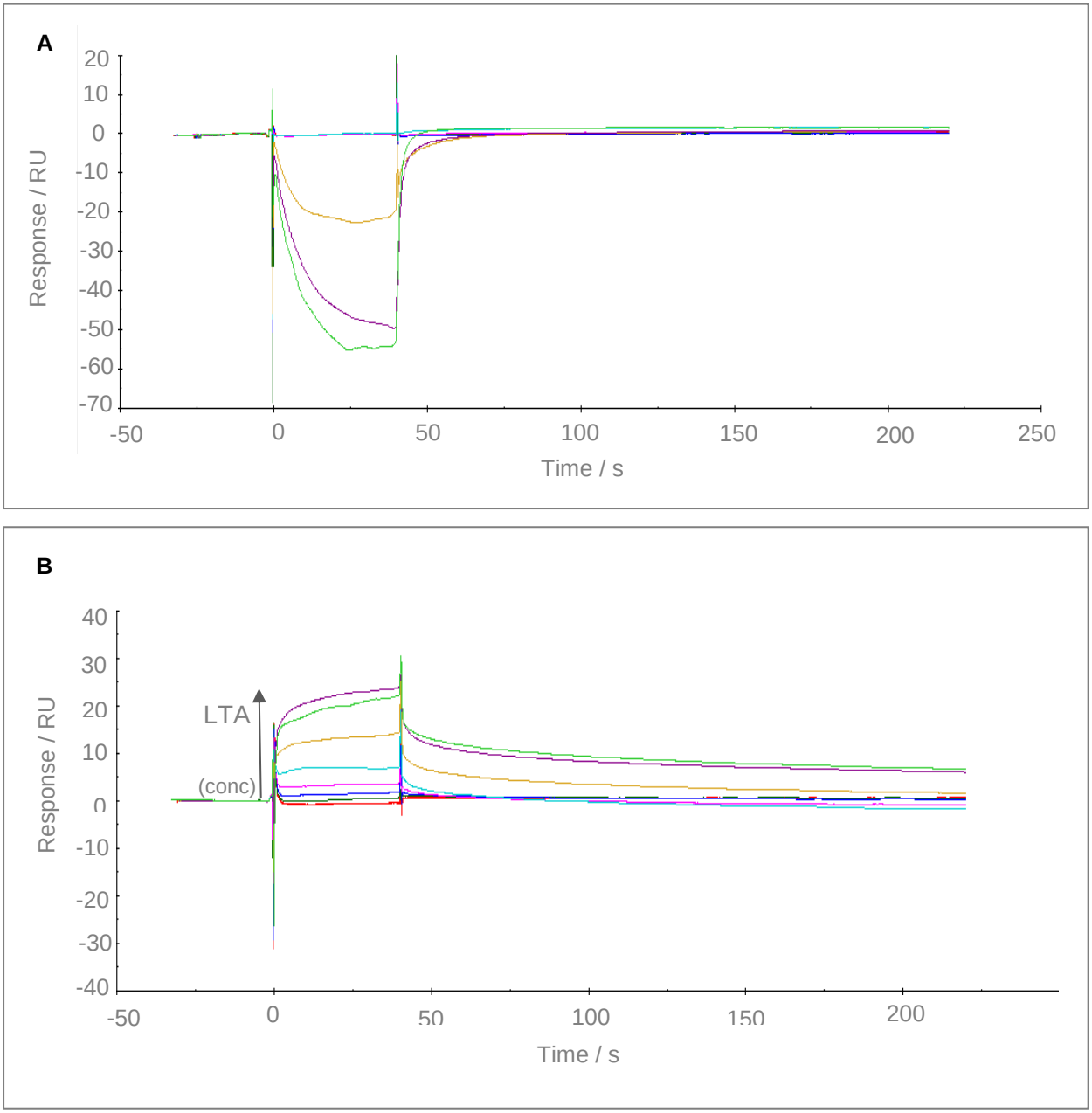

Fig. 3.26: OPG binding to Gram positive bacterial cell wall components. PGN (A) or LTA (B) binding to OPG.

3.4 Discussion

It was demonstrated in chapter 2 that OMLP-PCs possess antibacterial properties and that this was mediated through the release of soluble factors. Within this chapter the role of several different soluble factors, secreted by OMLP-PCs, was confirmed with the potential to explain their antibacterial mechanism of action. Additionally, it has been demonstrated that IDO and LL37, factors implicated in the BM-MSC mechanism (Krampera et al., 2006, Krasnodembskaya et al., 2010), are not involved in the OMLP-PC effects. This demonstrates that OMLP-PCs act by different mechanisms to those already identified for the BM-MSCs.

3.4.1 PGE2

The studies in this chapter demonstrate that in addition to the immunomodulatory properties, PGE2 is capable of directly affecting bacterial growth. At low levels, PGE2 can decrease the growth of both Gram positive and Gram negative bacteria, through a bacteriostatic mechanism. However, PGE2 was unable to affect the growth of one of the Gram negative bacteria investigated, *P aeruginosa*. This could be due to the complex cell wall structure of *P aeruginosa*, its potential mucoid phenotype and ability to create biofilms (Rybtke et al., 2015), which may limit the ability of the PGE2 lipid to penetrate the *P. aeruginosa* cell wall. The levels of PGE2 secreted from EFs are too low to demonstrate antibacterial effects. However, the secreted PGE2 from OMLP-PCs does not fully explain the antibacterial properties reported for OMLP-PCs. Blocking the secreted PGE2 could further delinate the involvement of PGE2. Blocking studies during this study were not possible. The availability of the one direct PGE2 blocking antibody (Cayman Chemical, USA) is limited. It is possible to block the COX2 enzyme, however this would not block PGE2 production specifically. Blocking COX2 would have further effects on COX2 mediated processes such as the production of other prostaglandins. It would therefore not be possible to definitively interpret any data as a direct result of blocking PGE2, but the effects may be related to other COX2 mediated factors. As not all of the antibacterial properties of OMLP-PCs could be explained by PGE2, further factors were investigated.

3.4.2 Haptoglobin

This chapter demonstrated the secretion of haptoglobin from OMLP-PCs, and the presence of the higher activity α1 chain (Sadrzadeh and Bozorgmehr, 2004). Haptoglobin's involvement in the antibacterial effects of OMLP-PCs was confirmed

when the secreted protein was blocked, preventing the direct antibacterial properties of OMLP-PCs on the Gram negative bacteria. However, the secretion of haptoglobin, along with the presence of the α1 chain was also detected in the non-antimicrobial EFs. The potent antibacterial activity of haptoglobin was recorded at 50pg/ml. The marginal differences in secreted levels of haptoglobin, which may account for the lack of antibacterial properties in EFs, are extremely difficult to quantify at such low levels. Commercial ELISA kits were unable to detect the secreted protein from either OMLP-PCs or EFs, with a sensitivity in the ng/ml range. Therefore it was not possible to undertake a direct comparison of the secreted levels of haptoglobin from OMLP-PCs and EFs. It is hypothesised that the ratios of different isoforms of haptoglobin vary between OMLP-PCs and EFs, with a greater abdundance of the higher activity isoforms containing the α1 chain secreted by OMLP-PCs. This could be investigated using pull down assays with an antibody specific to the α1 chain to isolate the higher activity isoforms.

Haptoglobin was shown to be antibacterial against Gram negative bacteria, with no effects on Gram positive bacteria, even at high levels. The bacteriostatic effects of haptglobin against *E. coli,* a Gram negative bacteria, through the depletion of iron have long been documented (Eaton et al., 1982). Whilst both Gram positive and Gram negative bacteria are dependant on iron, the levels and uptake mechanisms can vary dramatically between organisms. *S. pyogenes* is able to bind and transport ferric iron (Fe^{3+}), a stable form of iron, through an ATP-binding cassette transporter. However, both the *P. aeruginosa* and *P. mirabilis* are able to sequester iron from iron complexes, particularly when iron availability is restricted. FpvA (Shen et al., 2005) and FpvB (Ghysels et al., 2004) are the outer membrane transporters involved in iron uptake in *P. aeruginosa* which are capable of sequestering iron from ferripyoverdine binding (Cornelis and Dingemans, 2013). *P. mirabilis* iron uptake is mediated by a 64kDa iron-regulated outer membrane protein which is capable of sequestering iron from haem (Lima et al., 2007). As Gram positive bacteria lack the outer membrane, the outer membrane proteins involved in iron uptake during iron restriction are not present. The differences in iron uptake mechanisms could potentially explain the selective antibacterial properties of haptoglobin.

3.4.3 OPG

To my knowledge this is the first study to demonstrate that OPG possesses antibacterial properties, with decreased levels during inflammatory conditions

associated with infection such as periodontitis (Bostanci et al., 2007), potentially contributing to the disease. OPG decreased the growth of Gram positive bacteria in direct culture, with no effects observed on the growth of Gram negative bacteria. OPG was demonstrated to act in a bacteriostatic manner and was found to bind LTA on the surface of the Gram positive bacteria. This explains the lack of antibacterial effects against Gram negative bacteria, which do not express LTA on the surface of their cell wall, preventing binding of OPG to these bacteria. It was further shown that the antibacterial properties of OPG were not confined to the reference strains initially examined. OPG significantly reduced the growth of Gram positive, *Streptococcus salivaris* and *Streptococcus oralis* isolated from the oral mucosa of patients with oral squamous cell carcinoma, at the same level (5ng/ml) of the reference strains. These facultative anaerobes represent bacteria, which may lay near the surface of biofilms, due to the accessibility to oxygen. It is also known that OPG is detected within the oral fluids such as saliva (Buduneli et al., 2008) and grevicular fluid (Balli et al. 2015). With this knowledge and data from this study it is evident that OPG could affect bacteria on the surface of biofilms, highlighting the potential importance of OPG in maintaining the microflora of the oral cavity.

The involvement of OPG in the antibacterial mechanism of OMLP-PCs was confirmed when the secreted OPG was neutralised, inhibiting some of the antibacterial effects of OMLP-PCs. However, the expression and secretion of OPG was also noted in EFs at comparable levels. It was hypothesised that the secreted OPG from EFs was either bound to an inhibitor, or that the structure/conformation of the secreted OPG was different, blocking the LTA binding site, compared to the OMLP-PCs. RANKL and TRAIL are known to bind OPG (Baud'huin et al., 2013), which could potentially block the LTA binding site. However the expression levels within OMLP-PCs and EFs did not vary, indicating that the release of these factors and subsequent binding to OPG, most likely, did not account for the lack in antibacterial activities by OPG secreted from EFs. Western blot analysis was performed to continue to investigate this hypothesis. It was found that under non-reducing conditions, OPG secreted from EFs was not bound to a protein inhibitor (that was large enough to detect by Western blot analysis). It would not be possible to detect the molecular weight change in OPG if it was bound to a small protein or peptide. Further studies would be needed to fully rule out the possibility of a bound inhibitor to OPG secreted from EFs. For example, label transfer could be used to isolate proteins bound to OPG. The process would involve pre-labelled OPG which

would transfer its label (e.g. biotin) to an interacting protein. OPG could then be cleaved from the interaction and the OPG interacting protein isolated using the label. Isolated proteins could then be analysed using electrophoresis, protein sequence analysis or mass spectrometry.

Under reducing and non-reducing conditions (including native), it was oberserved that the monomers and dimers (respectively) which make up OPG were the same between the OPG secreted by OMLP-PCs and EFs, confirming that no structural differences affecting molecular weight were present. The secreted OPG was also separated by charge in addition to size, using 2D gel electrophoresis. It was found that there were differences in the charge of the secreted OPG, with the protein secreted from EFs displaying a more negative charge compared with that secreted from OMLP-PCs. This may be explained by differing levels of glycosylation on the OPG secreted from EFs and OMLP-PCs, as the OPG protein contains several N-glycosylation sites (Lerner, 2004). Glycosylation can affect both the molecular weight and isoelectric point of a protein, manifesting in differences during 2D gel electrophoresis. Further studies are required to determine any additional differences in the secreted OPG from the two different cell sources. Immunoprecipitation may be used to purify OPG from both the OMLP-PCs and EFs. The purified OPG could then be incubated with live bacteria to demonstrate the differences in antibacterial activity. Furthermore the isolated protein could be sequenced to identify differences in protein sequence and potential splice variants. Additionally crystallography could be undertaken to assess any differences in the crystal structure of OPG secreted from OMLP-PCs and EFs. Furthermore, crystallising the structure of OPG bound to LTA could identify the LTA binding site, and pinpoint any differences in bacterial binding capabilities of the secreted OPG. Crystallography is however a time consuming process and dependant on the sufficient levels of purified OPG. Purifying appropriate levels of OPG using immunoprecipitation may also prove a time consuming process with just 10ng/ml being secreted by both OMLP-PCs and EFs. It is also possible that by binding to an antibody during the immunoprecipitation process, OPG could change its structure. Whilst it is possible the structure could revert back to its original secreted structure when eluted, it is not guaranteed.

CM samples were stored at -80°C before thawing for analysis. It is important to consider the effect of freeze thawing on the samples and any possible degradation of potential antibacterial proteins or peptides sensitive to this process. Therefore further mechanisms must be considered and the presence of such proteins or peptides compared to freshly generated samples which have not undergone freeze thawing.

3.5 Conclusion

The aim of this chapter was to identify the soluble factors mediating the antibacterial effects of OMLP-PCs. It was demonstrated that several different factors were involved. The factors identified in mediating the BM-MSC antibacterial effects, IDO and LL37, were not implicated in the OMLP-PC mechanism. This highlights the difference in the antibacterial mechanisms by the different cell populations, which could be attributed to the differences in the environment from which the cells were isolated.

The direct antibacterial effects of PGE2, haptoglobin and for the first time OPG were reported in this study, with antibacterial levels secreted from OMLP-PCs. The lack of antibacterial effects of EFs, despite secreting active levels of OPG, is not fully understood. Differences in the charge of OPG secreted from EFs compared to OMLP-PCs was reported. Further studies are required to delineate the difference in OPG secreted by EFs and the antibacterial OMLP-PCs. Greater understanding in the differences may be assessed after isolating the secreted OPG and examining the protein sequences and structure.

Each antibacterial factor demonstrated selective antibacterial properties, with no one factor fully explaining the antibacterial properties of OMLP-PCs *in vitro*. It is likely that additional factors are involved in the antibacterial effects of OMLP-PCs. The oral cavity constantly displays a rich microbial diversity, and it is therefore essential that a diverse range of antibacterial factors is present within the oral cavity. This chapter highlights the potential involvement of OMLP-PCs in oral homeostasis by the secretion of several different antimicrobial factors.

4. Changes in the Antibacterial Potential of OMLP-PCs during Chronic GVHD

4 Changes in the Antibacterial Potential of OMLP-PCs during Chronic GVHD

4.1 Background

GVHD develops when donor T cells within transplanted material (HSCT) become activated and mount an intense inflammatory/immune response within the recipient (Ferrara et al., 2009). The development of the disease results from a multi-staged process. Initial chemotherapy or radiotherapy before HSCT results in tissue damage in the patient and the release of bacterial products such as LPS from the gut microflora. Accumulation of such products results in a pro-inflammatory cytokine response and the migration of host APCs to secondary lymphoid organs. APCs within the lymph nodes become activated and present antigen to the donor T cells, leading to their activation and proliferation. This in turn stimulates the production of IFNy and IL-2 from the donor T cells. The activated T cells then migrate to the target tissues of the host such as the skin, gut, liver and oral cavity (in the case of chronic GVHD [cGVHD]) where cell apoptosis is initiated and further cytokine release is stimulated to perpetuate the process (Ferrara and Reddy, 2006).

The disease is most associated with patients who receive HSCT with a mismatch in HLA proteins, with overall survival decreased with the increase in mismatched HLA proteins (Loiseau et al., 2007). The disease is grouped into two classifications; acute GVHD (aGVHD) and cGVHD. The aGVHD form traditionally manifests itself within 100 days of the transplantation, whereas cGVHD presents 100 post transplantation, potentially lasting the lifetime of the patient (Martin et al., 2015).

Up to 83% of patients undergoing HSCT who develop cGVHD display oral symptoms (Mays et al., 2013). Symptoms include mucosal atrophy, ulceration, erythema, microbial infections and pain (Granitto et al., 2014). Patients with oral cGVHD are thought to be more susceptible to infections such as candidiasis, potentially due to the steroid based treatment of the disease (Treister et al., 2012). It has been further hypothesised that a dysfunction in the stromal cells of the oral cavity manifests after HSCT treatment, resulting in the decreased immunoregulatory capacity of the cells (Garming-Legert et al., 2015). A further lack of anti-microbial and anti-inflammatory factors resulting from the dysfunctional stromal tissue is predicted, leading to

increased infections and poor wound healing of the affected areas. With potential increases in microbial infections during HSCT and GVHD, it is important to consider the pathological changes, which may occur within the oral mucosa and the implications they may have on infections. Changes in the secretion of antimicrobial or immunomodulatory factors may contribute to oral GVHD and the increased infections observed.

Chapters 2 and 3 have established the direct antibacterial properties of OMLP-PCs in healthy individuals. The increased microbial infections during GVHD may be attributed to the loss of antibacterial functions of the OMLP-PCs or a decrease in progenitor cell numbers in these patients. It is unknown whether potential changes in OMLP-PCs are modulated by GVHD, which therefore predisposes the oral cavity to infections. Furthermore, the oral cavity may be more vunerable to infections before the development of GVHD by the conditioning regimes prior to HSCT (Kedia et al., 2013). Conditioning regimes such as chemotherapy and radiotherapy target the immune cells within the bone marrow, limiting the innate defence in these patients. Immunosuppressive treatment, to prevent HSCT rejection, further limits the innate immune system. Overall this limits the patient's ability to overcome infection.

Mucosal damage has been documented in the gastrointestinal tract following HSCT. Colitis, pneumatosis intestinalis, thickening of the mucosal layer and increased infections by micro-organisms such as *Clostridium difficile* have been reported (Lee et al., 2008). Furthermore, conditioning regimes will damage the mucosal linings (Ferrara and Reddy, 2006). Similar effects of HSCT and the conditioning regimes on the oral mucosa have been documented, with oral mucositis the predominant side-effect reported. Oral mucositis is characterised by mucosal damage extending from mild inflammation to extensive ulcerations caused by epithelial cell apoptosis (Haverman et al., 2014). The resulting ulceration leads to a loss in mucosal integrity and facilitates microbial colonisation with further pro-inflammatory cytokine release initiated. Oral mucositis can cause severe pain and limited movement (limiting the patient's ability to eat), which has a detrimental effect on the patient's quality of life (Bellm et al., 2000). Whether the mucosal damage from HSCT results in the dysfunction of OMLP-PCs is unknown.

The migration of innate immune cells to the site of infection is crucial to limit the damage caused during infections. Chemokines such as TNFα, IL-8 and IL-1β are secreted by tissue-resident cells such as epithelial cells, providing concentration

gradients for the migration of innate cells, such as neutrophils, to affected sites (Kolaczkowska and Kubes, 2013). The secretion of the chemoattractant factor, IL-8, is reported from BM-MSCs, nasal mucosal MSCs and human salivary gland MSCs (Jakob et al., 2010, Jakob et al., 2013) demonstrating the potential of these stem cell populations to recruit immune cells such as neutrophils.

The release of stromal derived factor (SDF)-1 by bone marrow stromal cells ensures the retention of neutrophils within the marrow environment by binding the CXCR4 receptor on the neutrophil surface (Summers et al., 2010). Potentially, the release of SDF-1 could lead to the immobilisation of neutrophils at the site of infection. Furthermore, MSCs are known to decrease neutrophil apoptosis through IL-6 secretion (Raffaghello et al., 2008) and increase the phagocytosis of bacteria by neutrophils (Hall et al., 2013). Additionally neutrophil activation and chemotaxis is promoted by MSCs through the secretion of factors such as IL-8 (Chen et al., 2014).

The beneficial effects of BM-MSCs in patients with sepsis, including reduced mortality and improved organ function, have been reported to be dependent on BM-MSC effects on monocytes and macrophages (Németh et al., 2009). The secretion of factors such as prostaglandin E2 (PGE2) by BM-MSCs stimulates IL-10 secretion from monocytes and M2 macrophages. Depeletion of the monocyte and macrophage populations within a polymicorbial septic mouse model eliminated the beneficial effects of BM-MSCs. Furthermore, increased monocyte phagocytosis of bacteria such as *Escherichia coli* has been documented with BM-MSC treatment (Krasnodembskaya et al., 2012). It has also been reported that MSCs can modulate the phenotype of macrophages, shifting the population from the pro-inflammatory M1 to the anti-inflammatory M2 phenotype (Dayan et al., 2011, Nakajima et al., 2012, Melief et al., 2013). Overall, the effects of MSCs on innate immune cells enhances the anti-microbial properties of cells such as neutrophils and monocytes through direct effects on bacterial phagocytosis, chemotaxis and shifts in the inflammatory cytokine release, leading to beneficial effects during infections such as sepsis. It is hypothesised that OMLP-PCs may contribute to oral homeostasis in a similar manner with both direct antibacterial effects demonstrated in chapter 2, and indirect effects through modulating cells of the innate immune system.

This study aims to investigate the direct antibacterial potential of OMLP-PCs isolated from oral cGVHD patients. The ability of the cells to express and secrete cyto- and

chemokines relevant to the attraction of innate immune cells will also be examined, and whether this is altered during oral cGVHD.

4.1.1 Aims

1. To compare the antibacterial potential of oral cGVHD patient derived OMLP-PCs to those isolated from healthy donors.

2. To assess the involvement of OMLP-PCs in innate defence during GVHD by comparing the expression and secretion of antibacterial and chemoattractant factors from GVHD patient derived OMLP-PCs to those derived from healthy donors.

4.2 Materials and Methods

Cell isolation and the generation of CM and cDNA samples was performed by Dr Lindsay Davies and Dr Gregory Tour, Karolinska Institute as part of an on-going collaborative project. ELISAs (except PGE2) were carried out by Dr Gregory Tour, Karolinska Institute. All flow cytometry cell characterisation, qPCR, IDO activity assays, PGE2 quantification, haptoglobin Western blot analysis and antibacterial assays were carried out by myself, Emma Board-Davies, in addition to all data analysis.

All tissue culture reagents were purchased from Life Technologies Europe BV (Stockholm, Sweden) unless otherwise stated.

4.2.1 Isolation of OMLP-PCs and EFs from Healthy and GVHD patients

OMLP-PCs and EFs were isolated and expanded from healthy donors (hOMLP-PCs and hEFs) and moderate-severe grade oral cGVHD patients (gOMLP-PCs and gEFs) as described in section 2.2.1. The study was approved by Karolinska University Hospital, Stockholm Ethical Committee and conducted in accordance with the Declaration of Helsinki. All donors provided written consent. All GVHD patients were classified as having severe cGvHD using global severity scoring according to the National Institute of Health (NIH) Consensus Working Group for Diagnosis and Staging of cGvHD. Furthermore all patients included had a cGvHD organ score of 3/3 within the oral cavity, with evidence of non-healing oral lesions of the buccal mucosa. Five millimeter punch biopsies were taken from an area of the buccal mucosa unaffected by lesions.

4.2.2 Characterisation of OMLP-PCs and EFs from Healthy Donor and GVHD Patients

Flow cytometry was used to ensure that the cells from both healthy and GVHD donors displayed the same cell surface expression for the previously defined stem cell markers (Davies et al., 2010). OMLP-PCs and EFs from healthy donors (n=4, n=3 respectively) and OMLP-PCs and EFs from GVHD patients (n=6, n=3 respectively) were cultured in DMEM supplemented with 10% (v/v) FCS, 2mM L-glutamine and antibiotics/antimycotics (100 U/ml penicillin G, 100 µg/ml streptomycin sulphate and 0.25 µg/ml amphotericin B) herein referred to as complete medium to 90% confluence. Cells were subsequently removed from the plastic using Accutase® before pelleting cells at 500xg for 5mins. Cells were resuspended in 800µl complete

medium and aliquoted into 8 flow cytometry tubes (100ul/tube). Cells were stained with CD105-fluorescein isothiocyanate (FITC) (Clone SN6h, Ancell, USA; 5µl), CD73-phycoerythrin (PE) (500257, BD Bioscience, Sweden; 5µl), CD90-FITC (Clone 5E10; BD Bioscience, 2.5µl), CD14-PE/CD45-FITC Simultest™ (clone MφP9 and clone 2D1 respectively; BD Bioscience, Sweden; 5µl), CD31-FITC (Clone WM59 BD Bioscience; 2.5µl), HLAI-RPE (Clone W6/32, Dako, Sweden; 3.5µl) and HLAII-FITC (Clone CR3/43 Dako, Swden; 5µl) were added. BD Simultest™ Control γ_1/γ_{2a} (IgG_1 FITC/IgG_{2a} PE; 5ul) served as controls. All tubes were incubated for 15mins in the dark at room temperature before washing in 1ml PBS. Cells were pelleted at 500xg for 5mins and the supernatant aspirated. Cells were resuspended in 300µl fridge cold PBS + 0.1% (w/v) BSA and analysed on a BD FACSCalibur™ (BD Bioscience, Sweden) with 10,000 gated events recorded per sample. Data was analysed using FlowJo version 7.6 (Tree Star Inc., Ashland, OR).

4.2.3 Stimulation of OMLP-PCs and EFs with LPS

OMLP-PCs and EFs from healthy donors and GVHD patients were stimulated with LPS to assess the effect on their antibacterial potential. OMLP-PCs and EFs from healthy donors (n=4, n=3 respectively) and cGVHD patients (n=6, n=3 respectively) were seeded into 24 well culture plates ($1x10^5$ /well) in DMEM supplemented with 10% (v/v) FCS and 2mM L-glutamine and incubated overnight at 37°C/5% CO_2 to allow cells to adhere. Medium was aspirated and replaced with RPMI supplemented with 10% (v/v) FCS, 2mM L-glutamine, 20% (v/v) BHI +/- 10ng/ml LPS (Sigma). Samples were incubated for 1hr or 7hrs at 37°C/5% CO_2. Cells from the 1hr and 7hr time points were lysed in RLT buffer containing 1% (v/v) 2β-mercaptoethanol and samples stored at -80°C (RNeasy Kit, Qiagen, Sweden). CM was harvested from the 7hr samples, centrifuged at 500xg for 5mins to remove any cellular debris before storage at -80°C.

4.2.4 Susceptibility Testing of GVHD CM and Blocking of Identified Antibacterial Mediators

CM (90µl) derived from hOMLP-PCs (n=4), hEFs (n=3), gOMLP-PCs (n=6) and gEFs (n=3) were incubated with 100CFU of Gram positive bacteria (*E. faecalis* and *S. pyogenes*) +/- 0.6µg/ml of human osteoprotegerin neutralizing antibody (R&D Systems) or Gram negative bacteria (*P. aeruginosa* and *P. mirabilis*) +/- 24µg/ml of polyclonal rabbit anti-human haptoglobin antibody (Dako, UK) for 16hrs at 37ºC/5% CO_2 in a 96 well plate. Bacterial cultures were serially diluted and spiral plated (Don

Whitley Scientific Limited, UK) onto TSA or CLED (*P. mirabilis*) agar and incubated at 37°C overnight. The number of colonies grown on the agar plates was counted and bacterial CFU/ml was calculated from the counting table (WASP 2 User Manual Section 15.1, Don Whitely Scientific Limited, UK) as per section 2.2.4.

4.2.5 RNA Isolation

RNA was isolated from OMLP-PCs and EFs from healthy donors and GVHD patients +/- LPS from section 4.2.3, using the RNeasy kit (Qiagen, Sweden). Briefly, cells stored in the lysis solution were homogenised by vortexing samples for 1min. An equal volume of 70% (v/v) ethanol was added to each sample, mixed and directly added to a RNeasy spin column provided. Columns were centrifuged at 8000xg for 15s before 700µl of the buffer RW1 was added to the column. Columns were again centrifuged at 8000xg for 1min before 500µl of buffer RPE was applied. A centrifugation step at 500xg for 1min was carried out to wash the membrane of the column before a further 500µl of buffer RPE was applied, before a further 8000xg centrifugation for 2mins. RNA was then eluted into a clean tube using 50µl RNase-free water and centrifuged at 8000xg for 1min. RNA was quantified using a Nanodrop 2000C (Thermo Scientific, Sweden) and stored at -80ºC.

4.2.6 cDNA Synthesis

cDNA was generated from 200ng of RNA using the High-Capacity cDNA Reverse Transcription Kit (Life Technologies Europe BV, Sweden). A reaction mix was prepared as per the manufacturer's protocol, with 2µl x10 RT buffer, 0.8 µl x25 dNTP mix, 2 µl x10 RT random primers, 1µl MultiScribe™ Reverse Transcriptase and 4.2 µl nuclease-free water. Two hundred ng of RNA, made up to a 10µl volume using nuclease-free water, was added to the reaction mix and incubated using a thermal cycler at 25ºC for 10mins, 37ºC for 2hrs, 85ºC for 5mins and held at 4ºC. Synthesised cDNA was diluted 1 in 10 with nuclease-free water and stored at -20ºC.

4.2.7 Quantitative-Polymerase Chain Reaction (qPCR)

Two µl for the diluted cDNA from section 4.2.6 was added to 0.25µl of 10 µmol forward and reverse primer mix (Table 4.1), 5µl SYBR green Fast SYBR® Green Master Mix (Life Technologies, Sweden) and 2.75µl nuclease-free water. Samples were incubated using a thermal cycler at 95ºC for 20s before 40 cycles of 95ºC for 3s and 60ºC for 30s were applied.

Table 4.1: Primer sequences utilised for qPCR analysis of OMLP-PCs and EFs +/- LPS treatment. All primers were sourced from (MWG Biotech, Germany)

Primer target	**Primer sequence**
β actin (as per section 2.2.1.3)	F: 5' AGG GCA GTG ATC TCC TTC TGC ATC CT 3' R: 5' CCA CAC TGT GCC CAT CTA CGA GGG GT 3'
IDO (as per section 2.2.1.3)	F: 5' GCG ATG TTG GAA ATA GCT TC 3' R: 5' CAG GAC GTC AAA GCA CTA AA 3'
OPG (as per section 2.2.1.3)	F: 5' GAA GGG CGC TAC CTT GA GAT 3' R: 5' GCA AAC TGT ATT TCG CTC TGG 3'
COX2 (as per section 2.2.1.3)	F: 5' CTT CAC GCA TCA GTT TTT CAA G 3' R: 5' TCA CCG TAA ATA TGA TTT AAG TCC AC 3'
SDF-1a	F: 5' CCA AAC TGT GCC CTT CAG AT 3' R: 5' TGG CTG TTG TGC TTA CTT GTT TTG G 3'
IL-1β	F: 5' CAC GAT GCA CCT GTA CGA TCA 3' R: 5' GTT GCT CCA TAT CCT GTC CCT 3'
IL-8	F: 5' TTG CCA AGG AGT GCT AAA GAA 3' R: 5' GCC CTC TTC AAA AAC TTC TCC 3'

Data was analysed using the Δ ΔCT method, by which each sample was compared to its own β-actin level, before being compared to the control sample group (hOMLP-PCs, - LPS).

4.2.8 Examining the Levels of Antibacterial Factors

4.2.8.1 Quantification of IDO Activity in Conditioned Media from OMLP-PCs from Healthy Donors and GVHD Patients

The concentration of the IDO metabolite, L-kynurenine, was determined as a measure of IDO activity as per section 3.2.2.1, on CM samples generated in section 4.2.3.

4.2.8.2 Quantification of PGE_2 Secretion from OMLP-PCs from Healthy Donors and GVHD Patients

The secretion of PGE2 was determined using the Prostaglandin E2 Parameter Assay Kit (R&D Systems, UK) as per section 3.2.2.3, on CM samples generated in section 4.2.3.

4.2.8.3 Detection of Haptoglobin in the Secretome of OMLP-PCs from Healthy Donors and GVHD Patients

Total protein concentrations were determined in CM samples generated from section 4.2.3 using a bicinchoninic acid (BCA) protein assay (Pierce: Life Technologies, UK) as per section 3.2.2.4.1. Twenty five µg total protein was separated through a 4–15% Mini-PROTEAN® TGX™ Gel (Biorad, UK) as per section 3.2.2.4.1 with Western blot analysis performed to detect the secretion of haptoglobin as per section 3.2.2.4.4.

4.2.8.4 Quantification of OPG, IL-8, IL-1β and SDF-1a Secretion in Conditioned Media from OMLP-PCs from Healthy Donors and GVHD Patients

Secreted levels of OPG, IL-8, IL-1β and SDF-1α were determined in CM samples generated in section 4.2.3 using an enzyme-linked immunosorbent assay (ELISA: R&D Systems, UK) as per section 3.2.2.2.

4.2.8.5 Statistical Analysis

All statistical analysis was performed using SPSS statistics (IBM®, Version 20). Variance analysis was performed using Levene's test, where significant variability was assumed at $P<0.05$. Statistical analysis for comparing means was performed using a one-way ANOVA with a post hoc Tukey test (where equal variance) or a Games-Howell test (where variances were unequal). Statistical significance was assumed where $P<0.05$.

4.3 Results

4.3.1 OMLP-PCs and EFs in culture

Healthy OMLP-PCs (n=4) and EFs (n=3) and GVHD patient derived OMLP-PCs (n=6) and EFs (n=3) were expanded in complete media. All cell types demonstrated a typical bipolar, fibroblast-like morphology (Fig. 4.1 A-D).

4.3.2 Cell Surface Expression of GVHD Patient Derived Cells Mirror that of Healthy Donor Derived Cells

All OMLP-PC clones were phenotyped for their cell surface expression of CD73, CD105, CD90 and HLA I. The negative expression of the haematopoietic markers CD45 and CD34 and the endothelial marker CD31 was also examined, in addition to negative expression of CD14, CD80 and HLA II. OMLP-PCs from both healthy and GVHD sources expressed the typical stem cell markers above, with the lack of the expression of the haematopoietic markers noted (Fig. 4.2 - Fig. 4.5).

4.3.3 Investigating the Antibacterial Factors Secreted from GVHD Patient Derived OMLP-PCs

The expression and secretion of potential antibacterial factors was analysed in cells derived from healthy donors and GVHD patients to assess potential differences in the antibacterial secretome of these cells.

4.3.3.1 IDO is Not Expressed in OMLP-PCs Derived from Either Healthy Donors or GVHD Patients after Stimulation with LPS

Molecular expression of IDO and its activity was determined using qPCR and an activity assay respectively, in samples generated from section 4.2.3. Both the molecular expression (Fig. 4.6 A) and protein activity (Fig. 4.6 B) of IDO were undetectable in hOMLP-PCs and gOMLP-PCs after stimulation with LPS, irrespective of 1hr or 7hr initial culture period. A positive control of hOMLP-PCs primed with IFNγ was used.

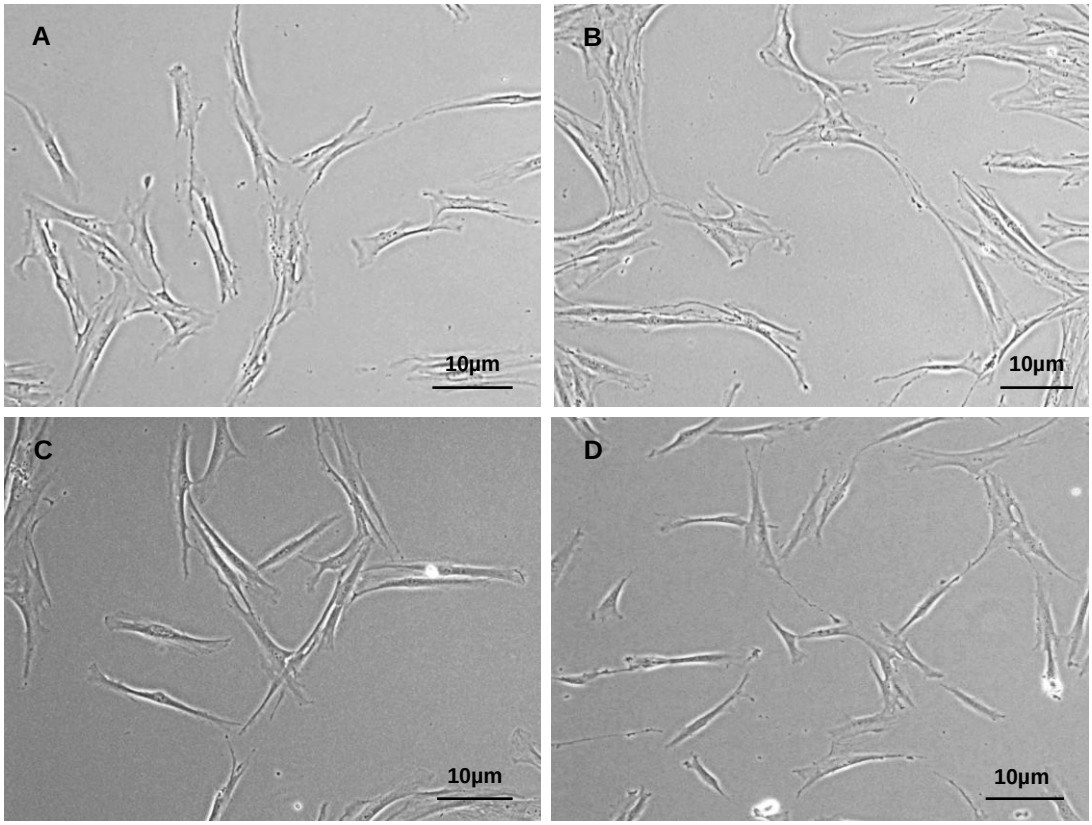

Fig. 4.1: Representative photomicrographs of (A) hOMLP-PC, (B) hEF, (C) gOMLP-PC and (D) gEF, PD 24-30. Bar = 10µM.

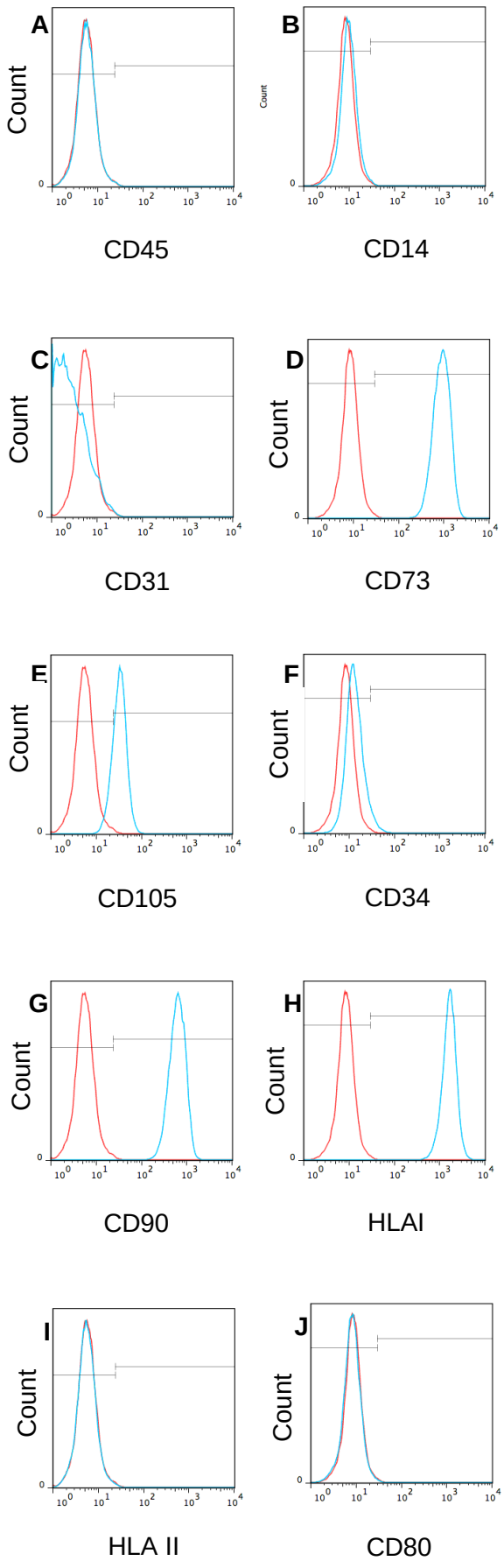

Fig. 4.2: Representative cell surface expression of (A) CD45, (B) CD14, (C) CD31, (D) CD73, (E) CD105, (F) CD34, (G) CD90, (H) HLA I, (I) HLA II and (J) CD80 in hOMLP-PC clones. Red line represents the Ig control, whilst the blue line demonstrates the cell surface expression of the sample.

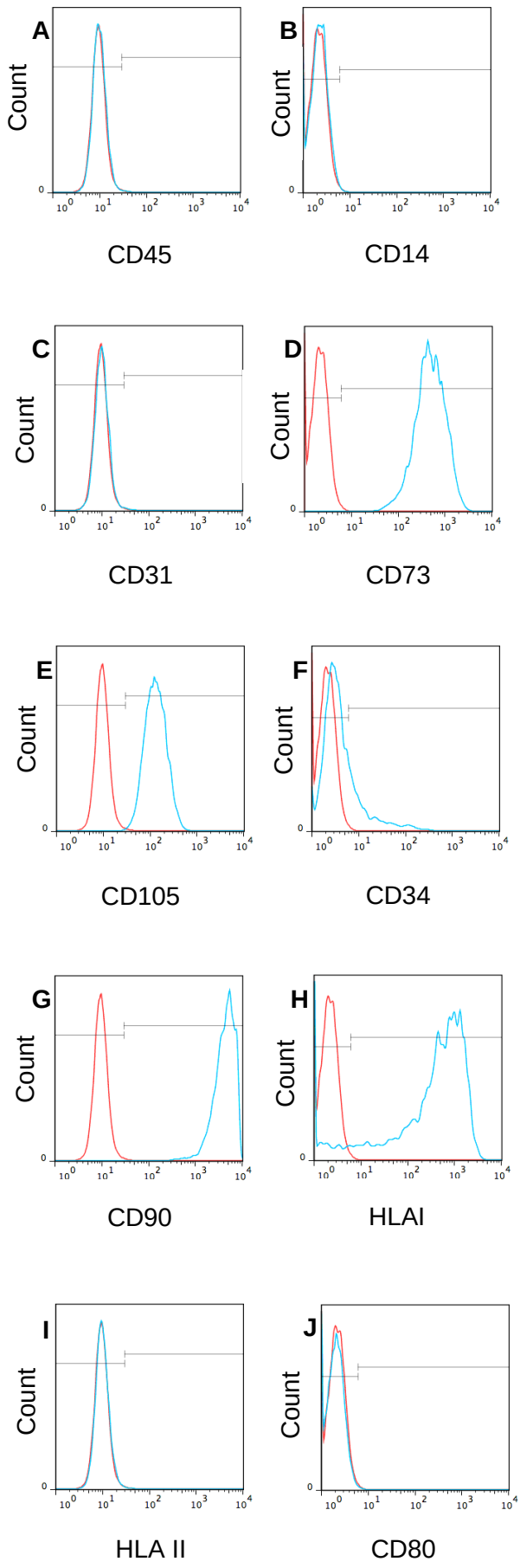

Fig. 4.3: Representative cell surface expression of (A) CD45, (B) CD14, (C) CD31, (D) CD73, (E) CD105, (F) CD34, (G) CD90, (H) HLA I, (I) HLA II and (J) CD80 in hEFs. Red line represents the Ig control, whilst the blue line demonstrates the cell surface expression of the sample. .

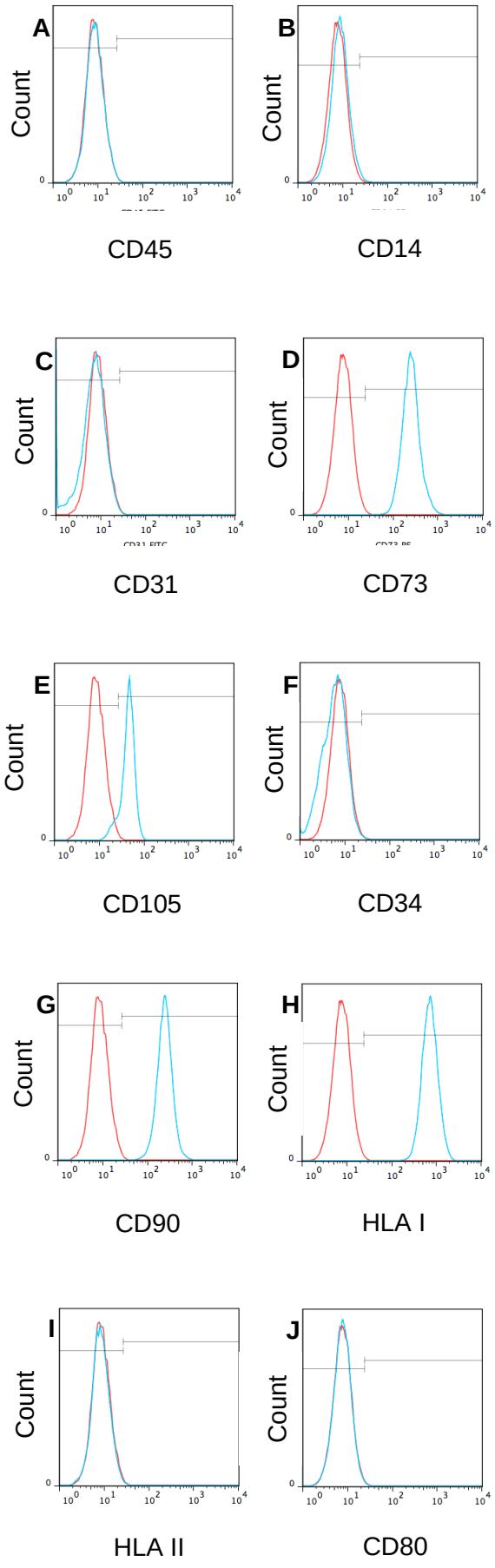

Fig. 4.4: Representative cell surface expression of (A) CD45, (B) CD14, (C) CD31, (D) CD73, (E) CD105, (F) CD34, (G) CD90, (H) HLA I, (I) HLA II and (J) CD80 in gOMLP-PC clones. Red line represents the Ig control, whilst the blue line demonstrates the cell surface expression of the sample.

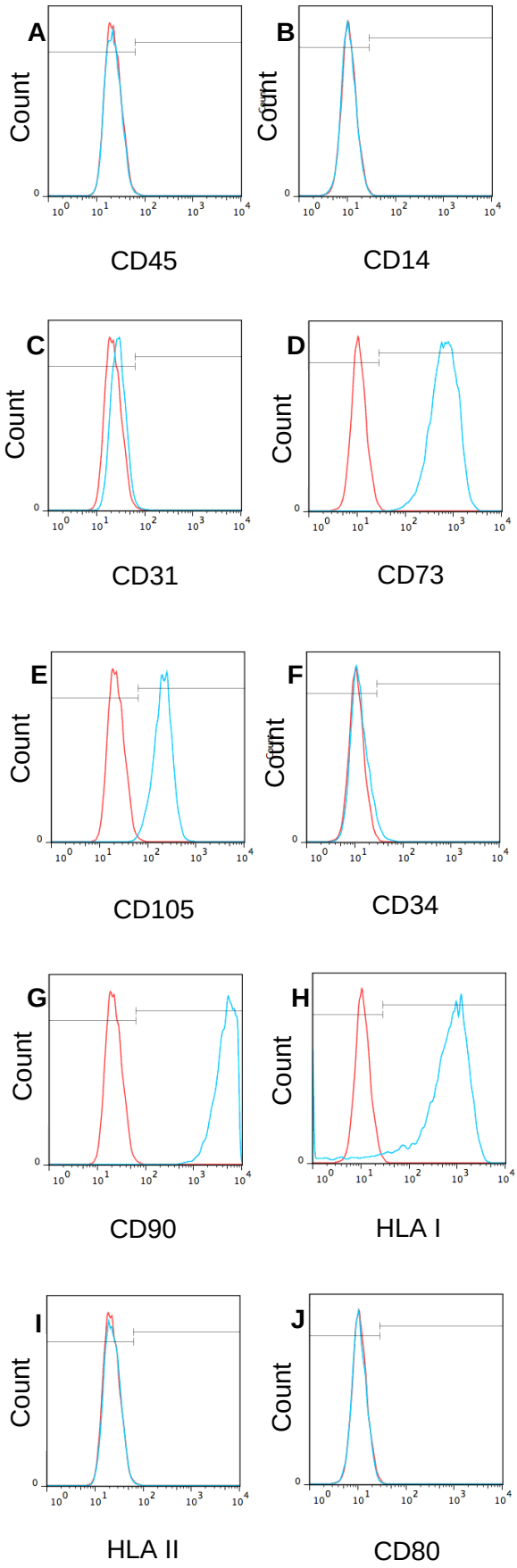

Fig. 4.5: Representative cell surface expression of (A) CD45, (B) CD14, (C) CD31, (D) CD73, (E) CD105, (F) CD34, (G) CD90, (H) HLA I, (I) HLA II and (J) CD80 in gEFs. Red line represents the Ig control, whilst the blue line demonstrates the cell surface expression of the sample.

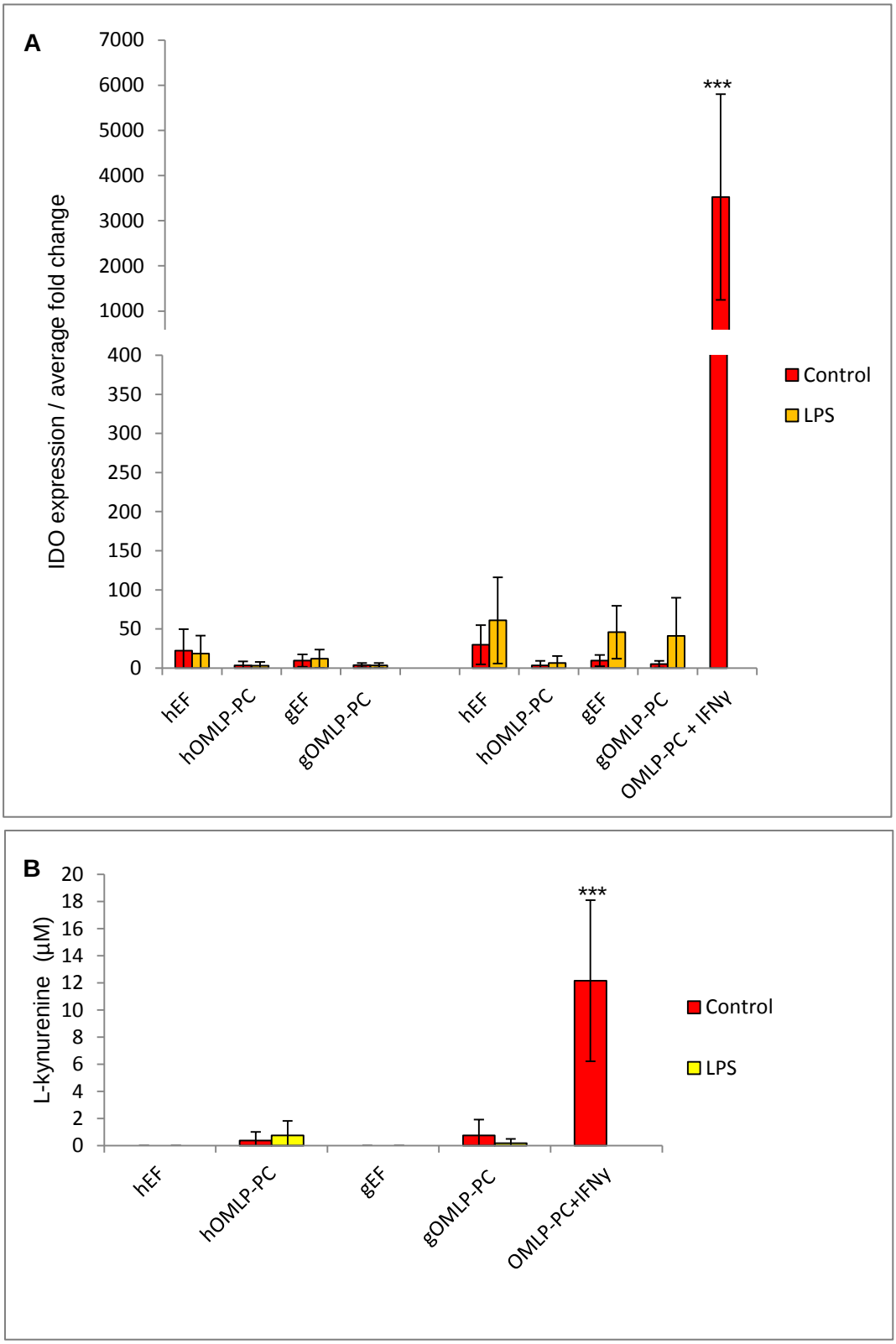

Fig. 4.6: IDO expression in OMLP-PCs and EFs. The expression (A) and activity (B) of IDO in hEFs (n=3), hOMLP-PCs (n=4), gEFs (n=3) and gOMLP-PCs (n=6) +/- LPS. Molecular expression data (A) expressed as average fold change compared to hOMLP-PCs. IDO activity determined in CM at 7hrs. All data +/- SD of the mean. Statistics compared to all other samples. ***P≤0.001.

4.3.3.2 GVHD Causes the Expression of COX2 to Increase in OMLP-PCs, but Not the Secretion of PGE2

RNA isolated from section 4.2.3 was synthesised into cDNA and levels of COX2 determined by qPCR. Secreted levels of PGE_2 in CM samples from section 4.2.3 were analysed using the Prostaglandin E2 Parameter Assay Kit (R&D Systems, UK). No significant differences were observed by LPS stimulus to any of the cell populations demonstrated at 1hr ($P \geq 0.05$). The baseline expression of COX2 at 7hrs was significantly higher in gOMLP-PCs than the expression in hOMLP-PCs ($P < 0.001$; Fig. 4.7 A). LPS stimulation significantly increased the expression of COX2 in hOMLP-PCs and gOMLP-PCs at 7hrs ($P \leq 0.01$; Fig. 4.7, A). The expression of COX2 was significantly greater in OMLP-PCs compared to EFs in samples derived from GVHD patients at 7hrs ($P \leq 0.05$; Fig. 4.7 A). No differences in expression were observed between hOMLP-PCs and hEFs +/- LPS stimulation ($P \geq 0.05$; Fig. 4.7 A).

The secretion of PGE_2 was unaffected by LPS stimulation in both OMLP-PCs and EFs from either healthy donors for GVHD patients ($P \geq 0.05$; Fig. 4.7 B). Both hOMLP-PCs and gOMLP-PCs displayed the same levels of secreted PGE_2 ($P \geq 0.05$; Fig. 4.7 B), which were significantly higher than the secretion from hEFs or gEFs ($P \leq 0.001$; Fig. 4.7 B).

4.3.3.3 Haptoglobin is Secreted from OMLP-PCs from Both Healthy Donors and GVHD Patients

The secretion of haptoglobin was investigated using Western blot analysis. The presence of the secreted protein was found in OMLP-PCs and EFs from both healthy donors and GVHD patients (Fig. 4.8).

4.3.3.4 OPG Expression is Constitutive

OPG expression and secretion in samples from section 4.2.3 were determined by qPCR and ELISA respectively. No statistical differences in either the mRNA expression or protein secretion of OPG were observed between hOMLP-PCs and gOMLP-PCs or EFs, irrespective of LPS stimulation ($P > 0.05$; Fig. 4.9 A, B).

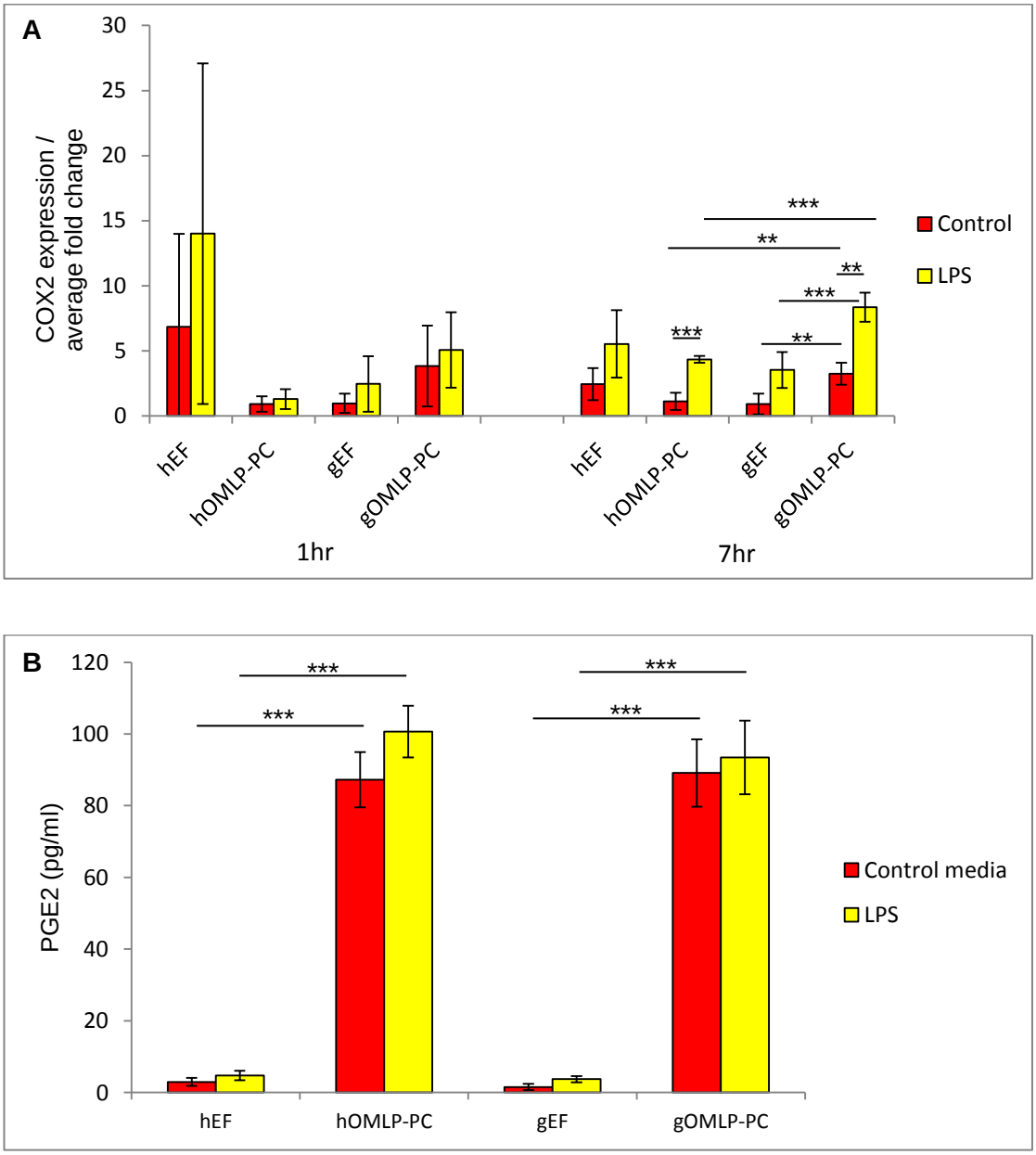

Fig. 4.7: Expression of COX2 and PGE_2 secretion from OMLP-PCs and EFs. The expression of COX2 (A) and secretion of PGE_2 (B) in hEFs (n=3), hOMLP-PCs (n=4), gEFs (n=3) and gOMLP-PCs (n=6), +/- LPS. Molecular expression data (A) expressed as average fold change compared to hOMLP-PCs. All data +/- SD of the mean, **P≤0.01 ***P≤0.001.

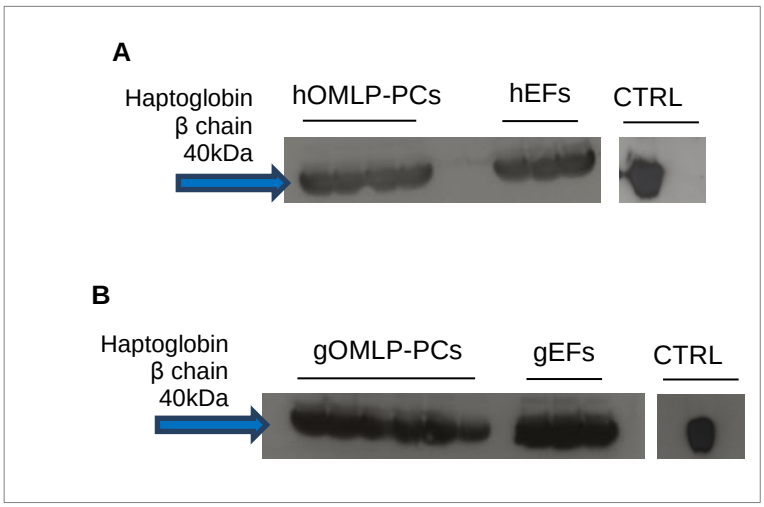

Fig. 4.8: Secretion of haptoglobin from OMLP-PCs and EFs. Haptoglobin secretion from healthy donor derived OMLP-PCs and EFs (A) and GVHD patient derived OMLP-PCs and EFs (B). A positive control of Haptoglobin is represented in the CTRL lane.

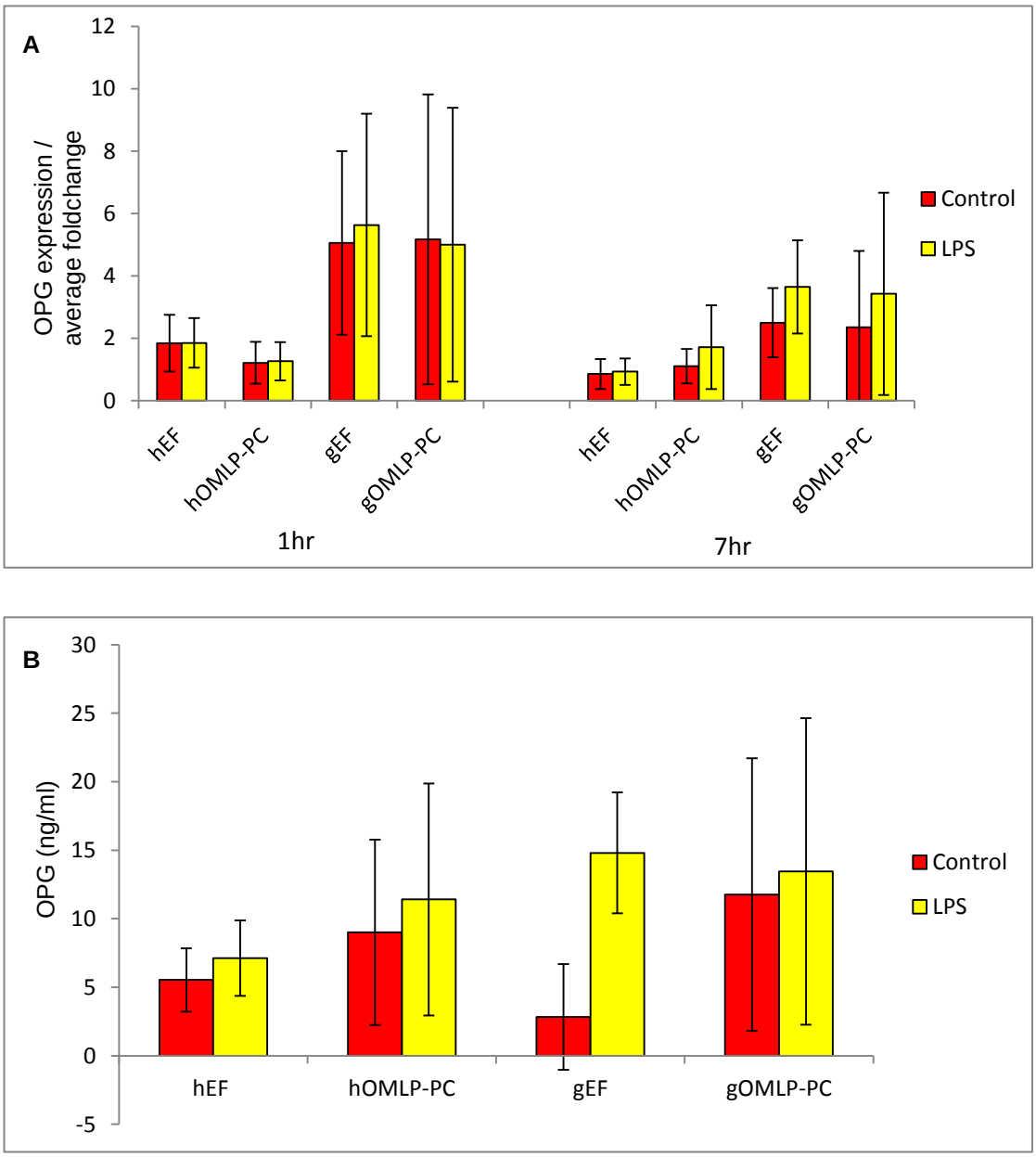

Fig. 4.9: OPG expression and secretion from OMLP-PCs and EFs. The expression (A) and secretion (B) of OPG from OMLP-PCs and EFs from healthy donors (n=3, n=4 respectively) and GVHD patients (n=3, n=6 respectively) +/- LPS. The molecular data was expressed as average fold change compared to hOMLP-PCs. All data +/- SD of the mean.

4.3.4 OMLP-PCs Derived from GVHD patients do not Display Antibacterial Properties

The fact that gOMLP-PCs (in a similar way to hOMLP-PCs) produced/secreted the antibacterial factors PGE2, haptoglobin and OPG, led to an investigation into the potential antibacterial properties of the disease cells. CM samples generated from section 4.2.3 were cultured with 100CFU of Gram positive and Gram negative bacteria to assess their effect on bacterial growth. As demonstrated in section 2.3.6, CM from hOMLP-PCs significantly reduced the growth of both Gram positive ($P \leq 0.001$; Fig. 4.10 A, B) and Gram negative bacteria ($P \leq 0.05$; Fig. 4.11 A, B). Prior stimulation of the cells with LPS had no further effect on the ability of the CM to reduce the bacterial growth. However, CM derived from gOMLP-PCs had no effect on the growth of any bacteria tested ($P \geq 0.05$; Fig. 4.10 A, B and Fig. 4.11 A, B) irrespective of LPS stimulation. EF derived media from both healthy donors and GVHD patients had no effect on bacteria growth ($P \geq 0.05$; Fig. 4.10 A, B and Fig. 4.11 A, B) irrespective of stimulation by LPS.

Blocking OPG or haptoglobin in hOMLP-PC CM significantly increased the growth of Gram positive or Gram negative bacteria respectively ($P \leq 0.01$; Fig. 4.10 A, B and $P \leq 0.05$; Fig. 4.11 A, B). Blocking OPG or haptoglobin within gOMLP-PCs CM samples had no effect on bacterial growth ($P \geq 0.05$; Fig. 4.10 A, B and Fig. 4.11 A, B).

4.3.4.1 IL-8 Expression but not Secretion is Upregulated by LPS in OMLP-PCs Derived from GVHD Patients

To analyse the potential of OMLP-PCs to recruit innate immune cells such as neutrophils, the chemoattractant IL-8 was analysed. The expression of IL-8 was determined using qPCR and secretion by ELISA in samples produced in section 4.2.3. At 7hrs, mRNA IL-8 expression was significantly increased by LPS stimulation in both OMLP-PCs and EFs ($P \leq 0.01$; Fig. 4.12 A), irrespective of the patient source, with no difference between disease and normal cells ($P > 0.05$). The secretion of IL-8 was significantly increased in hOMLP-PCs by LPS ($P \leq 0.01$; Fig. 4.12 B). However, LPS had no effect on the IL-8 secretion from gOMLP-PCs or either source of EFs ($P \geq 0.05$; Fig. 4.12).

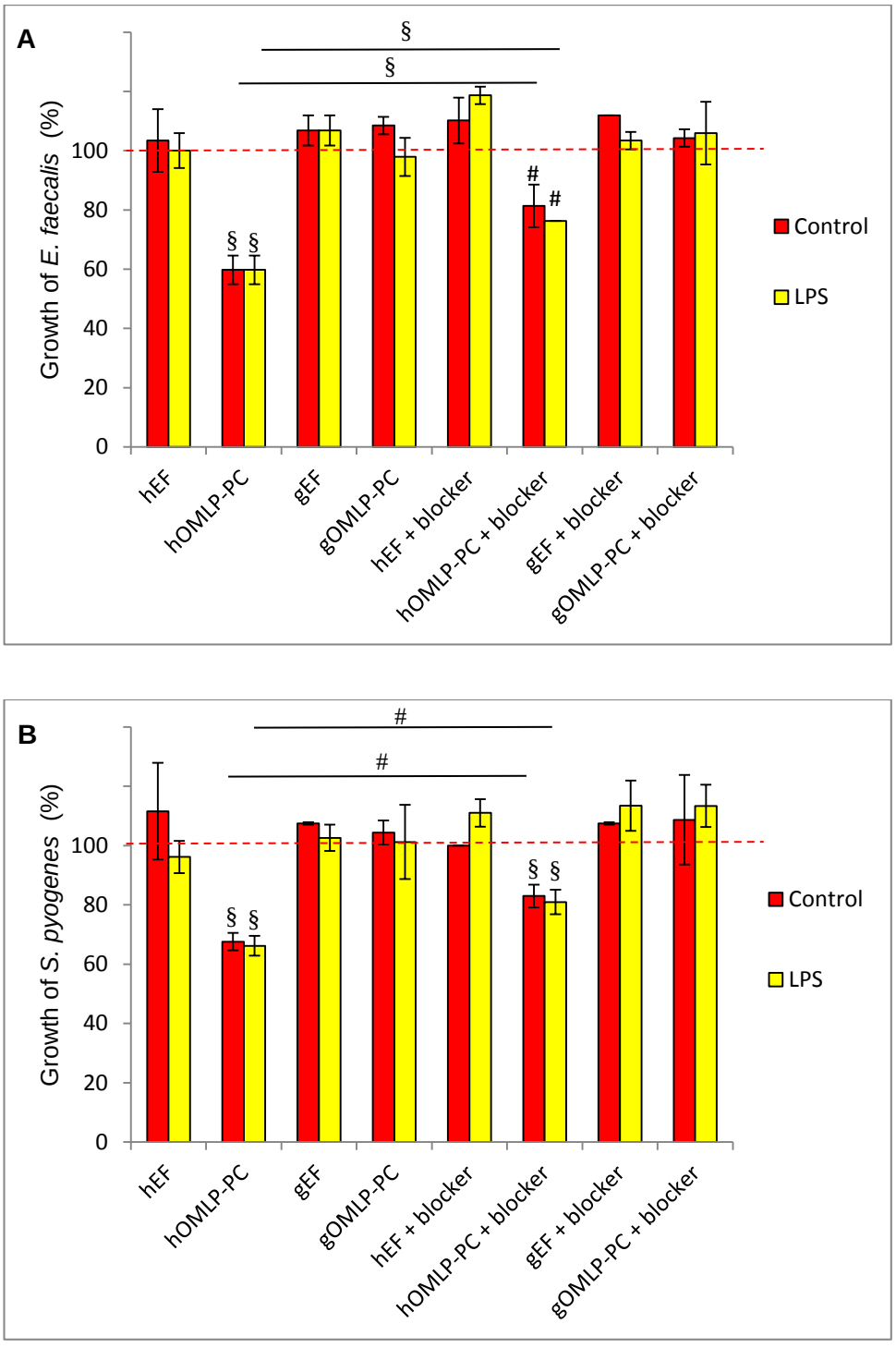

Fig. 4.10: The effect of CM on the growth of Gram positive bacteria. CM +/- LPS from hEFs (n=3), hOMLP-PCs (n=4), gEFs (n=3) and gOMLP-PCs (n=6) cultured with (A) *E. faecalis* and (B) *S. pyogenes*, +/- a neutralising antibody to OPG. Data expressed as percentage bacterial growth, +/- SD of the mean. Statistics compared to bacterial only controls (represented by the red dotted line), unless otherwise stated. #P≤0.01, §P≤0.001.

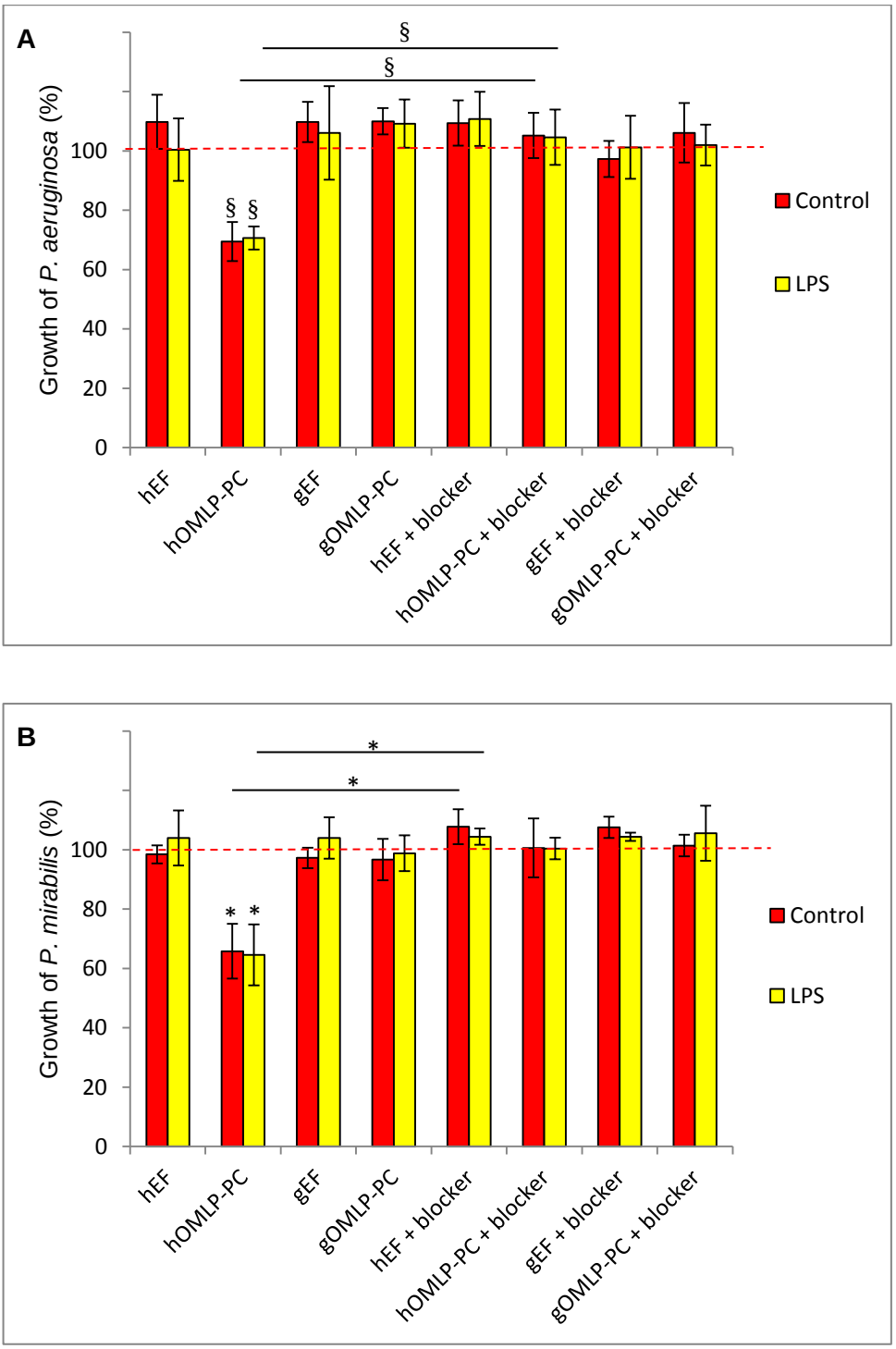

Fig. 4.11: The effect of CM on the growth of Gram negative bacteria. CM +/- LPS from hEFs (n=3), hOMLP-PCs (n=4), gEFs (n=3) and gOMLP-PCs (n=6) cultured with (A) *P. aeruginosa* and (B) *P. mirabilis*, +/- a blocking antibody to haptoglobin. Data expressed as percentage bacterial growth, +/- SD of the mean. Statistics compared to bacterial only controls (represented by the red dotted line), unless otherwise stated. *P≤0.05, §P≤0.001.

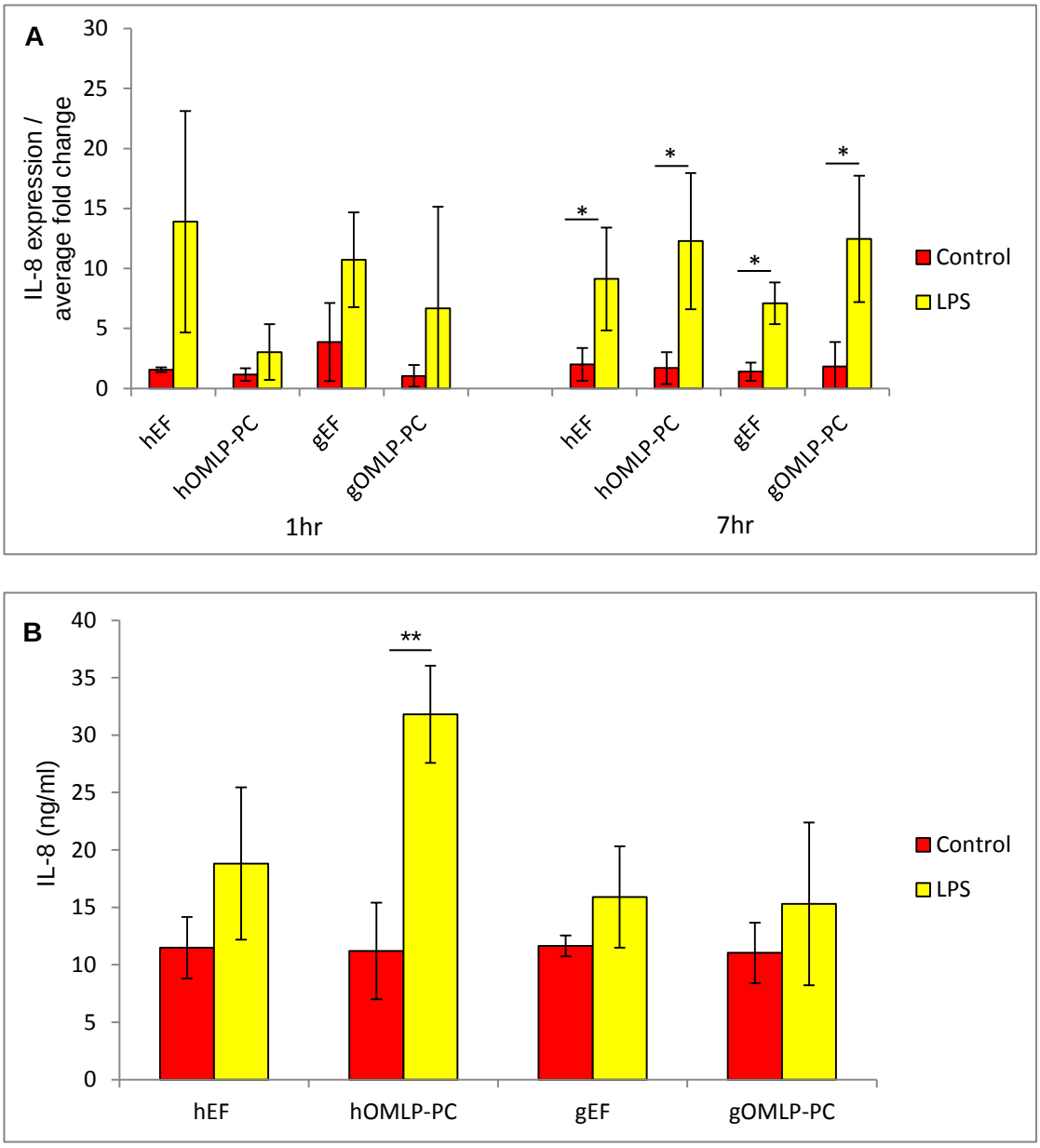

Fig. 4.12: IL-8 expression and secretion in OMLP-PCs and EFs. The expression (A) and secretion (B) of IL-8 from OMLP-PCs and EFs from healthy donors (n=3, n=4 respectively) and GVHD patients (n=3, n=6 respectively) +/- LPS. The molecular data expressed as average fold change compared to hOMLP-PCs. All data +/- SD of the mean. *P≤0.05.

4.3.4.2 The Expression of IL-1β is increased by LPS in hOMLP-PCs but not in gOMLP-PCs

To analyse the potential of OMLP-PCs to recruit innate immune cells such as neutrophils, the chemoattractant IL-1β was analysed. IL-1β expression was analysed in synthesised cDNA samples generated from section 4.2.3. LPS stimulation significantly increased the expression of IL-1β in hOMLP-PCs ($P \leq 0.05$; Fig. 4.13) but not in gOMLP-PCs ($P \geq 0.05$; Fig. 4.13). These findings did not translate to the protein level, with no secretion of IL-1β detected in any samples analysed.

4.3.4.3 Baseline Secreted Levels of SDF-1α are significantly higher in Healthy Donor Compared to GVHD Patient Cells

The levels of SDF-1α were analysed as potential mechanism for neutrophil retention. The expression and secretion of SDF-1α was analysed using qPCR and ELISA respectively, from samples generated in section 4.2.3. There were no significant differences in the expression of SDF-1 α +/-LPS treatment ($P>0.05$; Fig. 4.14, A). However, the secretion of SDF-1α was significantly higher from hOMLP-PCs compared to gOMLP-PCs +/- LPS treatment ($P \leq 0.01$; Fig. 4.14 B). LPS treated hOMLP-PCs secreted significantly more SDF-1α compared to LPS treated hEFs ($P \leq 0.05$; Fig. 4.14 B). No other differences between OMLP-PCs and EFs were observed from either healthy donors or GVHD patients ($P \geq 0.05$).

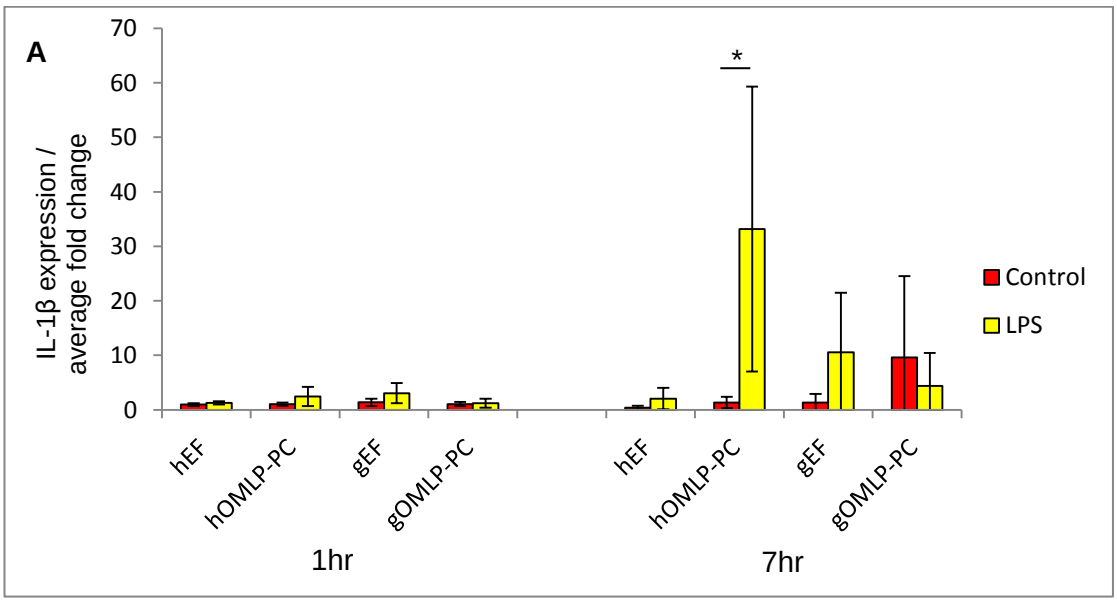

Fig. 4.13: IL-1β expression in OMLP-PCs and EFs. The expression of IL-1β from OMLP-PCs and EFs from healthy donors (n=3, n=4 respectively) and GVHD patients (n=3, n=6 respectively) +/- LPS. Molecular data expressed as average fold change compared to hOMLP-PCs. All data +/- SD of the mean.

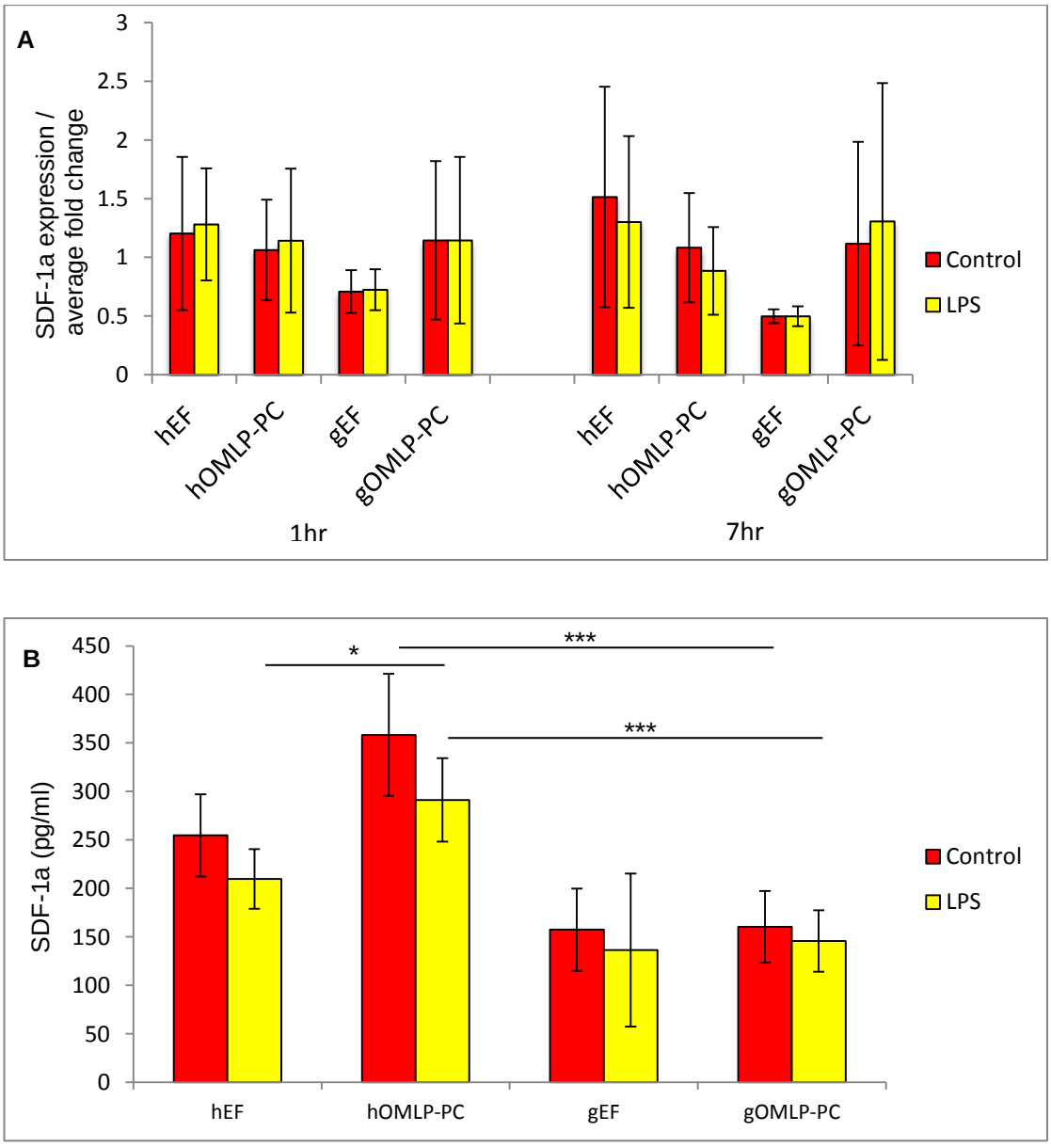

Fig. 4.14: SDF-1α expression and secretion in OMLP-PCs and EFs. (A) The expression SDF-1α from OMLP-PCs and EFs from healthy donors (n=3, n=4 respectively) and GVHD patients (n=3, n=6 respectively) +/- LPS. Data expressed as average fold change compared to hOMLP-PCs 1hr. (B) The secretion of SDF-1a from hOMLP-PCs (n=4) and gOMLP-PCs (n=6). All data +/- SD of the mean. *P≤0.05, ***P≤0.001.

Table 4.2: Summary of findings, a comparison between hOMLP-PCs and gOMLP-PCs

	hOMLP-PCs	**gOMLP-PCs**
IDO	None detected (+/- LPS)	None detected (+/- LPS)
COX2	Baseline expression lower than gOMLP-PCs Expression increased by LPS	Baseline expression higher than hOMLP-PCs Expression increased by LPS
PGE2	Constitutive secretion	Constitutive secretion
Haptoglobin	Constitutive secretion	Constitutive secretion
OPG	Constitutive expression and secretion	Constitutive expression and secretion
Antibacterial effects	Significantly reduces bacterial growth	No effects on bacterial growth
IL-8	Expression increased by LPS Secretion increased by LPS	Expression increased by LPS No effect of LPS on secretion
IL-1β	Expression increased by LPS	No effect of LPS on expression
SDF-1α	Secretion higher than gOMLP-PCs	Secretion lower than hOMLP-PCs

4.4 Discussion

Oral GVHD is associated with an increase in microbial infections (Treister et al., 2012), but the underlying reasons as to why are not fully understood. Both HSCT and the prior conditioning regimes can result in increased infections (Kedia et al., 2013). The conditioning regimes such as chemotherapy and radiotherapy target the bone marrow, eradicating the immune cells limiting the patient's ability to overcome infection. Furthermore, immunosuppressive therapy is given to patients before HSCT to prevent immune rejection of the stem cell therapy, which further limits the patient's immune system (Kedia et al., 2013). The HSCT and associated conditioning regimes may predispose the patient to increased infections, which further manifest during the development of GVHD post-HSCT treatment.

Mucosal surfaces are commonly affected by GVHD. Mucosal damage following HSCT (Lee et al., 2008) has been documented, predisposing these areas to developing GVHD. Changes in the microflora and increased infections are known in the gastrointestinal tract following HSCT (Lee et al., 2008). One study demonstrated that during allogeneic HSCT the bacterial diversity within the gut is decreased. It was demonstrated that *Enterococcus* species commonly dominated the gut of the patients (40%), with a further 37% of patients displaying a dominant *Streptococcus* species (Taur et al., 2012). Further studies have demonstrated that conditioning regimes such as chemotherapy have additional effects on the gut microflora (Montassier et al., 2014). Chemotherapy has been reported to reduce the bacterial diversity with a decrease in the abundance of *Faecalibacterium* species and an increase in *Escherichia* species associated with chemotherapy. The importance of the change in *Faecalibacterium* organisms has been highlighted with the reported anti-inflammatory effects of the bacteria *in vitro* and *in vivo* (Sokol et al., 2008). With the documented reduction in this bacterium following chemotherapy conditioning it has been hypothesised that chemotherapy results in a decrease of anti-inflammatory bacterial species within the gut, limiting the gut's ability to regulate the intestinal environment, thereby pre-disposing the gut to the inflammatory condition, mucositis (Montassier et al., 2014). The imbalance in the microbial populations following HSCT and the conditioning regimes have been linked to the development of GVHD (Jenq et al., 2012). Inflammation resulting from the development of GVHD has been associated with major shifts in microbial populations within both the human and murine intestine. After the development of GVHD, a loss of bacterial diversity has been reported. The elimination of *Lactobacillales* species prior to the transplantation therapy resulted in

the development of GVHD within murine models, with the reintroduction of the *Lactobacillales* species alleviating the disease (Jenq et al., 2012). This published study demonstrates the direct effects of microbial changes on the development of GVHD.

Oral mucositis is a common complication with both HSCT and GVHD. It could be hypothesised that this inflammatory condition is attributed to changes in the oral microbiome, with decreases in anti-inflammatory species directly affecting the oral mucosa. This chapter has demonstrated the loss of antibacterial properties of OMLP-PCs derived from GVHD patients. The resulting loss in antibacterial potential within the oral mucosa may further potentiate the effects of the remaining dominant bacterial species. With the potential loss in anti-inflammatory species and the decrease in antibacterial potential, a significant dysregulation within the oral mucosa may be present, inciting infections within the oral cavity.

In chapters 2 and 3, OMLP-PCs from healthy donors were shown to possess direct antibacterial properties through the release of soluble factors. As part of this results chapter, it was demonstrated that OMLP-PCs derived from patients with oral GVHD did not share this quality. CM from gOMLP-PCs had no effect on bacterial growth with any of the bacteria tested. Further studies would be needed to ensure gOMLP-PCs do not have any antibacterial properties as they may, for example, act through contact dependant mechanisms. Co-culture of gOMLP-PCs and live bacteria during this chapter was however, not possible due to logistical problems in the transfer of the gOMLP-PCs from the Karolinska Institutet to Cardiff University School of Dentistry microbiology laboratory. With changes in the oral cavity well documented during HSCT and the prior conditioning regimes, it is plausible that the OMLP-PCs lose antibacterial potential prior to developing GVHD. This loss of function may be attributed to mucosal damage during the conditioning regimes, further predisposing the oral cavity to the effects of GVHD. Examining the antibacterial effects of OMLP-PCs isolated from patients undergoing conditioning regimes, those undergoing HSCT and those who have developed chronic oral GVHD may determine the time at which the OMLP-PCs lose their antibacterial function.

The secretion of previously identified antibacterial factors (from Chapter 3) involved in the hOMLP-PCs mechanism of action were also investigated in gOMLP-PCs. PGE2 secretion was the same from OMLP-PCs isolated from both healthy donors and GVHD patients. It has been demonstrated that PGE2 can act in a synergistic

manner with TNFα. The ability of PGE2 to induce IL-12 production in human dendritic cells is significantly increased by TNFα (Rieser et al., 1997). It may be possible that PGE2 secreted by hOMLP-PCs functions as an antibacterial factor in synergy with another factor not present in the secretome of gOMLP-PCs. The expression of COX2 however, was significantly higher in gOMLP-PCs than hOMLP-PCs at 7hrs. This may indicate that other COX2 dependant factors, such as prostaglandin D2 (PGD2), may be regulated by the COX2 expressed in gOMLP-PCs. PGD2 has been shown to display immunomodulatory properties through its ability to act as a chemoattractant to monocytes and alter dendritic cell maturation (Gosset et al., 2003), but its effects compared to PGE2 are not well defined. Preliminary studies have demonstrated that PGD2 is not secreted by hOMLP-PCs (data not shown), eliminating any role within the antibacterial effects of hOMLP-PCs. Further studies are warranted to examine the secretion of PGD2 from gOMLP-PCs.

Haptoglobin secretion was demonstrated from both OMLP-PCs derived from healthy donors and those from GVHD patients. Concentrations of the OMLP-PCs derived protein are difficult to measure due to the low levels of secretion (pg/ml). It is possible that gOMLP-PCs secrete sub-active levels of haptoglobin, whilst hOMLP-PCs secrete above the antibacterial level of 50pg/ml (section 3.3.4.1). There are three isoforms of haptoglobin, with the differences between each isoform attributed to the differing α chains. Each isoform is comprised of either two α1 chains, two α2 chains or one α1 and one α2 chains. It is the α1 chain that conveys the highest level of activity, with the isoform containing two α1 chains demonstrating the greatest activity (Eaton et al., 1982). It is plausible that differences in the ratios of these isoforms explain the differences in antibacterial potential of the secreted haptoglobin from hOMLP-PCs and gOMLP-PCs. The resolution of the α chains was poor using Western blot analysis. A more specific technique, such as mass spectrometry, could be used to identify the chains present and the isoforms secreted by the cells.

The secretion of another identified antibacterial factor, OPG, was also investigated. The secreted of OPG was also noted to be the same from both gOMLP-PCs and hOMLP-PCs. It is possible that the OPG secreted from the gOMLP-PCs is secreted in a different conformation, blocking the bacterial binding site, or bound to an inhibitor (see section 3.4.3) hence resulting in the lack of gOMLP-PC antibacterial activity that was observed.

Both OMLP-PCs and EFs significantly increase the expression of the chemoattractant IL-8 in response to LPS, irrespective of whether the cells were derived from healthy donors or GVHD patients. However, the secretion of IL-8 was only upregulated by LPS in hOMLP-PCs and was impaired in gOMLP-PCs and EF populations. This suggests that the OMLP-PCs and EFs from both sources are able to sense the LPS stimulus and upregulate the expression of IL-8, however, the secretion of the protein in response to LPS is not realised by the gOMLP-PCs and EFs by 7hrs. This suggests that either the IL-8 protein is not translated in these cell populations, the secretion is impaired, or the protein is degraded. The expression of IL-1β was also significantly increased by LPS stimulation of hOMLP-PCs, but not of gOMLP-PCs, however secretion from neither hOMLP-PCs nor gOMLP-PCs was detected. The lack of secretion of the chemoattractant IL-8 by gOMLP-PCs in response to LPS could have potential downstream effects, preventing the gOMLP-PCs from recruiting innate immune cells, such as neutrophils (Kolaczkowska and Kubes, 2013) after bacterial exposure. The change in ratio of IL-8 and potentially other chemoattractants during GVHD may lead to compromised immune cell recruitment. The tissues targeted by GVHD are associated with an infiltration of immune cells such as T cells, monocytes and macrophages, which leads to tissue damage (Martin, 2008).

Oral cGVHD is also associated with an infiltration of immune cells such as lymphocytes within the oral mucosa (Soares et al., 2005). This could be a result of the differential expression in the chemoattractant factors within the oral mucosa, specifically the OMLP-PCs, leading to a dysregulation in immune cell recruitment. This chapter suggests that the recruitment of neutrophils by IL-8 and the retention by SDF-1α is impaired, leading to an imbalanced immune cell infiltration. LPS activation (Ward et al., 2009), and rhinovirus stimulation (Stokes et al., 2011) have been demonstrated to induce IL-1β in monocytes, demonstrating the ability of both bacterial and viral infections to induce IL-1β. IL-1β has been further identified as the factor controlling IL-8 release, a factor also known to be a potent neutrophil chemoattractant (Stokes et al., 2011). IL-8 is thought to activate neutrophils, facilitating their adhesion to the endothelium during neutrophil migration (Williams et al., 2011). The expression of IL-1β was increased by LPS in the healthy, but not GVHD OMLP-PCs. While the secretion of the protein was not detected even in healthy OMLP-PCs, it is possible that intracellular levels of IL-1β within OMLP-PCs may regulate the molecular levels and proteomic release of IL-8. The lack of IL-1β expression with gOMLP-PCs may lead to a dysregulation in the release of IL-8 and

therefore neutrophil recruitment with the oral cavity during GVHD. To further examine the importance of IL-8 secretion from OMLP-PCs, chemotaxis/cell migration assays (such as Boyden chambers) could be used to assess the ability of hOMLP-PC or gOMLP-PC CM to cause immune cell migration, such as neutrophils. The chemoattractive properties of BM-MSCs in addition to human salivary gland MSCs have been documented, with the induction of neutrophil chemotaxis reported from both cell types (Brandau et al., 2014). Direct neutralisation or blocking of the secreted IL-8 can be performed to investigate the role of this cytokine in the OMLP-PC mediated chemotaxis.

The retention of neutrophils within the bone-marrow environment is mediated by the release of SDF-1 by the BM-MSCs (Summers et al., 2010). Secreted SDF-1 binds the CXCR4 receptor on the surface of neutrophils, immobilising the immune cells. It can be hypothesised that the secretion of SDF-1 by OMLP-PCs would retain neutrophils after recruitment to the oral mucosa, facilitating bacterial clearance during infection. The expression and secretion of SDF-1α was observed from OMLP-PCs, however, the secretion was significantly higher from hOMLP-PCs compared with gOMLP-PCs. This demonstrates the greater potential of hOMLP-PCs to immobilise innate immune cells at the site of infection compared to gOMLP-PCs. The secretion of SDF-1α was reported irrespective of LPS stimulation, demonstrating the constitutive ability of the hOMLP-PCs to modulate neutrophil immobilisation. The expression of CXCR4 has also been reported on the surface of monocytes (Caulfield et al., 2002), with homing of monocytes to the bone-marrow by CXCR4 mediated mechanisms demonstrated (Wang et al., 2009). This further establishes the potential of hOMLP-PCs mediated SDF-1 α secretion to immobilise innate immune cells, such as neutrophils and monocytes, within the oral cavity.

4.4.1 Conclusion

The antibacterial properties of OMLP-PCs previously demonstrated in chapter 2 are absent in OMLP-PCs derived from GVHD patients who demonstrate oral symptoms. The development of oral GVHD and the increased infections during the disease may in part be attributed to the loss of antibacterial function of the OMLP-PCs, with the oral mucosa unable to regulate the oral microbiome during GVHD.

The loss of IL-8 and SDF-1α may prevent the migration and immobilisation of innate immune cells within the oral cavity during infection. With a lack of innate cell presence the immune response to bacterial challenge will be compromised, further potentiating the symptoms observed during oral GVHD.

The loss of direct antibacterial properties of OMLP-PCs, in addition to the loss of indirect properties (innate cell effects), may cause a severe dysregulation within the oral mucosa during GVHD. These changes may contribute to the increased infection rate in GVHD patients and limit the host innate immune responses.

This study demonstrates the loss of antibacterial function of OMLP-PCs isolated from GVHD patients, which may explain the increased infections during the disease.

5. General Discussion

5 General Discussion

5.1 Background

With over 700 different bacterial species identified in the human oral cavity (Kawamura and Kamiya, 2012) it is surprising that infections, particularly after invasive dental procedures for example, are rare (Parahitiyawa et al., 2010). The oral cavity harbours a dynamic microbial defence system vital for healthy homeostasis. The innate immune system, comprising of both cellular and protein components, provides a rapid but non-specific defence against pathogens. Innate immune cells are recruited to sites of infection by chemotactic stimuli such as cytokine gradients (Kolaczkowska and Kubes, 2013). Once at the infected site, innate immune cells exert their effects by the secretion of pro-inflammatory cytokines and phagocytosis (Fournier and Philpott, 2005). AMPs provide a further line of defence during the initial stages of infection; disrupting the phospholipid bacterial membrane, a structure vital to each bacterium (Teixeira et al., 2012). The mechanism of action for AMPs can vary, with many reducing the available nutrients such as iron, zinc or tryptophan to bacteria (Ellison and Giehl, 1991, Dale and Fredericks, 2005, Hucke et al., 2004). Over 45 AMPs have been identified in the oral cavity (Gorr, 2009), highlighting their importance in oral microbial defence. The diverse presence of factors such as defensins, histatins, LL37, lactoferrin and lysozyme demonstrates the multifactorial antimicrobial defence in the oral cavity. The secretion of AMPs have been identified from oral epithelial cells, neutrophils & salivary glands (Gorr, 2009), demonstrating the secretion of AMPs by cells found facing the external environment. However, little research has focused on the secretion of AMPs from cells residing within the deeper tissue, which may play a role when the epithelial layer is penetrated or disrupted. The secretion of AMPs from tissue resident stem cell populations within the oral cavity has also not been investigated. The secretion of one AMP, LL37, has been reported from a tissue resident stem cell population found within the bone marrow; the BM-MSCs (Krasnodembskaya et al., 2010). LL37 is thought to explain in part the antibacterial effects observed by BM-MSCs. No further literature has investigated the secretion of AMPs from BM-MSCs, which mediate the direct antibacterial properties of these cells.

Several stem cell populations, including the orally derived gingival mesenchymal stem cells (GMSCs), dental pulp-MSCs (DP-MSCs), periodontal ligament stem cells (PDLSCs) and OMLP-PCs have identified immunosuppressive properties (Zhang et

al., 2009, Tomic et al., 2011, Wada et al., 2009, Davies et al., 2012). The immunomodulatory properties of the stem cell populations are mediated by secreted factors such as PGE2 and IDO (Zhang et al., 2009, Wada et al., 2009). Many of these immunomodulatory factors, such as IDO, also have identified antibacterial properties (Hucke et al., 2004).

The aim of this thesis was to investigate the role of the OMLP-PCs in oral microbial defence. The low rate of infection within the oral cavity, despite a diverse microbial population is thought to result from a multifactorial antibacterial response which maintains a healthy homeostasis (Gorr, 2009). The role of oral stem cells within host defence is yet to be explored, in addition to the role of cells residing in the deeper tissue. It is not known whether the disruption of the epithelial layer and subsequent deeper infection may elicit an antimicrobial response from cells within the deeper tissue, or whether the response is confined to the surfaces of the oral cavity. The ability of the OMLP-PCs to modulate bacterial load was assessed to investigate any potential antibacterial effects in addition to identifying secreted antimicrobial factors, which may play a role in the antibacterial mechanism. To examine whether systemic disease disrupts the antibacterial effects of OMLP-PCs, cells isolated from oral cGVHD patients were also investigated.

5.2 The Antibacterial Properties of OMLP-PCs

This study demonstrates for the first time the direct antibacterial properties of OMLP-PCs, a property currently only investigated in a limited number of other stem cell populations, BM-MSCs and cord blood MSCs (Krasnodembskaya et al., 2010, Sung et al., 2016). Whilst similarities in the broad spectral antibacterial effects have been noted between the MSCs and OMLP-PCs, with both stem cell sources decreasing the growth of Gram positive and Gram negative bacteria, distinct differences in the mechanism of action are evident. Each of these stem cell populations mediate their antibacterial effects *in vitro* through the release of antimicrobial factors. Both the studies involving BM-MSCs and cord-blood MSCs demonstrated that MSCs must be exposed to bacteria before the cells secreted such factors to display an antibacterial phenotype (Krasnodembskaya et al., 2010, Sung et al., 2016). However, during this study it was demonstrated that OMLP-PCs constitutively secrete antimicrobial factors, making them ideal for cell based therapies where an antibacterial component

is required, with no modulation to the cells needed to display the full antibacterial phenotype.

Whilst it appears that the cells may unnecessarily expend energy by producing antibacterial factors in the absence of bacteria, the constitutive secretion may be explained through prior *in vivo* priming. OMLP-PCs are isolated from the buccal mucosa of human donors. The oral cavity is rich in microbial species (Kawamura and Kamiya, 2012), hence the OMLP-PCs may be primed by bacteria *in vivo*. This may also explain the increase in the directed migration of OMLP-PCs compared to the control EFs in control conditions. *In* vivo, the possible exposure to bacterial (or their products) gradients may have resulted in the stimulation of migration in OMLP-PCs. This would allow OMLP-PCs to migrate to the site of infection, leading to a more effective antimicrobial response by the cells. A positive migratory stimulus of FCS was not able to further enhance the migration of OMLP-PCs, potentially due to the stimulation of a maximal migratory phenotype resulting from the *in vivo* priming.

The antibacterial effects of OMLP-PCs have been demonstrated against both Gram positive and Gram negative bacteria, however only a limited number of bacteria were examined. A large panel of bacteria are required to fully assess the antibacterial potential of OMLP-PCs and confirm the broad spectral effects. The antibacterial effects against bacteria such as oral commensals, oral pathogens, non-orally derived bacteria and bacterial biofilms would determine the full spectrum of the OMLP-PC effect. This could determine whether OMLP-PCs elicit an antimicrobial effect against all bacteria, or whether the effect is confined to a subset of bacteria.

Currently the antibacterial properties of both BM-MSCs (Krasnodembskaya et al., 2010, Sung et al., 2016) and OMLP-PCs have focussed on the effects against aerobic or facultative anaerobic bacteria. These bacteria may represent the bacteria near the surface of biofilms, due to the accessible oxygen. However, anaerobic bacteria would be found deeper within biofilms (Thurnheer et al., 2015). To assess whether OMLP-PCs could affect anaerobic bacterial growth and therefore disrupt deeper layers of a biofilm, a co-culture with the OMLP-PCs and anaerobic bacteria could be used. The experimental system to co-culture stem cells and aerobic bacteria is simple, with both OMLP-PCs and microorganisms remaining healthy at 37ºC in 5% CO_2. However, a direct co-culture of OMLP-PCs and anaerobic bacteria is not possible with the current experimental setup. Under the current experimental conditions (5% CO_2) it would not be possible to culture anaerobic bacteria, whilst the

anaerobic conditions required for these bacteria would prevent the healthy culture of the progenitor cell populations causing cell death. While direct co-culture is difficult, susceptibility testing for the conditioned media (CM) may be more plausible. CM derived from OMLP-PCs could potentially be cultured in anaerobic conditions in the presence of bacteria. A redesign of the susceptibility testing protocol would be needed, as the current protocol would not allow the culture of anaerobic bacteria. These bacteria require a rich medium to grow and the CM does not provide the bacteria with such nutrients. However, by growing bacteria in biofilms, the growth of both aerobic bacteria on the surface and anaerobic bacteria deeper within the biofilm is facilitated. It is possible that OMLP-PCs could then be seeded on top of the biofilm and the diffusion of the OMLP-PC secretome could penetrate through to the anaerobic compartment of the biofilm. Using this system, potential interplay between a complex bacterial ecosystem and the OMLP-PCs could be investigated, rather than single bacterial species, allowing a more physiologically relevant approach.

5.3 Antibacterial Proteins and Peptides

The involvement of antibacterial soluble factors in the OMLP-PC effect was confirmed as a mechanism of action throughout the study, with the antibacterial properties retained within the CM of the cells. Krasnodembskaya et al., 2010 demonstrated that LL37 in-part mediates the antibacterial properties of BM-MSCs, with neutralisation of LL37 abolishing the antibacterial effects. The secretion of IDO, an antibacterial protein, is well established from MSCs after IFNγ stimulation (Wada et al., 2009). As BM-MSCs are the gold standard stem cell population for cell-based therapies, the BM-MSC identified LL37 and IDO expression and secretion was assessed in OMLP-PCs. A more recent study suggesting an involvement of hBD-2 (Sung et al., 2016) could steer future investigations to examine the role of the defensins in the OMLP-PC mediated antibacterial effects. The presence of hBD-2 has been identified in human saliva, in addition to hBD-1 and -3 and the α-defensins (HNP)-1,2 and 3 (Gorr, 2009). LPS activation of TLR4 and PGN activation of TLR2 has been demonstrated to induce the expression hBD-2 in intestinal epithelial cells (Vora et al., 2004). The TLR4 ligand LPS also stimulates granulocyte-colony stimulating factor (G-CSF) production in nasal mucosal MSCs (Jakob et al., 2010) in addition to the chemoattractant factor IL-8 (Jakob et al., 2013). The secretion of G-CSF by endothelial cells and immune cells such as monocytes is known to promote

the proliferation and differentiation of myeloid cells. This gives further evidence of the ability for bacterial stimuli, such as LPS, to modulate the immunomodulatory and antibacterial phenotype of immunomodulatory cell populations. The induction of human defensins during oral microbial infection has also been demonstrated (Sawaki et al., 2002, Wehkamp et al., 2004), suggests a role for defensins within the oral cavity. Examining the secretion of defensins from OMLP-PCs may further evaluate the role of these cells during infection. Investigating the surface expression of TLRs on OMLP-PCs may elucidate to the potential pathways regulating the antibacterial mechanisms.

This thesis has established that neither LL37 nor IDO are involved in the antibacterial effects of OMLP-PCs. OMLP-PCs demonstrated constitutive antibacterial effects with no expression of LL37 detected in OMLP-PCs, whilst the induction of IDO was dependent on IFNγ stimulation. This demonstrates that the antibacterial mechanism of OMLP-PCs differs from that reported for the BM-MSCs. This study identified three factors which mediate the antibacterial effects of the OMLP-PCs; PGE2, haptoglobin and OPG.

The immunomodulatory effects of PGE2 are well documented, with immunosuppressive effects on both innate and adaptive immune cells such as macrophages (Aronoff et al., 2004) and lymphocytes (Kalinski, 2012). The direct effects of PGE2 on bacterial growth have not fully been investigated. The literature suggests that PGE2 has a positive effect on bacterial growth through its immunosuppression (Agard et al., 2013). It is thought that PGE2 impairs the antibacterial functions of cells such as the phagocytosis of macrophages (Aronoff et al., 2004), thereby promoting bacterial infection. However, these studies examined the effects of PGE2 at 1µM (350ng/ml) (Serezani et al., 2007, Aronoff et al., 2004). The constitutive secretion of PGE2 from OMLP-PCs was reported at levels up to 2ng/ml or less, with increased levels induced by Gram negative bacteria and IFNγ to 8ng/ml. At the constitutive levels secreted by OMLP-PCs, PGE2 demonstrates antibacterial properties, decreasing the growth of bacteria. It is therefore likely that PGE2 acts in a biphasic manner, where at high concentrations the lipid induces imunosuppression and promotes bacterial growth, whereas at low concentrations PGE2 directly reduces bacterial growth. It is likely that the promotion of bacterial growth at high concentrations of PGE2 is an indirect result of the immunosuppression. With the innate immune system dampend due to the immunosuppession, a limited microbial defence from such innate cells would exist.

Further studies are needed to assess the direct antibacterial effects of PGE2 at concentrations above those already examined. The co-culture of peripheral blood PBMCs, OMLP-PCs and bacteria may indicate the potential interplay between the level of immunosupression and the level of antibacterial effects and whether these properties are inversely related.

The antibacterial effects of haptoglobin have long been established (Eaton et al., 1982). The chelation of iron by haptoglobin/haemoglobin binding limits the available iron to bacteria, an essential growth nutrient (Barclay, 1985). Although haptoglobin was detected in the secretome of the OMLP-PCs and blocking its activity restored bacterial growth, it was also detected in the secretome of the non-antibacterial EFs. There are 3 different human isoforms of haptoglobin, differing in the alpha chain composition (Sadrzadeh and Bozorgmehr, 2004). Each isoform contains two alpha chains, either two alpha 1 chains, two alpha 2 chains, or one alpha 1 and one alpha 2 chain. It is the alpha 1 chain which conveys the highest level of activity to the protein, with the isoform containing two alpha 1 chains demonstrating the greatest activity (Eaton et al., 1982). Whilst both the alpha 1 and alpha 2 chains of haptoglobin in the secretome of OMLP-PCs and EFs were detected, it is not possible to determine which isoforms each chain was associated with from the Western blots performed. The lack of antibacterial effects of EFs, despite the presence of haptoglobin, may be attributed to differing ratios of the three isoforms secreted by OMLP-PCs and EFs. Mass spectrometry could be used to identify the haptoglobin isoforms (Garibay-Cerdenares et al., 2014) present in the secretome of OMLP-PCs and EFs in further studies.

This is the first study to demonstrate the antibacterial effects of OPG. Normally associated with bone-remodelling (Jin et al., 2015), it has been demonstrated in this thesis that OPG can reduce the growth of Gram positive bacteria *in vitro*. Its involvement within the immune system has been investigated, with the inhibition of TRAIL-induced lymphocyte apoptosis by OPG known (Emery et al., 1998). OMLP-PCs are known to suppress lymphocyte proliferation (Davies et al., 2012) however, lymphocyte apoptosis was not reported. The secretion of OPG by OMLP-PCs may prevent lymphocyte apoptosis during OMLP-PC-mediated immunosuppression. Further immunomodulatory effects of OPG have been described, with an involvement in B cell development (Emery et al., 1998) and monocyte chemotaxis reported (Mosheimer et al., 2005). Additionally, the decrease in OPG during the inflammatory disease periodontitis is well documented (Bostanci et al., 2007, Mogi et al., 2004, Liu

et al., 2003, Balli et al., 2015). Periodontitis is associated with the bacterium *P. gingivalis*, but the correlation between the disease and OPG levels has not been fully explored. OPG levels during periodontitis are compared to levels of its ligand RANKL and their involvement in bone-remodelling. No study has investigated the potential direct effect of OPG on bacterial growth and whether the decrease in OPG levels pre-disposes patients to bacterial infection.

This study investigated the potential mechanism for the OPG-mediated antibacterial effects. A bacteriostatic effect was confirmed, by the lack of bacterial cell death after OPG incubation, while its binding site on Gram positive bacteria was identified. OPG binds to LTA embedded in the peptidoglycan layer on the surface of these bacteria. Gram negative bacteria lack the peptidoglycan layer (Labischinski et al., 1991) and therefore surface expression of LTA, explaining the lack of antibacterial effects of OPG on these bacteria. This finding has an important effect on the way OPG should be analysed during periodontitis. It is well known that OPG is decreased during the disease, but the knowledge that it has direct bacterial effects was not known, until this study. Whether a decrease in OPG leads to the increased infections during diseases such as periodontitis has not been examined.

Further investigations are warranted to fully characterise the OPG binding to bacteria, with crystallography able to identify the binding domain of OPG. To further assess the antibacterial mechanism of OPG, gene array analysis could be performed on the bacterial genome to assess the changes in gene expression after OPG binding. This may provide an insight into the downstream effects on bacterial growth by OPG.

It has been demonstrated that the antibacterial effects of OMLP-PCs are mediated by different factors to those already identified for BM-MSCs (LL37 and IDO). Further investigations are needed to assess whether the factors identified in this study play a role in the antibacterial effects of BM-MSCs. With such limited literature available in this new research area, it has been important to validate the effects that we see with pure peptide/protein for each of our factors of interest. This is the first study to demonstrate the secretion of haptoglobin by a stem cell population hence its involvement in the BM-MSC mediated antibacterial effect is also unknown. The secretion of PGE2 has been documented from BM-MSCs and it's immunosuppressive phenotype confirmed (Yañez et al., 2010). BM-MSCs are reported to secrete approximately 500pg/ml (Yañez et al., 2010, (Naderi et al., 2015),

which is increased to 1ng/ml with LPS stimulation (Yañez et al., 2010). The LPS stimulated PGE2 secretion is thought to mediate the immunosuppression by BM-MSCs, but direct effects on bacteria have not been assessed.

It has been reported that BM-MSCs secreted levels of OPG between 10-20ng/ml (Oshita et al., 2011, Le Blanc et al., 2004) however, neutralisation of OPG does not affect the immunosuppressive properties of the BM-derived cells. Further investigations are needed to assess whether OPG mediates any of the antibacterial effects demonstrated by MSCs *in vitro*. The negative control cells used in this study, EFs, were found to secrete similar levels of OPG to OMLP-PCs, yet did not display an antibacterial phenotype. The protein sequence of OPG should be analysed in future studies to determine if there are differences in this sequence between the OPG secreted from OMLP-PCs and that from EFs. Raman spectroscopy has been identified as a useful tool in detected changes in protein profiles in recent studies (Michael et al., 2014, Vrensen et al., 2015). A molecular fingerprint of the secreted OPG could therefore be investigated through the application of Raman spectroscopy, detecting any differences in the biochemical fingerprint between the secreted OPG from OMLP-PCs and EFs. It is possible that OPG secreted from the EFs may be conformationally different, blocking the LTA binding site, preventing antibacterial activity. The conformation and activity of BM-MSC secreted OPG would need to be assessed. Conformational differences may be attributed to differences in the glycosylation of the protein secreted from the different cell populations. Differences in the charge of the OMLP-PC and EF secreted OPG protein were alluded to through the 2D gel electrophoresis performed within this study, which may be explained by differences in the protein glycosylation. It is important to consider these differences when examining the potential antibacterial effects of OPG secreted from BM-MSCs.

5.4 *In vivo* potential of OMLP-PCs

This thesis has reported on the antibacterial effects of OMLP-PCs *in vitro*, demonstrating the potential therapeutic effects of a cell-based therapy. However, it is questionable as to whether the effects seen in *in vitro* would translate into clinical benefit. The significant reduction in the growth of bacteria demonstrated *in vitro* by OMLP-PCs may not be sufficient to clear a bacterial infection *in vivo.* However, it is likely that OMLP-PCs would have further antimicrobial effects *in vivo* due to the potential immunomodulatory properties of the cells. The immunomodulatory effects

on lymphocyte proliferation have been characterised for OMLP-PCs (Davies et al., 2012) and many other stem cell populations (Zhang et al., 2009, Tomic et al., 2011, Wada et al., 2009). Further immunomodulatory effects have been confirmed for stem cell populations, which have yet to be investigated for OMLP-PCs. BM-MSCs have been reported to increase the phagocytosis of immune cells, which have demonstrated encouraging potential as a cell-based therapy to treat polymicrobial sepsis. In a model of polymicrobial sepsis, the reduction of *P. aeruginosa* in the blood has been attributed to the increase in blood monocyte phagocytosis (Krasnodembskaya et al., 2012). It was demonstrated that isolated monocytes from MSC-treated mice displayed a higher phagocytic activity compared to those isolated from non-treated mice. No changes in the phagocytic activity in the isolated neutrophils was observed. These effects were seen in the absence of inflammatory cytokine (e.g. TNFα) or immunomodulatory factor (e.g. PGE2) changes, demonstrating the effect was directly mediated by the phagocytosis of the monocytes. Other studies however, have demonstrated effects of MSCs on the phagocytosis of neutrophils. BM-MSCs and human salivary gland MSCs were reported to increase the phagocytic activity of neutrophils *in vitro,* as demonstrated by the increase in intracellular bacterial uptake (Brandau et al., 2014) and BM-MSCs *in vivo* in a mouse model of polymicrobial sepsis (Hall et al., 2013). No phagocytosis has been observed from the BM-MSCs directly. However, these studies did not examine further effects on monocyte phagocytosis.

The effects of OMLP-PCs on immune cell phagocytosis are yet to be examined, but it is hypothesised that this may be another trait that OMLP-PCs share with BM-MSCs. Evaluating the effects of OMLP-PCs on innate immune cells will begin to examine the potential indirect antibacterial effects of OMLP-PCs *in vivo*. The ability of OMLP-PCs to cause innate cell migration and activation should be examined in addition to direct effects of OMLP-PCs on immune cells. MSCs, from both the bone-marrow and the salivary glands have been reported to induce neutrophil chemotaxis (Brandau et al., 2014), with LPS stimulation of MSCs enhancing the chemotactic effect. Furthermore, the secretion of CCL4, a pro-inflammatory cytokine involved in macrophage recruitment, from the neutrophils was induced by LPS stimulated BM-MSCs. The ability of OMLP-PCs to mediate changes in the monocyte and/or mature macrophage populations could lead to further antibacterial effects *in vivo*. Macrophages cultured with MSCs demonstrate an increased M2 phenotype charaterised by IL-10 and IL-6 secretion (Kim and Hematti, 2009). It is thought that M2 macrophages resolve the inflammation caused by infection to prevent tissue damage (Sica et al., 2015). The

ability of MSCs to induce an M2 phenotype suggests MSCs may be involved in the resolution of inflammation and infection. Shifts in the pro-inflammatory M1 and anti-inflammatory M2 macrophage phenotype by OMLP-PCs are yet to be explored, in addition to the effects of OMLP-PCs on monocyte differentiation into macrophage phenotypes. Future studies could examine the effects of OMLP-PCs on monocyte and macrophage populations, in addition to the effects on innate cell phagocytosis. The antibacterial effects of OMLP-PCs may be further enhanced *in vivo* due to indirect antimicrobial effects through the modulation of innate immune cells.

5.5 OMLP-PCs as a New Cell Source for Stem Cell Therapies

While BM-MSCs do display properties making them an ideal for a cell-based therapy such as the ability to home to sites of injury (Wei et al., 2013) and immune-privileged phenotype (Lee et al., 2011), the invasive procedure to obtain BM-MSCs prevents extensive harvesting. A bone marrow aspiration can cause a large amount of discomfort and pain for the donor (Chen et al., 2013), therefore identifying an alternative cell source with limited discomfort to the donor is needed. OMLP-PCs are harvested during a minimally invasive procedure, which can be carried out during routine dental procedures. The mucosa is easily accessible and pain to the donor is limited. Due to the rapid healing within the oral mucosa, donors display a rapid recovery with no scarring. The mucosa is therefore an ideal source of progenitor cells for stem cell-based therapies.

This study has demonstrated the constitutive antibacterial properties of OMLP-PCs, thought to be a result from *in vivo* priming. The effects of *in vivo* priming may offer further advantages of OMLP-PCs as a cell-based therapy compared to BM-MSCs. The exposure of OMLP-PCs to *S. pyogenes* resulted in an enhanced antibacterial effect against this bacterium. With *Streptococcus* species, including *S. pyogenes* (Ramachandran, 2014), regularly the causative organism of sepsis, OMLP-PCs may provide a distinct advantage over other stem based cell therapies. OMLP-PCs share the immune-privileged phenotype with BM-MSCs demonstrated by the low expression of HLA molecules (Davies et al., 2010). Additional studies are required to demonstrate further shared qualities, which make BM-MSCs ideal as a cell-therapy, such as the ability for OMLP-PCs to home to sites of injury. The secretion of SDF-1 is known to facilitate the retention of neutrophils within the bone-marrow. SDF-1 produced by BM-MSCs binds to its ligand, CXCR4, expressed on the neutrophil

surface (Summers et al., 2010), immobilising the neutrophils. Furthermore, the SDF-1/CXCR4 axis has been implicated in stem cell homing. The expression of CXCR4 on MSCs directly correlates to the increased migration and engraftment observed by during MSC therapy (Chen et al., 2012). The overexpression of CXCR4 in BM-MSCs used for the treatment of skin injuries enhances the migration of the BM-MSCs to the site of injury and reduces the wound healing time (Yang et al., 2013). The recruitment of BM-MSCs to the site of injury and the wound healing capacity of the tissue is diminished when CXCR4 is blocked (Xu et al., 2013). Moreover, the treatment of a GVHD murine model with MSCs overexpressing CXCR4 improves the mortality rate of the mice in addition to reducing the GVHD clinical scores (Chen et al., 2012). The expression of CXCR4 on the surface of OMLP-PCs (personal communication Dr Lindsay Davies, Karolinksa Institutet) and the secretion of SDF-1 demonstrated in chapter 4 suggests that OMLP-PCs are able to recruit further OMLP-PCs to sites of infection. The secretion of SDF-1α by OMLP-PCs has the potential to bind to the CXCR4 expressed on the surface of the OMLP-PCs, immobilising further OMLP-PCs at the site of infection. The loss of CXCR4 expression on OMLP-PCs isolated from cGVHD patients (personal communication Dr Lindsay Davies, Karolinksa Institutet) indicates the lack of homing capabilities of these cells during disease.

5.6 OMLP-PCs Lose their Antibacterial Effects during Oral GVHD

GVHD is an immune disorder, which can develop in patients who have undergone HSCT. During GVHD, immune-competent cells such as lymphocytes within the transplanted material become activated, giving rise to an immune response against the host recipient (Ferrara et al., 2009). Complications of GVHD are known to affect several different organs such as the skin, liver and GI tract (Margaix-Muñoz et al., 2015). The oral cavity can also be affected in up to 70% of patients who develop chronic GVHD (Pavletic et al., 2005) with pain, mucositis and increased bacterial infections, particularly gingivitis, reported (Margaix-Muñoz et al., 2015).

Patients undergoing HSCT are predisposed to changes in the microbial flora and increased bacterial infections due to the effects of the treatment and conditioning regimes. Patients are given immunosuppressive therapy prior to HSCT to limit immunorejection (Ferrara et al., 2009). Additionally, radiation targeting the bone-marrow may be prescribed to prevent immunorejection. However, dampening of the patient's immune system and the irradiation of immune cells in the marrow results in

a decreased ability to fight infection. Furthermore, neutropenia, a decrease in neutrophil numbers, has been observed in patients undergoing HSCT, further limiting microbial defence bacteria (Young et al., 2015). The effects of HSCT and the conditioning regimes may predispose the oral cavity to increased bacterial infections, with a reduction in the microbial diversity reported after chemotherapy (Ye et al., 2013) for example. Furthermore, the oral mucosa has a diminished ability to effectively manage the changes in the bacterial flora and changes in bacterial load through the loss of antibacterial effects of the OMLP-PCs demonstrated here. The CM from OMLP-PCs isolated from oral GVHD patients failed to reduce the growth of bacteria, compared to those isolated from healthy patients. This may further explain the increased infections and gingivitis seen in oral cGVHD patients. It is not known whether the loss of OMLP-PCs antibacterial properties occurs during the development of GVHD, or prior to the disease development during the HSCT and conditioning regimes. Isolation of cells and determination of antibacterial potential from patients at each stage can further determine the point at which these properties are lost.

The secretion of identified antibacterial factors from chapter 2 were assessed, however no changes in these factors were reported from OMLP-PCs isolated from GVHD patients compared to healthy donors. This suggests that there are further antibacterial mechanisms mediating the antibacterial effect of OMLP-PCs isolated from healthy donors. It may also be possible that the CM derived from OMLP-PCs isolated form GVHD patients contains an inhibitory factor(s), preventing the antibacterial effects of the secreted factors.

This study demonstrates the potential to re-introduce OMLP-PCs isolated from healthy patients into GVHD patients as a treatment. One case study has demonstrated the potential benefits of a stem cell treatment for chronic oral GVHD (Garming-Legert et al., 2015). Locally injected BM-MSCs reduced the redness and ulceration wound in a 59 year old male. OMLP-PCs may provide a further benefit, by contributing towards the regeneration of a ‘normal’ oral microbial defense.

5.7 Future Directions

This study has demonstrated the direct antibacterial effects of OMLP-PCs. Future studies should further define the OMLP-PC secretome and identify additional

antibacterial factors involved in the antimicrobial mechanism. The recent reports of hBD-2 involvement in the antibacterial effects of cord blood MSCs (Sung et al., 2016) and it's known presence within the oral cavity (Gorr, 2009) warrant the investigation of hBD-2 secretion from OMLP-PCs. A large scale analysis of the secretome is required to identify all factors involved in the antibacterial mechanism. A screening protocol may be established, with initial investigations focused on AMPs known to be present within the oral cavity such as defensins and histatins (Gorr, 2009).

A large scale study to examine the spectrum of antibacterial effects of OMLP-PCs should be undertaken to assess the antibacterial effects against further Gram positive and Gram negative bacteria. It is important to assess the effects against oral commensals, oral pathogens and non-oral bacteria to ascertain which subsets of bacteria are affected by OMLP-PCs and those which could be potential targets for an OMLP-PC based therapy. The effect on pathogenic oral anaerobic bacteria such as *P. gingivalis* should be evaluated to assess the therapeutic potential of OMLP-PCs in diseases caused by such bacteria such as periodontitis.

Importantly, future investigations should focus on the effect of OMLP-PCs on innate immune cells to evaluate the antibacterial potential of the cells *in vivo*. The chemotactic effect of OMLP-PCs on several immune cells such as monocytes and neutrophils using migration assays (such as boyden chambers) could be investigated in addition to the effect of OMLP-PCs on innate cell function. The secretion profiles of innate cells could be assessed to evaluate the effect of OMLP-PCs on innate cell cytokine release. Phagocytic assays could analyse the effects of OMLP-PCs on innate cell phagocytosis, and assess whether OMLP-PCs can affect the antibacterial mechanisms of the innate cells. The phenotype of differentiated monocytes or mature macrophages could be assessed after OMLP-PCs co-culture to evaluate the macrophage M1 pro- or M2 anti-inflammatory phenotype. Surface expression of M1 or M2 markers such as CD86 and CD163 respectively can be analysed to assess the macrophage phenotype in addition to the secretion of M1 and M2 related factors such as TNFα and IL-10 respectively. The ability of OMLP-PCs isolated from patients with oral cGVHD to modulate innate cells should also be considered, to assess whether it is only the direct antibacterial effects which are eradicated during the disease or whether the immunomodulatory capacity of the PCs is also affected.

Future investigations into the OMLP-PCs antibacterial secretome and innate cell effects will hope provide further evidence for the suitability of OMLP-PCs as a cell

based-therapy. The advantages over the gold-standard BM-MSCs have been discussed, including the ease of access to the cells. Further studies will examine whether the beneficial immunomodulatory properties of MSCs are also observed in OMLP-PCs, such as the increased innate cell phagocytosis during polymicrobial sepsis (Hall et al., 2013).

5.8 Conclusion

In conclusion this thesis generated new knowledge concerning the antibacterial properties of OMLP-PCs, with the constitutive property thought to be a result of *in vivo* priming. The effect is mediated by soluble factors secreted from the OMLP-PCs, as demonstrated by the ability of the CM to decrease the growth of bacteria, as with the cells directly. This illustrates the potential role of OMLP-PCs in the oral host defence, with the ability of the OMLP-PCs and their secretome to decrease the growth of both Gram positive and Gram negative bacteria. Three factors were identified to play a role in the OMLP-PC mediated antibacterial effects (PGE2, OPG and haptoglobin) highlighting the differences in the mechanism of action between OMLP-PCs and BM-MSCs. This is the first study to illustrate the antibacterial effects of OPG, with OPG binding to a Gram positive bacterial cell wall component, LTA, beginning to decipher its mechanism of action.

The antibacterial effects of OMLP-PCs isolated from oral GVHD patients did not demonstrate an antibacterial response, with the CM having no effect on bacterial growth. This may in part explain the increased infections observed during GVHD which may lead to inflammation and the symptoms of oral GVHD. Changes in the microbiome of the oral cavity prior to the development of GVHD may pre-dispose the patient to oral infections, which is potentiated by the loss of functional antibacterial OMLP-PCs. Changes in the antibacterial potential of the cells in GHVD were observed in the absence of any changes in the levels of the secreted antibacterial factors PGE2, OPG and haptoglobin. This suggests there are further mechanisms mediating the antibacterial effects of OMLP-PCs.

The importance of OMLP-PCs in the regulation of bacterial populations to help maintain a healthy homeostasis has been suggested in this study, with a loss of antibacterial functions potentially leading to the dysregulation of the oral mucosa and an increased infections during diseases such as oral cGVHD. OMLP-PCs and their

secretome demonstrate antibacterial properties against a range of bacteria, illustrating the potential for OMLP-PCs as a novel cell based or soluble factor based therapy for conditions with a bacterial involvement such sepsis.

6. References

6 References

AAS, J. A., PASTER, B. J., STOKES, L. N., OLSEN, I. & DEWHIRST, F. E. 2005. Defining the normal bacterial flora of the oral cavity. *J Clin Microbiol,* 43**,** 5721-32.

AERTS, A. M., FRANÇOIS, I. E., CAMMUE, B. P. & THEVISSEN, K. 2008. The mode of antifungal action of plant, insect and human defensins. *Cell Mol Life Sci,* 65**,** 2069-79.

AGARD, M., ASAKRAH, S. & MORICI, L. A. 2013. PGE(2) suppression of innate immunity during mucosal bacterial infection. *Front Cell Infect Microbiol,* 3**,** 45.

AGGARWAL, S. & PITTENGER, M. F. 2005. Human mesenchymal stem cells modulate allogeneic immune cell responses. *Blood,* 105**,** 1815-22.

ALEXOPOULOU, L., HOLT, A. C., MEDZHITOV, R. & FLAVELL, R. A. 2001. Recognition of double-stranded RNA and activation of NF-kappaB by Toll-like receptor 3. *Nature,* 413**,** 732-8.

ARAKI, Y. & ITO, E. 1989. Linkage units in cell walls of gram-positive bacteria. *Crit Rev Microbiol,* 17**,** 121-35.

ARCHIBALD, A. R., BADDILEY, J. & BLUMSOM, N. L. 1968. The teichoic acids. *Adv Enzymol Relat Areas Mol Biol,* 30**,** 223-53.

ARENDORF, T. M. & WALKER, D. M. 1979. Oral candidal populations in health and disease. *Br Dent J,* 147**,** 267-72.

ARONOFF, D. M., CANETTI, C. & PETERS-GOLDEN, M. 2004. Prostaglandin E2 inhibits alveolar macrophage phagocytosis through an E-prostanoid 2 receptor-mediated increase in intracellular cyclic AMP. *J Immunol,* 173**,** 559-65.

ARREDOUANI, M. S., KASRAN, A., VANOIRBEEK, J. A., BERGER, F. G., BAUMANN, H. & CEUPPENS, J. L. 2005. Haptoglobin dampens endotoxin-induced inflammatory effects both in vitro and in vivo. *Immunology,* 114**,** 263-71.

ASSIS, A. C., CARVALHO, J. L., JACOBY, B. A., FERREIRA, R. L., CASTANHEIRA, P., DINIZ, S. O., CARDOSO, V. N., GOES, A. M. & FERREIRA, A. J. 2010. Time-dependent migration of systemically delivered bone marrow mesenchymal stem cells to the infarcted heart. *Cell Transplant,* 19**,** 219-30.

ATOUI, R. & CHIU, R. C. 2012. Concise review: immunomodulatory properties of mesenchymal stem cells in cellular transplantation: update, controversies, and unknowns. *Stem Cells Transl Med,* 1**,** 200-5.

AWAWDEH, L. A., LUNDY, F. T., LINDEN, G. J., SHAW, C., KENNEDY, J. G. & LAMEY, P. J. 2002. Quantitative analysis of substance P, neurokinin A and calcitonin gene-related peptide in gingival crevicular fluid associated with painful human teeth. *Eur J Oral Sci,* 110**,** 185-91.

BAJAÑA, S., HERRERA-GONZÁLEZ, N., NARVÁEZ, J., TORRES-AGUILAR, H., RIVAS-CARVALHO, A., AGUILAR, S. R. & SÁNCHEZ-TORRES, C. 2007. Differential CD4(+) T-cell memory responses induced by two subsets of human monocyte-derived dendritic cells. *Immunology,* 122**,** 381-93.

BALLI, U., AYDOGDU, A., ONGOZ DEDE, F., TURER, C. C. & GUVEN, B. 2015. Gingival Crevicular Fluid Levels of Sclerostin, Osteoprotegerin, and Receptor Activator of Nuclear Factor-κB Ligand in Periodontitis. *J Periodontol***,** 1-16.

BARCLAY, R. 1985. The role of iron in infection. *Med Lab Sci,* 42**,** 166-77.

BARTON, G. M. & MEDZHITOV, R. 2003. Toll-like receptor signaling pathways. *Science,* 300**,** 1524-5.

BASSI, E. J., AITA, C. A. & CÂMARA, N. O. 2011. Immune regulatory properties of multipotent mesenchymal stromal cells: Where do we stand? *World J Stem Cells,* 3**,** 1-8.

BAUD'HUIN, M., DUPLOMB, L., TELETCHEA, S., LAMOUREUX, F., RUIZ-VELASCO, C., MAILLASSON, M., REDINI, F., HEYMANN, M. F. & HEYMANN, D. 2013. Osteoprotegerin: multiple partners for multiple functions. *Cytokine Growth Factor Rev,* 24**,** 401-9.

BECKER, M. R., PASTER, B. J., LEYS, E. J., MOESCHBERGER, M. L., KENYON, S. G., GALVIN, J. L., BOCHES, S. K., DEWHIRST, F. E. & GRIFFEN, A. L. 2002. Molecular analysis of bacterial species associated with childhood caries. *J Clin Microbiol,* 40**,** 1001-9.

BELGE, K. U., DAYYANI, F., HORELT, A., SIEDLAR, M., FRANKENBERGER, M., FRANKENBERGER, B., ESPEVIK, T. & ZIEGLER-HEITBROCK, L. 2002. The proinflammatory CD14+CD16+DR++ monocytes are a major source of TNF. *J Immunol,* 168**,** 3536-42.

BELLAMY, W., TAKASE, M., YAMAUCHI, K., WAKABAYASHI, H., KAWASE, K. & TOMITA, M. 1992. Identification of the bactericidal domain of lactoferrin. *Biochim Biophys Acta,* 1121**,** 130-6.

BELLM, L. A., EPSTEIN, J. B., ROSE-PED, A., MARTIN, P. & FUCHS, H. J. 2000. Patient reports of complications of bone marrow transplantation. *Support Care Cancer,* 8**,** 33-9.

BERLUTTI, F., MOREA, C., BATTISTONI, A., SARLI, S., CIPRIANI, P., SUPERTI, F., AMMENDOLIA, M. G. & VALENTI, P. 2005. Iron availability influences aggregation, biofilm, adhesion and invasion of Pseudomonas aeruginosa and Burkholderia cenocepacia. *Int J Immunopathol Pharmacol,* 18**,** 661-70.

BLASIUS, A. L. & BEUTLER, B. 2010. Intracellular toll-like receptors. *Immunity,* 32**,** 305-15.

BOOMSMA, R. A. & GEENEN, D. L. 2012. Mesenchymal stem cells secrete multiple cytokines that promote angiogenesis and have contrasting effects on chemotaxis and apoptosis. *PLoS One,* 7**,** e35685.

BOSTANCI, N., ILGENLI, T., EMINGIL, G., AFACAN, B., HAN, B., TÖZ, H., BERDELI, A., ATILLA, G., MCKAY, I. J., HUGHES, F. J. & BELIBASAKIS, G. N. 2007. Differential expression of receptor activator of nuclear factor-kappaB ligand and osteoprotegerin mRNA in periodontal diseases. *J Periodontal Res,* 42**,** 287-93.

BOWDISH, D. M., DAVIDSON, D. J., LAU, Y. E., LEE, K., SCOTT, M. G. & HANCOCK, R. E. 2005. Impact of LL-37 on anti-infective immunity. *J Leukoc Biol,* 77**,** 451-9.

BRANDAU, S., JAKOB, M., BRUDEREK, K., BOOTZ, F., GIEBEL, B., RADTKE, S., MAUEL, K., JÄGER, M., FLOHÉ, S. B. & LANG, S. 2014. Mesenchymal stem cells augment the anti-bacterial activity of neutrophil granulocytes. *PLoS One,* 9**,** e106903.

BRANDTZAEG, P., GABRIELSEN, T. O., DALE, I., MÜLLER, F., STEINBAKK, M. & FAGERHOL, M. K. 1995. The leucocyte protein L1 (calprotectin): a putative

nonspecific defence factor at epithelial surfaces. *Adv Exp Med Biol,* 371A**,** 201-6.

BRINKMANN, V., REICHARD, U., GOOSMANN, C., FAULER, B., UHLEMANN, Y., WEISS, D. S., WEINRAUCH, Y. & ZYCHLINSKY, A. 2004. Neutrophil extracellular traps kill bacteria. *Science,* 303**,** 1532-5.

BUDUNELI, N., BIYIKOĞLU, B., SHERRABEH, S. & LAPPIN, D. F. 2008. Saliva concentrations of RANKL and osteoprotegerin in smoker versus non-smoker chronic periodontitis patients. *J Clin Periodontol,* 35**,** 846-52.

BURNS, A. R., BOWDEN, R. A., MACDONELL, S. D., WALKER, D. C., ODEBUNMI, T. O., DONNACHIE, E. M., SIMON, S. I., ENTMAN, M. L. & SMITH, C. W. 2000. Analysis of tight junctions during neutrophil transendothelial migration. *J Cell Sci,* 113 (Pt 1)**,** 45-57.

BUTOVSKY, O., JEDRYCHOWSKI, M. P., MOORE, C. S., CIALIC, R., LANSER, A. J., GABRIELY, G., KOEGLSPERGER, T., DAKE, B., WU, P. M., DOYKAN, C. E., FANEK, Z., LIU, L., CHEN, Z., ROTHSTEIN, J. D., RANSOHOFF, R. M., GYGI, S. P., ANTEL, J. P. & WEINER, H. L. 2014. Identification of a unique TGF-β-dependent molecular and functional signature in microglia. *Nat Neurosci,* 17**,** 131-43.

BĄBOLEWSKA, E. & BRZEZIŃSKA-BŁASZCZYK, E. 2015. Human-derived cathelicidin LL-37 directly activates mast cells to proinflammatory mediator synthesis and migratory response. *Cell Immunol,* 293**,** 67-73.

CABEEN, M. T. & JACOBS-WAGNER, C. 2005. Bacterial cell shape. *Nat Rev Microbiol,* 3**,** 601-10.

CAULFIELD, J., FERNANDEZ, M., SNETKOV, V., LEE, T. & HAWRYLOWICZ, C. 2002. CXCR4 expression on monocytes is up-regulated by dexamethasone and is modulated by autologous CD3+ T cells. *Immunology,* 105**,** 155-62.

CHAMPLIN, R. 2003. *Selection of Autologous or Allogeneic Transplantation,* Holland, BC Decker.

CHAUDHARI, B. R., MURPHY, R. F. & AGRAWAL, D. K. 2006. Following the TRAIL to apoptosis. *Immunol Res,* 35**,** 249-62.

CHEN, J. Y., MOU, X. Z., DU, X. C. & XIANG, C. 2015a. Comparative analysis of biological characteristics of adult mesenchymal stem cells with different tissue origins. *Asian Pac J Trop Med,* 8**,** 739-46.

CHEN, P., HUANG, Y. & WOMER, K. L. 2015b. Effects of mesenchymal stromal cells on human myeloid dendritic cell differentiation and maturation in a humanized mouse model. *J Immunol Methods,* 427, 100-4.

CHEN, S. H., WANG, T. F. & YANG, K. L. 2013. Hematopoietic stem cell donation. *Int J Hematol,* 97**,** 446-55.

CHEN, W., LI, M., LI, Z., YAN, Z., CHENG, H., PAN, B., CAO, J., CHEN, C., ZENG, L. & XU, K. 2012. CXCR4-transduced mesenchymal stem cells protect mice against graft-versus-host disease. *Immunol Lett,* 143**,** 161-9.

CHEN, X., NIYONSABA, F., USHIO, H., OKUDA, D., NAGAOKA, I., IKEDA, S., OKUMURA, K. & OGAWA, H. 2005. Synergistic effect of antibacterial agents human beta-defensins, cathelicidin LL-37 and lysozyme against Staphylococcus aureus and Escherichia coli. *J Dermatol Sci,* 40**,** 123-32.

CHENG, Z., OU, L., ZHOU, X., LI, F., JIA, X., ZHANG, Y., LIU, X., LI, Y., WARD, C. A., MELO, L. G. & KONG, D. 2008. Targeted migration of mesenchymal stem

cells modified with CXCR4 gene to infarcted myocardium improves cardiac performance. *Mol Ther,* 16**,** 571-9.

CHEREDDY, K. K., HER, C. H., COMUNE, M., MOIA, C., LOPES, A., PORPORATO, P. E., VANACKER, J., LAM, M. C., STEINSTRAESSER, L., SONVEAUX, P., ZHU, H., FERREIRA, L. S., VANDERMEULEN, G. & PRÉAT, V. 2014. PLGA nanoparticles loaded with host defense peptide LL37 promote wound healing. *J Control Release,* 194**,** 138-47.

CHO, H., BAE, Y. C. & JUNG, J. S. 2006. Role of toll-like receptors on human adipose-derived stromal cells. *Stem Cells,* 24**,** 2744-52.

CLAES, A. K., ZHOU, J. Y. & PHILPOTT, D. J. 2015. NOD-Like Receptors: Guardians of Intestinal Mucosal Barriers. *Physiology (Bethesda),* 30**,** 241-50.

CLARKSON, S. B. & ORY, P. A. 1988. CD16. Developmentally regulated IgG Fc receptors on cultured human monocytes. *J Exp Med,* 167**,** 408-20.

CLAVERT, A., CHEVALLIER, P., GUILLAUME, T., DELAUNAY, J., LE GOUILL, S., MAHE, B., DUBRUILLE, V., GASTINNE, T., BLIN, N., MOREAU, P. & MOHTY, M. 2013. Safety and efficacy of rituximab in steroid-refractory chronic GVHD. *Bone Marrow Transplant,* 48**,** 734-6.

CLINICALTRIALS.GOV. *A service of the U.S. National Institutes of Health* [Online]. [Accessed 1.5.15 2015].

CLOHESSY, P. A. & GOLDEN, B. E. 1995. Calprotectin-mediated zinc chelation as a biostatic mechanism in host defence. *Scand J Immunol,* 42**,** 551-6.

CONROTTO, D., BROCCOLETTI, R., CARCIERI, P., GIACCONE, L. & ARDUINO, P. G. 2014. Topical tacrolimus and periodontal therapy in the management of a case of oral chronic GVHD characterized by specific gingival localization. *Case Rep Dent,* 2014**,** 127219.

CONSORTIUM, H. M. P. 2012. Structure, function and diversity of the healthy human microbiome. *Nature,* 486**,** 207-14.

CORALLINI, F., CELEGHINI, C., RIMONDI, E., DI IASIO, M. G., GONELLI, A., SECCHIERO, P. & ZAULI, G. 2011. Trail down-regulates the release of osteoprotegerin (OPG) by primary stromal cells. *J Cell Physiol,* 226**,** 2279-86.

CORNELIS, P. & DINGEMANS, J. 2013. Pseudomonas aeruginosa adapts its iron uptake strategies in function of the type of infections. *Front Cell Infect Microbiol,* 3**,** 75.

COWLAND, J. B. & BORREGAARD, N. 1997. Molecular characterization and pattern of tissue expression of the gene for neutrophil gelatinase-associated lipocalin from humans. *Genomics,* 45**,** 17-23.

CROS, J., CAGNARD, N., WOOLLARD, K., PATEY, N., ZHANG, S. Y., SENECHAL, B., PUEL, A., BISWAS, S. K., MOSHOUS, D., PICARD, C., JAIS, J. P., D'CRUZ, D., CASANOVA, J. L., TROUILLET, C. & GEISSMANN, F. 2010. Human CD14dim monocytes patrol and sense nucleic acids and viruses via TLR7 and TLR8 receptors. *Immunity,* 33**,** 375-86.

CRUZ, F. F., BORG, Z. D., GOODWIN, M., SOKOCEVIC, D., WAGNER, D. E., COFFEY, A., ANTUNES, M., ROBINSON, K. L., MITSIALIS, S. A., KOUREMBANAS, S., THANE, K., HOFFMAN, A. M., MCKENNA, D. H., ROCCO, P. R. & WEISS, D. J. 2015. Systemic Administration of Human Bone Marrow-Derived Mesenchymal Stromal Cell Extracellular Vesicles

Ameliorates Aspergillus Hyphal Extract-Induced Allergic Airway Inflammation in Immunocompetent Mice. *Stem Cells Transl Med,* 4**,** 1302-16.

CUTLER, C., MIKLOS, D., KIM, H. T., TREISTER, N., WOO, S. B., BIENFANG, D., KLICKSTEIN, L. B., LEVIN, J., MILLER, K., REYNOLDS, C., MACDONELL, R., PASEK, M., LEE, S. J., HO, V., SOIFFER, R., ANTIN, J. H., RITZ, J. & ALYEA, E. 2006. Rituximab for steroid-refractory chronic graft-versus-host disease. *Blood,* 108**,** 756-62.

D'IPPOLITO, G., SCHILLER, P. C., RICORDI, C., ROOS, B. A. & HOWARD, G. A. 1999. Age-related osteogenic potential of mesenchymal stromal stem cells from human vertebral bone marrow. *J Bone Miner Res,* 14**,** 1115-22.

DALE, B. A. & FREDERICKS, L. P. 2005. Antimicrobial peptides in the oral environment: expression and function in health and disease. *Curr Issues Mol Biol,* 7**,** 119-33.

DALL'AMICO, R. & MESSINA, C. 2002. Extracorporeal photochemotherapy for the treatment of graft-versus-host disease. *Ther Apher,* 6**,** 296-304.

DARVEAU, R. P., PHAM, T. T., LEMLEY, K., REIFE, R. A., BAINBRIDGE, B. W., COATS, S. R., HOWALD, W. N., WAY, S. S. & HAJJAR, A. M. 2004. Porphyromonas gingivalis lipopolysaccharide contains multiple lipid A species that functionally interact with both toll-like receptors 2 and 4. *Infect Immun,* 72**,** 5041-51.

DAVIES, L. C., LOCKE, M., WEBB, R. D., ROBERTS, J. T., LANGLEY, M., THOMAS, D. W., ARCHER, C. W. & STEPHENS, P. 2010. A multipotent neural crest-derived progenitor cell population is resident within the oral mucosa lamina propria. *Stem Cells Dev,* 19**,** 819-30.

DAVIES, L. C., LÖNNIES, H., LOCKE, M., SUNDBERG, B., ROSENDAHL, K., GÖTHERSTRÖM, C., LE BLANC, K. & STEPHENS, P. 2012. Oral mucosal progenitor cells are potently immunosuppressive in a dose-independent manner. *Stem Cells Dev,* 21**,** 1478-87.

DAWIDSON, I., BLOM, M., LUNDEBERG, T., THEODORSSON, E. & ANGMAR-MÅNSSON, B. 1997. Neuropeptides in the saliva of healthy subjects. *Life Sci,* 60**,** 269-78.

DAWSON, D. V., DRAKE, D. R., HILL, J. R., BROGDEN, K. A., FISCHER, C. L. & WERTZ, P. W. 2013. Organization, barrier function and antimicrobial lipids of the oral mucosa. *Int J Cosmet Sci,* 35**,** 220-3.

DAYAN, V., YANNARELLI, G., BILLIA, F., FILOMENO, P., WANG, X. H., DAVIES, J. E. & KEATING, A. 2011. Mesenchymal stromal cells mediate a switch to alternatively activated monocytes/macrophages after acute myocardial infarction. *Basic Res Cardiol,* 106**,** 1299-310.

DE HAAR, S. F., HIEMSTRA, P. S., VAN STEENBERGEN, M. T., EVERTS, V. & BEERTSEN, W. 2006. Role of polymorphonuclear leukocyte-derived serine proteinases in defense against Actinobacillus actinomycetemcomitans. *Infect Immun,* 74**,** 5284-91.

DE SMET, K. & CONTRERAS, R. 2005. Human antimicrobial peptides: defensins, cathelicidins and histatins. *Biotechnol Lett,* 27**,** 1337-47.

DEVOCELLE, M. 2012. Targeted antimicrobial peptides. *Front Immunol,* 3**,** 309.

DEWHIRST, F. E., CHEN, T., IZARD, J., PASTER, B. J., TANNER, A. C., YU, W. H., LAKSHMANAN, A. & WADE, W. G. 2010. The human oral microbiome. *J Bacteriol,* 192**,** 5002-17.

DHIR, S., SLATTER, M. & SKINNER, R. 2014. Recent advances in the management of graft-versus-host disease. *Arch Dis Child,* 99**,** 1150-7.

DIETRICH, T., JIMENEZ, M., KRALL KAYE, E. A., VOKONAS, P. S. & GARCIA, R. I. 2008. Age-dependent associations between chronic periodontitis/edentulism and risk of coronary heart disease. *Circulation,* 117**,** 1668-74.

DING, G., LIU, Y., WANG, W., WEI, F., LIU, D., FAN, Z., AN, Y., ZHANG, C. & WANG, S. 2010. Allogeneic periodontal ligament stem cell therapy for periodontitis in swine. *Stem Cells,* 28**,** 1829-38.

DJOUAD, F., BOUFFI, C., GHANNAM, S., NOËL, D. & JORGENSEN, C. 2009. Mesenchymal stem cells: innovative therapeutic tools for rheumatic diseases. *Nat Rev Rheumatol,* 5**,** 392-9.

DOMINICI, M., LE BLANC, K., MUELLER, I., SLAPER-CORTENBACH, I., MARINI, F., KRAUSE, D., DEANS, R., KEATING, A., PROCKOP, D. & HORWITZ, E. 2006. Minimal criteria for defining multipotent mesenchymal stromal cells. The International Society for Cellular Therapy position statement. *Cytotherapy,* 8**,** 315-7.

DOWTHWAITE, G. P., BISHOP, J. C., REDMAN, S. N., KHAN, I. M., ROONEY, P., EVANS, D. J., HAUGHTON, L., BAYRAM, Z., BOYER, S., THOMSON, B., WOLFE, M. S. & ARCHER, C. W. 2004. The surface of articular cartilage contains a progenitor cell population. *J Cell Sci,* 117**,** 889-97.

EATON, J. W., BRANDT, P., MAHONEY, J. R. & LEE, J. T. 1982. Haptoglobin: a natural bacteriostat. *Science,* 215**,** 691-3.

ECKARDT, A., STARKE, O., STADLER, M., REUTER, C. & HERTENSTEIN, B. 2004. Severe oral chronic graft-versus-host disease following allogeneic bone marrow transplantation: highly effective treatment with topical tacrolimus. *Oral Oncol,* 40**,** 811-4.

EDGERTON, M., KOSHLUKOVA, S. E., LO, T. E., CHRZAN, B. G., STRAUBINGER, R. M. & RAJ, P. A. 1998. Candidacidal activity of salivary histatins. Identification of a histatin 5-binding protein on Candida albicans. *J Biol Chem,* 273**,** 20438-47.

EGGENHOFER, E., BENSELER, V., KROEMER, A., POPP, F. C., GEISSLER, E. K., SCHLITT, H. J., BAAN, C. C., DAHLKE, M. H. & HOOGDUIJN, M. J. 2012. Mesenchymal stem cells are short-lived and do not migrate beyond the lungs after intravenous infusion. *Front Immunol,* 3**,** 297.

EL KARIM, I. A., LINDEN, G. J., ORR, D. F. & LUNDY, F. T. 2008. Antimicrobial activity of neuropeptides against a range of micro-organisms from skin, oral, respiratory and gastrointestinal tract sites. *J Neuroimmunol,* 200**,** 11-6.

ELLISON, R. T. & GIEHL, T. J. 1991. Killing of gram-negative bacteria by lactoferrin and lysozyme. *J Clin Invest,* 88**,** 1080-91.

EMERY, J. G., MCDONNELL, P., BURKE, M. B., DEEN, K. C., LYN, S., SILVERMAN, C., DUL, E., APPELBAUM, E. R., EICHMAN, C., DIPRINZIO, R., DODDS, R. A., JAMES, I. E., ROSENBERG, M., LEE, J. C. & YOUNG, P. R. 1998. Osteoprotegerin is a receptor for the cytotoxic ligand TRAIL. *J Biol Chem,* 273**,** 14363-7.

ENGLISH, K., TONLORENZI, R., COSSU, G. & WOOD, K. J. 2013. Mesoangioblasts suppress T cell proliferation through IDO and PGE-2-dependent pathways. *Stem Cells Dev,* 22**,** 512-23.

ERICKSEN, B., WU, Z., LU, W. & LEHRER, R. I. 2005. Antibacterial activity and specificity of the six human {alpha}-defensins. *Antimicrob Agents Chemother,* 49**,** 269-75.

ERIGUCHI, Y., TAKASHIMA, S., OKA, H., SHIMOJI, S., NAKAMURA, K., URYU, H., SHIMODA, S., IWASAKI, H., SHIMONO, N., AYABE, T., AKASHI, K. & TESHIMA, T. 2012. Graft-versus-host disease disrupts intestinal microbial ecology by inhibiting Paneth cell production of α-defensins. *Blood,* 120**,** 223-31.

ESEONU, O. I. & DE BARI, C. 2015. Homing of mesenchymal stem cells: mechanistic or stochastic? Implications for targeted delivery in arthritis. *Rheumatology (Oxford),* 54**,** 210-8.

FAGAN, M. 2013. *Philosophy of Stem Cell BiologyKnowledge in Flesh and Blood,* Basingstoke, Pal Grave McMillan.

FAKHARI, S., KALANTAR, E., NIKZABAN, M., HAKHAMNESHI, M. S., FATHI, F., NIKKHOO, B., RAHMANI, M. R., BEIRAGHDAR, M. & JALILI, A. 2014. Effect of Helicobacter pylori infection on stromal-derived factor-1/CXCR4 axis in bone marrow-derived mesenchymal stem cells. *Adv Biomed Res,* 3**,** 19.

FALLARINO, F., GROHMANN, U., VACCA, C., ORABONA, C., SPRECA, A., FIORETTI, M. C. & PUCCETTI, P. 2003. T cell apoptosis by kynurenines. *Adv Exp Med Biol,* 527**,** 183-90.

FERRARA, J. L., LEVINE, J. E., REDDY, P. & HOLLER, E. 2009. Graft-versus-host disease. *Lancet,* 373**,** 1550-61.

FERRARA, J. L. & REDDY, P. 2006. Pathophysiology of graft-versus-host disease. *Semin Hematol,* 43**,** 3-10.

FERRIS, L. K., MBURU, Y. K., MATHERS, A. R., FLUHARTY, E. R., LARREGINA, A. T., FERRIS, R. L. & FALO, L. D. 2013. Human beta-defensin 3 induces maturation of human langerhans cell-like dendritic cells: an antimicrobial peptide that functions as an endogenous adjuvant. *J Invest Dermatol,* 133**,** 460-8.

FIALKOW, L., WANG, Y. & DOWNEY, G. P. 2007. Reactive oxygen and nitrogen species as signaling molecules regulating neutrophil function. *Free Radic Biol Med,* 42**,** 153-64.

FISCHER, U. M., HARTING, M. T., JIMENEZ, F., MONZON-POSADAS, W. O., XUE, H., SAVITZ, S. I., LAINE, G. A. & COX, C. S. 2009. Pulmonary passage is a major obstacle for intravenous stem cell delivery: the pulmonary first-pass effect. *Stem Cells Dev,* 18**,** 683-92.

FJELL, C. D., HISS, J. A., HANCOCK, R. E. & SCHNEIDER, G. 2012. Designing antimicrobial peptides: form follows function. *Nat Rev Drug Discov,* 11**,** 37-51.

FLO, T. H., SMITH, K. D., SATO, S., RODRIGUEZ, D. J., HOLMES, M. A., STRONG, R. K., AKIRA, S. & ADEREM, A. 2004. Lipocalin 2 mediates an innate immune response to bacterial infection by sequestrating iron. *Nature,* 432**,** 917-21.

FOROUZANDEH, F., JALILI, R. B., GERMAIN, M., DURONIO, V. & GHAHARY, A. 2008. Differential immunosuppressive effect of indoleamine 2,3-dioxygenase (IDO) on primary human CD4+ and CD8+ T cells. *Mol Cell Biochem,* 309**,** 1-7.

FOURNIER, B. & PHILPOTT, D. J. 2005. Recognition of Staphylococcus aureus by the innate immune system. *Clin Microbiol Rev,* 18**,** 521-40.

FRANKLIN, C., CESKO, E., HILLEN, U., SCHILLING, B. & BRANDAU, S. 2015. Modulation and Apoptosis of Neutrophil Granulocytes by Extracorporeal Photopheresis in the Treatment of Chronic Graft-Versus-Host Disease. *PLoS One,* 10**,** e0134518.

FRIEDENSTEIN, A. J., PETRAKOVA, K. V., KUROLESOVA, A. I. & FROLOVA, G. P. 1968. Heterotopic of bone marrow. Analysis of precursor cells for osteogenic and hematopoietic tissues. *Transplantation,* 6**,** 230-47.

GALLO, R. L., MURAKAMI, M., OHTAKE, T. & ZAIOU, M. 2002. Biology and clinical relevance of naturally occurring antimicrobial peptides. *J Allergy Clin Immunol,* 110**,** 823-31.

GALLO, R. L. & NIZET, V. 2008. Innate barriers against infection and associated disorders. *Drug Discov Today Dis Mech,* 5**,** 145-152.

GARIBAY-CERDENARES, O. L., HERNÁNDEZ-RAMÍREZ, V. I., OSORIO-TRUJILLO, J. C., HERNÁNDEZ-ORTÍZ, M., GALLARDO-RINCÓN, D., CANTÚ DE LEÓN, D., ENCARNACIÓN-GUEVARA, S., VILLEGAS-PINEDA, J. C. & TALAMÁS-ROHANA, P. 2014. Proteomic identification of fucosylated haptoglobin alpha isoforms in ascitic fluids and its localization in ovarian carcinoma tissues from Mexican patients. *J Ovarian Res,* 7**,** 27.

GARMING-LEGERT, K., TOUR, G., SUGARS, R., VON BAHR, L., DAVIES, L. C. & LE BLANC, K. 2015. Enhanced oral healing following local mesenchymal stromal cell therapy. *Oral Oncol*, 51,97-99.

GAUDREAULT, E., FIOLA, S., OLIVIER, M. & GOSSELIN, J. 2007. Epstein-Barr virus induces MCP-1 secretion by human monocytes via TLR2. *J Virol,* 81**,** 8016-24.

GENEVROIS, S., STEEGHS, L., ROHOLL, P., LETESSON, J. J. & VAN DER LEY, P. 2003. The Omp85 protein of Neisseria meningitidis is required for lipid export to the outer membrane. *EMBO J,* 22**,** 1780-9.

GHANNAM, S., BOUFFI, C., DJOUAD, F., JORGENSEN, C. & NOËL, D. 2010a. Immunosuppression by mesenchymal stem cells: mechanisms and clinical applications. *Stem Cell Res Ther,* 1**,** 2.

GHANNAM, S., PÈNE, J., MOQUET-TORCY, G., TORCY-MOQUET, G., JORGENSEN, C. & YSSEL, H. 2010b. Mesenchymal stem cells inhibit human Th17 cell differentiation and function and induce a T regulatory cell phenotype. *J Immunol,* 185**,** 302-12.

GHANNOUM, M. A., JUREVIC, R. J., MUKHERJEE, P. K., CUI, F., SIKAROODI, M., NAQVI, A. & GILLEVET, P. M. 2010. Characterization of the oral fungal microbiome (mycobiome) in healthy individuals. *PLoS Pathog,* 6**,** e1000713.

GHYSELS, B., DIEU, B. T., BEATSON, S. A., PIRNAY, J. P., OCHSNER, U. A., VASIL, M. L. & CORNELIS, P. 2004. FpvB, an alternative type I ferripyoverdine receptor of Pseudomonas aeruginosa. *Microbiology,* 150**,** 1671-80.

GOETZ, D. H., HOLMES, M. A., BORREGAARD, N., BLUHM, M. E., RAYMOND, K. N. & STRONG, R. K. 2002. The neutrophil lipocalin NGAL is a bacteriostatic agent that interferes with siderophore-mediated iron acquisition. *Mol Cell,* 10**,** 1033-43.

GORR, S. U. 2009. Antimicrobial peptides of the oral cavity. *Periodontol 2000,* 51**,** 152-80.

GOSSET, P., BUREAU, F., ANGELI, V., PICHAVANT, M., FAVEEUW, C., TONNEL, A. B. & TROTTEIN, F. 2003. Prostaglandin D2 affects the maturation of human monocyte-derived dendritic cells: consequence on the polarization of naive Th cells. *J Immunol,* 170**,** 4943-52.

GRANITTO, M. H., FALL-DICKSON, J. M., NORTON, C. K. & SANDERS, C. 2014. Review of therapies for the treatment of oral chronic graft-versus-host disease. *Clin J Oncol Nurs,* 18**,** 76-81.

GRAVES, D. T. & COCHRAN, D. 2003. The contribution of interleukin-1 and tumor necrosis factor to periodontal tissue destruction. *J Periodontol,* 74**,** 391-401.

GRÖSCHL, M., WENDLER, O., TOPF, H. G., BOHLENDER, J. & KÖHLER, H. 2009. Significance of salivary adrenomedullin in the maintenance of oral health: stimulation of oral cell proliferation and antibacterial properties. *Regul Pept,* 154**,** 16-22.

GUANÍ-GUERRA, E., SANTOS-MENDOZA, T., LUGO-REYES, S. O. & TERÁN, L. M. 2010. Antimicrobial peptides: general overview and clinical implications in human health and disease. *Clin Immunol,* 135**,** 1-11.

GUPTA, N., KRASNODEMBSKAYA, A., KAPETANAKI, M., MOUDED, M., TAN, X., SERIKOV, V. & MATTHAY, M. A. 2012. Mesenchymal stem cells enhance survival and bacterial clearance in murine Escherichia coli pneumonia. *Thorax,* 67**,** 533-9.

GÜRGAN, C. A., ÖZCAN, M., KARAKUŞ, Ö., ZINCIRCIOĞLU, G., ARAT, M., SOYDAN, E., TOPCUOGLU, P., GÜRMAN, G. & BOSTANCI, H. S. 2013. Periodontal status and post-transplantation complications following intensive periodontal treatment in patients underwent allogenic hematopoietic stem cell transplantation conditioned with myeloablative regimen. *Int J Dent Hyg,* 11**,** 84-90.

HACKSTEIN, H., LIPPITSCH, A., KRUG, P., SCHEVTSCHENKO, I., KRANZ, S., HECKER, M., DIETERT, K., GRUBER, A. D., BEIN, G., BRENDEL, C. & BAAL, N. 2015. Prospectively defined murine mesenchymal stem cells inhibit Klebsiella pneumoniae-induced acute lung injury and improve pneumonia survival. *Respir Res,* 16**,** 123.

HALL, S. R., TSOYI, K., ITH, B., PADERA, R. F., LEDERER, J. A., WANG, Z., LIU, X. & PERRELLA, M. A. 2013. Mesenchymal stromal cells improve survival during sepsis in the absence of heme oxygenase-1: the importance of neutrophils. *Stem Cells,* 31**,** 397-407.

HANEY, E. F. & HANCOCK, R. E. 2013. Peptide design for antimicrobial and immunomodulatory applications. *Biopolymers,* 100**,** 572-83.

HARDER, J., MEYER-HOFFERT, U., TERAN, L. M., SCHWICHTENBERG, L., BARTELS, J., MAUNE, S. & SCHRÖDER, J. M. 2000. Mucoid Pseudomonas aeruginosa, TNF-alpha, and IL-1beta, but not IL-6, induce human beta-defensin-2 in respiratory epithelia. *Am J Respir Cell Mol Biol,* 22**,** 714-21.

HARRIS, A. C., YOUNG, R., DEVINE, S., HOGAN, W. J., AYUK, F., BUNWORASATE, U., CHANSWANGPHUWANA, C., EFEBERA, Y. A., HOLLER, E., LITZOW, M., ORDEMANN, R., QAYED, M., RENTERIA, A. S., RESHEF, R., WÖLFL, M., CHEN, Y. B., GOLDSTEIN, S., JAGASIA, M., LOCATELLI, F., MIELKE, S., PORTER, D., SCHECHTER, T., SHEKHOVTSOVA, Z., FERRARA, J. L. & LEVINE, J. E. 2015. International, Multicenter Standardization of Acute Graft-versus-Host Disease Clinical Data

Collection: A Report from the Mount Sinai Acute GVHD International Consortium. *Biol Blood Marrow Transplant,* 22, 4-10.

HARRIS, J., DE HARO, S. A., MASTER, S. S., KEANE, J., ROBERTS, E. A., DELGADO, M. & DERETIC, V. 2007. T helper 2 cytokines inhibit autophagic control of intracellular Mycobacterium tuberculosis. *Immunity,* 27**,** 505-17.

HAVERMAN, T. M., RABER-DURLACHER, J. E., RADEMACHER, W. M., VOKURKA, S., EPSTEIN, J. B., HUISMAN, C., HAZENBERG, M. D., DE SOET, J. J., DE LANGE, J. & ROZEMA, F. R. 2014. Oral complications in hematopoietic stem cell recipients: the role of inflammation. *Mediators Inflamm,* 2014**,** 378281.

HAYASHI, F., SMITH, K. D., OZINSKY, A., HAWN, T. R., YI, E. C., GOODLETT, D. R., ENG, J. K., AKIRA, S., UNDERHILL, D. M. & ADEREM, A. 2001. The innate immune response to bacterial flagellin is mediated by Toll-like receptor 5. *Nature,* 410**,** 1099-103.

HEGYI, B., KUDLIK, G., MONOSTORI, E. & UHER, F. 2012. Activated T-cells and pro-inflammatory cytokines differentially regulate prostaglandin E2 secretion by mesenchymal stem cells. *Biochem Biophys Res Commun,* 419**,** 215-20.

HEINE, H., MÜLLER-LOENNIES, S., BRADE, L., LINDNER, B. & BRADE, H. 2003. Endotoxic activity and chemical structure of lipopolysaccharides from Chlamydia trachomatis serotypes E and L2 and Chlamydophila psittaci 6BC. *Eur J Biochem,* 270**,** 440-50.

HERBST, S., SCHAIBLE, U. E. & SCHNEIDER, B. E. 2011. Interferon gamma activated macrophages kill mycobacteria by nitric oxide induced apoptosis. *PLoS One,* 6**,** e19105.

HESSLE, C. C., ANDERSSON, B. & WOLD, A. E. 2003. Gram-negative, but not Gram-positive, bacteria elicit strong PGE2 production in human monocytes. *Inflammation,* 27**,** 329-32.

HEUMANN, D. & ROGER, T. 2002. Initial responses to endotoxins and Gram-negative bacteria. *Clin Chim Acta,* 323**,** 59-72.

HIESHIMA, K., OHTANI, H., SHIBANO, M., IZAWA, D., NAKAYAMA, T., KAWASAKI, Y., SHIBA, F., SHIOTA, M., KATOU, F., SAITO, T. & YOSHIE, O. 2003. CCL28 has dual roles in mucosal immunity as a chemokine with broad-spectrum antimicrobial activity. *J Immunol,* 170**,** 1452-61.

HIRSCH, E., KATANAEV, V. L., GARLANDA, C., AZZOLINO, O., PIROLA, L., SILENGO, L., SOZZANI, S., MANTOVANI, A., ALTRUDA, F. & WYMANN, M. P. 2000. Central role for G protein-coupled phosphoinositide 3-kinase gamma in inflammation. *Science,* 287**,** 1049-53.

HOHL, T. M., RIVERA, A., LIPUMA, L., GALLEGOS, A., SHI, C., MACK, M. & PAMER, E. G. 2009. Inflammatory monocytes facilitate adaptive CD4 T cell responses during respiratory fungal infection. *Cell Host Microbe,* 6**,** 470-81.

HOVAV, A. H. 2014. Dendritic cells of the oral mucosa. *Mucosal Immunol,* 7**,** 27-37.

HUCKE, C., MACKENZIE, C. R., ADJOGBLE, K. D., TAKIKAWA, O. & DÄUBENER, W. 2004. Nitric oxide-mediated regulation of gamma interferon-induced bacteriostasis: inhibition and degradation of human indoleamine 2,3-dioxygenase. *Infect Immun,* 72**,** 2723-30.

HUME, D. A. 2015. The Many Alternative Faces of Macrophage Activation. *Front Immunol,* 6**,** 370.

HUNTOON, K. M., WANG, Y., EPPOLITO, C. A., BARBOUR, K. W., BERGER, F. G., SHRIKANT, P. A. & BAUMANN, H. 2008. The acute phase protein haptoglobin regulates host immunity. *J Leukoc Biol,* 84**,** 170-81.

IMAIZUMI, T., KUMAGAI, M., TAIMA, K., FUJITA, T., YOSHIDA, H. & SATOH, K. 2005. Involvement of retinoic acid-inducible gene-I in the IFN-{gamma}/STAT1 signalling pathway in BEAS-2B cells. *Eur Respir J,* 25**,** 1077-83.

INAMOTO, Y., MARTIN, P. J., CHAI, X., JAGASIA, M., PALMER, J., PIDALA, J., CUTLER, C., PAVLETIC, S. Z., ARORA, M., JACOBSOHN, D., CARPENTER, P. A., FLOWERS, M. E., KHERA, N., VOGELSANG, G. B., WEISDORF, D., STORER, B. E., LEE, S. J. & CONSORTIUM, C. G. 2012. Clinical benefit of response in chronic graft-versus-host disease. *Biol Blood Marrow Transplant,* 18**,** 1517-24.

INAZAWA, N., HORI, T., HATAKEYAMA, N., YAMAMOTO, M., YOTO, Y., NOJIMA, M., SUZUKI, N., SHIMIZU, N. & TSUTSUMI, H. 2015. Large-scale multiplex polymerase chain reaction assay for diagnosis of viral reactivations after allogeneic hematopoietic stem cell transplantation. *J Med Virol,* 87**,** 1427-35.

ISOLA, M., CABRAS, T., INZITARI, R., LANTINI, M. S., PROTO, E., COSSU, M. & RIVA, A. 2008. Electron microscopic detection of statherin in secretory granules of human major salivary glands. *J Anat,* 212**,** 664-8.

IZADPANAH, A. & GALLO, R. L. 2005. Antimicrobial peptides. *J Am Acad Dermatol,* 52**,** 381-90; quiz 391-2.

JAGASIA, M. H., GREINIX, H. T., ARORA, M., WILLIAMS, K. M., WOLFF, D., COWEN, E. W., PALMER, J., WEISDORF, D., TREISTER, N. S., CHENG, G. S., KERR, H., STRATTON, P., DUARTE, R. F., MCDONALD, G. B., INAMOTO, Y., VIGORITO, A., ARAI, S., DATILES, M. B., JACOBSOHN, D., HELLER, T., KITKO, C. L., MITCHELL, S. A., MARTIN, P. J., SHULMAN, H., WU, R. S., CUTLER, C. S., VOGELSANG, G. B., LEE, S. J., PAVLETIC, S. Z. & FLOWERS, M. E. 2015. National Institutes of Health Consensus Development Project on Criteria for Clinical Trials in Chronic Graft-versus-Host Disease: I. The 2014 Diagnosis and Staging Working Group report. *Biol Blood Marrow Transplant,* 21**,** 389-401.e1.

JAKOB, M., HEMEDA, H., BRUDEREK, K., H GERSTNER, A. O., BOOTZ, F., LANG, S. & BRANDAU, S. 2013. Comparative functional cell biological analysis of mesenchymal stem cells of the head and neck region: potential impact on wound healing, trauma, and infection. *Head Neck,* 35**,** 1621-9.

JAKOB, M., HEMEDA, H., JANESCHIK, S., BOOTZ, F., ROTTER, N., LANG, S. & BRANDAU, S. 2010. Human nasal mucosa contains tissue-resident immunologically responsive mesenchymal stromal cells. *Stem Cells Dev,* 19**,** 635-44.

JANEWAY, C., TRAVER, P., WALPORT, M. & SCHLOMCHIK, M. 2005. *Immunobiology: The Immune System in Health and Disease,* UK, Thomas Publishing Services.

JANZ, D. R., BASTARACHE, J. A., SILLS, G., WICKERSHAM, N., MAY, A. K., BERNARD, G. R. & WARE, L. B. 2013. Association between haptoglobin, hemopexin and mortality in adults with sepsis. *Crit Care,* 17**,** R272.

JENQ, R. R., UBEDA, C., TAUR, Y., MENEZES, C. C., KHANIN, R., DUDAKOV, J. A., LIU, C., WEST, M. L., SINGER, N. V., EQUINDA, M. J., GOBOURNE, A., LIPUMA, L., YOUNG, L. F., SMITH, O. M., GHOSH, A., HANASH, A. M.,

GOLDBERG, J. D., AOYAMA, K., BLAZAR, B. R., PAMER, E. G. & VAN DEN BRINK, M. R. 2012. Regulation of intestinal inflammation by microbiota following allogeneic bone marrow transplantation. *J Exp Med,* 209**,** 903-11.

JENSSEN, H. & HANCOCK, R. E. 2009. Antimicrobial properties of lactoferrin. *Biochimie,* 91**,** 19-29.

JEON, Y. J., KIM, J., CHO, J. H., CHUNG, H. M. & CHAE, J. I. 2015. Comparative Analysis of Human Mesenchymal Stem Cells Derived from Bone Marrow, Placenta, and Adipose Tissue as Sources of Cell Therapy. *J Cell Biochem,* 117, 1112-1125.

JIN, Z., LI, X. & WAN, Y. 2015. Minireview: nuclear receptor regulation of osteoclast and bone remodeling. *Mol Endocrinol,* 29**,** 172-86.

JOHANSSON, I., BRATT, P., HAY, D. I., SCHLUCKEBIER, S. & STRÖMBERG, N. 2000. Adhesion of Candida albicans, but not Candida krusei, to salivary statherin and mimicking host molecules. *Oral Microbiol Immunol,* 15**,** 112-8.

JOUAN-LANHOUET, S., ARSHAD, M. I., PIQUET-PELLORCE, C., MARTIN-CHOULY, C., LE MOIGNE-MULLER, G., VAN HERREWEGHE, F., TAKAHASHI, N., SERGENT, O., LAGADIC-GOSSMANN, D., VANDENABEELE, P., SAMSON, M. & DIMANCHE-BOITREL, M. T. 2012. TRAIL induces necroptosis involving RIPK1/RIPK3-dependent PARP-1 activation. *Cell Death Differ,* 19**,** 2003-14.

KALINSKI, P. 2012. Regulation of immune responses by prostaglandin E2. *J Immunol,* 188**,** 21-8.

KANG, D. C., GOPALKRISHNAN, R. V., LIN, L., RANDOLPH, A., VALERIE, K., PESTKA, S. & FISHER, P. B. 2004. Expression analysis and genomic characterization of human melanoma differentiation associated gene-5, mda-5: a novel type I interferon-responsive apoptosis-inducing gene. *Oncogene,* 23**,** 1789-800.

KAPAS, S., PAHAL, K., CRUCHLEY, A. T., HAGI-PAVLI, E. & HINSON, J. P. 2004. Expression of adrenomedullin and its receptors in human salivary tissue. *J Dent Res,* 83**,** 333-7.

KASSEM, A., HENNING, P., KINDLUND, B., LINDHOLM, C. & LERNER, U. H. 2015a. TLR5, a novel mediator of innate immunity-induced osteoclastogenesis and bone loss. *FASEB J,* 29**,** 4449-60.

KASSEM, A., HENNING, P., LUNDBERG, P., SOUZA, P. P., LINDHOLM, C. & LERNER, U. H. 2015b. Porphyromonas gingivalis Stimulates Bone Resorption by Enhancing RANKL (Receptor Activator of NF-κB Ligand) through Activation of Toll-like Receptor 2 in Osteoblasts. *J Biol Chem,* 290**,** 20147-58.

KATAYAMA, N., TAKANO, H., SUGIYAMA, M., TAKIO, S., SAKAI, A., TANAKA, K., KUROIWA, H. & ONO, K. 2003. Effects of antibiotics that inhibit the bacterial peptidoglycan synthesis pathway on moss chloroplast division. *Plant Cell Physiol,* 44**,** 776-81.

KAWAMURA, Y. & KAMIYA, Y. 2012. Metagenomic analysis permitting identification of the minority bacterial populations in the oral microbiota. *Journal of Oral Biosciences,* 54**,** 132-137.

KEDIA, S., ACHARYA, P., MOHAMMAD, F., NGUYEN, H., ASTI, D., MEHTA, S., PANT, M. & MOBARAKAI, N. 2013. Infectious Complications of Hematopoietic Stem Cell Transplantation. *Stem Cell Research & Therapy,* 83.

KHUNG, R., SHIBA, H., KAJIYA, M., KITTAKA, M., OUHARA, K., TAKEDA, K., MIZUNO, N., FUJITA, T., KOMATSUZAWA, H. & KURIHARA, H. 2014. LL37 induces VEGF expression in dental pulp cells through ERK signalling. *Int Endod J*.

KHURSHID, Z., NASEEM, M., SHEIKH, Z., SHAHAB, S. & ZAFAE, M. 2015. Oral antimicrobial peptides: Types and role in the oral cavity. *Saudi Pharmaceutical Journal,* In Press, doi:10.1016/j.jsps.2015.02.015.

KIM, J. & HEMATTI, P. 2009. Mesenchymal stem cell-educated macrophages: a novel type of alternatively activated macrophages. *Exp Hematol,* 37**,** 1445-53.

KIM, M. H., GRANICK, J. L., KWOK, C., WALKER, N. J., BORJESSON, D. L., CURRY, F. R., MILLER, L. S. & SIMON, S. I. 2011. Neutrophil survival and c-kit(+)-progenitor proliferation in Staphylococcus aureus-infected skin wounds promote resolution. *Blood,* 117**,** 3343-52.

KITTAKA, M., SHIBA, H., KAJIYA, M., OUHARA, K., TAKEDA, K., KANBARA, K., FUJITA, T., KAWAGUCHI, H., KOMATSUZAWA, H. & KURIHARA, H. 2013. Antimicrobial peptide LL37 promotes vascular endothelial growth factor-A expression in human periodontal ligament cells. *J Periodontal Res,* 48**,** 228-34.

KOCHAŃSKA, B., KEDZIA, A., KAMYSZ, W., MAĆKIEWICZ, Z. & KUPRYSZEWSKI, G. 2000. The effect of statherin and its shortened analogues on anaerobic bacteria isolated from the oral cavity. *Acta Microbiol Pol,* 49**,** 243-51.

KOLACZKOWSKA, E. & KUBES, P. 2013. Neutrophil recruitment and function in health and inflammation. *Nat Rev Immunol,* 13**,** 159-75.

KONERMANN, A., BEYER, M., DESCHNER, J., ALLAM, J. P., NOVAK, N., WINTER, J., JEPSEN, S. & JÄGER, A. 2012. Human periodontal ligament cells facilitate leukocyte recruitment and are influenced in their immunomodulatory function by Th17 cytokine release. *Cell Immunol,* 272**,** 137-43.

KORDELAS, L., REBMANN, V., LUDWIG, A. K., RADTKE, S., RUESING, J., DOEPPNER, T. R., EPPLE, M., HORN, P. A., BEELEN, D. W. & GIEBEL, B. 2014. MSC-derived exosomes: a novel tool to treat therapy-refractory graft-versus-host disease. *Leukemia,* 28**,** 970-3.

KRAITCHMAN, D. L., TATSUMI, M., GILSON, W. D., ISHIMORI, T., KEDZIOREK, D., WALCZAK, P., SEGARS, W. P., CHEN, H. H., FRITZGES, D., IZBUDAK, I., YOUNG, R. G., MARCELINO, M., PITTENGER, M. F., SOLAIYAPPAN, M., BOSTON, R. C., TSUI, B. M., WAHL, R. L. & BULTE, J. W. 2005. Dynamic imaging of allogeneic mesenchymal stem cells trafficking to myocardial infarction. *Circulation,* 112**,** 1451-61.

KRAMPERA, M., PASINI, A., PIZZOLO, G., COSMI, L., ROMAGNANI, S. & ANNUNZIATO, F. 2006. Regenerative and immunomodulatory potential of mesenchymal stem cells. *Curr Opin Pharmacol,* 6**,** 435-41.

KRASNODEMBSKAYA, A., SAMARANI, G., SONG, Y., ZHUO, H., SU, X., LEE, J. W., GUPTA, N., PETRINI, M. & MATTHAY, M. A. 2012. Human mesenchymal stem cells reduce mortality and bacteremia in gram-negative sepsis in mice in part by enhancing the phagocytic activity of blood monocytes. *Am J Physiol Lung Cell Mol Physiol,* 302**,** L1003-13.

KRASNODEMBSKAYA, A., SONG, Y., FANG, X., GUPTA, N., SERIKOV, V., LEE, J. W. & MATTHAY, M. A. 2010. Antibacterial effect of human mesenchymal

stem cells is mediated in part from secretion of the antimicrobial peptide LL-37. *Stem Cells,* 28**,** 2229-38.

KULKARNI, S., SITARU, C., JAKUS, Z., ANDERSON, K. E., DAMOULAKIS, G., DAVIDSON, K., HIROSE, M., JUSS, J., OXLEY, D., CHESSA, T. A., RAMADANI, F., GUILLOU, H., SEGONDS-PICHON, A., FRITSCH, A., JARVIS, G. E., OKKENHAUG, K., LUDWIG, R., ZILLIKENS, D., MOCSAI, A., VANHAESEBROECK, B., STEPHENS, L. R. & HAWKINS, P. T. 2011. PI3Kβ plays a critical role in neutrophil activation by immune complexes. *Sci Signal,* 4**,** ra23.

KURT-JONES, E. A., POPOVA, L., KWINN, L., HAYNES, L. M., JONES, L. P., TRIPP, R. A., WALSH, E. E., FREEMAN, M. W., GOLENBOCK, D. T., ANDERSON, L. J. & FINBERG, R. W. 2000. Pattern recognition receptors TLR4 and CD14 mediate response to respiratory syncytial virus. *Nat Immunol,* 1**,** 398-401.

KUSADASI, N. & GROENEVELD, A. B. 2013. A perspective on mesenchymal stromal cell transplantation in the treatment of sepsis. *Shock,* 40**,** 352-7.

LABISCHINSKI, H., GOODELL, E. W., GOODELL, A. & HOCHBERG, M. L. 1991. Direct proof of a "more-than-single-layered" peptidoglycan architecture of Escherichia coli W7: a neutron small-angle scattering study. *J Bacteriol,* 173**,** 751-6.

LE BLANC, K., FRASSONI, F., BALL, L., LOCATELLI, F., ROELOFS, H., LEWIS, I., LANINO, E., SUNDBERG, B., BERNARDO, M. E., REMBERGER, M., DINI, G., EGELER, R. M., BACIGALUPO, A., FIBBE, W., RINGDÉN, O. & TRANSPLANTATION, D. C. O. T. E. G. F. B. A. M. 2008. Mesenchymal stem cells for treatment of steroid-resistant, severe, acute graft-versus-host disease: a phase II study. *Lancet,* 371**,** 1579-86.

LE BLANC, K., RASMUSSON, I., GÖTHERSTRÖM, C., SEIDEL, C., SUNDBERG, B., SUNDIN, M., ROSENDAHL, K., TAMMIK, C. & RINGDÉN, O. 2004. Mesenchymal stem cells inhibit the expression of CD25 (interleukin-2 receptor) and CD38 on phytohaemagglutinin-activated lymphocytes. *Scand J Immunol,* 60**,** 307-15.

LE BLANC, K., TAMMIK, L., SUNDBERG, B., HAYNESWORTH, S. E. & RINGDÉN, O. 2003. Mesenchymal stem cells inhibit and stimulate mixed lymphocyte cultures and mitogenic responses independently of the major histocompatibility complex. *Scand J Immunol,* 57**,** 11-20.

LEE, J. H., LIM, G. Y., IM, S. A., CHUNG, N. G. & HAHN, S. T. 2008. Gastrointestinal complications following hematopoietic stem cell transplantation in children. *Korean J Radiol,* 9**,** 449-57.

LEE, J. W., FANG, X., KRASNODEMBSKAYA, A., HOWARD, J. P. & MATTHAY, M. A. 2011. Concise review: Mesenchymal stem cells for acute lung injury: role of paracrine soluble factors. *Stem Cells,* 29**,** 913-9.

LEE, J. W., KRASNODEMBSKAYA, A., MCKENNA, D. H., SONG, Y., ABBOTT, J. & MATTHAY, M. A. 2013. Therapeutic effects of human mesenchymal stem cells in ex vivo human lungs injured with live bacteria. *Am J Respir Crit Care Med,* 187**,** 751-60.

LEE, S. H. & BAEK, D. H. 2012. Antibacterial and neutralizing effect of human β-defensins on Enterococcus faecalis and Enterococcus faecalis lipoteichoic acid. *J Endod,* 38**,** 351-6.

LERNER, U. H. 2004. NEW MOLECULES IN THE TUMOR NECROSIS FACTOR LIGAND AND RECEPTOR SUPERFAMILIES WITH IMPORTANCE FOR PHYSIOLOGICAL AND PATHOLOGICAL BONE RESORPTION. *Crit Rev Oral Biol Med,* 15**,** 64-81.

LEÓN, B., LÓPEZ-BRAVO, M. & ARDAVÍN, C. 2007. Monocyte-derived dendritic cells formed at the infection site control the induction of protective T helper 1 responses against Leishmania. *Immunity,* 26**,** 519-31.

LIMA, A., ZUNINO, P., D'ALESSANDRO, B. & PICCINI, C. 2007. An iron-regulated outer-membrane protein of Proteus mirabilis is a haem receptor that plays an important role in urinary tract infection and in in vivo growth. *J Med Microbiol,* 56**,** 1600-7.

LINDE, V., BJØRN, S., KASTRUP, J. S. & FLODGAARD, H. 2000. Lipopolysaccharide affinity measurement by scintillation proximity assay: application to human heparin binding protein. *Biotechniques,* 28**,** 218-20, 222.

LIU, D., XU, J. K., FIGLIOMENI, L., HUANG, L., PAVLOS, N. J., ROGERS, M., TAN, A., PRICE, P. & ZHENG, M. H. 2003. Expression of RANKL and OPG mRNA in periodontal disease: possible involvement in bone destruction. *Int J Mol Med,* 11**,** 17-21.

LOISEAU, P., BUSSON, M., BALERE, M. L., DORMOY, A., BIGNON, J. D., GAGNE, K., GEBUHRER, L., DUBOIS, V., JOLLET, I., BOIS, M., PERRIER, P., MASSON, D., MOINE, A., ABSI, L., REVIRON, D., LEPAGE, V., TAMOUZA, R., TOUBERT, A., MARRY, E., CHIR, Z., JOUET, J. P., BLAISE, D., CHARRON, D. & RAFFOUX, C. 2007. HLA Association with hematopoietic stem cell transplantation outcome: the number of mismatches at HLA-A, -B, -C, -DRB1, or -DQB1 is strongly associated with overall survival. *Biol Blood Marrow Transplant,* 13**,** 965-74.

LOMBARDO, E., VAN DER POLL, T., DELAROSA, O. & DALEMANS, W. 2015. Mesenchymal stem cells as a therapeutic tool to treat sepsis. *World J Stem Cells,* 7**,** 368-79.

LOVERING, A. L., SAFADI, S. S. & STRYNADKA, N. C. 2012. Structural perspective of peptidoglycan biosynthesis and assembly. *Annu Rev Biochem,* 81**,** 451-78.

LUCCHINI, G., INTRONA, M., DANDER, E., ROVELLI, A., BALDUZZI, A., BONANOMI, S., SALVADÈ, A., CAPELLI, C., BELOTTI, D., GAIPA, G., PERSEGHIN, P., VINCI, P., LANINO, E., CHIUSOLO, P., OROFINO, M. G., MARKTEL, S., GOLAY, J., RAMBALDI, A., BIONDI, A., D'AMICO, G. & BIAGI, E. 2010. Platelet-lysate-expanded mesenchymal stromal cells as a salvage therapy for severe resistant graft-versus-host disease in a pediatric population. *Biol Blood Marrow Transplant,* 16**,** 1293-301.

LUNDY, F. T., O'HARE, M. M., MCKIBBEN, B. M., FULTON, C. R., BRIGGS, J. E. & LINDEN, G. J. 2006. Radioimmunoassay quantification of adrenomedullin in human gingival crevicular fluid. *Arch Oral Biol,* 51**,** 334-8.

LUQUE-ORTEGA, J. R., VAN'T HOF, W., VEERMAN, E. C., SAUGAR, J. M. & RIVAS, L. 2008. Human antimicrobial peptide histatin 5 is a cell-penetrating peptide targeting mitochondrial ATP synthesis in Leishmania. *FASEB J,* 22**,** 1817-28.

LÖNNERDAL, B. 2003. Nutritional and physiologic significance of human milk proteins. *Am J Clin Nutr,* 77**,** 1537S-1543S.

MAHANONDA, R., SA-ARD-IAM, N., MONTREEKACHON, P., PIMKHAOKHAM, A., YONGVANICHIT, K., FUKUDA, M. M. & PICHYANGKUL, S. 2007. IL-8 and

IDO expression by human gingival fibroblasts via TLRs. *J Immunol,* 178**,** 1151-7.

MAJORS, A. K., BOEHM, C. A., NITTO, H., MIDURA, R. J. & MUSCHLER, G. F. 1997. Characterization of human bone marrow stromal cells with respect to osteoblastic differentiation. *J Orthop Res,* 15**,** 546-57.

MARGAIX-MUÑOZ, M., BAGÁN, J. V., JIMÉNEZ, Y., SARRIÓN, M. G. & POVEDA-RODA, R. 2015. Graft-versus-host disease affecting oral cavity. A review. *J Clin Exp Dent,* 7**,** e138-45.

MARKOWSKI, J., HELBIG, G., WIDZISZOWSKA, A., LIKUS, W., KYRCZ-KRZEMIEŃ, S., JAROSZ, U., DZIUBDZIELA, W. & MARKIEWICZ, M. 2015. Fungal colonization of the respiratory tract in allogeneic and autologous hematopoietic stem cell transplant recipients: a study of 573 transplanted patients. *Med Sci Monit,* 21**,** 1173-80.

MARTIN, P. J. 2008. Biology of chronic graft-versus-host disease: implications for a future therapeutic approach. *Keio J Med,* 57**,** 177-83.

MARTIN, P. J., LEE, S. J., PRZEPIORKA, D., HOROWITZ, M. M., KORETH, J., VOGELSANG, G. B., WALKER, I., CARPENTER, P. A., GRIFFITH, L. M., AKPEK, G., MOHTY, M., WOLFF, D., PAVLETIC, S. Z. & CUTLER, C. S. 2015. National Institutes of Health Consensus Development Project on Criteria for Clinical Trials in Chronic Graft-versus-Host Disease: VI. The 2014 Clinical Trial Design Working Group Report. *Biol Blood Marrow Transplant,* 21**,** 1343-59.

MARTIN, P. J., RIZZO, J. D., WINGARD, J. R., BALLEN, K., CURTIN, P. T., CUTLER, C., LITZOW, M. R., NIETO, Y., SAVANI, B. N., SCHRIBER, J. R., SHAUGHNESSY, P. J., WALL, D. A. & CARPENTER, P. A. 2012. First- and second-line systemic treatment of acute graft-versus-host disease: recommendations of the American Society of Blood and Marrow Transplantation. *Biol Blood Marrow Transplant,* 18**,** 1150-63.

MARTINON, F., BURNS, K. & TSCHOPP, J. 2002. The inflammasome: a molecular platform triggering activation of inflammatory caspases and processing of proIL-beta. *Mol Cell,* 10**,** 417-26.

MATSUZAWA, T., KIM, B. H., SHENOY, A. R., KAMITANI, S., MIYAKE, M. & MACMICKING, J. D. 2012. IFN-γ elicits macrophage autophagy via the p38 MAPK signaling pathway. *J Immunol,* 189**,** 813-8.

MAYR, F. B., YENDE, S. & ANGUS, D. C. 2014. Epidemiology of severe sepsis. *Virulence,* 5**,** 4-11.

MAYS, J. W., FASSIL, H., EDWARDS, D. A., PAVLETIC, S. Z. & BASSIM, C. W. 2013. Oral chronic graft-versus-host disease: current pathogenesis, therapy, and research. *Oral Dis,* 19**,** 327-46.

MCCLURE, R. & MASSARI, P. 2014. TLR-Dependent Human Mucosal Epithelial Cell Responses to Microbial Pathogens. *Front Immunol,* 5**,** 386.

MEISEL, R., BROCKERS, S., HESELER, K., DEGISTIRICI, O., BÜLLE, H., WOITE, C., STUHLSATZ, S., SCHWIPPERT, W., JÄGER, M., SORG, R., HENSCHLER, R., SEISSLER, J., DILLOO, D. & DÄUBENER, W. 2011. Human but not murine multipotent mesenchymal stromal cells exhibit broad-spectrum antimicrobial effector function mediated by indoleamine 2,3-dioxygenase. *Leukemia,* 25**,** 648-54.

MEISEL, R., ZIBERT, A., LARYEA, M., GÖBEL, U., DÄUBENER, W. & DILLOO, D. 2004. Human bone marrow stromal cells inhibit allogeneic T-cell responses by indoleamine 2,3-dioxygenase-mediated tryptophan degradation. *Blood,* 103**,** 4619-21.

MELIEF, S. M., GEUTSKENS, S. B., FIBBE, W. E. & ROELOFS, H. 2013. Multipotent stromal cells skew monocytes towards an anti-inflammatory interleukin-10-producing phenotype by production of interleukin-6. *Haematologica,* 98**,** 888-95.

MEZEY, E. 2011. The therapeutic potential of bone marrow-derived stromal cells. *J Cell Biochem,* 112**,** 2683-7.

MICHAEL, R., OTTO, C., LENFERINK, A., GELPI, E., MONTENEGRO, G. A., ROSANDIĆ, J., TRESSERRA, F., BARRAQUER, R. I. & VRENSEN, G. F. 2014. Absence of amyloid-beta in lenses of Alzheimer patients: a confocal Raman microspectroscopic study. *Exp Eye Res,* 119**,** 44-53.

MOFFA, E. B., MUSSI, M. C., XIAO, Y., GARRIDO, S. S., MACHADO, M. A., GIAMPAOLO, E. T. & SIQUEIRA, W. L. 2015. Histatin 5 inhibits adhesion of C. albicans to Reconstructed Human Oral Epithelium. *Front Microbiol,* 6**,** 885.

MOGI, M., OTOGOTO, J., OTA, N. & TOGARI, A. 2004. Differential expression of RANKL and osteoprotegerin in gingival crevicular fluid of patients with periodontitis. *J Dent Res,* 83**,** 166-9.

MONSEL, A., ZHU, Y. G., GENNAI, S., HAO, Q., HU, S., ROUBY, J. J., ROSENZWAJG, M., MATTHAY, M. A. & LEE, J. W. 2015. Therapeutic Effects of Human Mesenchymal Stem Cell-derived Microvesicles in Severe Pneumonia in Mice. *Am J Respir Crit Care Med,* 192**,** 324-36.

MONTASSIER, E., BATARD, E., MASSART, S., GASTINNE, T., CARTON, T., CAILLON, J., LE FRESNE, S., CAROFF, N., HARDOUIN, J., MOREAU, P., POTEL, G., LE VACON, F. & DE LA COCHETIÈRE, M. 2014. 16S rRNA gene pyrosequencing reveals shift in patient faecal microbiota during high-dose chemotherapy as conditioning regimen for bone marrow transplantation. *Microbial ecology,* 67.

MORAES, T. J. & DOWNEY, G. P. 2003. Neutrophil cell signaling in infection: role of phosphatidylinositide 3-kinase. *Microbes Infect,* 5**,** 1293-8.

MOSHEIMER, B. A., KANEIDER, N. C., FEISTRITZER, C., DJANANI, A. M., STURN, D. H., PATSCH, J. R. & WIEDERMANN, C. J. 2005. Syndecan-1 is involved in osteoprotegerin-induced chemotaxis in human peripheral blood monocytes. *J Clin Endocrinol Metab,* 90**,** 2964-71.

MUNN, D. H., SHAFIZADEH, E., ATTWOOD, J. T., BONDAREV, I., PASHINE, A. & MELLOR, A. L. 1999. Inhibition of T cell proliferation by macrophage tryptophan catabolism. *J Exp Med,* 189**,** 1363-72.

NADERI, E. H., SKAH, S., UGLAND, H., MYKLEBOST, O., SANDNES, D. L., TORGERSEN, M. L., JOSEFSEN, D., RUUD, E., NADERI, S. & BLOMHOFF, H. K. 2015. Bone marrow stroma-derived PGE2 protects BCP-ALL cells from DNA damage-induced p53 accumulation and cell death. *Mol Cancer,* 14**,** 14.

NAKAJIMA, H., UCHIDA, K., GUERRERO, A. R., WATANABE, S., SUGITA, D., TAKEURA, N., YOSHIDA, A., LONG, G., WRIGHT, K. T., JOHNSON, W. E. & BABA, H. 2012. Transplantation of mesenchymal stem cells promotes an alternative pathway of macrophage activation and functional recovery after spinal cord injury. *J Neurotrauma,* 29**,** 1614-25.

NG, K. P., KUAN, C. S., KAUR, H., NA, S. L., ATIYA, N. & VELAYUTHAN, R. D. 2015. Candida species epidemiology 2000-2013: a laboratory-based report. *Trop Med Int Health,* 20**,** 1447-1453.

NGKELO, A., MEJA, K., YEADON, M., ADCOCK, I. & KIRKHAM, P. A. 2012. LPS induced inflammatory responses in human peripheral blood mononuclear cells is mediated through NOX4 and Giα dependent PI-3kinase signalling. *J Inflamm (Lond),* 9**,** 1.

NIGORIKAWA, K., HAZEKI, K., KUMAZAWA, T., ITOH, Y., HOSHI, M. & HAZEKI, O. 2012. Class-IA phosphoinositide 3-kinase p110β Triggers GPCR-induced superoxide production in p110γ-deficient murine neutrophils. *J Pharmacol Sci,* 120**,** 270-9.

NISAPAKULTORN, K., MAKRUDTHONG, J., SA-ARD-IAM, N., RERKYEN, P., MAHANONDA, R. & TAKIKAWA, O. 2009. Indoleamine 2,3-dioxygenase expression and regulation in chronic periodontitis. *J Periodontol,* 80**,** 114-21.

NISHIDA, S., ENDO, N., YAMAGIWA, H., TANIZAWA, T. & TAKAHASHI, H. E. 1999. Number of osteoprogenitor cells in human bone marrow markedly decreases after skeletal maturation. *J Bone Miner Metab,* 17**,** 171-7.

NORDER GRUSELL, E., DAHLÉN, G., RUTH, M., NY, L., QUIDING-JÄRBRINK, M., BERGQUIST, H. & BOVE, M. 2013. Bacterial flora of the human oral cavity, and the upper and lower esophagus. *Dis Esophagus,* 26**,** 84-90.

NÉMETH, K., LEELAHAVANICHKUL, A., YUEN, P. S., MAYER, B., PARMELEE, A., DOI, K., ROBEY, P. G., LEELAHAVANICHKUL, K., KOLLER, B. H., BROWN, J. M., HU, X., JELINEK, I., STAR, R. A. & MEZEY, E. 2009. Bone marrow stromal cells attenuate sepsis via prostaglandin E(2)-dependent reprogramming of host macrophages to increase their interleukin-10 production. *Nat Med,* 15**,** 42-9.

O'CONNOR, J. C., LAWSON, M. A., ANDRÉ, C., MOREAU, M., LESTAGE, J., CASTANON, N., KELLEY, K. W. & DANTZER, R. 2009. Lipopolysaccharide-induced depressive-like behavior is mediated by indoleamine 2,3-dioxygenase activation in mice. *Mol Psychiatry,* 14**,** 511-22.

OSHITA, K., YAMAOKA, K., UDAGAWA, N., FUKUYO, S., SONOMOTO, K., MAESHIMA, K., KURIHARA, R., NAKANO, K., SAITO, K., OKADA, Y., CHIBA, K. & TANAKA, Y. 2011. Human mesenchymal stem cells inhibit osteoclastogenesis through osteoprotegerin production. *Arthritis Rheum,* 63**,** 1658-67.

PANDA, S., EL KHADER, I., CASELLAS, F., LÓPEZ VIVANCOS, J., GARCÍA CORS, M., SANTIAGO, A., CUENCA, S., GUARNER, F. & MANICHANH, C. 2014. Short-term effect of antibiotics on human gut microbiota. *PLoS One,* 9**,** e95476.

PARAHITIYAWA, N. B., SCULLY, C., LEUNG, W. K., YAM, W. C., JIN, L. J. & SAMARANAYAKE, L. P. 2010. Exploring the oral bacterial flora: current status and future directions. *Oral Dis,* 16**,** 136-45.

PARK, J. Y., PILLINGER, M. H. & ABRAMSON, S. B. 2006. Prostaglandin E2 synthesis and secretion: the role of PGE2 synthases. *Clin Immunol,* 119**,** 229-40.

PASSLICK, B., FLIEGER, D. & ZIEGLER-HEITBROCK, H. W. 1989. Identification and characterization of a novel monocyte subpopulation in human peripheral blood. *Blood,* 74**,** 2527-34.

PASSWEG, J. R., BALDOMERO, H., PETERS, C., GASPAR, H. B., CESARO, S., DREGER, P., DUARTE, R. F., FALKENBURG, J. H., FARGE-BANCEL, D., GENNERY, A., HALTER, J., KRÖGER, N., LANZA, F., MARSH, J., MOHTY, M., SUREDA, A., VELARDI, A., MADRIGAL, A. & EBMT, E. S. F. B. A. M. T. 2014. Hematopoietic SCT in Europe: data and trends in 2012 with special consideration of pediatric transplantation. *Bone Marrow Transplant,* 49**,** 744-50.

PATEL, P. K., ERLANDSEN, J. E., KIRKPATRICK, W. R., BERG, D. K., WESTBROOK, S. D., LOUDEN, C., CORNELL, J. E., THOMPSON, G. R., VALLOR, A. C., WICKES, B. L., WIEDERHOLD, N. P., REDDING, S. W. & PATTERSON, T. F. 2012. The Changing Epidemiology of Oropharyngeal Candidiasis in Patients with HIV/AIDS in the Era of Antiretroviral Therapy. *AIDS Res Treat,* 2012**,** 262471.

PAVLETIC, S. Z., SMITH, L. M., BISHOP, M. R., LYNCH, J. C., TARANTOLO, S. R., VOSE, J. M., BIERMAN, P. J., HADI, A., ARMITAGE, J. O. & KESSINGER, A. 2005. Prognostic factors of chronic graft-versus-host disease after allogeneic blood stem-cell transplantation. *Am J Hematol,* 78**,** 265-74.

PESCHEL, A. & SAHL, H. G. 2006. The co-evolution of host cationic antimicrobial peptides and microbial resistance. *Nat Rev Microbiol,* 4**,** 529-36.

PISANO, E., CABRAS, T., MONTALDO, C., PIRAS, V., INZITARI, R., OLMI, C., CASTAGNOLA, M. & MESSANA, I. 2005. Peptides of human gingival crevicular fluid determined by HPLC-ESI-MS. *Eur J Oral Sci,* 113**,** 462-8.

POLAK, G., BARCZYŃSKI, B., BEDNAREK, W., KWAŚNIEWSKI, W., WERTELL, I., DEREWIANKA-POLAK, M., MAKARA-STUDZIŃSKA, M. & KOTARSKI, J. 2015. Increased levels of proteins of the acute inflammatory phase in the peritoneal fluid of women with advanced stages of endometriosis. *Ginekol Pol,* 86**,** 414-8.

PRESHAW, P. M. & HEASMAN, P. A. 2002. Prostaglandin E2 concentrations in gingival crevicular fluid: observations in untreated chronic periodontitis. *J Clin Periodontol,* 29**,** 15-20.

PÜTSEP, K., CARLSSON, G., BOMAN, H. G. & ANDERSSON, M. 2002. Deficiency of antibacterial peptides in patients with morbus Kostmann: an observation study. *Lancet,* 360**,** 1144-9.

RAFEI, M., HSIEH, J., FORTIER, S., LI, M., YUAN, S., BIRMAN, E., FORNER, K., BOIVIN, M. N., DOODY, K., TREMBLAY, M., ANNABI, B. & GALIPEAU, J. 2008. Mesenchymal stromal cell-derived CCL2 suppresses plasma cell immunoglobulin production via STAT3 inactivation and PAX5 induction. *Blood,* 112**,** 4991-8.

RAFFAGHELLO, L., BIANCHI, G., BERTOLOTTO, M., MONTECUCCO, F., BUSCA, A., DALLEGRI, F., OTTONELLO, L. & PISTOIA, V. 2008. Human mesenchymal stem cells inhibit neutrophil apoptosis: a model for neutrophil preservation in the bone marrow niche. *Stem Cells,* 26**,** 151-62.

RAMACHANDRAN, G. 2014. Gram-positive and gram-negative bacterial toxins in sepsis: a brief review. *Virulence,* 5**,** 213-8.

REBELATTO, C. K., AGUIAR, A. M., MORETÃO, M. P., SENEGAGLIA, A. C., HANSEN, P., BARCHIKI, F., OLIVEIRA, J., MARTINS, J., KULIGOVSKI, C., MANSUR, F., CHRISTOFIS, A., AMARAL, V. F., BROFMAN, P. S., GOLDENBERG, S., NAKAO, L. S. & CORREA, A. 2008. Dissimilar

differentiation of mesenchymal stem cells from bone marrow, umbilical cord blood, and adipose tissue. *Exp Biol Med (Maywood),* 233**,** 901-13.

RIESER, C., BÖCK, G., KLOCKER, H., BARTSCH, G. & THURNHER, M. 1997. Prostaglandin E2 and Tumor Necrosis Factor α Cooperate to Activate Human Dendritic Cells: Synergistic Activation of Interleukin 12 Production. *Journal of Experimental Medicine,* 186**,** 1603-1608.

RINGDÉN, O., UZUNEL, M., RASMUSSON, I., REMBERGER, M., SUNDBERG, B., LÖNNIES, H., MARSCHALL, H. U., DLUGOSZ, A., SZAKOS, A., HASSAN, Z., OMAZIC, B., ASCHAN, J., BARKHOLT, L. & LE BLANC, K. 2006. Mesenchymal stem cells for treatment of therapy-resistant graft-versus-host disease. *Transplantation,* 81**,** 1390-7.

RUBINCHIK, E., DUGOURD, D., ALGARA, T., PASETKA, C. & FRIEDLAND, H. D. 2009. Antimicrobial and antifungal activities of a novel cationic antimicrobial peptide, omiganan, in experimental skin colonisation models. *Int J Antimicrob Agents,* 34**,** 457-61.

RYAN, J. M., BARRY, F., MURPHY, J. M. & MAHON, B. P. 2007. Interferon-gamma does not break, but promotes the immunosuppressive capacity of adult human mesenchymal stem cells. *Clin Exp Immunol,* 149**,** 353-63.

RYBTKE, M., HULTQVIST, L. D., GIVSKOV, M. & TOLKER-NIELSEN, T. 2015. Pseudomonas aeruginosa Biofilm Infections: Community Structure, Antimicrobial Tolerance and Immune Response. *J Mol Biol,* 427, 3628-45.

SADRZADEH, S. M. & BOZORGMEHR, J. 2004. Haptoglobin phenotypes in health and disorders. *Am J Clin Pathol,* 121 Suppl**,** S97-104.

SAITO, A., MOTOMURA, N., KAKIMI, K., NARUI, K., NOGUCHI, N., SASATSU, M., KUBO, K., KOEZUKA, Y., TAKAI, D., UEHA, S. & TAKAMOTO, S. 2008. Vascular allografts are resistant to methicillin-resistant Staphylococcus aureus through indoleamine 2,3-dioxygenase in a murine model. *J Thorac Cardiovasc Surg,* 136**,** 159-67.

SAKAKI-YUMOTO, M., KATSUNO, Y. & DERYNCK, R. 2013. TGF-β family signaling in stem cells. *Biochim Biophys Acta,* 1830**,** 2280-96.

SANDRA, F., HENDARMIN, L. & NAKAMURA, S. 2006. Osteoprotegerin (OPG) binds with tumor necrosis factor-related apoptosis-inducing ligand (TRAIL): suppression of TRAIL-induced apoptosis in ameloblastomas. *Oral Oncol,* 42**,** 415-20.

SAWAKI, K., MIZUKAWA, N., YAMAAI, T., FUKUNAGA, J. & SUGAHARA, T. 2002. Immunohistochemical study on expression of alpha-defensin and beta-defensin-2 in human buccal epithelia with candidiasis. *Oral Dis,* 8**,** 37-41.

SCANNAPIECO, F. A. & HO, A. W. 2001. Potential associations between chronic respiratory disease and periodontal disease: analysis of National Health and Nutrition Examination Survey III. *J Periodontol,* 72**,** 50-6.

SCHROEDER, B. O., EHMANN, D., PRECHT, J. C., CASTILLO, P. A., KÜCHLER, R., BERGER, J., SCHALLER, M., STANGE, E. F. & WEHKAMP, J. 2015. Paneth cell α-defensin 6 (HD-6) is an antimicrobial peptide. *Mucosal Immunol,* 8**,** 661-71.

SCHROTEN, H., SPORS, B., HUCKE, C., STINS, M., KIM, K. S., ADAM, R. & DÄUBENER, W. 2001. Potential role of human brain microvascular endothelial cells in the pathogenesis of brain abscess: inhibition of

Staphylococcus aureus by activation of indoleamine 2,3-dioxygenase. *Neuropediatrics,* 32**,** 206-10.

SCHRÖDER, N. W., MORATH, S., ALEXANDER, C., HAMANN, L., HARTUNG, T., ZÄHRINGER, U., GÖBEL, U. B., WEBER, J. R. & SCHUMANN, R. R. 2003. Lipoteichoic acid (LTA) of Streptococcus pneumoniae and Staphylococcus aureus activates immune cells via Toll-like receptor (TLR)-2, lipopolysaccharide-binding protein (LBP), and CD14, whereas TLR-4 and MD-2 are not involved. *J Biol Chem,* 278**,** 15587-94.

SCHÄFFER, C. & MESSNER, P. 2005. The structure of secondary cell wall polymers: how Gram-positive bacteria stick their cell walls together. *Microbiology,* 151**,** 643-51.

SERBINA, N. V., JIA, T., HOHL, T. M. & PAMER, E. G. 2008. Monocyte-mediated defense against microbial pathogens. *Annu Rev Immunol,* 26**,** 421-52.

SERBINA, N. V., SALAZAR-MATHER, T. P., BIRON, C. A., KUZIEL, W. A. & PAMER, E. G. 2003. TNF/iNOS-producing dendritic cells mediate innate immune defense against bacterial infection. *Immunity,* 19**,** 59-70.

SEREZANI, C. H., CHUNG, J., BALLINGER, M. N., MOORE, B. B., ARONOFF, D. M. & PETERS-GOLDEN, M. 2007. Prostaglandin E2 suppresses bacterial killing in alveolar macrophages by inhibiting NADPH oxidase. *Am J Respir Cell Mol Biol,* 37**,** 562-70.

SHACHOR-MEYOUHAS, Y., FESENKO, A., KRA-OZ, Z., ZAIDMAN, I., SZWARCWORT-COHEN, M., SHAFRAN, E. & KASSIS, I. 2015. Human Herpes Virus-6 Following Pediatric Allogeneic Hematopoietic Stem Cell Transplantation. *Isr Med Assoc J,* 17**,** 302-5.

SHEN, J. S., GEOFFROY, V., NESHAT, S., JIA, Z., MELDRUM, A., MEYER, J. M. & POOLE, K. 2005. FpvA-mediated ferric pyoverdine uptake in Pseudomonas aeruginosa: identification of aromatic residues in FpvA implicated in ferric pyoverdine binding and transport. *J Bacteriol,* 187**,** 8511-5.

SHI, C. & PAMER, E. G. 2011. Monocyte recruitment during infection and inflammation. *Nat Rev Immunol,* 11**,** 762-74.

SHIREY, K. A., JUNG, J. Y., MAEDER, G. S. & CARLIN, J. M. 2006. Upregulation of IFN-gamma receptor expression by proinflammatory cytokines influences IDO activation in epithelial cells. *J Interferon Cytokine Res,* 26**,** 53-62.

SICA, A., ERRENI, M., ALLAVENA, P. & PORTA, C. 2015. Macrophage polarization in pathology. *Cell Mol Life Sci,* 72, 4111-26.

SILHAVY, T. J., KAHNE, D. & WALKER, S. 2010. The bacterial cell envelope. *Cold Spring Harb Perspect Biol,* 2**,** a000414.

SILVA, G. K., GUTIERREZ, F. R., GUEDES, P. M., HORTA, C. V., CUNHA, L. D., MINEO, T. W., SANTIAGO-SILVA, J., KOBAYASHI, K. S., FLAVELL, R. A., SILVA, J. S. & ZAMBONI, D. S. 2010. Cutting edge: nucleotide-binding oligomerization domain 1-dependent responses account for murine resistance against Trypanosoma cruzi infection. *J Immunol,* 184**,** 1148-52.

SMITH, J. G., SILVESTRY, M., LINDERT, S., LU, W., NEMEROW, G. R. & STEWART, P. L. 2010. Insight into the mechanisms of adenovirus capsid disassembly from studies of defensin neutralization. *PLoS Pathog,* 6**,** e1000959.

SOARES, A. B., FARIA, P. R., MAGNA, L. A., CORREA, M. E., DE SOUSA, C. A., ALMEIDA, O. P. & CINTRA, M. L. 2005. Chronic GVHD in minor salivary

glands and oral mucosa: histopathological and immunohistochemical evaluation of 25 patients. *J Oral Pathol Med,* 34**,** 368-73.

SOCIÉ, G. & RITZ, J. 2014. Current issues in chronic graft-versus-host disease. *Blood,* 124**,** 374-84.

SOEHNLEIN, O. & LINDBOM, L. 2009. Neutrophil-derived azurocidin alarms the immune system. *J Leukoc Biol,* 85**,** 344-51.

SOKOL, H., PIGNEUR, B., WATTERLOT, L., LAKHDARI, O., BERMÚDEZ-HUMARÁN, L. G., GRATADOUX, J. J., BLUGEON, S., BRIDONNEAU, C., FURET, J. P., CORTHIER, G., GRANGETTE, C., VASQUEZ, N., POCHART, P., TRUGNAN, G., THOMAS, G., BLOTTIÈRE, H. M., DORÉ, J., MARTEAU, P., SEKSIK, P. & LANGELLA, P. 2008. Faecalibacterium prausnitzii is an anti-inflammatory commensal bacterium identified by gut microbiota analysis of Crohn disease patients. *Proc Natl Acad Sci U S A,* 105**,** 16731-6.

SOTIROPOULOU, P. A., PEREZ, S. A., GRITZAPIS, A. D., BAXEVANIS, C. N. & PAPAMICHAIL, M. 2006. Interactions between human mesenchymal stem cells and natural killer cells. *Stem Cells,* 24**,** 74-85.

STENDERUP, K., JUSTESEN, J., CLAUSEN, C. & KASSEM, M. 2003. Aging is associated with decreased maximal life span and accelerated senescence of bone marrow stromal cells. *Bone,* 33**,** 919-26.

STEPHENS, P., DAVIES, K. J., AL-KHATEEB, T., SHEPHERD, J. P. & THOMAS, D. W. 1996. A comparison of the ability of intra-oral and extra-oral fibroblasts to stimulate extracellular matrix reorganization in a model of wound contraction. *J Dent Res,* 75**,** 1358-64.

STEPHENS, P. & GENEVER, P. 2007. Non-epithelial oral mucosal progenitor cell populations. *Oral Dis,* 13**,** 1-10.

STOKES, C. A., ISMAIL, S., DICK, E. P., BENNETT, J. A., JOHNSTON, S. L., EDWARDS, M. R., SABROE, I. & PARKER, L. C. 2011. Role of interleukin-1 and MyD88-dependent signaling in rhinovirus infection. *J Virol,* 85**,** 7912-21.

SU, W. R., ZHANG, Q. Z., SHI, S. H., NGUYEN, A. L. & LE, A. D. 2011. Human gingiva-derived mesenchymal stromal cells attenuate contact hypersensitivity via prostaglandin E2-dependent mechanisms. *Stem Cells,* 29**,** 1849-60.

SUDA, Y., KIM, Y. M., OGAWA, T., YASUI, N., HASEGAWA, Y., KASHIHARA, W., SHIMOYAMA, T., AOYAMA, K., NAGATA, K., TAMURA, T. & KUSUMOTO, S. 2001. Chemical structure and biological activity of a lipid A component from Helicobacter pylori strain 206. *J Endotoxin Res,* 7**,** 95-104.

SUGIMOTO, J., KANEHIRA, T., MIZUGAI, H., CHIBA, I. & MORITA, M. 2006. Relationship between salivary histatin 5 levels and Candida CFU counts in healthy elderly. *Gerodontology,* 23**,** 164-9.

SUMMERS, C., RANKIN, S. M., CONDLIFFE, A. M., SINGH, N., PETERS, A. M. & CHILVERS, E. R. 2010. Neutrophil kinetics in health and disease. *Trends Immunol,* 31**,** 318-24.

SUNDIN, M., RINGDÉN, O., SUNDBERG, B., NAVA, S., GÖTHERSTRÖM, C. & LE BLANC, K. 2007. No alloantibodies against mesenchymal stromal cells, but presence of anti-fetal calf serum antibodies, after transplantation in allogeneic hematopoietic stem cell recipients. *Haematologica,* 92**,** 1208-15.

SUNG, D. K., CHANG, Y. S., SUNG, S. I., YOO, H. S., AHN, S. Y. & PARK, W. S. 2016. Antibacterial effect of mesenchymal stem cells against Escherichia coli

is mediated by secretion of beta-defensin-2 via toll-like receptor 4 signalling. *Cell Microbiol,* 18, 424-36.

SÁNCHEZ-TORRES, C., GARCÍA-ROMO, G. S., CORNEJO-CORTÉS, M. A., RIVAS-CARVALHO, A. & SÁNCHEZ-SCHMITZ, G. 2001. CD16+ and CD16- human blood monocyte subsets differentiate in vitro to dendritic cells with different abilities to stimulate CD4+ T cells. *Int Immunol,* 13**,** 1571-81.

TAKAHASHI, K. & YAMANAKA, S. 2006. Induction of pluripotent stem cells from mouse embryonic and adult fibroblast cultures by defined factors. *Cell,* 126**,** 663-76.

TAKEUCHI, O., HOSHINO, K., KAWAI, T., SANJO, H., TAKADA, H., OGAWA, T., TAKEDA, K. & AKIRA, S. 1999. Differential roles of TLR2 and TLR4 in recognition of gram-negative and gram-positive bacterial cell wall components. *Immunity,* 11**,** 443-51.

TANIDA, T., OKAMOTO, T., OKAMOTO, A., WANG, H., HAMADA, T., UETA, E. & OSAKI, T. 2003. Decreased excretion of antimicrobial proteins and peptides in saliva of patients with oral candidiasis. *J Oral Pathol Med,* 32**,** 586-94.

TAUR, Y., XAVIER, J. B., LIPUMA, L., UBEDA, C., GOLDBERG, J., GOBOURNE, A., LEE, Y. J., DUBIN, K. A., SOCCI, N. D., VIALE, A., PERALES, M. A., JENQ, R. R., VAN DEN BRINK, M. R. & PAMER, E. G. 2012. Intestinal domination and the risk of bacteremia in patients undergoing allogeneic hematopoietic stem cell transplantation. *Clin Infect Dis,* 55**,** 905-14.

TEIXEIRA, V., FEIO, M. J. & BASTOS, M. 2012. Role of lipids in the interaction of antimicrobial peptides with membranes. *Prog Lipid Res,* 51**,** 149-77.

THURNHEER, T., BOSTANCI, N. & BELIBASAKIS, G. N. 2015. Microbial dynamics during conversion from supragingival to subgingival biofilms in an in vitro model. *Mol Oral Microbiol,* 31, 125-35.

TOMIC, S., DJOKIC, J., VASILIJIC, S., VUCEVIC, D., TODOROVIC, V., SUPIC, G. & COLIC, M. 2011. Immunomodulatory properties of mesenchymal stem cells derived from dental pulp and dental follicle are susceptible to activation by toll-like receptor agonists. *Stem Cells Dev,* 20**,** 695-708.

TOMITA, M., BELLAMY, W., TAKASE, M., YAMAUCHI, K., WAKABAYASHI, H. & KAWASE, K. 1991. Potent antibacterial peptides generated by pepsin digestion of bovine lactoferrin. *J Dairy Sci,* 74**,** 4137-42.

TORRES-JUAREZ, F., CARDENAS-VARGAS, A., MONTOYA-ROSALES, A., GONZÁLEZ-CURIEL, I., GARCIA-HERNANDEZ, M. H., ENCISO-MORENO, J. A., HANCOCK, R. E. & RIVAS-SANTIAGO, B. 2015. LL-37 immunomodulatory activity during Mycobacterium tuberculosis infection in macrophages. *Infect Immun,* 83, 4495-503.

TREISTER, N., DUNCAN, C., CUTLER, C. & LEHMANN, L. 2012. How we treat oral chronic graft-versus-host disease. *Blood,* 120**,** 3407-18.

VARIN, A., MUKHOPADHYAY, S., HERBEIN, G. & GORDON, S. 2010. Alternative activation of macrophages by IL-4 impairs phagocytosis of pathogens but potentiates microbial-induced signalling and cytokine secretion. *Blood,* 115**,** 353-62.

VAVILOV, V. N., AVER'IANOVA, M. I. U., BONDARENKO, S. N., STANCHEVA, N. V., ZUBAROVSKAIA, L. S. & AFANAS'EV, B. V. 2015. [Bacterial infections in the early period after allogeneic bone marrow transplantation]. *Ter Arkh,* 87**,** 88-93.

VIEIRA COLOMBO, A. P., MAGALHÃES, C. B., HARTENBACH, F. A., MARTINS DO SOUTO, R. & MACIEL DA SILVA-BOGHOSSIAN, C. 2015. Periodontal-disease-associated biofilm: A reservoir for pathogens of medical importance. *Microb Pathog,* 94, 27-34.

VORA, P., YOUDIM, A., THOMAS, L. S., FUKATA, M., TESFAY, S. Y., LUKASEK, K., MICHELSEN, K. S., WADA, A., HIRAYAMA, T., ARDITI, M. & ABREU, M. T. 2004. Beta-defensin-2 expression is regulated by TLR signaling in intestinal epithelial cells. *J Immunol,* 173**,** 5398-405.

VON BAHR, L., BATSIS, I., MOLL, G., HÄGG, M., SZAKOS, A., SUNDBERG, B., UZUNEL, M., RINGDEN, O. & LE BLANC, K. 2012. Analysis of tissues following mesenchymal stromal cell therapy in humans indicates limited long-term engraftment and no ectopic tissue formation. *Stem Cells,* 30**,** 1575-8.

VRENSEN, G. F., OTTO, C., LENFERINK, A., LISZKA, B., MONTENEGRO, G. A., BARRAQUER, R. I. & MICHAEL, R. 2015. Protein profiles in cortical and nuclear regions of aged human donor lenses: A confocal Raman microspectroscopic and imaging study. *Exp Eye Res,* 145:100-9.

WADA, N., MENICANIN, D., SHI, S., BARTOLD, P. M. & GRONTHOS, S. 2009. Immunomodulatory properties of human periodontal ligament stem cells. *J Cell Physiol,* 219**,** 667-76.

WADE, W. G. 2013. The oral microbiome in health and disease. *Pharmacol Res,* 69**,** 137-43.

WANG, D. & DUBOIS, R. N. 2006. Prostaglandins and cancer. *Gut,* 55**,** 115-22.

WANG, X. & QUINN, P. J. 2010. Lipopolysaccharide: Biosynthetic pathway and structure modification. *Prog Lipid Res,* 49**,** 97-107.

WANG, Y., CUI, L., GONSIOREK, W., MIN, S. H., ANILKUMAR, G., ROSENBLUM, S., KOZLOWSKI, J., LUNDELL, D., FINE, J. S. & GRANT, E. P. 2009. CCR2 and CXCR4 regulate peripheral blood monocyte pharmacodynamics and link to efficacy in experimental autoimmune encephalomyelitis. *J Inflamm (Lond),* 6**,** 32.

WARD, J. B. 1981. Teichoic and teichuronic acids: biosynthesis, assembly, and location. *Microbiol Rev,* 45**,** 211-43.

WARD, J. R., FRANCIS, S. E., MARSDEN, L., SUDDASON, T., LORD, G. M., DOWER, S. K., CROSSMAN, D. C. & SABROE, I. 2009. A central role for monocytes in Toll-like receptor-mediated activation of the vasculature. *Immunology,* 128**,** 58-68.

WEHKAMP, J., HARDER, J., WEHKAMP, K., WEHKAMP-VON MEISSNER, B., SCHLEE, M., ENDERS, C., SONNENBORN, U., NUDING, S., BENGMARK, S., FELLERMANN, K., SCHRÖDER, J. M. & STANGE, E. F. 2004. NF-kappaB- and AP-1-mediated induction of human beta defensin-2 in intestinal epithelial cells by Escherichia coli Nissle 1917: a novel effect of a probiotic bacterium. *Infect Immun,* 72**,** 5750-8.

WEI, X., YANG, X., HAN, Z. P., QU, F. F., SHAO, L. & SHI, Y. F. 2013. Mesenchymal stem cells: a new trend for cell therapy. *Acta Pharmacol Sin,* 34**,** 747-54.

WELSH, C. T., SUMMERSGILL, J. T. & MILLER, R. D. 2004. Increases in c-Jun N-terminal kinase/stress-activated protein kinase and p38 activity in monocyte-derived macrophages following the uptake of Legionella pneumophila. *Infect Immun,* 72**,** 1512-8.

WENG, J. Y., DU, X., GENG, S. X., PENG, Y. W., WANG, Z., LU, Z. S., WU, S. J., LUO, C. W., GUO, R., LING, W., DENG, C. X., LIAO, P. J. & XIANG, A. P. 2010. Mesenchymal stem cell as salvage treatment for refractory chronic GVHD. *Bone Marrow Transplant,* 45**,** 1732-40.

WESTPHAL, H. 2002. International stem cell research considerations. *C R Biol,* 325**,** 1045-8.

WILLIAMS, M. R., AZCUTIA, V., NEWTON, G., ALCAIDE, P. & LUSCINSKAS, F. W. 2011. Emerging mechanisms of neutrophil recruitment across endothelium. *Trends Immunol,* 32**,** 461-9.

WILMARTH, P. A., RIVIERE, M. A., RUSTVOLD, D. L., LAUTEN, J. D., MADDEN, T. E. & DAVID, L. L. 2004. Two-dimensional liquid chromatography study of the human whole saliva proteome. *J Proteome Res,* 3**,** 1017-23.

WOO, J. S., JEONG, J. Y., HWANG, Y. J., CHAE, S. W., HWANG, S. J. & LEE, H. M. 2003. Expression of cathelicidin in human salivary glands. *Arch Otolaryngol Head Neck Surg,* 129**,** 211-4.

WRIGHT, S. D., RAMOS, R. A., TOBIAS, P. S., ULEVITCH, R. J. & MATHISON, J. C. 1990. CD14, a receptor for complexes of lipopolysaccharide (LPS) and LPS binding protein. *Science,* 249**,** 1431-3.

XAGORARI, A. & CHLICHLIA, K. 2008. Toll-like receptors and viruses: induction of innate antiviral immune responses. *Open Microbiol J,* 2**,** 49-59.

XU, X., ZHU, F., ZHANG, M., ZENG, D., LUO, D., LIU, G., CUI, W., WANG, S., GUO, W., XING, W., LIANG, H., LI, L., FU, X., JIANG, J. & HUANG, H. 2013. Stromal cell-derived factor-1 enhances wound healing through recruiting bone marrow-derived mesenchymal stem cells to the wound area and promoting neovascularization. *Cells Tissues Organs,* 197**,** 103-13.

YANG, D., SUN, S., WANG, Z., ZHU, P., YANG, Z. & ZHANG, B. 2013. Stromal cell-derived factor-1 receptor CXCR4-overexpressing bone marrow mesenchymal stem cells accelerate wound healing by migrating into skin injury areas. *Cell Reprogram,* 15**,** 206-15.

YANG, R. B., MARK, M. R., GRAY, A., HUANG, A., XIE, M. H., ZHANG, M., GODDARD, A., WOOD, W. I., GURNEY, A. L. & GODOWSKI, P. J. 1998. Toll-like receptor-2 mediates lipopolysaccharide-induced cellular signalling. *Nature,* 395**,** 284-8.

YANG, S. H., PARK, M. J., YOON, I. H., KIM, S. Y., HONG, S. H., SHIN, J. Y., NAM, H. Y., KIM, Y. H., KIM, B. & PARK, C. G. 2009. Soluble mediators from mesenchymal stem cells suppress T cell proliferation by inducing IL-10. *Exp Mol Med,* 41**,** 315-24.

YAÑEZ, R., OVIEDO, A., ALDEA, M., BUEREN, J. A. & LAMANA, M. L. 2010. Prostaglandin E2 plays a key role in the immunosuppressive properties of adipose and bone marrow tissue-derived mesenchymal stromal cells. *Exp Cell Res,* 316**,** 3109-23.

YE, Y., CARLSSON, G., AGHOLME, M. B., WILSON, J. A., ROOS, A., HENRIQUES-NORMARK, B., ENGSTRAND, L., MODÉER, T. & PÜTSEP, K. 2013. Oral bacterial community dynamics in paediatric patients with malignancies in relation to chemotherapy-related oral mucositis: a prospective study. *Clin Microbiol Infect,* 19**,** E559-67.

YEN, C. A., DAMOULIS, P. D., STARK, P. C., HIBBERD, P. L., SINGH, M. & PAPAS, A. S. 2008. The effect of a selective cyclooxygenase-2 inhibitor (celecoxib) on chronic periodontitis. *J Periodontol,* 79**,** 104-13.

YONEYAMA, M., KIKUCHI, M., NATSUKAWA, T., SHINOBU, N., IMAIZUMI, T., MIYAGISHI, M., TAIRA, K., AKIRA, S. & FUJITA, T. 2004. The RNA helicase RIG-I has an essential function in double-stranded RNA-induced innate antiviral responses. *Nat Immunol,* 5**,** 730-7.

YOSHIMURA, A., LIEN, E., INGALLS, R. R., TUOMANEN, E., DZIARSKI, R. & GOLENBOCK, D. 1999. Cutting edge: recognition of Gram-positive bacterial cell wall components by the innate immune system occurs via Toll-like receptor 2. *J Immunol,* 163**,** 1-5.

YOUNG, J. H., LOGAN, B. R., WU, J., WINGARD, J. R., WEISDORF, D. J., MUDRICK, C., KNUST, K., HOROWITZ, M. M., CONFER, D. L., DUBBERKE, E. R., PERGAM, S. A., MARTY, F. M., STRASFELD, L. M., BROWN, J. W., LANGSTON, A. A., SCHUSTER, M. G., KAUL, D. R., MARTIN, S. I., ANASETTI, C. & 0201, B. A. M. T. C. T. N. T. 2015. Infections after Transplantation of Bone Marrow or Peripheral Blood Stem Cells from Unrelated Donors. *Biol Blood Marrow Transplant*, 22, 359-70.

YOUNT, N. Y. & YEAMAN, M. R. 2013. Peptide antimicrobials: cell wall as a bacterial target. *Ann N Y Acad Sci,* 1277**,** 127-38.

YUN, T. J., TALLQUIST, M. D., AICHER, A., RAFFERTY, K. L., MARSHALL, A. J., MOON, J. J., EWINGS, M. E., MOHAUPT, M., HERRING, S. W. & CLARK, E. A. 2001. Osteoprotegerin, a crucial regulator of bone metabolism, also regulates B cell development and function. *J Immunol,* 166**,** 1482-91.

ZANETTI, M. 2005. The role of cathelicidins in the innate host defenses of mammals. *Curr Issues Mol Biol,* 7**,** 179-96.

ZASLOFF, M. 2002. Antimicrobial peptides of multicellular organisms. *Nature,* 415**,** 389-95.

ZHANG, Q., SHI, S., LIU, Y., UYANNE, J., SHI, Y. & LE, A. D. 2009. Mesenchymal stem cells derived from human gingiva are capable of immunomodulatory functions and ameliorate inflammation-related tissue destruction in experimental colitis. *J Immunol,* 183**,** 7787-98.

ZHOU, H., GUO, M., BIAN, C., SUN, Z., YANG, Z., ZENG, Y., AI, H. & ZHAO, R. C. 2010. Efficacy of bone marrow-derived mesenchymal stem cells in the treatment of sclerodermatous chronic graft-versus-host disease: clinical report. *Biol Blood Marrow Transplant,* 16**,** 403-12.

ZHU, L., COURIEL, D. R. & CHANG, C. H. 2015. The effect of extracorporeal photopheresis on T cell response in chronic graft-versus-host disease. *Leuk Lymphoma***,** 1-9.

ZIEGLER-HEITBROCK, L. & HOFER, T. P. 2013. Toward a refined definition of monocyte subsets. *Front Immunol,* 4**,** 23.

7. Supplementary Data

7 Supplementary Data

7.1 Bacterial growth profiles

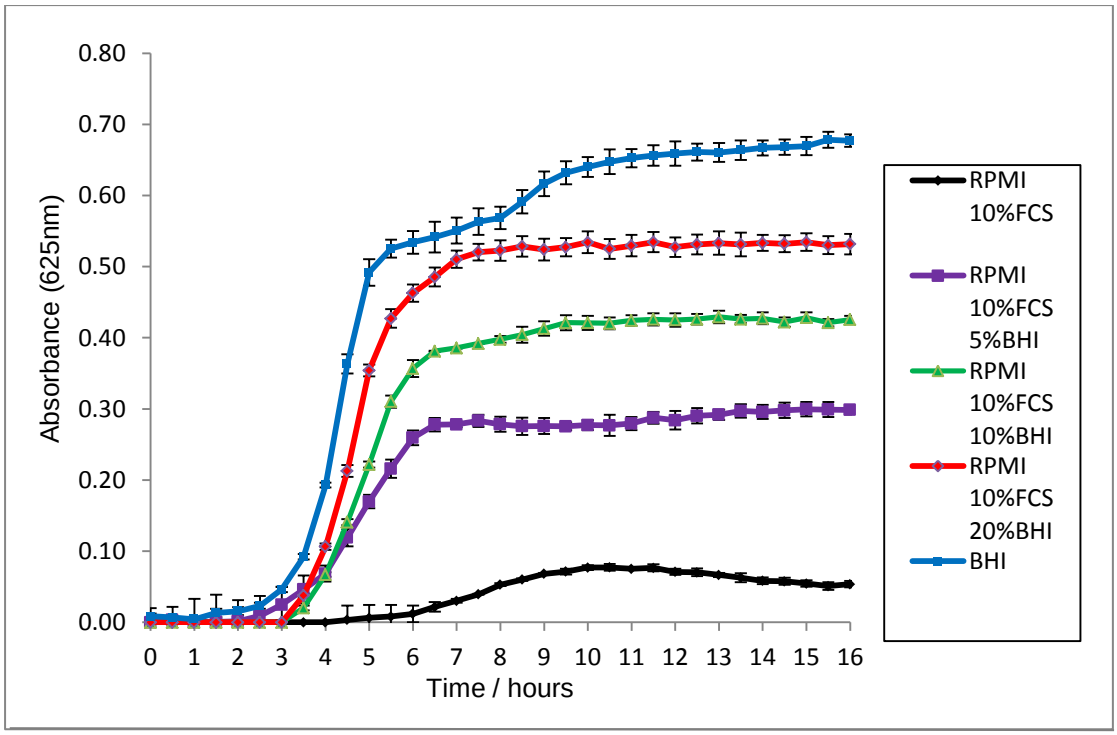

Figure S1: The growth profile of *E. faecalis* in BHI, RPMI + 10%FCS (+/- 5-20% BHI) from a 1:100 of a 0.5 McFarland.

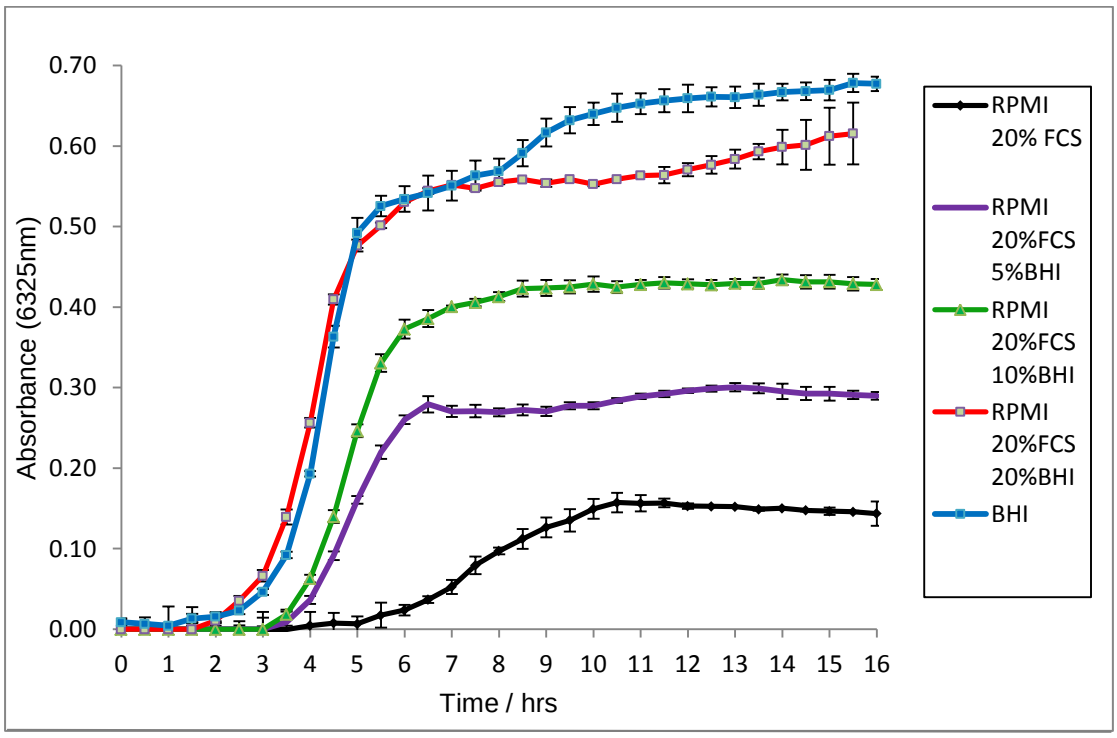

Figure S2: The growth profile of *E. faecalis* in BHI, RPMI + 20%FCS (+/- 5-20% BHI) from a 1:100 of a 0.5 McFarland.

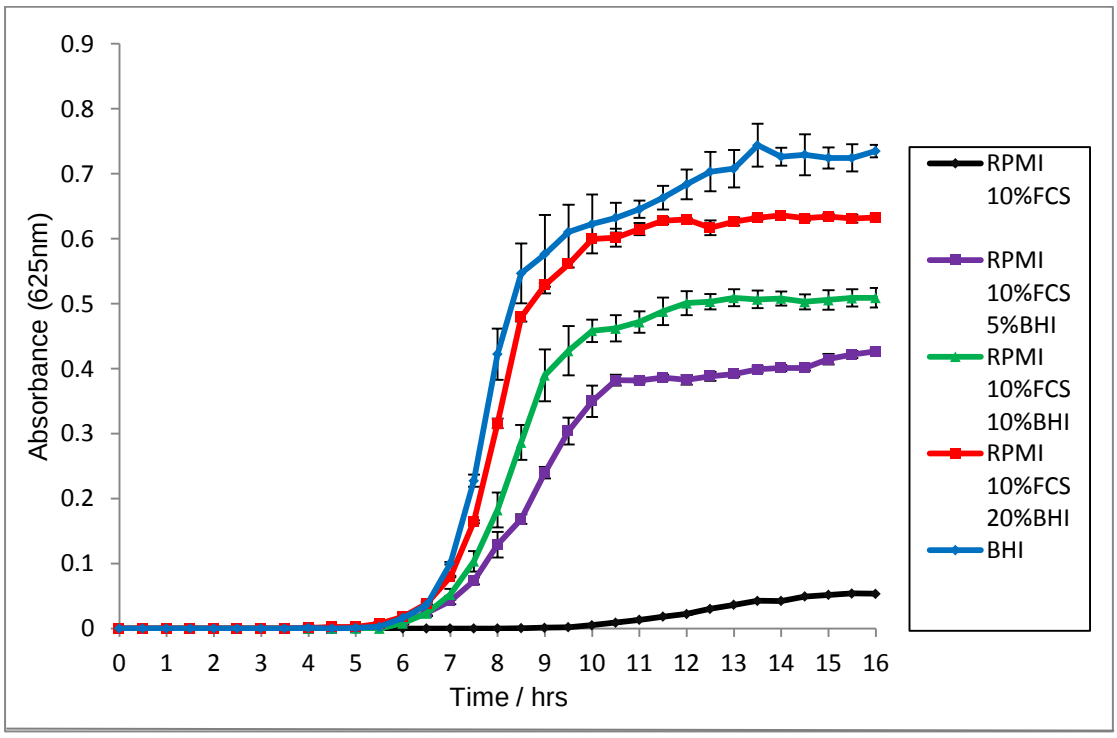

Figure S3: The growth profile of *E. faecalis* in BHI, RPMI + 10%FCS (+/- 5-20% BHI) from 150CFU.

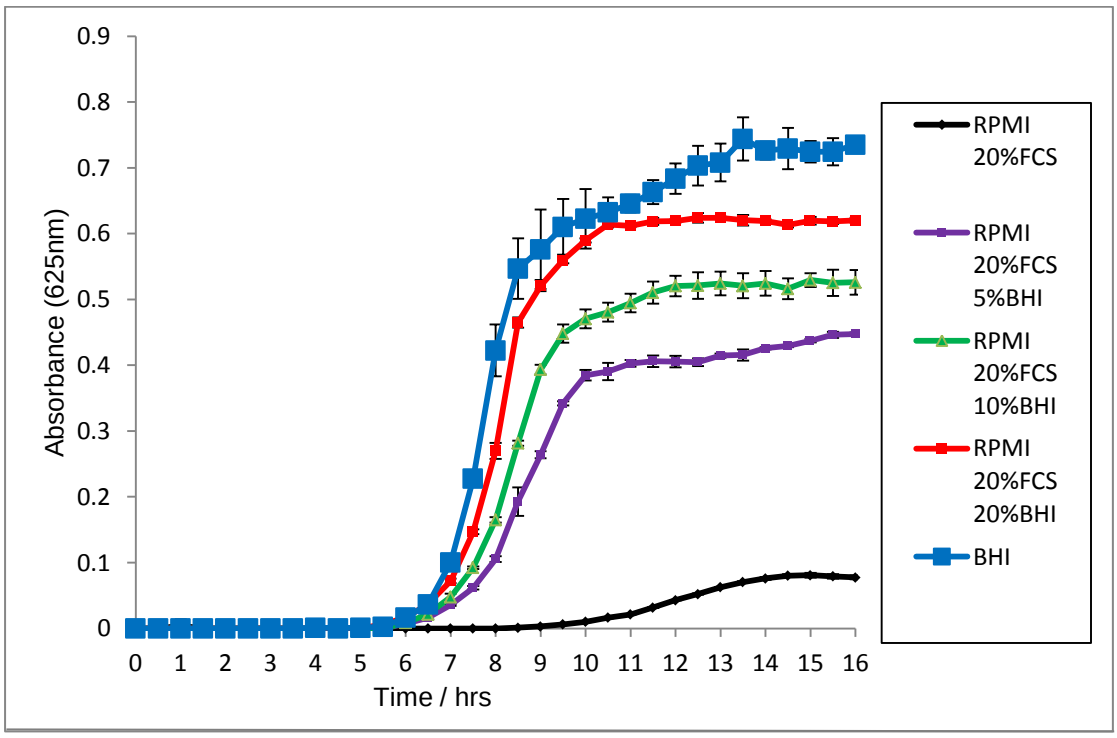

Figure S4: The growth profile of *E. faecalis* in BHI, RPMI + 20%FCS (+/- 5-20% BHI) from 150CFU.

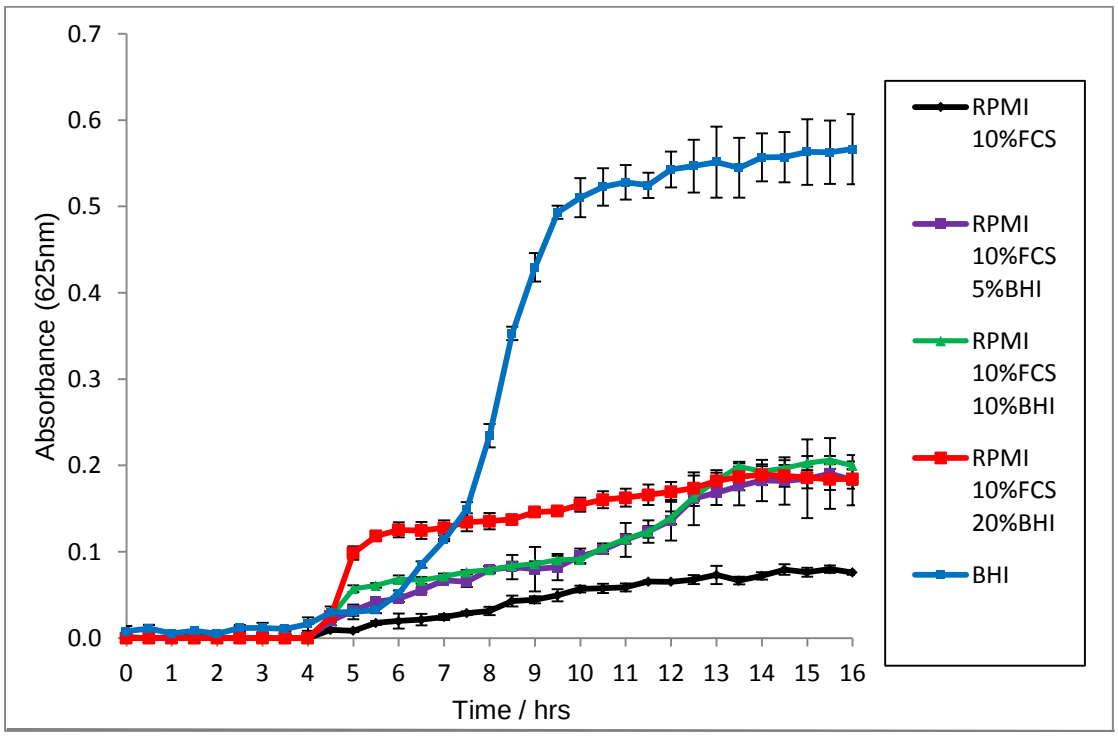

Figure S5: The growth profile of *S. pyogenes* in BHI, RPMI + 10%FCS (+/- 5-20% BHI) from a 1:100 of a 0.5 McFarland..

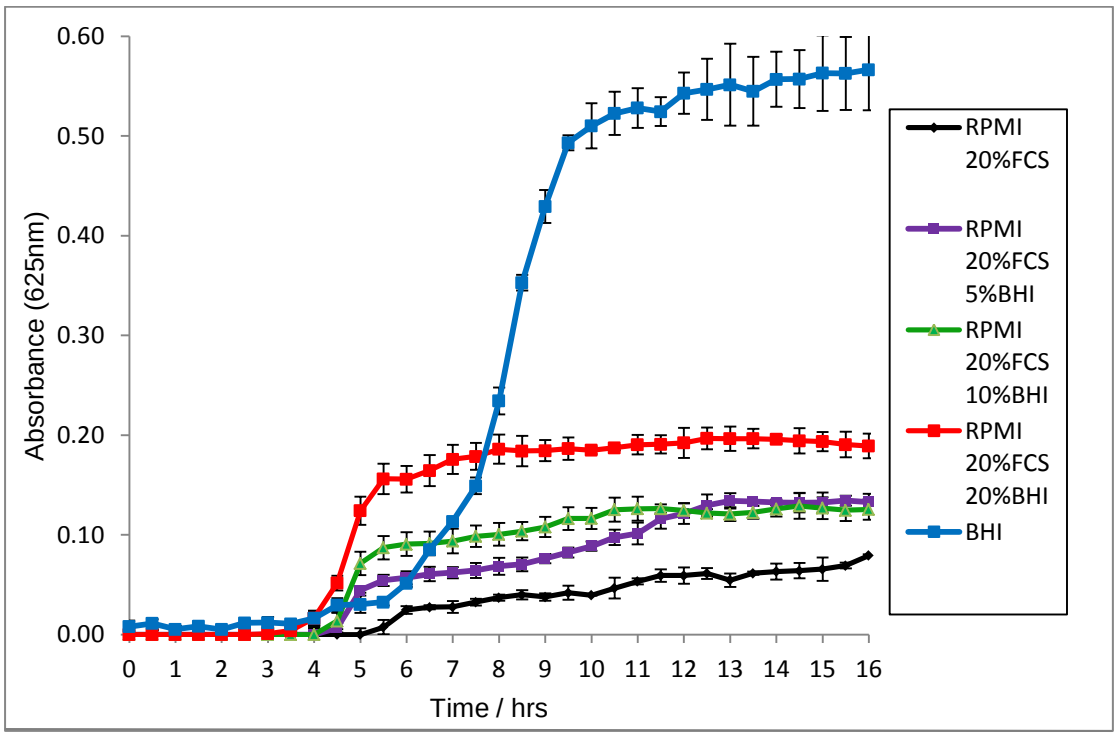

Figure S6: The growth profile of *S. pyogenes* in BHI, RPMI + 20%FCS (+/- 5-20% BHI) from a 1:100 of a 0.5 McFarland.

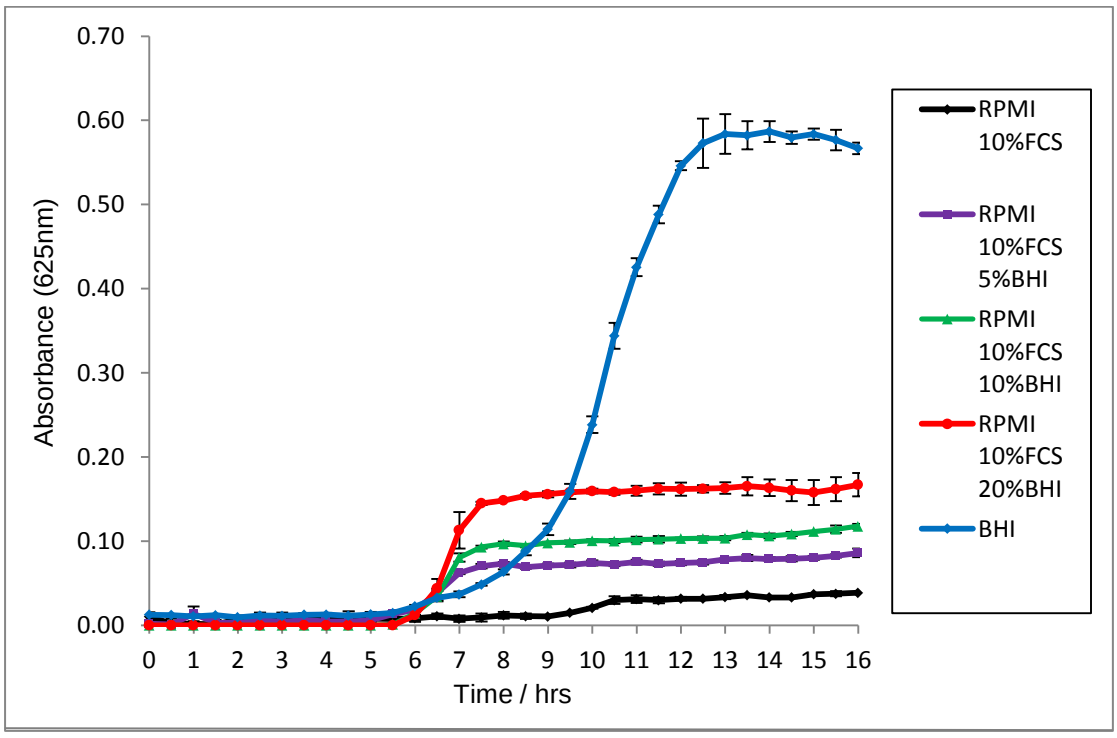

Figure S7: The growth profile of *S. pyogenes* in BHI, RPMI + 10%FCS (+/- 5-20% BHI) from 150CFU.

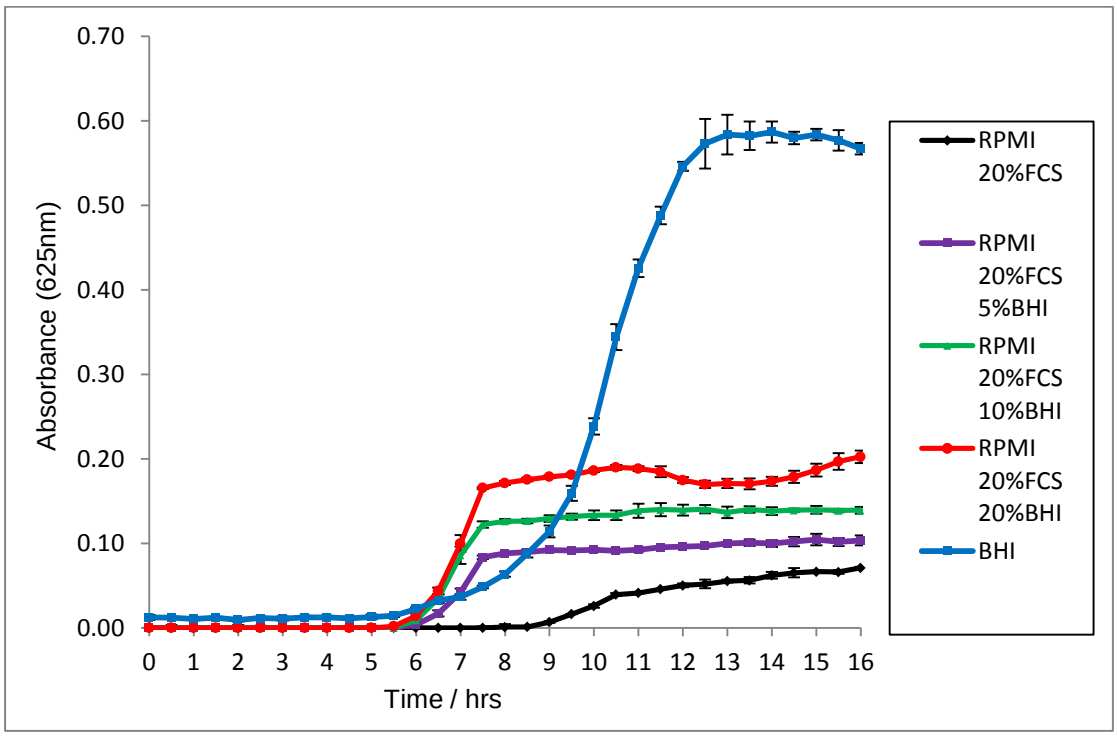

Figure S8: The growth profile of *S. pyogenes* in BHI, RPMI + 20%FCS (+/- 5-20% BHI) from 150CFU.

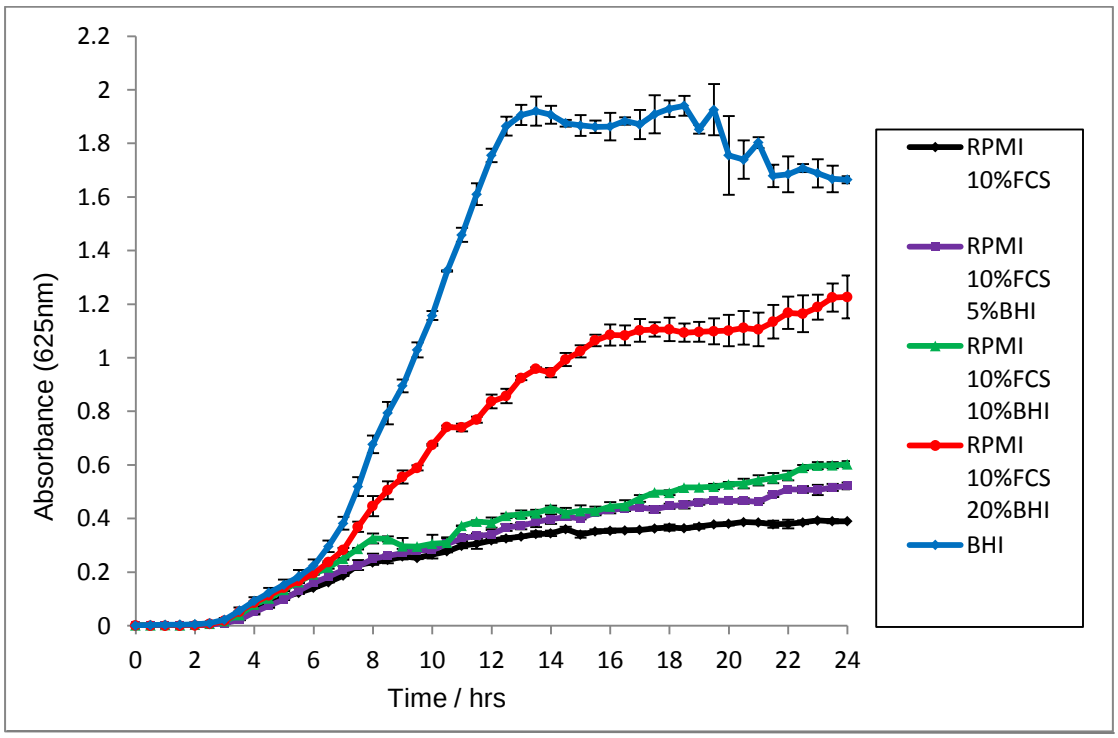

Figure S9: The growth profile of *P. aeruginosa* in BHI, RPMI + 10%FCS (+/- 5-20% BHI) from a 1:100 of a 0.5 McFarland.

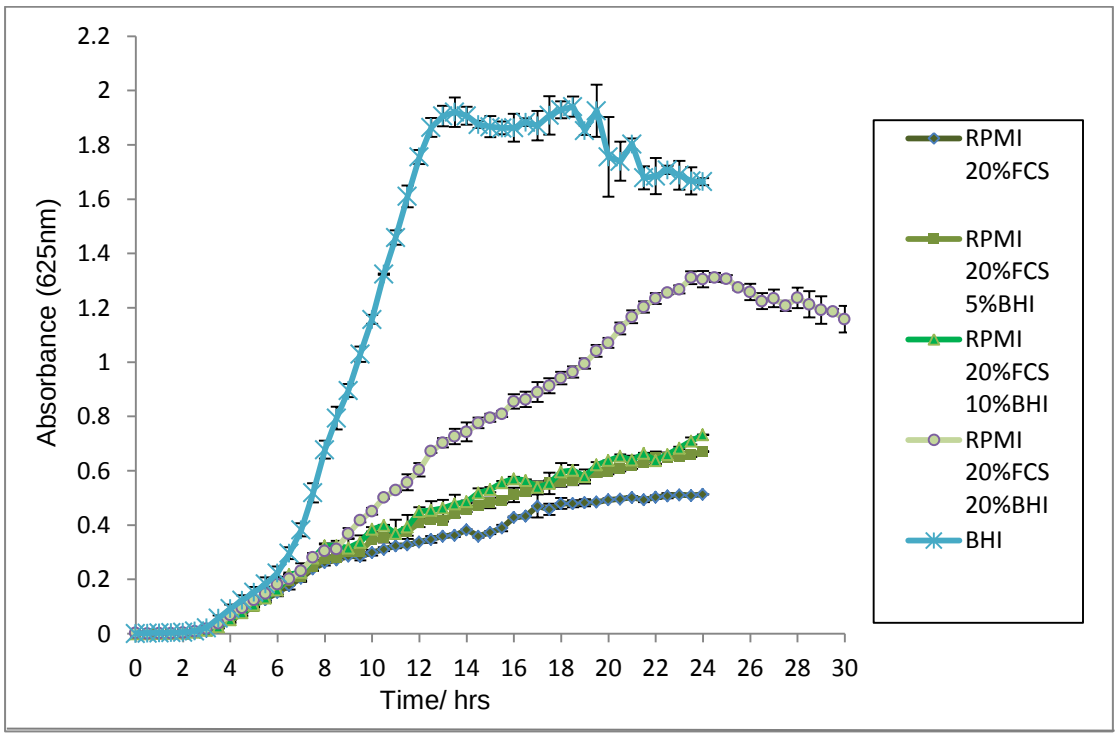

Figure S10: The growth profile of *P. aeruginosa* in BHI, RPMI + 20%FCS (+/- 5-20% BHI) from a 1:100 of a 0.5 McFarland.

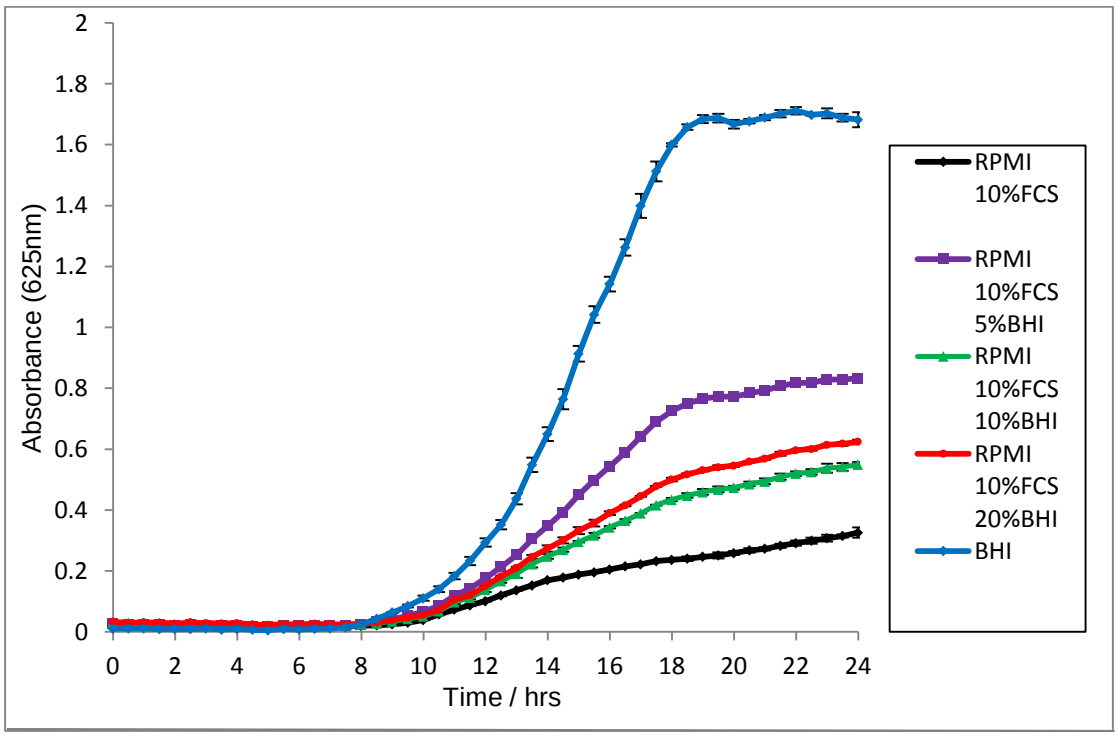

Figure S11: The growth profile of *P. aeruginosa* in BHI, RPMI + 10%FCS (+/- 5-20% BHI) from 150CFU.

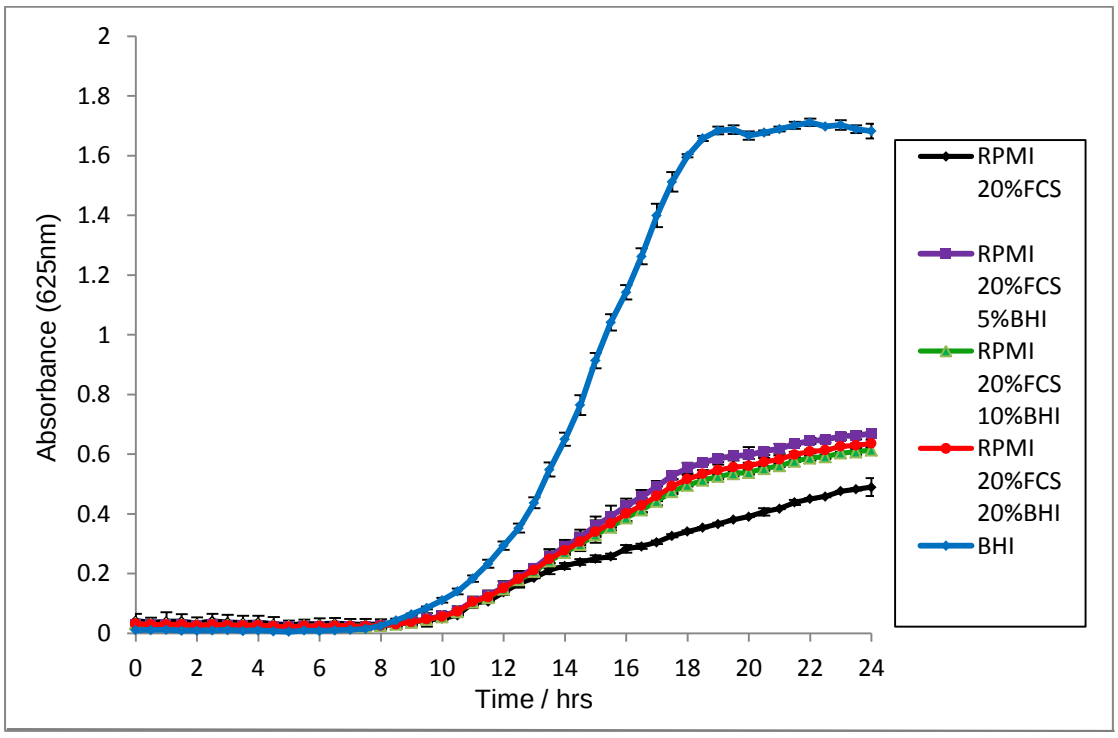

Figure S12: The growth profile of *P. aeruginosa* in BHI, RPMI + 20%FCS (+/- 5-20% BHI) from 150CFU.

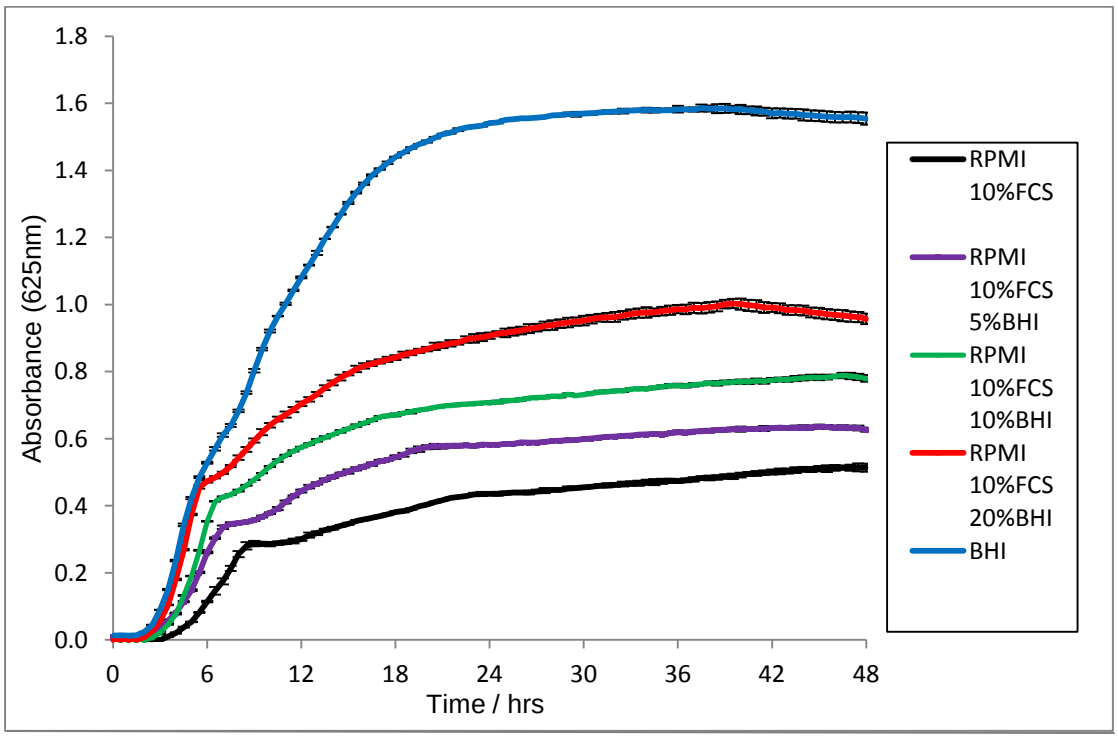

Figure S13: The growth profile of *P. mirabilis* in BHI, RPMI + 10%FCS (+/- 5-20% BHI) from a 1:100 of a 0.5 McFarland.

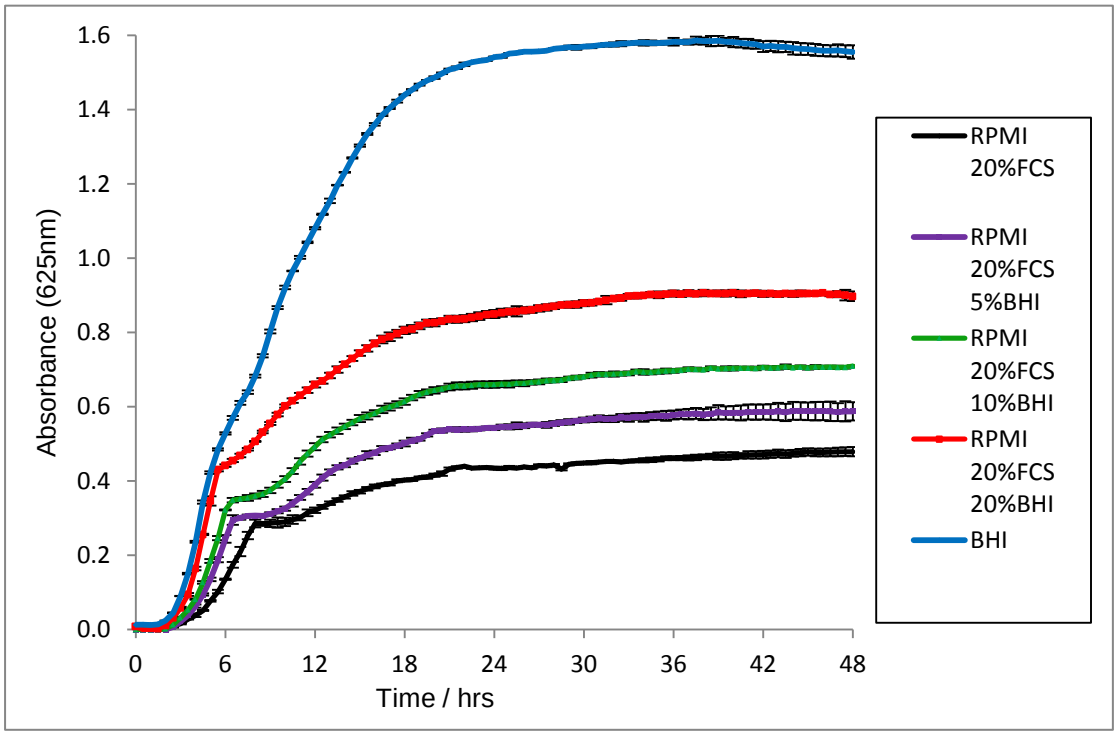

Figure S14: The growth profile of *P. mirabilis* in BHI, RPMI + 20%FCS (+/- 5-20% BHI) from a 1:100 of a 0.5 McFarland.

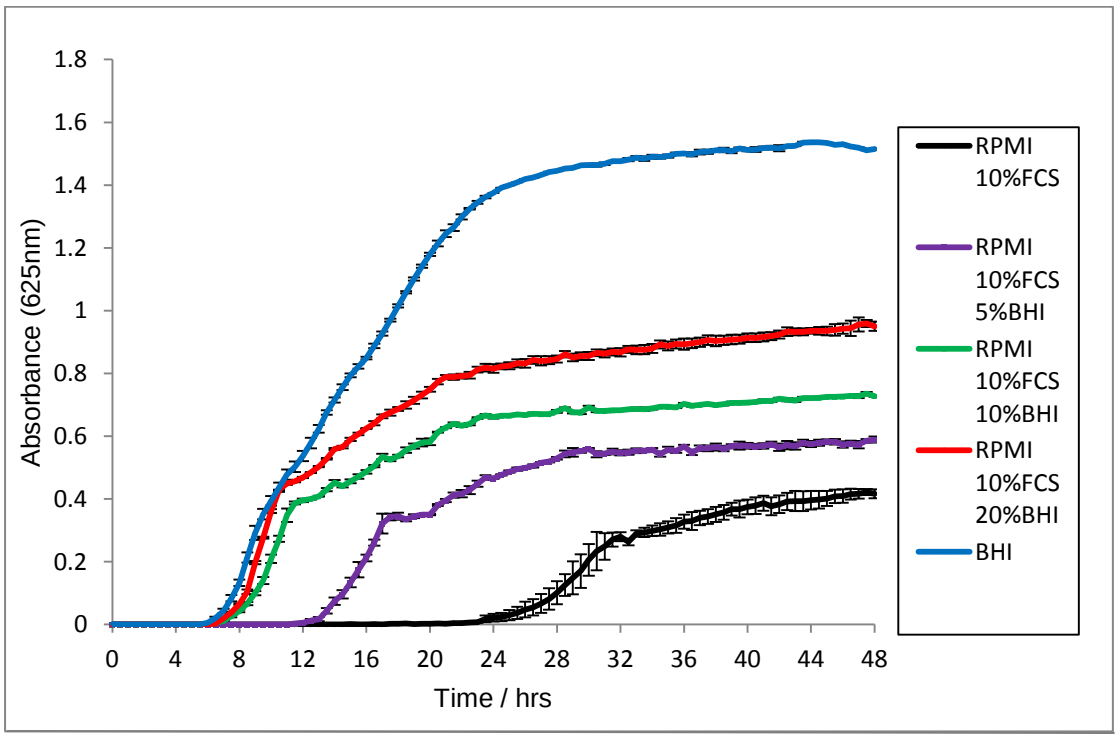

Figure S15: The growth profile of *P. mirabilis* in BHI, RPMI + 10%FCS (+/- 5-20% BHI) from 150CFU.

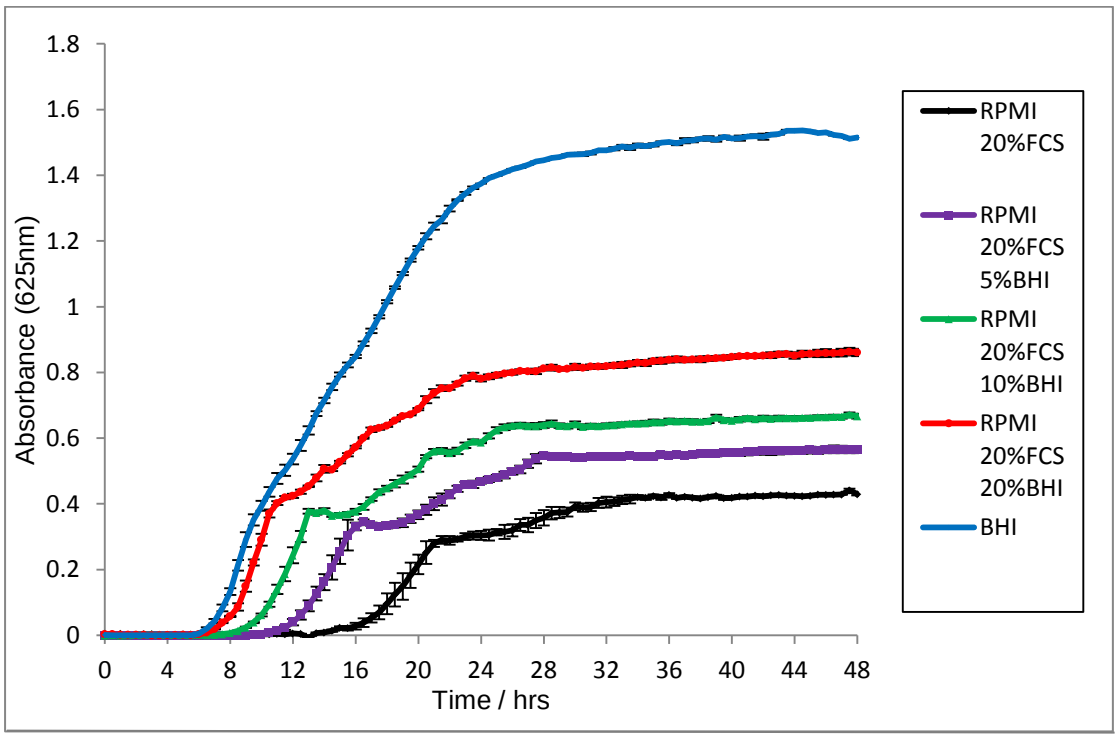

Figure S16: The growth profile of *P. mirabilis* in BHI, RPMI + 20%FCS (+/- 5-20% BHI) from 150CFU.

8. Publications and Prizes

8 Publications and Prizes

8.1 Publications:

Board-Davies EL, Sloan A, Stephens P and Davies LC, 2013 Determining the Antibacterial Potential of Oral Mucosal Lamina Propria-Progenitor Cells. *European Cell and Materials,* 26(7):47. (Conference abstract)

Board-Davies EL, Moses R, Sloan A, Stephens P and Davies LC, 2015 Oral Mucosal Lamina Propria-Progenitor Cells Exert Antibacterial Properties via the Secretion of Osteoprotegerin and Haptoglobin. *Stem Cells Translational Medicine,* 4(11): 1283-93.

8.2 Prizes

Cardiff Institute of Tissue Engineering and Repair (CITER) Annual Scientific Meeting, 2012. Postgraduate Oral Presentation Prize.

British Society for Oral and Dental Research (BSODR), 2012. Senior Colgate Award: Commendation.

Published Ahead of Print on September 16, 2015 as 10.5966/sctm.2015-0043.

STEM CELLS TRANSLATIONAL MEDICINE®

TISSUE-SPECIFIC PROGENITOR AND STEM CELLS

Oral Mucosal Lamina Propria-Progenitor Cells Exert Antibacterial Properties via the Secretion of Osteoprotegerin and Haptoglobin

EMMA BOARD-DAVIES,[a,b] RACHAEL MOSES,[a,b] ALASTAIR SLOAN,[a,b] PHIL STEPHENS,[a,b] LINDSAY C. DAVIES[a,b,c]

Key Words. Oral mucosa • Progenitor cell • Antibacterial agents • Osteoprotegerin • Haptoglobin

[a]Wound Biology Group, Tissue Engineering and Reparative Dentistry, School of Dentistry, College of Biomedical and Life Sciences, and [b]Cardiff Institute of Tissue Engineering and Repair, Cardiff University, Cardiff, United Kingdom; [c]Centre for Hematology and Regenerative Medicine, Department of Laboratory Medicine, Karolinska Institutet, Huddinge, Sweden

Correspondence: Lindsay C. Davies, Ph.D., Centre for Haematology and Regenerative Medicine, Karolinska University Hospital, Huddinge HERM, Novum, Floor 4, Stockholm 141 86, Sweden. Telephone: 46 8-585-813-61; E-Mail: Lindsay.davies@ki.se

Received March 5, 2015; accepted for publication July 27, 2015.

1066-5099/2015/$20.00/0

http://dx.doi.org/10.5966/sctm.2015-0043

ABSTRACT

The oral cavity possesses a diverse microflora, yet recurrent infections within healthy individuals are rare. Wound healing within the buccal mucosa is preferential, potentially because of the presence of oral mucosal lamina propria-progenitor cells (OMLP-PCs). In addition to their multipotency, OMLP-PCs demonstrate potent immunosuppressive properties. The present study investigated whether OMLP-PCs possess antibacterial properties, directly interacting with microorganisms and contributing to the maintenance of a balanced oral microflora. Gram-positive and -negative bacteria were cocultured with OMLP-PCs, buccal mucosal fibroblasts, or their respective conditioned media (CM). Bacterial growth was significantly inhibited when cocultured with OMLP-PCs or their CM. No antibacterial activity was apparent within the fibroblasts. Analysis of the OMLP-PC CM indicated constitutive secretion of osteoprotegerin (OPG) and haptoglobin (Hp). Exposure of the bacteria to OPG or Hp demonstrated their differential antibacterial properties, with neutralization/blocking studies confirming that the growth of Gram-positive bacteria was partially restored by neutralizing OPG within OMLP-PC CM; blocking Hp restored the growth of Gram-negative bacteria. The present study demonstrates, for the first time, the broad-spectrum antibacterial properties of OMLP-PCs. We report the direct and constitutive antibacterial nature of OMLP-PCs, with retention of this effect within the CM suggesting a role for soluble factors such as OPG and Hp. Knowledge of the immunomodulatory and antibacterial properties of these cells could potentially be exploited in the development of novel cell- or soluble factor-based therapeutics for the treatment of infectious diseases such as pneumonia or ailments such as chronic nonhealing wounds. STEM CELLS TRANSLATIONAL MEDICINE *2015; 4:1–11*

SIGNIFICANCE

Oral mucosal lamina propria-progenitor cells (OMLP-PCs) are a cell source with known immunomodulatory properties. The present report demonstrates the novel finding that OMLP-PCs possess potent antibacterial properties, halting the growth of Gram-positive and -negative bacteria through the secretion of soluble factors. OMLP-PCs constitutively secrete osteoprotegerin (OPG) and haptoglobin (Hp) at levels high enough to exert antibacterial action. OPG, a glycoprotein not previously known to be antibacterial, can suppress Gram-positive bacterial growth. Hp is only active against Gram-negative microorganisms. These findings indicate that OMLP-PCs could offer great potential in the development of novel cell- or soluble factor-based therapies for the treatment of infectious illness, such as bacterial pneumonia, through systemic infusion and of chronic wounds through local administration.

INTRODUCTION

Oral soft tissues are continually exposed to the external environment and are thus a critical entry point for potentially harmful bacteria [1]. However, chronic infections are rare, potentially because of antimicrobial factors secreted by resident cells within tissues such as the salivary glands [2]. A decrease in specific antimicrobial factors has been linked to the onset of oral diseases such as periodontitis and deficiencies in the human cathelicidin protein LL-37 [3].

Oral mucosal lamina propria-progenitor cells (OMLP-PCs) are isolated from buccal mucosal biopsies by differential adhesion to fibronectin [4]. These cells are clonally expanded and are CD44+CD90+CD105+CD166+ and CD34−CD45−. They are of neural crest origin (Slug+, Snail+, Sox10+, and Twist+) and are multipotent (mesenchymal and neural lineages) [4]. In addition to their plasticity, OMLP-PCs demonstrate potent

Published Ahead of Print on September 16, 2015 as 10.5966/sctm.2015-0043.

immunosuppressive properties, suppressing lymphocyte proliferation in a contact- and dose-independent manner, indicating the importance of secreted factors in mediating their mechanism of action [5].

The immunosuppressive properties of bone marrow-derived mesenchymal stem cells (BMMSCs) are well documented [6]. BMMSCs require licensing to an anti-inflammatory phenotype, termed "MSC2," by exposure to proinflammatory cytokines, such as interferon-γ (IFN-γ), to display these properties [7]. IFN-γ induces the expression of indoleamine 2,3-dioxygenase (IDO), the enzyme responsible for depleting tryptophan, an essential factor in suppressing lymphocyte proliferation [8].

Immunosuppressive factors, such as IDO, are also known to have prominent antibacterial actions. This enzyme also inhibits tryptophan-dependent bacteria such as group B streptococci [9] and *Escherichia coli* [10, 11] by the depletion of tryptophan. This knowledge has led to the hypothesis that stem cells can act with dual properties, displaying both immunomodulatory and antibacterial characteristics. However, limited studies have been reported with respect to the potential antibacterial properties of stem/progenitor cells. BMMSCs have been demonstrated to decrease the growth of a restricted number of bacteria in vitro by the secretion of antibacterial factors such as LL-37 [12]. In vivo studies have also documented the antibacterial nature of BMMSCs for the treatment of conditions such as sepsis. For example, BMMSCs stimulate bacterial clearance within the blood in both polymicrobial [13] and Gram-negative sepsis mouse models [14], potentially owing to an increase in the phagocytosis of bacteria.

Haptoglobin (Hp) is a multifunctional glycoprotein with known antibacterial and immunomodulatory properties affecting both the innate and the adaptive immune systems [15]. It is composed of two α and two β chains, with the type of α chain (α1 or α2) conveying the level of Hp activity. Three human forms are known: Hp1-1, Hp2-1, and Hp2-2. Hp1-1 with two α1 chains demonstrating the highest level of activity. Its ability to effectively bind hemoglobin and thereby deplete iron from the environment provides Hp with excellent antibacterial effects against multiple bacterial and fungal pathogens [10]. Normally associated as a positive acute phase protein, produced by the liver and found in increasing concentrations within the plasma as inflammation occurs, no association with stem/progenitor cells has yet been reported [16].

Osteoprotegerin (OPG) is a glycoprotein predominantly described as a decoy receptor for the receptor activator of nuclear factor κB ligand (RANKL), preventing nuclear κB activation. Activation of this pathway is central to the regulation of a number of key immune pathways and the process of osteoclastogenesis [17]. OPG is known to be a component of the BMMSC secretome, although it has been reported to not play a significant role in MSC-mediated immunosuppression [18], but rather in regulating bone resorption [19]. Numerous reports have highlighted a correlation among bone resorption, OPG, and periodontitis; a condition associated with the bacteria *Porphyromonas gingivalis* [20–22].

In the present report, we demonstrate, for the first time, the broad-spectrum antibacterial properties of OMLP-PCs. These findings suggest that this is an inherent and distinct property of this PC population that does not extend to stromal fibroblasts. We demonstrate that OMLP-PC-mediated antibacterial activity is through the constitutive secretion of soluble factors, including Hp and OPG, confirming that the OMLP-PC secretome is able to directly modulate bacterial growth in the absence of immune cell involvement. To our knowledge, this is the first report documenting the antibacterial properties of OPG and its ability to inhibit Gram-positive bacterial growth through a bacteriostatic mechanism. Future investigations will focus on identifying the potential for OMLP-PC usage as a cell- or soluble factor-based therapeutic in the treatment of infectious diseases.

Materials and Methods

Isolation and Maintenance of OMLP-PCs and Enriched Fibroblasts in Culture

Disease-free buccal mucosa biopsies (n = 4) were obtained from healthy donors undergoing orthognathic surgery at Cardiff and Vale University Health Board (Cardiff, U.K.). The local research ethical committee had previously approved the present study, and the donors were informed in accordance with the Declaration of Helsinki.

Single cell suspensions of the lamina propria were obtained by enzymatic digestion of the biopsy specimens, and OMLP-PCs were isolated and characterized as previously described [4, 23]. In brief, OMLP-PCs were separated from the lamina propria cell suspension by differential adhesion to fibronectin and expanded in monolayer culture. Cells remaining in suspension after multiple adhesion steps on fibronectin (i.e., the OMLP-PC-depleted stromal fraction) were termed "enriched fibroblasts" (EFs) and used as a control oral fibroblast cell population throughout the present study.

OMLP-PCs and EFs were maintained at 37°C in a 5% CO_2 humidified atmosphere in Dulbecco's modified Eagle's medium supplemented with 10% (vol/vol) fetal calf serum (FCS), 2 mM L-glutamine, and antibiotics/antimycotics (100 U/ml penicillin G, 100 μg/ml streptomycin sulfate, and 0.25 μg/ml amphotericin B; Life Technologies, Paisley, U.K., http://www.thermofisher.com). To remove cells from plastic for subsequent experimental procedures, 0.05% (wt/vol) trypsin/0.53 mM EDTA (Life Technologies) was used, unless otherwise stated.

Maintenance of Microbiology Stocks

Enterococcus faecalis (NCTC 775), *Pseudomonas aeruginosa* (ATCC 15692), and *Staphylococcus pyogenes* (NCTC 8198) were maintained on tryptone soya agar (TSA; Oxoid Ltd., Basingstoke, U.K., http://www.oxoid.com). *Proteus mirabilis* (NCTC 11938) was maintained on cysteine lactose electrolyte deficient (CLED; Oxoid Ltd.) agar to prevent swarming of the bacteria. Bacteria were subcultured onto fresh agar plates weekly and grown overnight at 37°C. Agar plates were then stored at 4°C.

Coculture of OMLP-PCs, EFs, OPG, and Human Hp With Live Bacteria

OMLP-PCs and EFs (n = 4 donors) were used at 24–30 population doublings for the following experiments. OMLP-PCs were treated $\pm$100 U/ml recombinant human IFN-γ (Sigma-Aldrich, Gillingham, U.K., http://www.sigmaaldrich.com) for 7 days before coculture with bacteria to induce an anti-inflammatory phenotype as confirmed by quantification of the IDO-inducing metabolite L-kynurenine [5].

Published Ahead of Print on September 16, 2015 as 10.5966/sctm.2015-0043.

OMLP-PCs with or without IFN-γ and EFs were seeded into 24-well plates at a density of 1×10^5 cells per well in Roswell Park Memorial Institute (RPMI) medium supplemented with 10% (vol/vol) FCS and 2 mM L-glutamine. The cells were allowed to adhere overnight at 37°C in 5% CO_2. Subsequent to adhesion, the culture medium was removed and exchanged for RPMI supplemented with 10% (vol/vol) FCS, 20% (vol/vol) brain heart infusion broth, and 2 mM L-glutamine with or without inoculation with 150 colony-forming units (CFUs) of bacteria. For the OPG and human Hp coculture experiments, recombinant human OPG (rhOPG; R&D Systems, Abingdon, U.K., http://www.rndsystems.com) or Hp (Sigma-Aldrich) was added to 150 CFU bacteria in suspension at 1–100 ng/ml or 10 pg/ml to 1 μg/ml, respectively.

The CFUs of each bacterium were previously calculated from 10- or 20-ml (*S. pyogenes* only) overnight cultures derived from single colonies. Cultures were spiral plated using a Whitley automatic spiral plater (Don Whitley Scientific, Shipley, U.K., http://www.dwscientific.co.uk) onto appropriate agar after 16 hours (for cocultures) and 23 hours (for susceptibility testing) at 37°C (and 5% CO_2 for *S. pyogenes*). The bacterial colonies were subsequently counted in accordance with the manufacturer's instructions, and the dilution for 150 CFUs was determined for each culture period.

The cocultures were incubated at 37°C and 5% CO_2 for the calculated time to reach the mid-log phase for the control cultures (individual mid-log time points were previously determined for each bacterium using growth curves starting from an inoculation of 150 CFUs). Bacteria and OMLP-PC/EF-only cultures served as controls. The conditioned media (CM) was removed, serially diluted, and spiral plated onto TSA or CLED agar (*P. mirabilis*) and incubated overnight at 37°C before counting the bacterial colonies. The remaining CM was centrifuged at 500*g* for 5 minutes to remove any cell debris. For samples containing bacteria, the CM was further centrifuged at 14,000*g* for 2 minutes through a Pall Nanosep MF centrifugal device, Bio-Inert pore size of 0.2 μm (Sigma-Aldrich) to remove bacteria, and stored at −80°C.

Susceptibility Testing of Live Bacteria With OMLP-PC Secretome

A total of 100 CFUs of bacteria in phosphate-buffered saline was added to 90 μl of CM from the above coculture experiments. The cocultures were then incubated at 37°C and 5% CO_2 for 16 hours. The bacterial cultures were serially diluted, spiral plated onto TSA or CLED (*P. mirabilis)* agar, and incubated overnight at 37°C before the bacterial colonies were counted as described above. The experiments were repeated with the addition of 0.6 μg/ml of human osteoprotegerin/TNFRSF11B neutralizing antibody (R&D Systems) or 24 μg/ml of the polyclonal rabbit anti-human Hp antibody (Dako, Ely, U.K., http://www.dako.com).

Quantification of OPG Gene Expression by OMLP-PCs

Total RNA was extracted from the OMLP-PCs after coculture with bacteria using the Illustra RNAspin Mini RNA isolation kit (GE Healthcare Life Sciences, Little Chalfont, U.K., http://www.gelifesciences.com) and stored at −80°C before use. cDNA was synthesized from 0.5 μg of total RNA using random hexamer primers and Moloney murine leukemia virus reverse transcriptase in accordance with the manufacturer's instructions (Promega, Southampton, U.K., http://www.promega.com). The genomic level of OPG (forward: 5′-GAAGGGCGCTACCTTGAGAT-3′ and reverse: 5′-GCAAATGTATTTCGCTCTGG-3′) and β-actin (forward: 5′-AGCTACGAGCTGCCTGAC-3′ and reverse: 5′-AAGGTAGTTTCGTGGATGC-3′) within OMLP-PCs was determined by quantitative reverse transcription-polymerase chain reaction (qRT-PCR) using Fast SYBR Green Master Mix (Life Technologies) according to the manufacturer's instructions.

Quantification of OPG Level in OMLP-PC Secretome

The protein levels of secreted OPG were determined in CM samples from the coculture experiments using the human osteoprotegerin/TNFRSF11B DuoSet enzyme-linked immunosorbent assay (ELISA) (R&D Systems). The concentration of OPG in the samples was assessed using a standard curve of rhOPG from 0 to 4000 pg/ml.

Detection of Hp in OMLP-PC Secretome

CM derived from OMLP-PCs cultured with and without 100 U/ml IFN-γ for 7 days was combined with Laemmli buffer (62 mM Tris-HCL [pH 6.8], 10% [vol/vol] glycerol, 5% sodium dodecyl sulfate, 0.005% bromophenol blue, and 5% β-mercaptoethanol) and reduced by heating to 100°C for 2 minutes. The total protein concentration was determined using the bicinchoninic acid protein assay (ThermoFisher) to ensure equal loading.

Samples (35 μg) of total protein were separated on NuPAGE Novex 4%–12% Bis-Tris gels (Life Technologies). A positive control of 1 μg human Hp was added to one well (Sigma-Aldrich). The proteins were transferred to nitrocellulose membrane (HybondECL; GE Healthcare Life Sciences) overnight at 4°C, before rinsing the membrane in deionized water. The membrane was placed in 5% (wt/vol) nonfat milk for 1 hour at room temperature with agitation before probing with polyclonal rabbit anti-human Hp (1.2 μg/ml; Dako) diluted in 2% (wt/vol) nonfat milk in phosphate-buffered saline (PBS) with 0.1% Tween20 (PBS-T) for 1 hour at room temperature with agitation. The membrane was washed in PBS-T before being incubated with horseradish peroxidase-conjugated polyclonal swine anti-rabbit immunoglobulins (0.1 μg/ml; Dako) in 2% (wt/vol) nonfat milk diluted in PBS-T for 1 hour at room temperature. The membrane was washed in PBS-T before development using ECL Prime and exposure to Hyperfilm (GE Healthcare Life Sciences).

Assessing Effect of OMLP-PC Secretome, OPG, and Hp on Bacterial Viability

Bacteria were assessed for viability after exposure to OMLP-PC CM, rhOPG, and Hp, as detailed above. Bacteria were stained using the LIVE/DEAD *Bac*Light Bacterial Viability Kit (Life Technologies) as per the manufacturer's instructions. Bacteria were stained for 15 minutes before mounting onto poly-L-lysine microscope slides under a coverslip, using the *Bac*Light mounting oil provided. The bacteria were visualized using a fluorescent microscope at ×100 objective under oil immersion (Olympus, Southend-on-Sea, U.K., http://www.olympus-lifescience.com). Live (green) and dead (red) bacterial cells were subsequently counted using Image Pro-Plus software, version 6.0 (Media Cybernectics, Bethesda, MD, http://www.mediacy.com). Individual bacteria in a minimum of four fields of view were counted per condition.

Published Ahead of Print on September 16, 2015 as 10.5966/sctm.2015-0043.

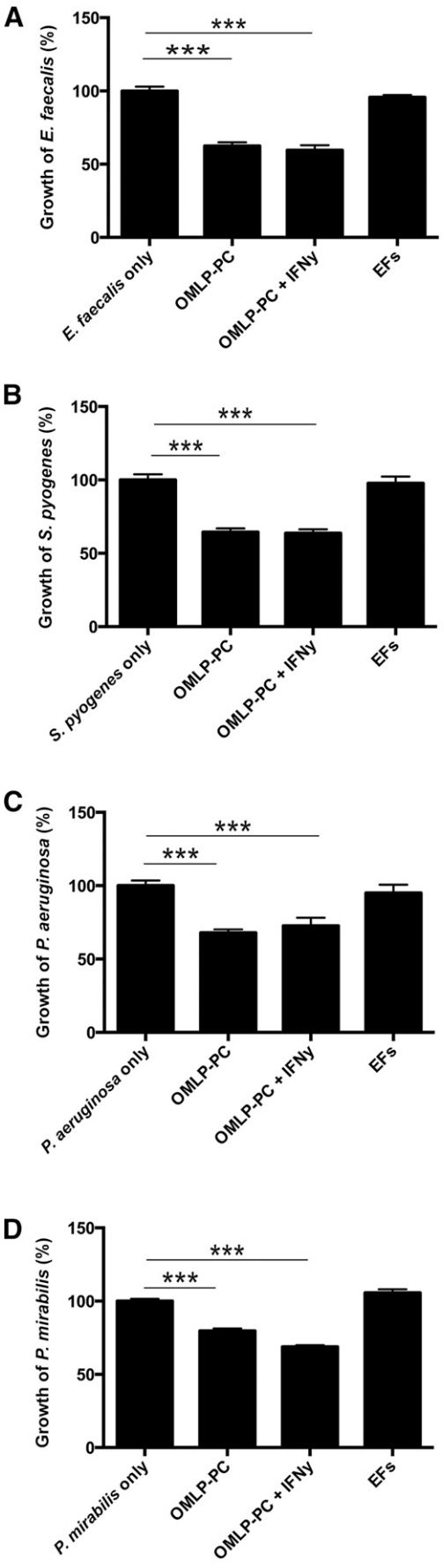

Statistical Analysis

All statistical analyses were performed using SPSS statistics, version 20 (IBM Corp., Armonk, NY, http://www-01.ibm.com/software/analytics/spss/). Statistical analysis to compare mean values was performed using one-way analysis of variance with post hoc Tukey test (equal variances assumed) or a Games-Howell test (unequal variances determined). Variance analysis was performed using Levene's test. Significance was assumed at $p \leq .05$.

Results

OMLP-PCs Significantly Reduce Growth of Both Gram-Positive and Gram-Negative Bacteria

OMLP-PCs were cultured with Gram-positive (*E. faecalis* and *S. pyogenes*) and Gram-negative (*P. aeruginosa* and *P. mirabilis*) bacteria to the calculated mid-log time point. The growth of each bacterium, both Gram-positive ($p < .001$; Fig. 1A, 1B) and Gram-negative ($p < .001$; Fig. 1C, 1D), was significantly reduced when cocultured with OMLP-PCs. No further inhibitory effect was evident with previous IFN-γ licensing of the PCs (confirmation of IDO activity on IFN-γ licensing shown in supplemental online Fig. 1). Coculturing of the PC-depleted EFs with bacteria had no significant effect on the growth of any bacterium (Fig. 1A–1D).

OMLP-PC Secretome Constitutively Reduces Growth of Gram-Positive and Gram-Negative Bacteria

CM from OMLP-PCs significantly reduced the growth of each bacterium ($p < .001$; Fig. 2A–2D). No further inhibitory effect was demonstrated with CM derived from OMLP-PCs previously licensed with IFN-γ or primed by pre-exposure to the bacterium, with the exception of *S. pyogenes*. CM derived from OMLP-PCs previously exposed to *S. pyogenes* further suppressed the growth of this bacterium compared with CM derived from unprimed OMLP-PCs ($p < .001$; Fig. 2B). CM from EFs with or without previous exposure to each bacterium had no significant effect on the growth of any of the bacteria (Fig. 2A–2D).

OPG Is Constitutively Expressed and Secreted by OMLP-PCs

mRNA expression levels of OPG from OMLP-PCs were examined using qRT-PCR, and the secreted levels within CM were measured using ELISA. OPG was constitutively expressed (Fig. 3A–3D) and secreted (average secretion of 13 ng/ml in resting OMLP-PCs;

Figure 1. OMLP-PCs demonstrate broad-spectrum antibacterial effects in coculture with bacteria. OMLP-PCs significantly reduced the growth of Gram-positive *E. faecalis* **(A)** and *S. pyogenes* **(B)** and Gram-negative *P. aeruginosa* **(C)** and *P. mirabilis* **(D)** bacteria. This effect was observed irrespective of OMLP-PCs prestimulation with IFN-γ or not. EFs had no effect on bacterial growth. Data are expressed as the percentage of growth $\pm$ SEM, with bacteria-only cultures set to 100%. ***, $p \leq .001$. Abbreviations: EFs, enriched fibroblasts; IFN-γ, interferon-γ; OMLP-PCs, oral mucosal lamina propria-progenitor cells.

Published Ahead of Print on September 16, 2015 as 10.5966/sctm.2015-0043.

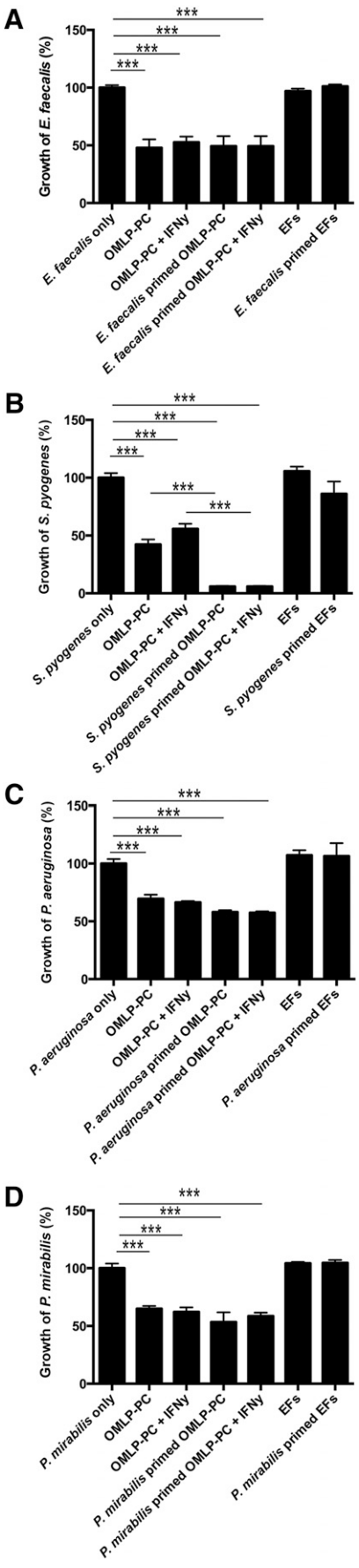

Fig. 3E–3H) by OMLP-PCs, with IFN-γ and/or bacterial exposure having no further effect on these levels.

OPG Exerts Antibacterial Activity Against Gram-Positive Bacteria

Bacteria were incubated with rhOPG at concentrations relevant to those secreted by OMLP-PCs to examine whether OPG possesses antibacterial properties. OPG significantly decreased the growth of Gram-positive bacteria (*E. faecalis* significant at 5 ng/ml, $p \leq .01$; Fig. 4A; and *S. pyogenes* significant at 5 ng/ml, $p \leq .001$; Fig. 4B). However, OPG demonstrated no significant effect on the growth of either Gram-negative bacteria (Fig. 4C, 4D).

Neutralizing OPG Partially Inhibits Antibacterial Properties of OMLP-PCs Against Gram-Positive Bacteria

CM derived from OMLP-PCs (with or without previous bacterial exposure) was incubated with live, Gram-positive bacteria in the presence or absence of an OPG-neutralizing antibody. Neutralization of the OMLP-PC (with or without bacterial exposure) secreted OPG significantly increased the growth of *E. faecalis* (OMLP-PC CM, $p \leq .01$, and bacterially exposed OMLP-PC CM, $p \leq .05$; Fig. 4E) and *S. pyogenes* (OMLP-PC CM, $p \leq .001$, and bacterially exposed OMLP-PC CM, $p \leq .001$; Fig. 4F) compared with CM that had not been neutralized. However, neither the growth of *E. faecalis* nor the growth of *S. pyogenes* was fully restored to control levels by neutralization of OPG ($p \leq .01$, Fig. 4E; and $p \leq .001$, Fig. 4F, respectively).

Hp Is Constitutively Secreted by OMLP-PCs

Hp secretion from OMLP-PCs was detected in the CM by Western blot, with all three chain variants detected, suggesting the constitutive secretion of the higher activity forms, Hp1-1 and Hp2-1 (Fig. 5A). Hp was secreted from OMLP-PCs, irrespective of IFN-γ stimulation of the cells.

Hp Exerts Antibacterial Activity Against Gram-Negative Bacteria

Bacteria were incubated with Hp to examine its antibacterial properties. Hp significantly decreased the growth of both Gram-negative bacteria (*P. aeruginosa* was significant at 50 pg/ml, $p \leq .001$ [Fig. 5B] and *P. mirabilis* was significant at 50 pg/ml, $p \leq .001$ [Fig. 5C]). However, Hp demonstrated no significant effect on the growth of either Gram-positive bacterium (Fig. 5D, 5E).

Figure 2. OMLP-PCs exert antibacterial effects through the secretion of soluble factors. Conditioned media (CM) derived from OMLP-PCs significantly reduced the growth of Gram-positive *E. faecalis***(A)** and *S. pyogenes* **(B)** and Gram-negative *P. aeruginosa* **(C)** and *P. mirabilis* **(D)** bacteria. CM from EFs had no significant effect on bacterial growth. Data are expressed as the percentage of growth $\pm$ SEM, with bacteria-only cultures set to 100%. ***, $p \leq .001$. Abbreviations: EFs, enriched fibroblasts; IFN-γ, interferon-γ; OMLP-PCs, oral mucosal lamina propria-progenitor cells.

Published Ahead of Print on September 16, 2015 as 10.5966/sctm.2015-0043.

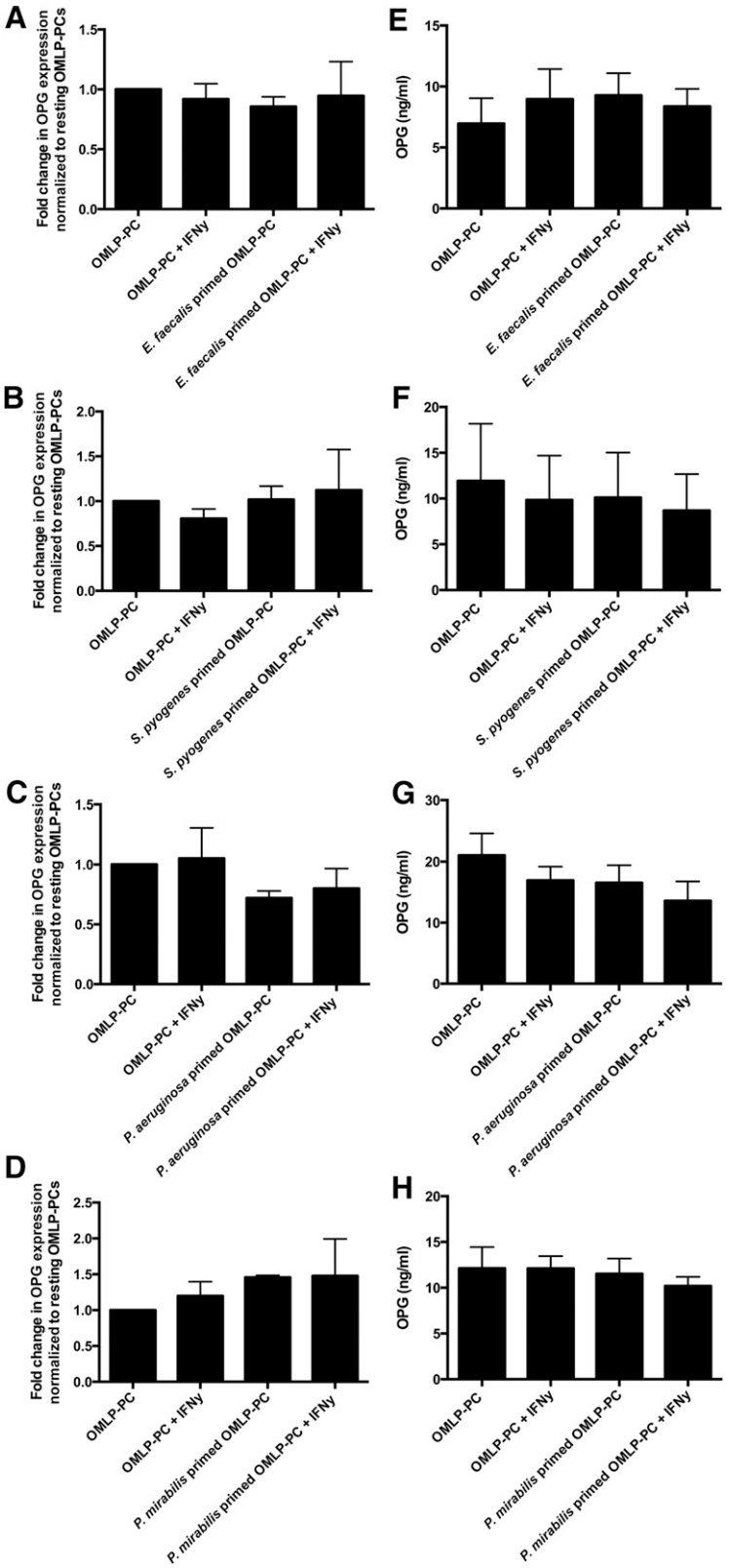

Figure 3. OMLP-PCs constitutively express and secrete OPG. OPG expression and secretion was unchanged by IFN-γ priming of OMLP-PCs and/or exposure to Gram-positive *E. faecalis* **(A, E)** and *S. pyogenes* **(B, F)** or Gram-negative *P. aeruginosa* **(C, G)** and *P. mirabilis* **(D, H)** bacteria. Genomic expression data are presented as the fold change from resting OMLP-PCs ± SEM and OPG secretion data as ng/ml ± SEM. Abbreviations: EFs, enriched fibroblasts; IFN-γ, interferon-γ; OMLP-PCs, oral mucosal lamina propria-progenitor cells; OPG, osteoprotegerin.

Published Ahead of Print on September 16, 2015 as 10.5966/sctm.2015-0043.

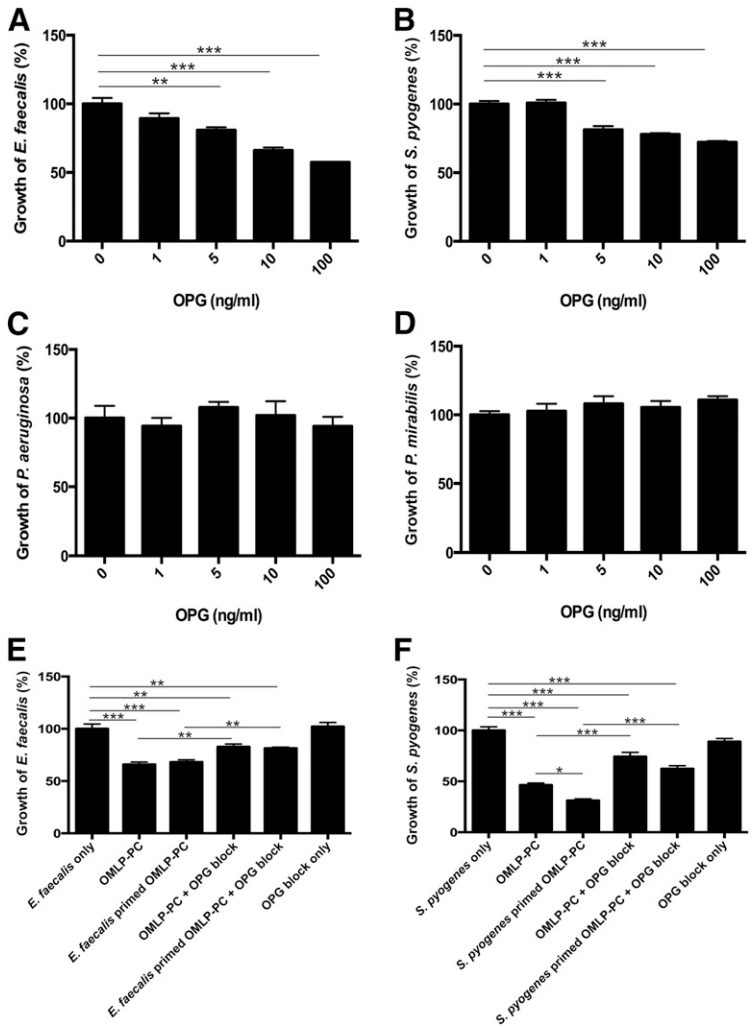

Figure 4. OPG demonstrated antibacterial properties against Gram-positive bacteria. OPG reduced the growth of Gram-positive bacteria *E. faecalis* **(A)** and *S. pyogenes* **(B)** only (no effect on Gram-negative bacteria **[C, D]**). Blocking OPG within the conditioned media of OMLP-PCs significantly restored the growth of Gram-positive *E. faecalis* **(E)** and *S. pyogenes* **(F)** bacteria. Data are expressed as the percentage of growth ± SEM, with bacteria-only cultures set to 100%. *, $p \leq .05$; **, $p \leq .01$; ***, $p \leq .001$. Abbreviations: EFs, enriched fibroblasts; IFN-γ, interferon-γ; OMLP-PCs, oral mucosal lamina propria-progenitor cells; OPG, osteoprotegerin.

Blocking Hp Inhibits Antibacterial Properties of OMLP-PCs Against Gram-Negative Bacteria

CM derived from OMLP-PCs (with or without previous bacterial exposure) was incubated with live, Gram-negative bacteria in the presence or absence of an anti-human Hp antibody. By blocking the secreted Hp in the CM samples of OMLP-PCs (with or without bacterial exposure), the growth of *P. aeruginosa* ($p \leq .001$ for both, with or without bacterial exposure; Fig. 5F) and *P. mirabilis* ($p \leq .01$ for both, with or without bacterial exposure; Fig. 5G) was significantly increased compared with samples in which Hp had not been blocked. The growth of *P. aeruginosa* and *P. mirabilis* was fully restored to control levels by blocking Hp.

OMLP-PC-Mediated Antibacterial Action Is Bacteriostatic

Bacterial cultures were incubated with CM derived from OMLP-PCs, rhOPG (Gram-positive bacteria), or Hp (Gram-negative bacteria), as previously stated. Subsequent to incubation, the bacterial cultures were stained using the LIVE/DEAD *Bac*Light staining kit. Bacterial viability was not compromised when bacteria were incubated with CM with or without bacterial exposure, rhOPG, or Hp (Fig. 6A–6D).

Discussion

We have previously reported the potent immunomodulatory potential of OMLP-PCs and their mode of action through the release of soluble factors [5]. In addition to their immunosuppressive properties, BMMSCs have recently been reported to display antibacterial properties [12, 24], leading to the hypothesis that immunomodulatory OMLP-PCs might also exhibit equivalent or potentially enhanced antibacterial properties because of their anatomical site of origin. The present study has demonstrated a reproducible direct antibacterial action by OMLP-PCs against both Gram-positive and Gram-negative bacteria in a bacteriostatic manner through the constitutive release of the differentially acting soluble factors, OPG and Hp.

Published Ahead of Print on September 16, 2015 as 10.5966/sctm.2015-0043.

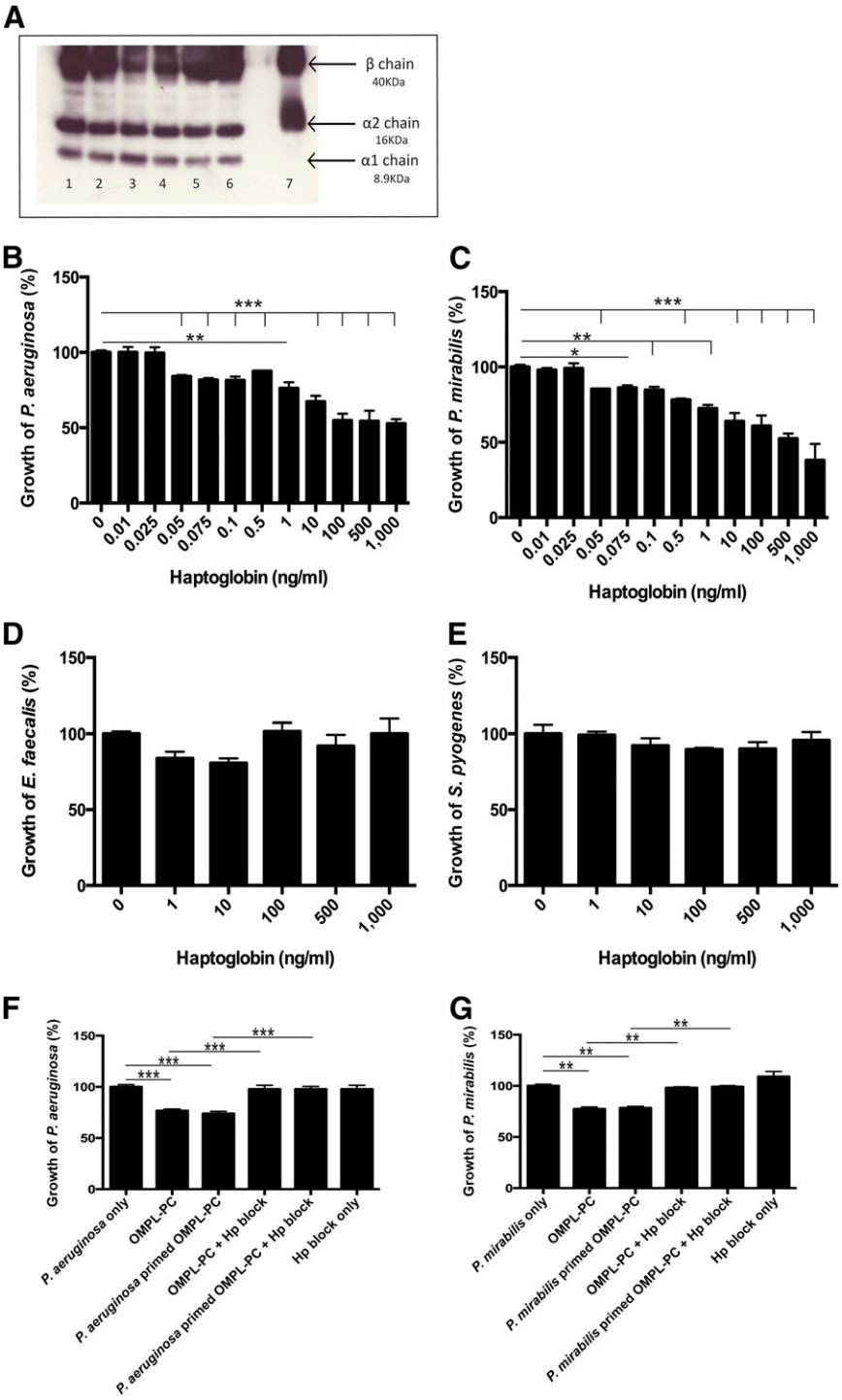

Figure 5. Haptoglobin is constitutively secreted by OMLP-PCs and demonstrates antibacterial properties against Gram-negative bacteria. **(A):** Hp was constitutively detected in the conditioned media (CM) of OMLP-PCs ($n = 3$ donors; lanes 2, 4, and 6, irrespective of IFN-γ stimulation of the cells [lanes 1, 3, 5]). Lane 7 indicates the Hp-positive control. Hp reduced the growth of *P. aeruginosa* **(B)** and *P. mirabilis* **(C)** bacteria only (no effect was seen on Gram-positive bacteria **[D, E]**). Blocking Hp in the CM restored the growth of the Gram-negative *P. aeruginosa* **(F)** and *P. mirabilis* **(G)** bacteria. Data are expressed as the percentage of growth ± SEM, with bacteria-only cultures set to 100%. *, $p \leq .05$; **, $p \leq .01$; ***, $p \leq .001$. Abbreviations: EFs, enriched fibroblasts; Hp, haptoglobin; IFN-γ, interferon-γ; OMLP-PCs, oral mucosal lamina propria-progenitor cells.

To date, limited evidence of stem cell-mediated antibacterial action has been documented. Both IDO and LL-37 have been implicated in the BMMSC mechanism of action [12, 24]. Within the present study, we found evidence for the importance of soluble factors in OMLP-PC-mediated antibacterial activity. However, in contrast to the BMMSC reports, no expression of LL-37 was seen within the OMLP-PCs (data not shown), and IDO, as we have previously reported, is only inducible by

Published Ahead of Print on September 16, 2015 as 10.5966/sctm.2015-0043.

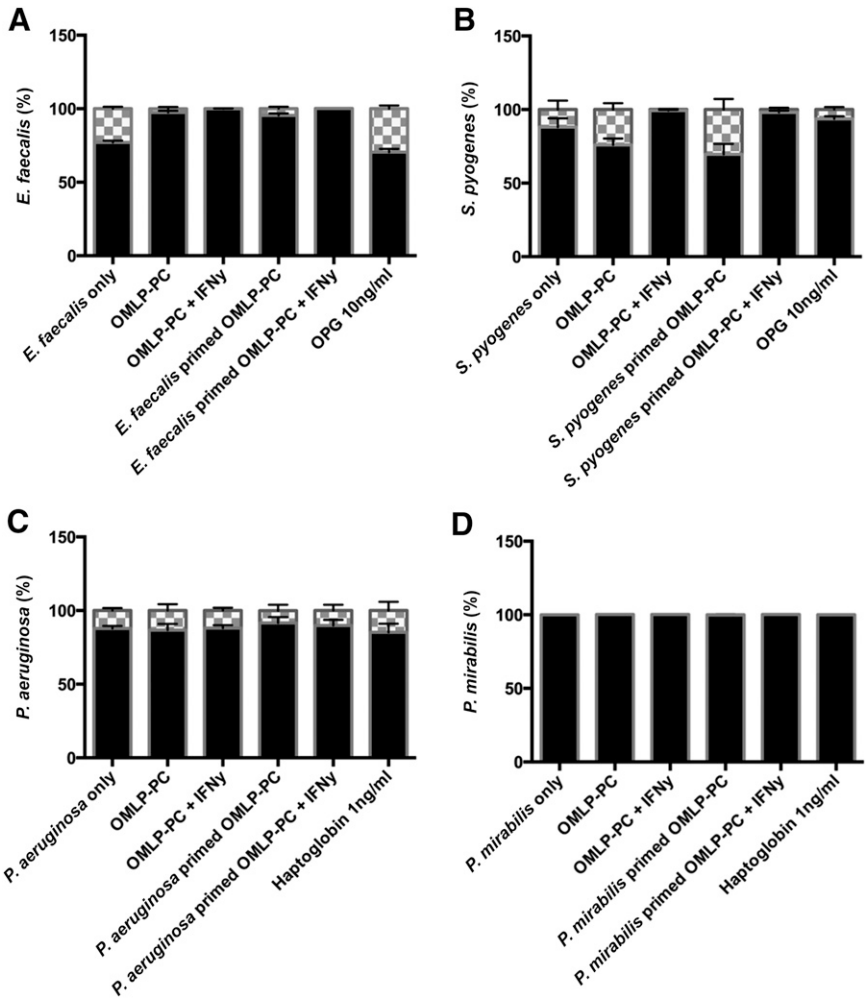

Figure 6. OMLP-PCs exert their antimicrobial actions via bacteriostatic mechanisms. LIVE/DEAD staining of *E. faecalis* **(A)**, *S. pyogenes* **(B)**, *P. aeruginosa* **(C)**, and *P. mirabilis* **(D)** cultures after incubation with OMLP-PC conditioned media with or without bacterial exposure, recombinant human OPG and haptoglobin. No bactericidal effect was seen with any of the test conditions. Data are expressed as the percentage of live/dead cells ± SEM. Black bars indicate the percentage of live cells; and checkered bars, the percentage of dead cells. Abbreviations: EFs, enriched fibroblasts; IFN-γ, interferon-γ; OMLP-PCs, oral mucosal lamina propria-progenitor cells; OPG, osteoprotegerin.

inflammatory stimuli and not constitutively expressed, as per the antibacterial effect shown [5].

Similar antibacterial effects of MSCs have been noted in murine models, with an increase in bacterial clearance on MSC treatment of sepsis [25] and *E. coli*-induced pneumonia [26], with lipocalin 2 thought to play a role in the latter. Our data have demonstrated that OMLP-PCs are antibacterial via the release of soluble factors. Additionally, we have shown that CM from OMLP-PCs is antibacterial through a bacteriostatic mechanism, ruling out soluble factors, which act in a bactericidal manner, such as the family of defensins and LL-37 [27]. The constitutive antibacterial nature of OMLP-PCs also differs from the reported mechanism seen in BMMSCs, for which exposure to bacteria is necessary for the cells to exert their effect by secreting soluble factors [12]. These differential modes of action among sources of stem cells is to be expected, and we hypothesize that in vivo priming and the niche environment from which the cells are derived will have a significant effect on their antibacterial properties.

OPG is vital in bone remodeling, regulating the process by acting as a decoy receptor for RANKL and influencing osteoclastogenesis [28]. The major bacterium involved in periodontal disease, *P. gingivalis* [29], is known to be capable of inducing OPG in human cells. The induction of OPG by *P. gingivalis* has been demonstrated in both endothelial cells [30] and gingival fibroblasts from both healthy and periodontitis patients, with the varying levels potentially correlating with disease status [31]. Patients with periodontitis display lower levels of OPG within the gingival crevicular fluid [20, 21] and gingival tissue [22] compared with healthy controls. However, each published study to date has compared OPG to RANKL within the context of bone remodeling and osteoclastogenesis. The clinical importance of OPG alone regarding bacterial infection during periodontal disease has not yet been explored.

We have demonstrated, for the first time, the novel antibacterial properties of OPG, which exerts a direct antibacterial action specifically against Gram-positive bacteria, through a bacteriostatic mechanism. OPG is constitutively secreted by OMLP-PCs at concentrations high enough to exert antibacterial effects. Furthermore, neutralization of OPG within the CM significantly restored the growth of the Gram-positive bacteria tested. However, because complete restoration in the growth of either bacterium to control levels was not

Published Ahead of Print on September 16, 2015 as 10.5966/sctm.2015-0043.

observed, we hypothesize that OPG is not the only factor involved in this antibacterial mechanism against *S. pyogenes* and *E. faecalis*.

In contrast to the other Gram-positive bacteria used in the present study, the antibacterial effect of the CM was greater against *S. pyogenes* when previous exposure of the OMLP-PCs to the bacteria had occurred. We hypothesize that this might be a consequence of in vivo priming. OMLP-PCs will have been exposed to streptococcal species in vivo, because these are one of the predominate bacterial genera within the oral cavity [32]. This could explain the heightened response of the primed CM to *S. pyogenes*, because the cells might have been sensitized to recognize this genus. Further investigations will determine whether the CM acts in a similar manner to other bacteria commonly found within the oral cavity.

Hp has long been known to display antibacterial properties against the Gram-negative bacterium *E. coli* [11]. Hp's mechanism of action is simple, sequestering iron and, therefore, reducing the iron available for bacteria [10]. Importantly, iron is crucial for bacterial growth, with a deficiency causing bacterial growth inhibition [33]. Although iron is essential for most bacteria, the levels required and uptake mechanisms vary considerably between microorganisms. Generally, Gram-negative bacteria recognize iron sources via an outer membrane receptor. The iron is then transported into the cell by an ATP-binding cassette transporter within the inner membrane [34]. Because Gram-positive bacteria lack an outer membrane, iron uptake mechanisms differ from that of the Gram-negative bacteria. The differences in iron uptake mechanisms are the likely reason Hp only demonstrated antibacterial properties against the Gram-negative bacteria examined. The studies confirmed the efficacy of Hp's antibacterial properties, with bacteriostatic effects evident down to levels as low as 50 pg/ml. Western blot analysis identified multiple isoforms of Hp constitutively expressed within the secretome of the OMLP-PCs, with the presence of the α1 chain suggesting the production of the higher affinity Hp1-1 and/or Hp2-1 isoforms. Blocking of this protein was sufficient to completely restore bacterial growth, suggesting this is the major mechanism of OMLP-PC antibacterial action against Gram-negative bacteria.

Wound healing within the oral mucosa is well documented to be preferential, characterized by rapid re-epithelialization, remodeling of the extracellular matrix, and rapid transition through the inflammatory phase [23, 35–38]. Our previous work suggested a potential role for immunomodulatory OMLP-PCs resident within the lamina propria in orchestrating this healing response [4, 5]. The finding that this cell source possesses additional innate antibacterial properties supports the hypothesis that OMLP-PCs offer a novel cell source for the development of cell- or soluble factor-based local treatment of chronic nonhealing wounds or systemic infusions for infectious disorders such as bacterial pneumonia.

Additional studies are required to examine further the antibacterial factors secreted by the OMLP-PCs, particularly against Gram-positive bacteria as the presence of OPG did not fully explain the antibacterial properties of the cells. Future work will concentrate on investigating the potential factors involved in these antibacterial mechanisms and how these findings can be exploited for clinical translation.

Conclusion

Within the present study, we have demonstrated, for the first time, the broad spectrum antibacterial properties of OMLP-PCs. These PCs constitutively secrete antimicrobial soluble factors with bacteriostatic activity against both Gram-positive and Gram-negative bacteria. Analysis of the OMLP-PC secretome confirmed a role for OPG in the suppression of Gram-positive bacterial growth and for Hp in inhibiting Gram-negative bacteria. The findings we have reported illustrate the potential for OMLP-PCs in the development of novel antibacterial cell- or soluble factor-based therapies for conditions such as pneumonia or chronic nonhealing wounds.

Acknowledgments

This work was funded by Cardiff University, the Medical Research Council (Grant G0901562), Cardiff Institute of Tissue Engineering and Repair, and the Welsh Livery Guild. Buccal mucosal biopsy samples were kindly obtained from patients undergoing routine oral surgery by Andrew Cronin, Consultant Oral and Maxillofacial Surgeon (Cardiff and Vale University Health Board, Cardiff, U.K.). The present work is subjected to patent filing (patent application nos. PCT/GB2009/001443, AU2009259053, EP09761964.7, CN200980122121.0, JP501125275, HK1155775, and US12/997,363).

Author Contributions

E.B.-D.: conception and design, collection and assembly of data, data analysis and interpretation, manuscript writing; R.M.: collection and assembly of data; A.S.: conception and design, financial support, final approval of manuscript; P.S.: conception and design, financial support, provision of study material or patients, final approval of manuscript; L.C.D.: conception and design, financial support, provision of study material or patients, data analysis and interpretation, manuscript writing, final approval of manuscript.

Disclosure of Potential Conflicts of Interest

L.C.D. and P.S. have filed for patents. The other authors indicated no potential conflicts of interest.

References

1 Parahitiyawa NB, Scully C, Leung WK et al. Exploring the oral bacterial flora: Current status and future directions. Oral Dis 2010;16:136–145.

2 Gorr SU. Antimicrobial peptides of the oral cavity. Periodontol 2000 2009;51:152–180.

3 Pütsep K, Carlsson G, Boman HG et al. Deficiency of antibacterial peptides in patients with morbus Kostmann: An observation study. Lancet 2002;360:1144–1149.

4 Davies LC, Locke M, Webb RD et al. A multipotent neural crest-derived progenitor cell population is resident within the oral mucosa lamina propria. Stem Cells Dev 2010;19:819–830.

5 Davies LC, Lönnies H, Locke M et al. Oral mucosal progenitor cells are potently immunosuppressive in a dose-independent manner. Stem Cells Dev 2012;21:1478–1487.

6 Abumaree M, Al Jumah M, Pace RA et al. Immunosuppressive properties of mesenchymal stem cells. Stem Cell Rev 2012;8:375–392.

7 Waterman RS, Tomchuck SL, Henkle SL et al. A new mesenchymal stem cell (MSC) paradigm: Polarization into a pro-inflammatory MSC1 or an immunosuppressive MSC2 phenotype. PLoS One 2010;5:e10088.

8 Krampera M, Pasini A, Pizzolo G et al. Regenerative and immunomodulatory potential

Published Ahead of Print on September 16, 2015 as 10.5966/sctm.2015-0043.

of mesenchymal stem cells. Curr Opin Pharmacol 2006;6:435–441.

9 Hucke C, MacKenzie CR, Adjogble KD et al. Nitric oxide-mediated regulation of gamma interferon-induced bacteriostasis: Inhibition and degradation of human indoleamine 2,3-dioxygenase. Infect Immun 2004;72:2723–2730.

10 Barclay R. The role of iron in infection. Med Lab Sci 1985;42:166–177.

11 Eaton JW, Brandt P, Mahoney JR et al. Haptoglobin: A natural bacteriostat. Science 1982;215: 691–693.

12 Krasnodembskaya A, Song Y, Fang X et al. Antibacterial effect of human mesenchymal stem cells is mediated in part from secretion of the antimicrobial peptide LL-37. STEM CELLS 2010;28:2229–2238.

13 Hall SR, Tsoyi K, Ith B et al. Mesenchymal stromal cells improve survival during sepsis in the absence of heme oxygenase-1: The importance of neutrophils. STEM CELLS 2013;31:397–407.

14 Krasnodembskaya A, Samarani G, Song Y et al. Human mesenchymal stem cells reduce mortality and bacteremia in gram-negative sepsis in mice in part by enhancing the phagocytic activity of blood monocytes. Am J Physiol Lung Cell Mol Physiol 2012;302:L1003–L1013.

15 Sadrzadeh SM, Bozorgmehr J. Haptoglobin phenotypes in health and disorders. Am J Clin Pathol 2004;121(suppl):S97–S104.

16 Huntoon KM, Wang Y, Eppolito CA et al. The acute phase protein haptoglobin regulates host immunity. J Leukoc Biol 2008;84:170–181.

17 Jin Z, Li X, Wan Y. Minireview: Nuclear receptor regulation of osteoclast and bone remodeling. Mol Endocrinol 2015;29:172–186.

18 Le Blanc K, Rasmusson I, Götherström C et al. Mesenchymal stem cells inhibit the expression of CD25 (interleukin-2 receptor) and CD38 on phytohaemagglutinin-activated lymphocytes. Scand J Immunol 2004;60:307–315.

19 Oshita K, Yamaoka K, Udagawa N et al. Human mesenchymal stem cells inhibit osteoclastogenesis through osteoprotegerin production. Arthritis Rheum 2011;63:1658–1667.

20 Bostanci N, Ilgenli T, Emingil G et al. Differential expression of receptor activator of nuclear factor-kappaB ligand and osteoprotegerin mRNA in periodontal diseases. J Periodontal Res 2007;42:287–293.

21 Mogi M, Otogoto J, Ota N et al. Differential expression of RANKL and osteoprotegerin in gingival crevicular fluid of patients with periodontitis. J Dent Res 2004;83:166–169.

22 Liu D, Xu JK, Figliomeni L et al. Expression of RANKL and OPG mRNA in periodontal disease: Possible involvement in bone destruction. Int J Mol Med 2003;11:17–21.

23 Stephens P, Davies KJ, al-Khateeb T et al. A comparison of the ability of intra-oral and extra-oral fibroblasts to stimulate extracellular matrix reorganization in a model of wound contraction. J Dent Res 1996;75:1358–1364.

24 Meisel R, Brockers S, Heseler K et al. Human but not murine multipotent mesenchymal stromal cells exhibit broad-spectrum antimicrobial effector function mediated by indoleamine 2,3-dioxygenase. Leukemia 2011;25:648–654.

25 Mei SH, Haitsma JJ, Dos Santos CC et al. Mesenchymal stem cells reduce inflammation while enhancing bacterial clearance and improving survival in sepsis. Am J Respir Crit Care Med 2010;182:1047–1057.

26 Gupta N, Krasnodembskaya A, Kapetanaki M et al. Mesenchymal stem cells enhance survival and bacterial clearance in murine *Escherichia coli* pneumonia. Thorax 2012;67:533–539.

27 Zasloff M. Antimicrobial peptides, innate immunity, and the normally sterile urinary tract. J Am Soc Nephrol 2007;18: 2810–2816.

28 Martin TJ. Historically significant events in the discovery of RANK/RANKL/OPG. World J Orthop 2013;4:186–197.

29 Slots J, Ting M. Systemic antibiotics in the treatment of periodontal disease. Periodontol 2000 2002;28:106–176.

30 Kobayashi-Sakamoto M, Hirose K, Isogai E et al. NF-kappaB-dependent induction of osteoprotegerin by *Porphyromonas gingivalis* in endothelial cells. Biochem Biophys Res Commun 2004;315:107–112.

31 Baek KJ, Choi Y, Ji S. Gingival fibroblasts from periodontitis patients exhibit inflammatory characteristics in vitro. Arch Oral Biol 2013;58:1282–1292.

32 Aas JA, Paster BJ, Stokes LN et al. Defining the normal bacterial flora of the oral cavity. J Clin Microbiol 2005;43:5721–5732.

33 Cherayil BJ. The role of iron in the immune response to bacterial infection. Immunol Res 2011;50:1–9.

34 Krewulak KD, Vogel HJ. . Structural biology of bacterial iron uptake. . Biochim Biophys Acta 2008;1778:1781–1804.

35 Stephens P, Hiscox S, Cook H et al. Phenotypic variation in the production of bioactive hepatocyte growth factor/scatter factor by oral mucosal and skin fibroblasts. Wound Repair Regen 2001;9:34–43.

36 Stephens P, Davies KJ, Occleston N et al. Skin and oral fibroblasts exhibit phenotypic differences in extracellular matrix reorganization and matrix metalloproteinase activity. Br J Dermatol 2001;144:229–237.

37 Enoch S, Wall I, Peake M et al. Increased oral fibroblast lifespan is telomerase-independent. J Dent Res 2009;88:916–921.

38 Enoch S, Peake MA, Wall I et al. "Young" oral fibroblasts are geno/phenotypically distinct. J Dent Res 2010;89:1407–1413.

See www.StemCellsTM.com for supporting information available online.

